

# NORTH CAROLINA STATE UNIVERSITY | AT RALEIGH

SCHOOL OF ENGINEERING

DEPARTMENT OF ENGINEERING SCIENCE AND MECHANICS  
Box 5130, Zip 27607

October 29, 1974

(NASA-CR-141949) [METHOD OF CHARACTERISTICS  
CALCULATIONS AND COMPUTER CODE FOR MATERIALS  
WITH ARBITRARY EQUATIONS OF STATE AND USING  
ORTHOGONAL POLYNOMIAL LEAST SQUARE SURFACE  
FITS] Final Report (North Carolina State

N75-15329

Unclas  
G3/61 04939

Dr. Robert G. Thompson  
Technical Representative of the  
Contracting Officer (TRCO)  
Mail Stop 230  
NASA-Langley Research Center  
Hampton, Virginia 23665

RE: Final Report, NASA Research Grant NGL 34-002-084

Dear Bob:

How are you?

I am enclosing two (2) copies of the Final Report of the above Research Grant. Three (3) additional copies have been forwarded directly to:

NASA Scientific and Technical  
Information Facility  
Post Office Box 33  
College Park, Maryland 20740

This report is subdivided into three sections as follows:

Section I Journal Papers and Technical Reports of Research Projects directly related to and partially supported by the research grant.

- I.1. "Stress Waves Resulting from Hypervelocity Impact," AIAA paper No. 69-355, Presented at the 1969 AIAA Hypervelocity Impact Conference in Cincinnati, Ohio (Authored by R. Madden and T. S. Chang) Results from a numerical scheme based on the method of characteristics are presented for the axially symmetric, hypervelocity impact of similar materials. The analysis is restricted to the early stages of the impact of a right circular cylinder on a halfspace. The resulting rarefaction and shock waves produced by the impact are considered as discrete wavefronts which divide the impacted zone into regions. Numerical diffusion is then controlled by requiring that the values of the dependent variables at a given point in the impacted zone to depend on only the calculated values at earlier times at points in the same region as the point in question. The numerical results give

accurate representations of the stress wave profiles (i.e., rarefaction and shock waves) which should be useful as inputs for a later stage elastoplastic analysis and/or spallation analysis. The effects of "numerical diffusion" on the calculated pressure and flow fields when the rarefaction wave is not considered as discrete is investigated and the "diffused" results are compared with the more exact analysis.

- I.2. "Nonlinear Waves in a Rate-Sensitive, Elastoplastic Material," International Journal of Engineering Science, Volume 10, pp. 353-367, 1972. (Authored by E. E. Burniston and T. S. Chang).  
Two classes of closed form solutions of one-dimensional, nonlinear waves in a rate-sensitive, elastoplastic material are reported. One class of these solutions is self-similar and the other class consists of constant speed propagations. Applications of these solutions to unsteady motions behind propagating discontinuities are also considered.
- I.3. "Curved Characteristics Behind Blast Waves," The Physics of Fluids, Volume 15, pp. 502-504, 1972. (Authored by O. Laporte and T. S. Chang)  
Exact solutions, expressed in closed form in terms of elementary functions, are presented for the three sets of curved characteristics behind a self-similar, strong blast wave.
- I.4. "On Dispersion and Characteristic Motions of Temperature-Rate Dependent Materials," National Aeronautics and Space Administration Report CR-1795, 1971.  
A general three-dimensional theory of a thermomechanical material which can be a metallic or polymeric medium, or a structured composite, is developed using the modern techniques of axiomatic continuum mechanics and the laws of thermodynamics. One-dimensional linear spatial gradient temperature-rate dependent theories are presented for both thermoviscoelastic and thermoelastic materials. The characteristic motions are considered and it is shown that, due to the presence of temperature-rate effects, thermal propagation speeds have finite values. A comprehensive study of the dispersion relations is presented and illustrated graphically for typical values of the material constants. Analytical expressions are obtained for both high and low frequency responses. It is demonstrated that the characteristic speeds coincide with the high frequency asymptotic phase velocities in both cases. Physical and numerical limitations on the material constants are obtained for stable wave propagations. A class of self-similar solutions is obtained for the temperature-rate dependent thermoelastic medium using the theory of continuous group of transformations.
- I.5. "Comments on Application of Singular Eigenfunction Expansions to the Propagation of Periodic Disturbances in a Radiating Grey Gas," The Physics of Fluids, Volume 16, pp. 159-160, 1973. (Authored by T. S. Chang, K. H. Kim and M. N. Osizik)  
Recently, we have been extending our analysis of sound propagation



in dissociative, radiative media to include the effects of scattering. It is of interest to note that the set of pertinent integrodifferential equations can also be solved exactly using the singular eigenfunction expansion technique.

## Section II Computer Programs and Numerical Results of Hypervelocity Impact Calculations

- II.1. Method of Characteristics Calculations and the Computer Code Using Orthogonal Polynomial Least Square Surface Fits.  
Very recently, we have developed a new numerical scheme using the method of characteristics to calculate the flow properties and pressures behind decaying shock waves for materials under hypervelocity impact. This procedure is quite different from our earlier methods (see paper I.1). We are now able to replace the time-consuming double interpolation subroutines used in paper I.1 by a technique based on Orthogonal Polynomial Least Square Surface Fits. Typical calculated results are given and in Tables 1-19. These results are compared with the double-interpolation results. The complete computer program is also included.
- II.2. Method of Characteristics Calculations and the Computer Code for Materials with Arbitrary Equations of State.  
As reported in our earlier status reports, we have developed a numerical code capable of calculating flow properties and pressures behind decaying shock waves for materials under hypervelocity impact with arbitrary equations of state. For comparison purposes, we have made some sample calculations using the new code for impact conditions similar to those reported in I.1. These results are quite encouraging and are displayed graphically in Figures 1-3. A listing of the numerical code is also attached.

## Section III Fundamental Research on Equations of State and Non-Equilibrium Statistical Mechanics Generated by the Research Grant.

Materials under hypervelocity impact experience extreme changes of stresses, strains, and thermodynamic states. We have looked into some basic research areas related to (1) the non-equilibrium statistical mechanical aspects of heat transfer with discontinuous velocity boundary conditions, and (2) the fundamental understanding of the equations of state, phase transitions, and critical phenomena of materials under extreme thermodynamic environments. Our research efforts along these directions are found in the following research papers:

- III.1. "Elementary Solutions of Coupled Model Equations in the Kinetic Theory of Gases," International Journal of Engineering Science, Volume 12, pp. 441-470, 1974. (Authors: J. T. Kriese, T. S. Chang, and C. E. Siewert.)

The method of elementary solutions is employed to solve two coupled integrodifferential equations sufficient for determining temperature - density effects in a linearized BGK model in the kinetic theory of gases. Full-range completeness and orthogonality theorems are proved for the developed normal modes and the infinite-medium Green's function is constructed as an illustration of the full-range formalism. The appropriate homogeneous matrix Riemann problem is discussed, and half-range completeness and orthogonality theorems are proved for a certain subset of the normal modes. The required existence and uniqueness theorems relevant to the H matrix, basic to the half-range analysis, are proved, and an accurate and efficient computational method is discussed. The half-space temperature-slip problem is solved analytically, and a highly accurate value of the temperature-slip coefficient is reported.

- III.2. "Tricritical Points in Multicomponent Fluid Mixtures," Physical Review, Volume A9, pp. 2573-2578, 1974. (Authors: A. Hankey, T. S. Chang, and H. E. Stanley)

In view of experimental considerations, we give a model-independent argument that the novel tricritical points in multicomponent fluid mixtures, where three phases simultaneously become critical, are points on the boundary of a single two-dimensional surface of critical points. This result is corroborated by the Landau model suggested by Griffiths. The relationship between these tricritical points and the complex "higher-order" critical points proposed to exist in certain magnetic systems is elucidated.

- III.3. "Generalized Scaling Hypothesis in Multicomponent Systems. I. Classification of Critical Points by Order and Scaling at Tricritical Points," Physical Review, Volume B8, pp. 346-364. (Authored by T. S. Chang, A. Hankey, and H. E. Stanley.)

The goal of this work is to provide an analysis of spaces of critical points for multicomponent systems. First, we propose the geometric concept of order  $O$  for critical points; we distinguish it from a previous definition of a "multicritical" point. Specifically, we may define the intersection of space of critical points of order  $O$  to be a space of critical points of order  $(O + 1)$ . Ordinary critical points are defined to be of order  $O = 2$ , so that the tricritical points introduced by Griffiths are of order  $O = 3$ . We discuss more general examples of critical spaces of order  $O = 3$  which are known for a wide variety of systems; we also propose several examples of models of magnetic systems showing critical points of order  $O = 4$  - i.e., systems having intersecting lines of tricritical points. The analysis of critical and coexistence spaces also provides a new form of the Gibbs phase rule suitable for complex magnetic models. Next we define - for the critical points of order  $O$  of which examples have been given - special directions in terms of which to make a scaling hypothesis. We give the hypothesis for simple systems and then for tricritical points, and then, in a subsequent paper, part II, the special directions are used to make a scaling hypothesis at spaces of critical points of any order. Certain predictions (e.g., scaling laws and "single-power"

October 29, 1974

scaling functions) follow in a simple and straightforward fashion. We consider the scaling hypothesis at a critical space of order  $\bar{0}$  in terms of a group of transformations. We can define a set of invariants of the group. It is possible, for  $\bar{0} > 3$ , to make a second scaling hypothesis for the space of order  $\bar{0} - 1$  using certain of these invariants as independent variables. This is advantageous because certain "double-power" scaling functions then follow directly; these predict that for  $\bar{0} = 3$ , experimental data collapse from a volume onto a line. This prediction is to be contrasted with ordinary scaling function, which predict that data collapse by only a single dimension (e.g., from a volume onto a surface or from a surface onto a line).

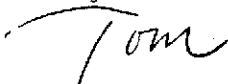
III.4. "Double-Power Scaling Functions Near Tricritical Points," Physical Review, Volume B7, pp. 4263-4266, 1973. (Authored by T. S. Chang, A. Hankey, and H. E. Stanley.)

We introduce invariants of the scaling equation about the tricritical point. Using these invariants, a modified version of the scaling hypothesis about the three critical lines meeting at the tricritical point is presented. From it we demonstrate that the thermodynamic equation of state near a tricritical point and near a critical line may be expressed as double-power scaling functions. These imply that experimental data should collapse from a volume onto a line (i.e., by two dimensions). This behavior is in contrast to ordinary "single-power" scaling functions, which predict data collapsing from a volume onto a surface or from a surface onto a line (i.e., by one dimension).

In conclusion, we have obtained much information pertaining to the behavior materials under impact, particularly hypervelocity impact. Two useful numerical codes have been developed for calculations of axisymmetric hypervelocity impact for materials with rather general equations of state. Fundamental research in the areas of critical equations of state and non-equilibrium statistical mechanics and heat transfer have also been considered.

With best wishes, I am

Very sincerely yours,



Tien Sun Chang  
Professor

C:mlm

closures

: NASA Scientific and Technical  
Information Facility (3 copies)

- I.1. "Stress Waves Resulting from Hypervelocity Impact"
- I.2. "Nonlinear Waves in a Rate-Sensitive, Elastoplastic Material"
- I.3. "Curved Characteristics Behind Blast Waves"
- I.4. "On Dispersion and Characteristic Motions of Temperature-Rate  
Dependent Materials"  
NASA Report - copies not enclosed
- I.5. "Comments on Application of Singular Eigenfunction Expansions  
to the Propagation of Periodic Disturbances in a Radiating  
Grey Gas"

PAPERS INTENTIONALLY OMITTED

II.1. Method of Characteristics Calculations and the Computer Code  
Using Orthogonal Polynomial Least Square Surface Fits

### List of Symbols

$t$  = time ( $\mu\text{sec}$ )

$r$  = radial coordinate (cm)

$Z$  = axial coordinate (cm)

$U$  = radial velocity (cm/ $\mu\text{sec}$ )

$V$  = axial velocity (cm/ $\mu\text{sec}$ )

$\rho$  = mass density ( $\text{gm}/\text{cm}^3$ )

$e$  = internal energy per unit mass (megabar  $\text{cm}^3/\text{gm}$ )

$a$  = sound speed (cm/ $\mu\text{sec}$ )

$P$  = pressure (megabars)

$\cos \alpha_0$  = direction cosine of normal with respect to  $r$  axis

$\sin \alpha_0$  = direction cosine of normal with respect to  $Z$  axis

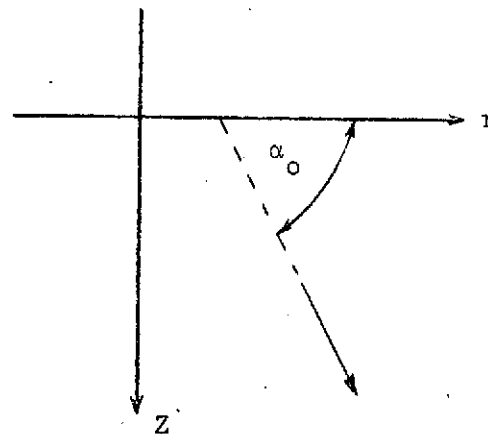


Table 1. Flow properties in Projectile Shock at  $t = 1.18 \mu\text{sec}$  after impact of a 2.5-cm-diameter projectile at 0.76 cm/ $\mu\text{sec}$  on an aluminum half-space based on (1) Double Interpolation and (2) Othogonal Polynomials Least Square Surface Fit with Double Interpolation after  $t = 1.1 \mu\text{sec}$ .

(1)					(2)				
Z	r	P	U	V	Z	r	P	U	V
$\rho$	e	a	$\cos \alpha_o$	$\sin \alpha_o$	$\rho$	e	a	$\cos \alpha_o$	$\sin \alpha_o$
-0.3532	0.0	1.0869	0.0	0.3800	-0.3532	0.0	1.0869	0.0	0.3800
4.2103	0.0722	1.0038	0.0	1.0000	4.2103	0.0722	1.0038	0.0	1.0000
-0.3532	0.2500	1.0869	0.0	0.3800	-0.3532	0.2500	1.0869	0.0	0.3800
4.2103	0.0722	1.0038	0.0	1.0000	4.2103	0.0722	1.0038	0.0	1.0000
-0.3521	0.5012	1.0412	0.0025	0.3910	-0.3509	0.5009	0.9911	0.0017	0.4033
4.1738	0.0681	0.9934	-0.0068	1.0000	4.1325	0.0636	0.9820	-0.0049	1.0000
-0.3312	0.7611	0.8591	0.0209	0.4372	-0.3312	0.7630	0.7891	0.0106	0.4554
4.0185	0.0521	0.9500	-0.0648	0.9976	3.9533	0.0463	0.9318	-0.0348	0.9991
-0.2120	1.0183	0.4162	0.0124	0.5679	-0.2117	1.0177	0.4090	0.0116	0.5704
3.5399	0.0183	0.8122	-0.0667	0.9968	3.5303	0.0178	0.8094	-0.0613	0.9972

Table 2. Flow properties in Target Shock at  $t = 1.18 \mu\text{sec}$  after impact of a 2.5-cm-diameter projectile at  $0.76 \text{ cm}/\mu\text{sec}$  on an aluminum half-space based on (1) Double Interpolation and (2) Orthogonal Polynomials Least Square Surface Fit with Double Interpolation after  $t = 1.1 \mu\text{sec}$ .

(1)					(2)				
Z $\rho$	r e	P a	U $\cos \alpha_o$	V $\sin \alpha_o$	Z $\rho$	r e	P a	U $\cos \alpha_o$	V $\sin \alpha_o$
1.2500	0.0	1.0869	0.0	0.3800	1.2500	0.0	1.0869	0.0	0.3800
4.2103	0.0722	1.0038	0.0	1.0000	4.2103	0.0722	1.0038	0.0	1.0000
1.2500	0.2500	1.0869	0.0	0.3800	1.2500	0.2500	1.0869	0.0	0.3800
4.2103	0.0722	1.0038	0.0	1.0000	4.2103	0.0722	1.0038	0.0	1.0000
1.2500	0.5007	1.0686	0.0029	0.3756	1.2497	0.5007	1.0685	0.0029	0.3756
4.1957	0.0750	0.9997	0.0078	1.0000	4.1957	0.0705	0.9997	0.0078	1.0000
1.2398	0.7544	0.9647	0.0058	0.3501	1.2398	0.7544	0.9647	0.0058	0.3501
4.1106	0.0613	0.9758	0.0165	0.9998	4.1106	0.0613	0.9758	0.0165	0.9998
1.2143	1.0281	0.8382	0.0192	0.3169	1.2143	1.0281	0.8382	0.0192	0.3169
3.9996	0.0503	0.9446	0.0605	0.9979	3.9996	0.0503	0.9446	0.0605	0.9979
1.1235	1.3139	0.5624	0.0302	0.2368	1.1236	1.3139	0.5679	0.0304	0.2384
3.7190	0.0285	0.8649	0.1265	0.9910	3.7252	0.0290	0.8666	0.1265	0.9910
0.7683	1.7372	0.1558	0.0540	0.0691	0.7678	1.7377	0.1546	0.0528	0.0694
3.1170	0.0038	0.6776	0.6152	0.7870	3.1144	0.0037	0.6768	0.6050	0.7948
0.5808	1.8634	0.0670	0.0330	0.0263	0.5807	1.8634	0.0664	0.0327	0.0261
2.9088	0.0008	0.6045	0.7817	0.6227	2.9071	0.0008	0.6039	0.7816	0.6227
0.3716	1.9378	0.0	0.0	0.0	0.3716	1.9377	0.0	0.0	0.0
2.7000	0.0	0.5277	0.9289	0.3690	2.7000	0.0	0.5277	0.9289	0.3690



Table 3. Flow properties in Rarefaction at  $t = 1.18 \mu\text{sec}$  after impact of a 2.5-cm-diameter projectile at 0.76 cm/ $\mu\text{sec}$  on an aluminum half-space based on (1) Double Interpolation and (2) Orthogonal Polynomials Least Square Surface Fit with Double Interpolation after  $t = 1.1 \mu\text{sec}$ .

(1)				(2)			
Z	r	$\cos \alpha_o$	$\sin \alpha_o$	Z	r	$\cos \alpha_o$	$\sin \alpha_o$
1.2500	0.3781	0.6768	-0.7362	1.2500	0.3781	0.6768	-0.7362
1.1356	0.2852	0.5801	-0.8145	1.1355	0.2852	0.5801	-0.8145
1.0210	0.2132	0.4834	-0.8754	1.0210	0.2132	0.4834	-0.8754
0.9065	0.1577	0.3867	-0.9222	0.9065	0.1577	0.3867	-0.9222
0.7920	0.1165	0.2901	-0.9570	0.7920	0.1165	0.2901	-0.9570
0.6774	0.0879	0.1934	-0.9811	0.6774	0.0879	0.1934	-0.9811
0.5629	0.0711	0.0967	-0.9953	0.5629	0.0711	0.0967	-0.9953
0.4484	0.0656	-0.0000	-1.0000	0.4484	0.0656	-0.0000	-1.0000
0.3339	0.0711	-0.0967	-0.9953	0.3339	0.0711	-0.0967	-0.9953
0.2194	0.0879	-0.1934	-0.9811	0.2194	0.0879	-0.1934	-0.9811
0.1048	0.1165	-0.2901	-0.9570	0.1048	0.1165	-0.2901	-0.9570
-0.0097	0.1577	-0.3867	-0.9222	-0.0097	0.1577	-0.3867	-0.9222
-0.1242	0.2132	-0.4834	-0.8754	-0.1242	0.2132	-0.4834	-0.8754
-0.2387	0.2852	-0.5801	-0.8145	-0.2387	0.2852	-0.5801	-0.8145
-0.3532	0.3781	-0.6768	-0.7362	-0.3532	0.3781	-0.6768	-0.7362

Table 4. Flow properties in Interior Region at  $t = 1.18 \mu\text{sec}$  after impact of a 2.5-cm-diameter projectile at  $0.76 \text{ cm}/\mu\text{sec}$  on an aluminum half-space based on (1) Double Interpolation and (2) Orthogonal Polynomial Least Square Surface Fit with Double Interpolation after  $t = 1.1 \mu\text{sec}$  at  $Z = -0.25 \text{ cm}$ .

$Z = -0.25 \text{ cm}$	$r$	$P$	$U$	$V$	$\rho$	$e$	$a$
(1)	0.0	1.0869	0.0	0.3800	4.2103	0.0722	1.0038
	0.2500	1.0869	0.0	0.3800	4.2103	0.0722	1.0038
	0.5000	0.9289	0.0167	0.4159	4.050	0.0622	0.9654
	0.7500	0.6891	0.0558	0.3987	3.8200	0.0422	0.9012
	1.0000	0.0	0.0	0.0	2.7000	0.0	0.5277
	1.2500	0.0	0.0	0.0	2.7000	0.0	0.5277
	1.5000	0.0	0.0	0.0	2.7000	0.0	0.5277
	1.7500	0.0	0.0	0.0	2.7000	0.0	0.5277
	2.0000	0.0	0.0	0.0	2.7000	0.0	0.5277
(2)	0.0	1.0869	0.0	0.3800	4.2103	0.0722	1.0038
	0.2500	1.0869	0.0	0.3800	4.2103	0.0722	1.0038
	0.5000	0.6710	-0.1555	0.4333	3.7854	0.0425	0.8946
	0.7500	2.2439	-0.0865	0.9374	5.2602	0.1201	1.2174
	1.0000	0.0	0.0	0.0	2.7000	0.0	0.5277
	1.2500	0.0	0.0	0.0	2.7000	0.0	0.5277
	1.5000	0.0	0.0	0.0	2.7000	0.0	0.5277
	1.7500	0.0	0.0	0.0	2.7000	0.0	0.5277
	2.0000	0.0	0.0	0.0	2.7000	0.0	0.5277

Table 5. Flow properties in Interior Region at  $t = 1.18$   $\mu\text{sec}$  after impact of a 2.5-cm-diameter projectile at 0.76 cm/ $\mu\text{sec}$  on an aluminum half-space based on (1) Double Interpolation and (2) Orthogonal Polynomial Least Square Surface Fit with Double Interpolation after  $t = 1.1 \mu\text{sec}$  at  $Z = 0.0$  cm.

$Z = 0.0$ cm	$r$	$P$	$U$	$V$	$\rho$	$e$	$a$
(1)	0.0	1.0869	0.0	0.3800	4.2103	0.0722	1.0038
	0.2500	0.9644	0.0130	0.3829	4.0861	0.0646	0.9743
	0.5000	0.6875	0.0985	0.4466	3.7705	0.0478	0.8972
	0.7500	0.4822	0.2065	0.5931	3.5022	0.0348	0.8269
	1.0000	0.1931	0.2829	0.7128	3.0774	0.0132	0.6916
	1.2500	0.0	0.6160	0.3904	2.7000	0.0	0.5277
	1.5000	0.0	0.1923	-0.0971	2.7000	0.0	0.5277
	1.7500	0.0	0.1103	-0.1452	2.7000	0.0	0.5277
	2.0000	0.0	0.0303	-0.0074	2.7000	0.0	0.5277
(2)	0.0	1.0869	0.0	0.3800	4.2103	0.0722	1.0038
	0.2500	0.4956	-0.1726	0.3333	3.5563	0.0318	0.8347
	0.5000	0.5533	0.0033	0.4539	3.6020	0.0395	0.8537
	0.7500	0.7227	0.2308	0.6779	3.8156	0.0497	0.9081
	1.0000	0.0112	0.3021	0.6287	2.6397	0.0053	0.5362
	1.2500	0.0	0.3460	0.4024	2.7000	0.0	0.5277
	1.5000	0.0	0.2988	-0.1707	2.7000	0.0	0.5277
	1.7500	0.0	0.0076	-0.0333	2.7000	0.0	0.5277
	2.000	0.0	1.0304	0.0920	2.7000	0.0	0.5277

18

Table 6. Flow properties in Interior Region at  $t = 1.18$   $\mu\text{sec}$  after impact of a 2.5-cm-diameter projectile at 0.76 cm/ $\mu\text{sec}$  on an aluminum half-space based on (1) Double Interpolation and (2) Orthogonal Polynomial Least Square Surface Fit with Double Interpolation after  $t = 1.1 \mu\text{sec}$  at  $Z = 0.25$  cm.

Z = 0.25 cm		r	P	U	V	$\rho$	e	a
(1)	0.0	1.0869	0.0	0.3800	4.2103	0.0722	1.0038	
	0.2500	0.9018	0.0414	0.3889	4.0190	0.0608	0.9582	
	0.5000	0.6611	0.1029	0.3898	3.7383	0.0461	0.8890	
	0.7500	0.5468	0.1589	0.4410	3.5875	0.0393	0.8504	
	1.0000	0.4078	0.2552	0.5698	3.3982	0.0296	0.7973	
	1.2500	0.2713	0.3356	0.2505	3.1741	0.0216	0.7328	
	1.5000	0.1800	0.2782	-0.0038	3.0497	0.0126	0.6831	
	1.7500	0.1452	0.1345	-0.0307	3.0979	0.0032	0.6704	
	2.0000	0.0	0.0	0.0	2.7000	0.0	0.5277	
(2)	0.0	1.0869	0.0	0.3800	4.2103	0.0722	1.0038	
	0.2500	0.9041	0.0405	0.4685	4.0212	0.0610	0.9588	
	0.5000	0.6238	0.1083	0.3428	3.6922	0.0436	0.8770	
	0.7500	0.4999	0.1591	0.4221	3.5219	0.0365	0.8332	
	1.0000	0.4384	0.1553	0.5946	3.4452	0.0314	0.8102	
	1.2500	0.3310	0.3414	0.2448	3.2767	0.0250	0.7629	
	1.5000	0.1820	0.2935	0.0031	3.0507	0.0130	0.6841	
	1.7500	0.1509	0.1379	-0.0592	3.1113	0.0033	0.6746	
	2.0000	0.0	0.0	0.0	2.7000	0.0	0.5277	

Table 7. Flow properties in Interior Region at  $t = 1.18$   $\mu\text{sec}$  after impact of a 2.5-cm-diameter projectile at 0.76 cm/ $\mu\text{sec}$  on an aluminum half-space based on (1) Double Interpolation and (2) Orthogonal Polynomial Least Square Surface Fit with Double Interpolation after  $t = 1.1 \mu\text{sec}$  at  $Z = 0.50$  cm.

$Z = 0.50$ cm	r	P	U	V	$\rho$	e	a
(1)	0.0	1.0869	0.0	0.3800	4.2103	0.0722	1.0038
	0.2500	0.9285	0.0338	0.3758	4.0475	0.0625	0.9651
	0.5000	0.7314	0.0768	0.3523	3.8244	0.0504	0.9106
	0.7500	0.6101	0.1090	0.3385	3.6714	0.0432	0.8723
	1.0000	0.5674	0.1441	0.3850	3.6154	0.0406	0.8577
	1.2500	0.3240	0.2039	0.1874	3.2650	0.0246	0.7595
	1.5000	0.2336	0.1796	0.0690	3.2048	0.0115	0.7206
	1.7500	0.1461	0.0865	0.0345	3.1018	0.0031	0.6713
	2.0000	0.0	0.0	0.0	2.7000	0.0	0.5277
(2)	0.0	1.0869	0.0	0.3800	4.2103	0.0722	1.0038
	0.2500	0.9477	0.0025	0.4235	4.0676	0.0637	0.9700
	0.5000	0.7109	0.0920	0.3266	3.8004	0.0491	0.9045
	0.7500	0.5934	0.0993	0.3379	3.6493	0.0422	0.8666
	1.0000	0.5876	0.1442	0.3938	3.6421	0.0418	0.8647
	1.2500	0.3056	0.2154	0.1785	3.2283	0.0241	0.7501
	1.5000	0.2380	0.1708	0.0771	3.2140	0.0117	0.7232
	1.7500	0.1611	0.1319	0.0292	3.1346	0.0036	0.6820
	2.000	0.0	0.0	0.0	2.7000	0.0	0.5277

Table 8. Flow properties in Interior Region at  
 $t = 1.18 \mu\text{sec}$  after impact of a 2.5-  
 cm-diameter projectile at 0.76 cm/ $\mu\text{sec}$   
 on an aluminum half-space based on (1)  
 Double Interpolation and (2) Orthogonal  
 Polynomial Least Square Surface Fit with  
 Double Interpolation after  $t = 1.1 \mu\text{sec}$  at  $Z = 0.75 \text{ cm}$ .

$Z = 0.75 \text{ cm}$	$r$	$P$	$U$	$V$	$\rho$	$e$	$a$
(1)	0.0	1.0869	0.0	0.3800	4.2103	0.0722	1.0038
	0.2500	1.0006	0.0200	0.3730	4.1231	0.0669	0.9832
	0.5000	0.8307	0.0490	0.3472	3.9397	0.0565	0.9391
	0.7500	0.7051	0.0710	0.3163	3.7917	0.0489	0.9026
	1.0000	0.6166	0.0937	0.3127	3.6908	0.0423	0.8752
	1.2500	0.4242	0.1292	0.1985	3.4661	0.0263	0.8077
	1.5000	0.3014	0.1187	0.1145	3.3803	0.0108	0.7624
	1.7500	0.0	0.0	0.0	2.7000	0.0	0.5277
	2.0000	0.0	0.0	0.0	2.7000	0.0	0.5277
(2)	0.0	1.0869	0.0	0.3800	4.2103	0.0722	1.0038
	0.2500	0.9148	-0.0201	0.4072	4.0334	0.0615	0.9616
	0.5000	0.8167	0.0542	0.3333	3.9244	0.0556	0.9352
	0.7500	0.6996	0.0658	0.3149	3.7846	0.0486	0.9009
	1.0000	0.5993	0.0982	0.3095	3.6667	0.0414	0.8693
	1.2500	0.4229	0.1272	0.1785	3.4620	0.0265	0.8070
	1.5000	0.3248	0.1134	0.1264	3.4247	0.0115	0.7744
	1.7500	0.0	0.0	0.0	2.7000	0.0	0.5277
	2.0000	0.0	0.0	0.0	2.7000	0.0	0.5277

Table 9. Flow properties in Interior Region at  $t = 1.18 \mu\text{sec}$  after impact of a 2.5-cm-diameter projectile at 0.76 cm/ $\mu\text{sec}$  on an aluminum half-space based on (1) Double Interpolation and (2) Orthogonal Polynomial Least Square Surface Fit with Double Interpolation after  $t = 1.1 \mu\text{sec}$  at  $Z = 1.00 \text{ cm}$ .

Z = 1.00 cm	r	P	U	V	$\rho$	e	a
	0.0	1.0869	0.0	0.3800	4.2103	0.0722	1.0038
(1)	0.2500	1.0869	0.0	0.3800	4.2103	0.0722	1.0038
	0.5000	0.9551	0.0239	0.3569	4.0754	0.0642	0.9719
	0.7500	0.8458	0.0404	0.3263	3.9658	0.0562	0.9438
	1.0000	0.7492	0.0545	0.3053	3.8760	0.0477	0.9180
	1.2500	0.5566	0.0703	0.2330	3.6866	0.0306	0.8607
	1.5000	0.0	0.0	0.0	2.7000	0.0	0.5277
	1.7500	0.0	0.0	0.0	2.7000	0.0	0.5277
	2.0000	0.0	0.0	0.0	2.7000	0.0	0.5277
	0.0	1.0869	0.0	0.3800	4.2103	0.0722	1.0038
(2)	0.2500	1.0869	0.0	0.3800	4.2103	0.0722	1.0038
	0.5000	0.9137	0.0337	0.3572	4.0315	0.0616	0.9613
	0.7500	0.8233	0.0460	0.3269	3.9397	0.0549	0.9376
	1.0000	0.7430	0.0646	0.3254	3.8604	0.0465	0.9137
	1.2500	0.5142	0.0880	0.2854	3.6369	0.0275	0.8463
	1.5000	0.0	0.0	0.0	2.7000	0.0	0.5277
	1.7500	0.0	0.0	0.0	2.7000	0.0	0.5277
	2.0000	0.0	0.0	0.0	2.7000	0.0	0.5277

Table 10. Flow properties in Interior Region  
 at  $t = 1.18 \mu\text{sec}$  after impact of  
 a 2.5-cm-diameter projectile at 0.76  
 cm/ $\mu\text{sec}$  on an aluminum half-space  
 based on (1) Double Interpolation and  
 (2) Orthogonal Polynomial Least Square  
 Surface Fit with Double Interpolation  
 after  $t = 1.1 \mu\text{sec}$  at  $Z = 1.25 \text{ cm}$ .

(1)	$Z = 1.25 \text{ cm}$						
	r	P	U	V	$\rho$	e	a
	0.0	1.0869	0.0	0.3800	4.2103	0.0722	1.0038
	0.2500	1.0869	0.0	0.3800	4.2103	0.0722	1.0038
	0.5000	0.0	0.0	0.0	2.7000	0.0	0.5277
	0.7500	0.0	0.0	0.0	2.7000	0.0	0.5277
	1.0000	0.0	0.0	0.0	2.7000	0.0	0.5277
	1.2500	0.0	0.0	0.0	2.7000	0.0	0.5277
	1.5000	0.0	0.0	0.0	2.7000	0.0	0.5277
	1.7500	0.0	0.0	0.0	2.7000	0.0	0.5277
	2.0000	0.0	0.0	0.0	2.7000	0.0	0.5277
(2)	0.0	1.0869	0.0	0.3800	4.2103	0.0722	1.0038
	0.2500	1.0869	0.0	0.3800	4.2103	0.0722	1.0038
	0.5000	0.0	0.0	0.0	2.7000	0.0	0.5277
	0.7500	0.0	0.0	0.0	2.7000	0.0	0.5277
	1.0000	0.0	0.0	0.0	2.7000	0.0	0.5277
	1.2500	0.0	0.0	0.0	2.7000	0.0	0.5277
	1.5000	0.0	0.0	0.0	2.7000	0.0	0.5277
	1.7500	0.0	0.0	0.0	2.7000	0.0	0.5277
	2.0000	0.0	0.0	0.0	2.7000	0.0	0.5277



Table 11. Flow properties in Projectile Shock at  $t = 1.25 \mu\text{sec}$  after impact of a 2.5-cm-diameter projectile 0.76 cm/ $\mu\text{sec}$  on an aluminum half-space based on (1) Double Interpolation and (2) Orthogonal Polynomials Least Square Surface Fit with Double Interpolation after  $t = 1.1 \mu\text{sec}$ .

(1)					(2)				
Z $\rho$	r e	P a	U $\cos \alpha_o$	V $\sin \alpha_o$	Z $\rho$	r e	P a	U $\cos \alpha_o$	V $\sin \alpha_o$
-0.3742	0.0	1.0869	0.0	0.3800	-0.3742	0.0	1.0869	0.0	0.3800
4.2103	0.0722	1.0038	0.0	1.0000	4.2103	0.0722	1.0038	0.0	1.0000
-0.3742	0.2500	1.0869	0.0	0.3800	-0.3742	0.2500	1.0869	0.0	0.3800
4.2103	0.0722	1.0038	0.0	1.0000	4.2103	0.0722	1.0038	0.0	1.0000
-0.3713	0.5018	1.0071	0.0029	0.3993	-0.3684	0.5014	0.9280	0.0019	0.4191
4.1460	0.0650	0.9857	-0.0079	0.9999	4.0789	0.0581	0.9670	-0.0057	1.0000
-0.3468	0.7660	0.8343	0.0217	0.4438	-0.3437	0.7655	0.7182	0.0104	0.4750
3.9954	0.0501	0.9436	-0.0685	0.9973	3.8844	0.0405	0.9123	-0.0366	0.9990
-0.2153	1.0232	0.4007	0.0144	0.5731	-0.2140	1.0213	0.3767	0.0113	0.5816
3.5195	0.0173	0.8060	-0.0775	0.9958	3.4869	0.0157	0.7961	-0.0636	0.9970

Table 12. Flow properties in Target Shock at  $t = 1.25 \mu\text{sec}$  after impact of a 2.5-cm-diameter projectile at 0.76 cm/ $\mu\text{sec}$  or an aluminum half-space based on (1) Double Interpolation and (2) Orthogonal Polynomials Least Square Surface Fit with Double Interpolation after  $t = 1.1 \mu\text{sec}$ .

(1)					(2)				
Z $\rho$	r e	P a	U $\cos \alpha_o$	V $\sin \alpha_o$	Z $\rho$	r e	P a	U $\cos \alpha_o$	V $\sin \alpha_o$
1.3242	0.0	1.0869	0.0	0.3800	1.3242	0.0	1.0869	0.0	0.3800
4.2103	0.0722	1.0038	0.0	1.0000	4.2103	0.0722	1.0038	0.0	1.0000
1.3242	0.2500	1.0869	0.0	0.3800	1.3242	0.2500	1.0869	0.0	0.3800
4.2103	0.0722	1.0038	0.0	1.0000	4.2103	0.0722	1.0038	0.0	1.0000
1.3233	0.5015	1.0568	0.0039	0.3724	1.3232	0.5014	1.0550	0.0034	0.3723
4.1863	0.0695	0.9970	0.0105	0.9999	4.2848	0.0693	0.9966	0.0092	1.0000
1.3110	0.7558	0.9511	0.0066	0.3467	1.3109	0.7558	0.9506	0.0066	0.3465
4.0991	0.0601	0.9726	0.0190	0.9998	4.0986	0.0600	0.9725	0.0190	0.9998
1.2823	1.0325	0.8208	0.0203	0.3122	1.2823	1.0325	0.8240	0.0204	0.3130
3.9830	0.0490	0.9401	0.0650	0.9976	3.9859	0.0492	0.9409	0.0649	0.9976
1.1836	1.3220	0.5493	0.0312	0.2325	1.1840	1.3224	0.5610	0.0332	0.2359
3.7041	0.0276	0.8654	0.1328	0.9901	3.7174	0.0284	0.8645	0.1390	0.9892
0.8044	1.7655	0.1534	0.0550	0.0669	0.8039	1.7655	0.1475	0.0512	0.0664
3.1120	0.0037	0.6759	0.6341	0.7718	3.0997	0.0035	0.6717	0.6098	0.7910
0.6060	1.8958	0.0637	0.0318	0.0248	0.6060	1.8957	0.0621	0.0310	0.0242
2.9000	0.0007	0.6013	0.7876	0.6152	2.8955	0.0007	0.5997	0.7875	0.6152
0.3853	1.9721	0.0	0.0	0.0	0.3853	1.9722	0.0	0.0	0.0
2.7000	0.0	0.5277	0.9354	0.3522	2.7000	0.0	0.5277	0.9354	0.3524

Table 13. Flow properties in Rarefaction at  $t = 1.25 \mu\text{sec}$  after impact of a 2.5-cm-diameter projectile at  $0.76 \text{ cm}/\mu\text{sec}$  on an aluminum half-space based on (1) Double Interpolation and (2) Orthogonal Polynomials Least Square Surface Fit with Double Interpolation after  $t = 1.1 \mu\text{sec}$ .

(1)				(2)			
Z	r	$\cos \alpha_o$	$\sin \alpha_o$	Z	r	$\cos \alpha_o$	$\sin \alpha_o$
1.3242	0.3263	0.6768	-0.7362	1.3242	0.3263	0.6768	-0.7362
1.2029	0.2280	0.5801	-0.8145	1.2029	0.2280	0.5801	-0.8145
1.0816	0.1517	0.4834	-0.8754	1.0816	0.1517	0.4834	-0.8754
0.9602	0.0929	0.3867	-0.9222	0.9602	0.0929	0.3867	-0.9222
0.8389	0.0493	0.2901	-0.9570	0.8389	0.0493	0.2901	-0.9570
0.7176	0.0190	0.1934	-0.9811	0.7176	0.0190	0.1934	-0.9811
0.5963	0.0012	0.0967	-0.9953	0.5963	0.0012	0.0967	-0.9953
0.4750	-0.0047	0.0000	-1.0000	0.4750	-0.0047	0.0000	-1.0000
0.3537	0.0012	-0.0967	-0.9953	0.3537	0.0012	-0.0967	-0.9953
0.2324	0.0190	-0.1934	-0.9811	0.2324	0.0190	-0.1934	-0.9811
0.1111	0.0493	-0.2901	-0.9570	0.1111	0.0493	-0.2901	-0.9570
-0.0102	0.0929	-0.3867	-0.9222	-0.0102	0.0929	-0.3867	-0.9222
-0.1316	0.1517	-0.4834	-0.8754	-0.1316	0.1517	-0.4834	-0.8754
-0.2529	0.2280	-0.5801	-0.8145	-0.2529	0.2280	-0.5801	-0.8145
-0.3742	0.3263	-0.6768	-0.7362	-0.3742	0.3263	-0.6768	-0.7362

Table 14. Flow properties in Interior Region at  $t = 1.11 \mu\text{sec}$  after impact of a 2.5-cm-diameter projectile at 0.76 cm/ $\mu\text{sec}$  on an aluminum half-space based on (1) Double Interpolation and (2) Orthogonal Polynomials Least Square Surface Fit with Double Interpolation after  $t = 1.1 \mu\text{sec}$  at  $Z = -0.25 \text{ cm}$ .

$Z = -0.25 \text{ cm}$	$r$	$P$	$U$	$V$	$\rho$	$e$	$a$
(1)	0.0	1.0869	0.0	0.3800	4.2103	0.0722	1.0038
	0.2500	1.0869	0.0	0.3800	4.2103	0.0722	1.0038
	0.5000	1.0000	0.0011	0.3947	4.1232	0.0668	0.9832
	0.7500	0.9432	0.0686	0.4380	4.1035	0.0579	0.9715
	1.0000	0.0	0.0	0.0	2.70000	0.0	0.5277
	1.2500	0.0	0.0	0.0	2.7000	0.0	0.5277
	1.5000	0.0	0.0	0.0	2.7000	0.0	0.5277
	1.7500	0.0	0.0	0.0	2.7000	0.0	0.5277
	2.0000	0.0	0.0	0.0	2.7000	0.0	0.5277
(2)	0.0	1.0869	0.0	0.3800	4.2103	0.0722	1.0038
	0.2500	1.0869	0.0	0.3800	4.2103	0.0722	1.0038
	0.5000	0.9865	-0.0923	0.4746	4.1090	0.0660	0.9798
	0.7500	1.6829	0.0102	0.7228	4.7963	0.0979	1.1264
	1.0000	0.0	0.0	0.0	2.7000	0.0	0.5277
	1.2500	0.0	0.0	0.0	2.7000	0.0	0.5277
	1.5000	0.0	0.0	0.0	2.7000	0.0	0.5277
	1.7500	0.0	0.0	0.0	2.7000	0.0	0.5277
	2.0000	0.0	0.0	0.0	2.7000	0.0	0.5277

Table 15. Flow properties in Interior Region at  $t = 1.11 \mu\text{sec}$  after impact of a 2.5-cm-diameter projectile at 0.76 cm/ $\mu\text{sec}$  on an aluminum half-space based on (1) Double Interpolation and (2) Orthogonal Polynomials Least Square Surface Fit with Double Interpolation after  $t = 1.1 \mu\text{sec}$  at  $Z = 0.0 \text{ cm}$ .

$Z = 0.0 \text{ cm}$	$r$	$P$	$U$	$V$	$\rho$	$e$	$a$
(1)	0.0	1.0869	0.0	0.38000	4.2103	0.0722	1.0038
	0.2500	1.0869	0.0	0.3800	4.2103	0.0722	1.0038
	0.5000	0.7294	0.0887	0.4327	3.8222	0.0503	0.9100
	0.7500	0.5505	0.1836	0.5982	3.5915	0.0396	0.8517
	1.0000	0.1969	0.2836	0.7136	3.0808	0.0137	0.6937
	1.2500	0.0	0.6041	0.3687	2.7000	0.0	0.5277
	1.5000	0.0	0.2022	-0.1010	2.7000	0.0	0.5277
	1.7500	0.0	0.1250	-0.1445	2.7000	0.0	0.5277
	2.0000	0.0	0.0672	0.0310	2.7000	0.0	0.5277
(2)	0.0	1.0869	0.0	0.3800	4.2103	0.0722	1.0038
	0.2500	1.0869	0.0	0.3800	4.2103	0.0722	1.0038
	0.5000	0.6684	0.0649	0.4247	3.7487	0.0464	0.8914
	0.7500	0.5433	0.2089	0.5837	3.5837	0.0390	0.8493
	1.0000	0.1233	0.2851	0.6878	2.9268	0.0100	0.6429
	1.2500	0.0	0.5798	0.3784	2.7000	0.0	0.5277
	1.5000	0.0	0.2384	-0.1266	2.7000	0.0	0.5277
	1.7500	0.0	0.0790	-0.1272	2.7000	0.0	0.5277
	2.0000	0.0	0.7397	0.1453	2.7000	0.0	0.5277

Table 16. Flow properties in Interior Region at  $t = 1.11 \mu\text{sec}$  after impact of a 2.5-cm-diameter projectile at 0.76 cm/ $\mu\text{sec}$  on an aluminum half space based on (1) Double Interpolation and (2) Orthogonal Polynomials Least Square Surface Fit with Double Interpolation after  $t = 1.1 \mu\text{sec}$  at  $Z = 0.25 \text{ cm}$ .

$Z = 0.25 \text{ cm}$	$r$	$P$	$U$	$V$	$\rho$	$e$	$a$
(1)	0.0	1.0869	0.0	0.3800	4.2103	0.0722	1.0038
	0.2500	0.9839	0.0272	0.3851	4.1059	0.0659	0.9791
	0.5000	0.7084	0.0902	0.3852	3.7971	0.0489	0.9037
	0.7500	0.5403	0.1560	0.4163	3.5790	0.0388	0.8481
	1.0000	0.4323	0.2422	0.5445	3.4320	0.0315	0.8073
	1.2500	0.2618	0.3301	0.2324	3.1521	0.0215	0.7274
	1.5000	0.1760	0.2720	0.0015	3.0472	0.0120	0.6809
	1.7500	0.1315	0.1172	-0.0253	3.0716	0.0025	0.6606
	2.0000	0.0	0.0	0.0	2.7000	0.0	0.5277
(2)	0.0	1.0869	0.0	0.3800	4.2103	0.0722	1.0038
	0.2500	0.9982	0.0263	0.4170	4.1207	0.0668	0.9826
	0.5000	0.6946	0.0922	0.3700	3.7806	0.0480	0.8995
	0.7500	0.5285	0.1555	0.4120	3.5626	0.0381	0.8439
	1.0000	0.4507	0.2414	0.5557	3.4600	0.0325	0.8148
	1.2500	0.2818	0.3320	0.2294	3.1875	0.0226	0.7380
	1.5000	0.1784	0.2771	0.0039	3.0516	0.0122	0.6825
	1.7500	0.1331	0.1192	-0.0361	3.0754	0.0025	0.6618
	2.0000	0.0	0.0	0.0	2.7000	0.0	0.5277

Table 17. Flow properties in Interior Region at  $t = 1.11 \mu\text{sec}$  after impact of a 2.5-cm-diameter projectile at 0.76 cm/ $\mu\text{sec}$  on an aluminum half space based on (1) Double Interpolation and (2) Orthogonal Polynomials Least Square Surface Fit with Double Interpolation after  $t = 1.1 \mu\text{sec}$  at  $Z = 2.50 \text{ cm}$ .

$Z = 0.50 \text{ cm}$	$r$	$P$	$U$	$y$	$\rho$	$e$	$a$
(1)	0.0	1.0869	0.0	0.3800	4.2103	0.0722	1.0038
	0.2500	1.0058	0.0224	0.3776	4.1284	0.0672	0.9845
	0.5000	0.7873	0.0644	0.3560	3.8904	0.0538	0.9270
	0.7500	0.6405	0.1002	0.3370	3.7108	0.0450	0.8823
	1.0000	0.5742	0.1362	0.3663	3.6236	0.0410	0.8600
	1.2500	0.3283	0.1942	0.1842	3.2750	0.0246	0.7618
	1.5000	0.2347	0.1758	0.0773	3.2145	0.0110	0.7219
	1.7500	0.1343	0.0741	0.0354	3.0770	0.0026	0.6626
	2.0000	0.0	0.0	0.0	2.7000	0.0	0.5277
(2)	0.0	1.0869	0.0	0.3800	4.2103	0.0722	1.0038
	0.2500	1.0122	0.0136	0.3928	4.1350	0.0676	0.9860
	0.5000	0.7791	0.0687	0.3477	3.8810	0.0533	0.9246
	0.7500	0.6353	0.0971	0.3368	3.7042	0.0447	0.8806
	1.0000	0.5763	0.1374	0.3665	3.6261	0.0412	0.8607
	1.2500	0.3191	0.1977	0.1809	3.2574	0.0243	0.7572
	1.5000	0.2371	0.1742	0.0802	3.2194	0.0111	0.7233
	1.7500	0.1428	0.0846	0.0336	3.0931	0.0028	0.6679
	2.0000	0.0	0.0	0.0	2.7000	0.0	0.5277

Table 18. Flow properties in Interior Region at  $t = 1.1 \mu\text{sec}$  after impact of a 2.5-cm-diameter projectile at 0.76 cm/ $\mu\text{sec}$  on an aluminum half space based on (1) Double Interpolation and (2) Orthogonal Polynomials Least Square Surface Fit with Double Interpolation after  $t = 1.1 \mu\text{sec}$  at  $Z = 0.75 \text{ cm}$ .

$Z = 0.75 \text{ cm}$	$r$	$P$	$U$	$V$	$\rho$	$e$	$a$
(1)	0.0	1.0869	0.0	0.3800	4.2103	0.0722	1.0038
	0.2500	1.0575	0.0069	0.3782	4.1810	0.0704	0.9969
	0.5000	0.8898	0.0374	0.3551	4.0054	0.0601	0.9550
	0.7500	0.7535	0.0622	0.3208	3.8501	0.0518	0.9171
	1.0000	0.6515	0.0859	0.3099	3.7372	0.0442	0.8867
	1.2500	0.4555	0.1199	0.2073	3.5178	0.0276	0.8208
	1.5000	0.3195	0.1068	0.1168	3.4168	0.0112	0.7720
	1.7500	0.0	0.0	0.0	2.7000	0.0	0.5277
	2.0000	0.0	0.0	0.0	2.7000	0.0	0.5277
(2)	0.0	1.0869	0.0	0.3800	4.2103	0.0722	1.0038
	0.2500	0.9930	-0.0229	0.3930	4.1156	0.0664	0.9814
	0.5000	0.8864	0.0404	0.3514	4.1108	0.0599	0.9541
	0.7500	0.7504	0.0603	0.3195	3.8462	0.0517	0.9162
	1.0000	0.6505	0.0868	0.3100	3.7355	0.0442	0.8864
	1.2500	0.4552	0.1210	0.2011	3.5168	0.0277	0.8263
	1.5000	0.3313	0.1054	0.1197	3.4382	0.0116	0.7778
	1.7500	0.0	0.0	0.0	2.7000	0.0	0.5277
	2.0000	0.0	0.0	0.0	2.7000	0.0	0.5277



Table 19. Flow properties in Interior Region at  $t = 1.1 \mu\text{sec}$  after impact of a 2.5-cm-diameter projectile at 0.76 cm/ $\mu\text{sec}$  on an aluminum half space based on (1) Double Interpolation and (2) Orthogonal Polynomials Least Square Surface Fit with Double Interpolation after  $t = 1.1 \mu\text{sec}$  at  $Z = 1.00 \text{ cm}$ .

$Z = 1.00 \text{ cm}$	$r$	$P$	$U$	$V$	$\rho$	$e$	$a$
(1)	0.0	1.0869	0.0	0.3800	4.2103	0.0722	1.0038
	0.2500	1.0869	0.0	0.3800	4.2103	0.0722	1.0038
	0.5000	1.0119	0.0131	0.3673	4.1346	0.0676	0.9860
	0.7500	0.8990	0.0297	0.3359	4.0258	0.0593	0.9581
	1.0000	0.7910	0.0414	0.3143	3.9271	0.0499	0.9302
	1.2500	0.6043	0.0512	0.2428	3.7526	0.0330	0.8773
	1.5000	0.0	0.0	0.0	2.7000	0.0	0.5277
	1.7500	0.0	0.0	0.0	2.7000	0.0	0.5277
	2.0000	0.0	0.0	0.0	2.7000	0.0	0.5277
(2)	0.0	1.0369	0.0	0.3800	4.2103	0.0722	1.0038
	0.2500	1.0869	0.0	0.3800	4.2103	0.0722	1.0038
	0.5000	1.0110	0.0122	0.3680	4.1335	0.0676	0.9857
	0.7500	0.8941	0.0332	0.3364	4.0203	0.0590	0.9568
	1.0000	0.7734	0.0489	0.3178	3.9067	0.0488	0.9252
	1.2500	0.6046	0.0551	0.2587	3.7552	0.0328	0.8776
	1.5000	0.0	0.0	0.0	2.7000	0.0	0.5277
	1.7500	0.0	0.0	0.0	2.7000	0.0	0.5277
	2.0000	0.0	0.0	0.0	2.7000	0.0	0.5277

	COMMON CASEID(14),ITS1,ITS2,ITS3,ITS4,ITI1,ITI2,ITI3,ITI4,EPS1,EPS	1
	12, EPS3, EPS4, EPS5, EPS6, EPI1, EPI2, EPI3, EPI4, EPI5, EPI6, EPI7, VP, AR, LEN	2
	1GTH, APR, BPR, BIGAPR, BIGBPR, ESTAR, ALPHA, BETA, RHOSTR, EPRS, RHOS	3
	COMMON XMESH(20,20,6),XMESH2(20,20,6),Z(20),R(20),SURF(15,8),SURF2	4
	1(15,8),TAB(15,14,2),TAB2(15,14,2),SPART(15,2,2),RARF(15,11),RARF2(	5
	115,4),RPART(15,2)	6
C		7
C		8
	COMMON ZO,RO,PO,UO,VO,LO,MO,RHOO,EQ,AO,UBARO,VBARO	9
C		10
	COMMON NP,NT,NR,NI,NDEL,ISUB	11
C		12
	COMMON ZMIN,ZMAX,RMIN,RMAX,RADIUS,GZ,GR,DELTA,H	13
	COMMON DIRCOS	14
	COMMON TIME	15
	COMMON IRARF	16
	COMMON KSTOP	17
	COMMON TPSI	18
	COMMON KKK	19
C		20
C		21
	REAL LO,MO,LENGTH,MU,KO	22
	DOUBLE PRECISION PHI(20,20,6)	
	KR=7	
	EPS=.0000001	24
	KSTOP=0	25
1	FORMAT (1H1)	26
	CALL DVCHK(KEY)	27
	KICK=0	28
	IF (KEY.EQ.1) GO TO 9980	29
C		30
	DO 2 K=1,6	31
	DO 2 J=1,20	32
	DO 2 I=1,20	33
	XMESH(I,J,K)=0.	34
	XMESH2(I,J,K)=0.	35

2	CONTINUE	36
C	KRW=0	37
	NUZON=0	38
C		39
C		40
	WRITE (3,4)	41
C		42
C	DATA INPUT SECTION	43
C		44
4	FORMAT (52H1HYPERVELOCITY IMPACT METHOD OF CHARACTERISTICS CODE///	45
	1)	46
C	ID AND FX. PT. CONSTANTS	47
C		48
	READ (1,8) CASEID,ITS1,ITS2,ITS3,ITS4,ITI1,ITI2,ITI3,ITI4,NDEL	49
8	FORMAT (13A6,A2/9I3)	50
	IRARF=ITI2	51
C		52
C	FL. PT. CONSTANTS	53
C		54
	READ (1,15) EPS1,EPS2,EPS3,EPS4,EPS5,EPS6,EPI1,EPI2,EPI3,EPI4,EPI5	55
	1,EPI6,EPI7	56
	READ (1,14) NP,NT,NR	57
14	FORMAT (3I3)	58
	READ (1,15) APR,BPR,BIGAPR,BIGBPR,ESTAR,ALPHA,BETA,RHOSTR,EPRS,REF	59
	1L	60
	READ (1,15) ZMIN,ZMAX,RMIN,RMAX,GR,GZ,DELTA,VP,LENGTH,RADIUS,HSTAR	61
15	FORMAT (6E12.8)	62
	READ (1,15) RST	63
	IF (RST.GT.0.) GO TO 16	64
	REWIND 5	
C	DO 1529 JTP=1,200	66
	READ (5)TIME	67
C	IF (ABS(RST+TIME).LT..001) GO TO 1530	68
C	READ(5)BLOB	
C1529	CONTINUE	70
1530	CONTINUE	71

C	KRW=1	72
	READ (5)((X(MESH(I,J,K),I=1,20),J=1,20),K=1,6),(Z(I),I=1,20),(R(I	73
	1,I=1,20),(SURF(I,J),I=1,15),J=1,8),((TAB(I,J,K),I=1,15),J=1,14),	74
	1K=1,2),(RARF(I,J),I=1,15),J=1,11),TIME,ZMIN,ZMAX,RMIN,RMAX,GR,GZ,	75
	1AR	76
	DO 1500 J=1,20	77
	DO 1500 I=1,20	78
	DO 1500 K=1,6	79
1500	XMESH2(I,J,K)=XMESH(I,J,K)	80
	DO 1501 I=1,15	81
	DO 1501 J=1,8	82
1501	SURF2(I,J)=SURF(I,J)	83
	WRITE (3,145) TIME	84
	CALL SOUT	85
	CALL PRINT(XMESH2,Z,R,1)	86
	KREFL=0	87
16	CONTINUE	88
	WRITE (3,10) CASEID,ITS1,ITS2,ITS3,ITS4,ITI1,ITI2,ITI3,ITI4,NDEL	89
10	FORMAT (1X13A6,A2//17H SHOCK ITERATIONS6X,4I4//20H INTERIOR ITERAT	90
	1IONS3X,4I4//7H NDEL =,I4//)	91
	WRITE (3,18) EPS1,EPS2,EPS3,EPS4,EPS5,EPS6,EPI1,EPI2,EPI3,EPI4,EPI	92
	15,EPI6,EPI7,ZMIN,ZMAX,RMIN,RMAX,DELTA,VP,LENGTH,RADIUS,APR,BPR,BIG	93
	1APR,BIGBPR,ESTAR,ALPHA,BETA,RHOSTR,EPRS,REFL	94
18	FORMAT (///38H ERROR CRITERIA FOR SHOCK COMPUTATIONS//5X8HDELTA Z1	95
	18X8HDELTA R18X9HDELTA RHO7X7HDELTA E9X7HDELTA P9X7HDELTA U/6E16.6/	96
	1//41H ERROR CRITERIA FOR INTERIOR COMPUTATIONS//5X8HDELTA ZI8X8HDE	97
	1LTA RI8X7HDELTA P9X7HDELTA U9X7HDELTA V9X9HDELTA RHO7X7HDELTA E/7E	98
	116.6///5X4HZMIN12X4HZMAX12X4HRMIN12X4HRMAX12X5HDELTA11X2HVP14X6HLE	99
	1NGTH10X6HRADIUS/8E16.6///5X2HA'14X2HB'14X6HBIG A'10X6HBIG B'10X2HE	100
	1*14X5HALPHA11X4HBETA12X4HRHO*/8E16.6//5X3HE'S13X4HREFL/2E16.6///)	101
	IF (RST.LT.0.) GO TO 140	102
C		103
C	STORE RHO* IN ALL XMESH	104
C		105
	DO 22 J=1,20	106
	DO 22 I=1,20	107

22	XMESH(I,J,4)=RHOSTR	108
40	FORMAT (5E12.8)	109
C		110
C	PROJECTILE SHOCK	111
C		112
	CALL EQOS1(PRHO,PPP,PVV,PEE,TEE,TRHO,KICK)	113
	IF (KICK.EQ.2200) GO TO 9980	114
	DO 230 N=1,NP	115
	TAB(N,1,1)=(PRHO*PVV-RHOSTR*VP)*HSTAR/(PRHO-RHOSTR)	116
	EE=N-1	117
	FNP=NP	118
	TAB(N,2,1)=RMIN+EE*(RADIUS-RMIN)/FNP	119
	TAB(N,3,1)=PPP	120
	TAB(N,4,1)=0.0	121
	TAB(N,5,1)=PVV	122
	TAB(N,6,1)=PRHO	123
	TAB(N,7,1)=PEE	124
	TAB(N,9,1)=0.0	125
	TAB(N,10,1)=1.0	126
230	CONTINUE	127
C		128
C	TARGET SHOCK	129
C		130
	M=0	131
	DO 240 N=1,NT	132
	EE=N-1	133
	FNT=NT-4	134
	TAB(N,2,2)=RMIN+EE*(RADIUS-RMIN)/FNT	135
	TAB(N,7,2)=TEE	136
	TAB(N,6,2)=TRHO	137
	TAB(N,3,2)=PPP	138
	IF (TAB(N,2,2).GT.RADIUS) GO TO 250	139
	TAB(N,1,2)=TRHO*PVV*HSTAR/(TRHO-RHOSTR)	140
	TAB(N,4,2)=0.0	141
	TAB(N,5,2)=PVV	142
	TAB(N,9,2)=0.0	143

	TAB(N,10,2)=1.0	144
	GO TO 240	145
250	EF=M	146
	TAB(N,9,2)=SIN(.5236+EF*.2618)	147
	TAB(N,10,2)=COS(.5236+EF*.2618)	148
	TAB(N,4,2)=PVV*TAB(N,9,2)	149
	TAB(N,5,2)=PVV*TAB(N,10,2)	150
	TAB(N,1,2)=TAB(1,1,2)*TAB(N,10,2)	151
	TAB(N,2,2)=RADIUS+TAB(1,1,2)*TAB(N,9,2)	152
	M=M+1	153
240	CONTINUE	154
C		155
C	RAREFACTION	156
C		157
	CALL EQOS2(PPP,PRHO,PEE)	158
	EE=NR-1	159
	ADEL=(TAB(1,1,2)-TAB(1,1,1))/EE	160
	RARF(1,1)=TAB(1,1,2)	161
	DO 205 N=2,NR	162
	RARF(N,1)=RARF(N-1,1)-ADEL	163
205	CONTINUE	164
	DO 210 N=1,NR	165
	RARF(N,10)=(RARF(N,1)/HSTAR-.5*VP)/AR	166
	RARF(N,9)=-SQRT(1.-RARF(N,10)**2)	167
	RARF(N,2)=RADIUS+HSTAR*AR*RARF(N,9)	168
210	CONTINUE	169
	DO 220 N=1,NR	170
	RARF(N,3)=TAB(1,3,1)	171
	RARF(N,4)=0.	172
	RARF(N,5)=TAB(1,5,1)	173
	RARF(N,6)=TAB(1,6,1)	174
	RARF(N,7)=TAB(1,7,1)	175
220	CONTINUE	176
C	REGION INTERIOR TO SHOCKS	177
	I=-ZMIN/GZ+1.2	178
	J=0	179

260	J=J+1	180
	XMESH(I,J,1)=PPP	181
	XMESH(I,J,3)=PVV	182
	XMESH(I,J,4)=PRHO	183
	XMESH(I,J,5)=PEE	184
	EE=(J-1)	185
	IF ((EE*GR-RADIUS).LT.-EPS) GO TO 260	186
	XMESH(I,J,1)=0.	187
	XMESH(I,J,4)=RHOSTR	188
	XMESH(I,J,5)=0.	189
C		190
C	FREE SURFACE	191
C		192
	DO 50 I=1,NP	193
	SURF(I,1)=-LENGTH+VP*HSTAR	194
	SURF(I,2)=TAB(I,2,1)	195
	SURF(I,3)=0.	196
	SURF(I,4)=0.	197
	SURF(I,5)=VP	198
	SURF(I,6)=RHOSTR	199
	SURF(I,7)=0.	200
	SURF(I,8)=SQRT(BIGAPR/RHOSTR)	201
50	CONTINUE	202
	DO 51 I=1,NP	203
	DO 51 J=1,8	204
51	SURF2(I,J)=SURF(I,J)	205
	IF (NUZON.EQ.0) GO TO 5001	206
5000	GR=GR*2.	207
	GZ=GZ*2.	208
	ZMAX=ZMAX*2.-ZMIN	209
	RMAX=RMAX*2.	210
	NUZON=1	211
	WRITE (3,5003)	212
5003	FORMAT (7H REZONE///)	213
5001	CONTINUE	214
C		215

C	DO 55 I=1,20	216
	EE=I-1	217
	Z(I)=ZMIN+EE*GZ	218
	R(I)=RMIN+EE*GR	219
55	CONTINUE	220
	IF (NUZON.EQ.0) GO TO 5101	221
	DO 5100 I=1,10	222
	DO 5100 J=1,10	223
	DO 5100 K=1,6	224
	L=2*I-1	225
	M=2*J-1	226
	XMESH(I,J,K)=XMESH(L,M,K)	227
5100	CONTINUE	228
	GO TO 157	229
5101	CONTINUE	230
C		231
C	COMPUTE A FOR 2 SHOCKS AND MESH	232
C		233
	DO 86 K=1,3	234
	GO TO (57,59,61),K	235
57	NN=NP	236
	JJ=1	237
	GO TO 63	238
59	NN=NT	239
	JJ=1	240
	GO TO 63	241
61	NN=20	242
	JJ=20	243
63	DO 84 N=1,NN	244
	DO 82 J=1,JJ	245
	GO TO (65,65,68),K	246
65	P=TAB(N,3,K)	247
	RHO=TAB(N,6,K)	248
	E=TAB(N,7,K)	249
	GO TO 70	250
		251



68	P=XMESH(J,N,1)	252
	RHO=XMESH(J,N,4)	253
	E=XMESH(J,N,5)	254
70	CONTINUE	255
	CALL EQOS3(RHO,AA,E,P)	256
	GO TO (76,76,78),K	257
76	TAB(N,8,K)=AA	258
	GO TO 82	259
78	XMESH(J,N,6)=AA	260
82	CONTINUE	261
84	CONTINUE	262
86	CONTINUE	263
	KICK=86	264
	CALL DVCHK(KQ)	265
	IF (KQ.EQ.1) GO TO 9980	266
C		267
C	STORE A FOR RAREFACTION	268
C		269
	DO 90 I=1,NR	270
90	RARF(I,8)=AR	271
C		272
C	COMPLETE SHOCK TABLES	273
C		274
	DO 99 K=1,2	275
	GO TO (92,94),K	276
92	NN=NP	277
	GO TO 95	278
94	NN=NT	279
	US=0.	280
95	DO 97 N=1,NN	281
	GO TO (93,96),K	282
93	CONTINUE	283
	US=VP*TAB(N,10,1)	284
96	CONTINUE	285
	TAB(N,11,K)=TAB(N,9,K)*TAB(N,4,K)+TAB(N,10,K)*TAB(N,5,K)	286
	TAB(N,12,K)=TAB(N,9,K)*TAB(N,5,K)-TAB(N,10,K)*TAB(N,4,K)	287

	TAB(N,13,K)=((TAB(N,6,K)*ABS(TAB(N,11,K)))/(TAB(N,6,K)-RHOSTR)-US)	288
	1*(-1.)**K	289
	TAB(N,14,K)=1.	290
97	CONTINUE	291
99	CONTINUE	292
C		293
C		294
C	STORE ALL XMESH IN XMESH2	295
C		296
130	DO 135 K=1,6	297
	DO 135 J=1,20	298
	DO 135 I=1,20	299
	XMESH2(I,J,K)=XMESH(I,J,K)	300
135	CONTINUE	301
	TIME=HSTAR	302
	WRITE (3,145) TIME	303
	CALL SOUT	304
C	CALL PRINT(XMESH2,Z,R,1)	
	CALL PRINT(XMESH2,Z,R,1,PHI,NMAX,MMAX)	
C		306
	KREFL=0	307
139	IF (KREFL.NE.0) GO TO 143	308
C	ENTRY FOR TIME STEP	309
C		310
140	READ (1,142) H	311
142	FORMAT (E12.8)	312
143	CONTINUE	313
	TIME=TIME+H	314
	WRITE (3,145) TIME	315
145	FORMAT (1H1///6H TIME=,E15.8///)	316
	WRITE (3,999) KR	317
999	FORMAT (5X,4H KR=,I5)	318
C		319
C		320
C	ADVANCE SHOCK POINTS	321
C		322

	DO 159 N=1,NP	323
	IF (TAB(N,14,1).LT.0.) GO TO 156	324
	IF ((TAB(N,1,1)-SURF(N,1)).GT.EPS) GO TO 154	325
156	TAB2(N,1,1)=TAB(N,1,1)	326
	TAB2(N,2,1)=TAB(N,2,1)	327
	TAB(N,14,1)=-1.	328
	GO TO 159	329
154	TAB2(N,1,1)=TAB(N,1,1)+TAB(N,13,1)*H*TAB(N,10,1)-VP*TAB(N,9,1)*TAB	330
	1(N,10,1)*H	331
150	TAB2(N,2,1)=TAB(N,2,1)+TAB(N,13,1)*H*TAB(N,9,1)-VP*TAB(N,9,1)**2*H	332
159	CONTINUE	333
	DO 155 N=1,NT	334
	TAB2(N,1,2)=TAB(N,1,2)+TAB(N,13,2)*H*TAB(N,10,2)	335
155	TAB2(N,2,2)=TAB(N,2,2)+TAB(N,13,2)*H*TAB(N,9,2)	336
	DO 158 M=1,NT	337
	IF (TAB2(M,1,2).GT.ZMAX) GO TO 5000	338
	IF (TAB2(M,2,2).GT.RMAX) GO TO 5000	339
158	CONTINUE	340
157	NUZON=0	341
C	ADVANCE RAREFACTION	342
C		343
	IF (RARF(1,2).LT.0.)IRARF=1	344
	IF (IRARF.EQ.1) GO TO 516	345
	ENR=NR-1	346
	ADEL=(TAB2(1,1,2)-TAB2(1,1,1))/ENR	347
	RARF2(1,1)=TAB2(1,1,2)	348
	DO 510 N=2,NR	349
	RARF2(N,1)=RARF2(N-1,1)-ADEL	350
510	CONTINUE	351
	DO 515 N=1,NR	352
	RARF2(N,3)=(RARF2(N,1)/TIME-.5*VP)/AR	353
	RARF2(N,4)=-SQRT(1.-RARF2(N,3)**2)	354
	RARF2(N,2)=RADIUS+TIME*AR*RARF2(N,4)	355
515	CONTINUE	356
516	CONTINUE	357
	CALL SHOCK	358

C		359
C		360
	IF (ITS3.EQ.1) GO TO 569	361
C	SHOCK COMPUTATIONS COMPLETED	362
C	COMPUTE PARTICLE CURVES	363
C		364
	TMP=.5*VP*H	365
	DO 520 N=1,NP	366
	SPART(N,1,1)=TAB(N,1,1)+TAB(N,5,1)*H	367
520	SPART(N,2,1)=TAB(N,2,1)+TAB(N,4,1)*H	368
	DO 525 N=1,NT	369
	SPART(N,1,2)=TAB(N,1,2)+TAB(N,5,2)*H	370
525	SPART(N,2,2)=TAB(N,2,2)+TAB(N,4,2)*H	371
	IF (IRARF.EQ.1) GO TO 531	372
	DO 530 N=1,NR	373
	RPART(N,1)=RARF(N,1)+TMP	374
530	RPART(N,2)=RARF(N,2)	375
531	CONTINUE	376
C		377
C		378
568	CALL SOUT2	379
569	CONTINUE	380
C	ADVANCE PROJECTILE REAR SURFACE	381
	DO 5300 I=1,NP	382
	DO 5300 J=1,8	383
5300	SURF2(I,J)=SURF(I,J)	384
	KICK=568	385
	CALL DVCHK(KQ)	386
	IF (KQ.EQ.1) GO TO 9980	387
C		388
C	START INTERIOR REGION COMPUTATIONS	389
C		390
C	CALL INTER	
	CALL INTER(PHI,NMAX,MMAX)	
C		392
C	INTERIOR REGION COMPUTATIONS COMPLETED	393

C		394
C	CALL PRINT(XMESH2,Z,R,2)	
	CALL PRINT(XMESH2,Z,R,2,PHI,NMAX,MMAX)	
570	CONTINUE	396
C		397
C	INITIALIZE FOR NEXT TIME STEP	398
C		399
	DO 920 K=1,6	400
	DO 920 J=1,20	401
	DO 920 I=1,20	402
	XMESH(I,J,K)=XMESH2(I,J,K)	403
920	CONTINUE	404
	DO 930 J=1,13	405
	DO 930 I=1,NP	406
	TAB(I,J,1)=TAB2(I,J,1)	407
930	CONTINUE	408
	DO 940 J=1,13	409
	DO 940 I=1,NT	410
	TAB(I,J,2)=TAB2(I,J,2)	411
940	CONTINUE	412
	IF (IRARF.EQ.1) GO TO 951	413
	DO 950 I=1,NR	414
	RARF(I,1)=RARF2(I,1)	415
	RARF(I,2)=RARF2(I,2)	416
950	CONTINUE	417
951	CONTINUE	418
	DO 960 I=1,NP	419
	DO 959 J=1,5	420
	SURF(I,J)=SURF2(I,J)	421
959	CONTINUE	422
960	CONTINUE	423
777	IF (KREFL.EQ.0) GO TO 980	442
	KREFL=0	443
	H=H1	444
	GO TO 143	445
980	CONTINUE	446

	CALL DVCHK(KICK)	447
	IF (KICK.EQ.2) GO TO 140	448
	WRITE (3,970)	449
970	FORMAT (28HODIVIDE CHECK AT END OF CASE/1H1)	450
	CALL EXIT	451
C		452
C	DIVIDE CHECK	453
C		454
9980	WRITE (3,9985) KICK	455
9985	FORMAT (32HODIVIDE CHECK NEAR STATEMENT NO.,I5/1H1)	456
	RETURN	457
	DEBUG SUBCHK	
	END	458
	SUBROUTINE DBLTRP(ZX,RX,ANS)	1
C		2
C	1ST ORDER DOUBLE INTERPOLATION THAT CONSIDERS	3
C	LINES OF DISCONTINUITY IF IN CONSIDERED REGION	4
C		5
	COMMON CASEID(14),ITS1,ITS2,ITS3,ITS4,ITI1,ITI2,ITI3,ITI4,EPS1,EPS	6
	12,EPS3,EPS4,EPS5,EPS6,EPI1,EPI2,EPI3,EPI4,EPI5,EPI6,EPI7,VP,AR,LEN	7
	1GTH,APR,BPR,BIGAPR,BIGBPR,ESTAR,ALPHA,BETA,RHOSTR,EPRS,RHOS	8
	COMMON XMESH(20,20,6),XMESH2(20,20,6),Z(20),R(20),SURF(15,8),SURF2	9
	1(15,8),TAB(15,14,2),TAB2(15,14,2),SPART(15,2,2),RARF(15,11),RARF2(	10
	115,4),RPART(15,2)	11
C		12
C		13
	COMMON ZO,RO,PO,UO,VO,LO,MO,RHOO,E0,A0,UBARO,VBARO	14
C		15
	COMMON NP,NT,NR,NI,NDEL,ISUB	16
C		17
	COMMON ZMIN,ZMAX,RMIN,RMAX,RADIUS,GZ,GR,DELTA,H	18
	COMMON DIRCOS	19
	COMMON TIME	20
	COMMON IRARF	21
	COMMON KSTOP	22
	COMMON TPSI	23

	COMMON KKK	24
	REAL LO,MO,LENGTH,MU,KO	25
C		26
	DIMENSION ANS(6),ANS1(2,8),ANS2(2,8),ZI(4),RI(4),IK(4)	27
	CALL DVCHK(KEY)	28
	IF (KEY.EQ.2) GO TO 4	29
	NO=0	30
	GO TO 940	31
C		32
C	FIND SUBSCRIPTS FOR GRID	33
C		34
4	I1=(ZX-ZMIN)/GZ+1.000001	35
	I2=I1+1	36
	J1=(RX-RMIN)/GR+1.000001	37
	J2=J1+1	38
	NN=NP	39
	IF (ITS3.EQ.1) GO TO 3	40
	DO 1 K=1,2	41
	IF (K.EQ.2) NN=NT	42
	DO 1 I=1,NN	43
	ALF=SQRT((TAB(I,1,K)-ZX)**2+(TAB(I,2,K)-RX)**2)	44
	IF (ALF.GT.EPS1) GO TO 1	45
	ANS(1)=TAB(I,3,K)	46
	ANS(2)=TAB(I,4,K)	47
	ANS(3)=TAB(I,5,K)	48
	ANS(4)=TAB(I,6,K)	49
	ANS(5)=TAB(I,7,K)	50
	ANS(6)=TAB(I,8,K)	51
	RETURN	52
1	CONTINUE	53
	IF (IRARF.EQ.1) GO TO 3	54
	DO 2 I=1,NR	55
	ALF=SQRT((RARF(I,1)-ZX)**2+(RARF(I,2)-RX)**2)	56
	IF (ALF.GT.EPI1) GO TO 2	57
	ANS(1)=RARF(I,3)	58
	ANS(2)=RARF(I,4)	59

	ANS(3)=RARF(I,5)	60
	ANS(4)=RARF(I,6)	61
	ANS(5)=RARF(I,7)	62
	ANS(6)=RARF(I,8)	63
	RETURN	64
2	CONTINUE	65
3	CONTINUE	66
C		67
C		68
	ZXX=ZX+.01	69
	RXX=RX+.01	70
C		71
C	I LOOP FOR UPPER AND LOWER Z GRID LINES	72
C		73
	DO 800 I=1,2	74
	IF (ITS3.EQ.1) GO TO 14	75
	IF (I.EQ.2) GO TO 8	76
	II=I1	77
	GO TO 12	78
8	II=I2	79
12	M=COMP(ZX,RX,Z(II),R(J1))	80
	IF (M.EQ.1) GO TO 13	81
	MCOM=1	82
	GO TO 20	83
13	M=COMP(ZX,RX,Z(II),R(J2))	84
	IF (M.EQ.1) GO TO 14	85
	MCOM=2	86
	GO TO 20	87
C		88
C	GET 6 VALUES ON GRID LINES	89
C		90
14	DO 15 K=1,6	91
	ANS1(I,K+2)=XMESH(II,J1,K)+(XMESH(II,J2,K)-XMESH(II,J1,K))*(RX-R(J	92
	11))/(R(J2)-R(J1))	93
15	CONTINUE	94
	CALL DVCHK(NO)	95



	IF (NO.EQ.2) GO TO 17	96
	NO=15	97
	GO TO 940	98
17	ANS1(I,1)=Z(II)	99
	ANS1(I,2)=RX	100
	GO TO 800	101
C		102
C		103
20	ZZ=Z(II)	104
	RR=RX	105
	M=COMP(ZX,RX,ZZ,RR)	106
	IF (M.EQ.1) GO TO 300	107
C		108
C		109
	DO 25 K=1,2	110
	KATCH=0	111
	GO TO (21,22),K	112
21	NN=NP	113
	GO TO 23	114
22	NN=NT	115
23	JJJ=NN-1	116
	DO 24 M=1,JJJ	117
	IF (M.EQ.JJJ) GO TO 210	118
	IF (RX.GT.TAB(M+1,2,K).OR.RX.LT.TAB(M,2,K)) GO TO 24	119
210	ZI(K)=TAB(M+1,1,K)+(TAB(M,1,K)-TAB(M+1,1,K))*(RX-TAB(M+1,2,K))/(TA	120
	IB(M,2,K)-TAB(M+1,2,K))	121
	NO=210	122
	CALL DVCHK(KQ)	123
	IF (KQ.EQ.1) GO TO 940	124
	IF (I.EQ.2) GO TO 211	125
	IF (KATCH.EQ.1) GO TO 212	126
	KATCH=1	127
	GO TO 213	128
212	IF ((ZX-ZI(K)).GT.(ZX-ZM)) GO TO 24	129
	IF (ZI(K).GT.ZX) GO TO 24	130
213	ZM=ZI(K)	131

	IF (K.EQ.2) GO TO 215	132
	NPS=M	133
	GO TO 24	134
215	NTS=M	135
	GO TO 24	136
211	CONTINUE	137
	IF (KATCH.EQ.1) GO TO 26	138
	KATCH=1	139
	GO TO 213	140
26	IF ((ZI(K)-ZX).GT.(ZM-ZX)) GO TO 24	141
	IF (ZI(K).LT.ZX) GO TO 24	142
	GO TO 213	143
24	CONTINUE	144
	ZI(K)=ZM	145
	IF (KATCH.NE.0) GO TO 25	146
	ZI(K)=ZMAX+1.	147
25	CONTINUE	148
	IF (IRARF.EQ.1) ZI(3)=ZMAX+1.	149
	IF (IRARF.EQ.1) GO TO 2504	150
	KATCH=0	151
	JJJ=NR-1	152
	DO 27 M=1, JJJ	153
	ZI(3)=RARF(M+1,1)+(RARF(M,1)-RARF(M+1,1))*(RX-RARF(M+1,2))/(RARF(M	154
	1,2)-RARF(M+1,2))	155
	NO=25	156
	CALL DVCHK(KQ)	157
	IF (KQ.EQ.1) GO TO 940	158
	IF (ABS(ZI(3)-ZX).GT.1.E-5) GO TO 279	159
	DO 2799 LN=1,6	160
	LNN=LN+2	161
	ANS(LN)=RARF(1,LNN)	162
2799	CONTINUE	163
	GO TO 820	164
279	CONTINUE	165
	IF (I.EQ.2) GO TO 28	166
	IF (ZI(3).GT.ZX) GO TO 27	167

	IF (KATCH.EQ.1) GO TO 280	168
	KATCH=1	169
	GO TO 281	170
280	IF ((ZX-ZI(3)).GT.(ZX-ZM)) GO TO 27	171
281	ZM=ZI(3)	172
	MR=M	173
	GO TO 27	174
28	IF (ZI(3).LT.ZX) GO TO 27	175
	IF (KATCH.EQ.1) GO TO 282	176
	KATCH=1	177
	GO TO 281	178
282	IF ((ZI(3)-ZX).GT.(ZM-ZX)) GO TO 27	179
	GO TO 281	180
27	CONTINUE	181
	ZI(3)=ZM	182
2504	CONTINUE	183
	KATCH=0	184
	K=4	185
	JJJ=NP-1	186
	DO 2700 M=1,JJJ	187
	IF (M.EQ.JJJ) GO TO 2710	188
	IF (RX.GT.SURF(M+1,2).OR.RX.LT.SURF(M,2)) GO TO 2700	189
2710	ZI(4)=SURF(M+1,1)+(SURF(M,1)-SURF(M+1,1))*(RX-SURF(M+1,2))/(SURF(M	190
	1,2)-SURF(M+1,2))	191
	IF (KQ.EQ.1) GO TO 940	192
	CALL DVCHK(KQ)	193
	NO=2710	194
	IF (I.EQ.2) GO TO 2711	195
	IF (KATCH.EQ.1) GO TO 2712	196
	KATCH=1	197
	GO TO 2713	198
2712	IF ((ZX-ZI(K)).GT.(ZX-ZM)) GO TO 2700	199
2713	ZM=ZI(4)	200
	MS=M	201
	GO TO 2700	202
2711	CONTINUE	203

	IF (KATCH.EQ.1) GO TO 2726	204
	KATCH=1	205
	GO TO 2713	206
2726	IF ((ZI(K)-ZX).GT.(ZM-ZX)) GO TO 2700	207
	GO TO 2713	208
2700	CONTINUE	209
	ZI(4)=ZM	210
	IF (KATCH.NE.0) GO TO 2701	211
	ZI(4)=ZMAX+1.	212
2701	CONTINUE	213
	RI(1)=RX	214
	RI(2)=RX	215
	RI(3)=RX	216
	RI(4)=RX	217
C	FIND INTERSECTION TO USE	218
C		219
30	KEY=0	220
	IF (I.EQ.2) GO TO 50	221
C		222
C	UPPER GRID LINE	223
C		224
	DO 40 KK=1,4	225
	IF (Z(II).GT.ZI(KK)) GO TO 40	226
	IF (ABS(ZI(KK)-ZX).LT.1.E-5) GO TO 35	227
	IF (ZI(KK).GT.ZX) GO TO 40	228
	IF (KEY.EQ.0) GO TO 35	229
	IF (ZI(KK).LE.ZI(KEEP)) GO TO 40	230
	KEEP=KK	231
	GO TO 40	232
35	KEEP=KK	233
	KEY=1	234
40	CONTINUE	235
	GO TO 65	236
C		237
C	LOWER GRID LINE	238
C		239

50	DO 60 KK=1,4	240
	IF (Z(II).LT.ZI(KK)) GO TO 60	241
	IF (ABS(ZI(KK)-ZX).LT.1.E-5) GO TO 55	242
	IF (ZI(KK).LT.ZX) GO TO 60	243
	IF (KEY.EQ.0) GO TO 55	244
	IF (ZI(KK).GE.ZI(KEEP)) GO TO 60	245
	KEEP=KK	246
	GO TO 60	247
55	KEEP=KK	248
	KEY=1	249
60	CONTINUE	250
C		251
65	IF (KEY.NE.0) GO TO 70	252
	WRITE (6,67) ZX,RX,I,(ZI(KEY),KEY=1,4),(RI(KEY),KEY=1,4)	253
67	FORMAT (34HOERROR NEAR STATEMENT 65 IN DBLTRP/1X3HZX=,E15.8,4X3HRX	254
	1=,E15.8,4X2HI=,I3/1X3HZI=,4E20.8/1X3HRI=,4E20.8/1H1)	255
	XYZ=-2.	256
	ZYX=SQRT(XYZ)	257
	CALL EXIT	258
C		259
C	FIND 6 VALUES ON SELECTED DISCONTINUITY	260
C		261
70	IF (KEEP.EQ.3) GO TO 80	262
	IF (KEEP.EQ.4) GO TO 81	263
	IF (KEEP.EQ.2) GO TO 71	264
	N=NPS	265
	GO TO 72	266
71	N=NTS	267
72	CONTINUE	268
	ZY=ZI(KEEP)	269
	RY=RX	270
	DO 75 K=3,8	271
	ANS1(I,K)=TAB(N,K,KEEP)+(TAB(N+1,K,KEEP)-TAB(N,K,KEEP))*SQRT(((RY-	272
	1TAB(N,2,KEEP))*2+(ZY-TAB(N,1,KEEP))*2)/((TAB(N+1,2,KEEP)-TAB(N,2	273
	1,KEEP))*2+(TAB(N+1,1,KEEP)-TAB(N,1,KEEP))*2))	274
	NO=75	275

	CALL DVCHK(KQ)	276
	IF (KQ.EQ.1) GO TO 940	277
75	CONTINUE	278
	GO TO 90	279
80	N=MR	280
	ZY=ZI(3)	281
	RY=RX	282
	DO 85 K=3,8	283
	ANS1(I,K)=RARF(N,K)+(RARF(N+1,K)-RARF(N,K))*SQRT(((RY-RARF(N,2))**	284
	12+(ZY-RARF(N,1))**2)/((RARF(N+1,2)-RARF(N,2))**2+(RARF(N+1,1)-RARF	285
	1(N,1))**2))	286
	NO=85	287
	CALL DVCHK(KQ)	288
	IF (KQ.EQ.1) GO TO 940	289
85	CONTINUE	290
	GO TO 90	291
81	N=MS	292
	ZY=ZI(4)	293
	RY=RX	294
	DO 86 K=3,8	295
	ANS1(I,K)=SURF(N,K)+(SURF(N+1,K)-SURF(N,K))*SQRT(((RY-SURF(N,2))**	296
	12+(ZY-SURF(N,1))**2)/((SURF(N+1,2)-SURF(N,2))**2+(SURF(N+1,1)-SURF	297
	1(N,1))**2))	298
86	CONTINUE	299
90	CALL DVCHK(NO)	300
	IF (NO.EQ.2) GO TO 92	301
	NO=90	302
	GO TO 940	303
92	ANS1(I,1)=ZY	304
	ANS1(I,2)=RY	305
	GO TO 800	306
C		307
C	FIND INTERSECTIONS OF 3 DISCONTINUITIES AND Z GRID LINE	308
C		309
300	CONTINUE	310
	KATCHP=0	311

	KATCHR=0	312
	KATCHT=0	313
	KATCHS=0	314
	DO 310 K=1,2	315
	KATCH=0	316
	GO TO (303,301),K	317
303	NN=NP	318
	GO TO 302	319
301	NN=NT	320
302	JJJ=NN-1	321
	DO 309 M=1,JJJ	322
	IF ((TAB(M,1,K)-TAB(M+1,1,K)).GT.1.E-6) GO TO 3030	323
	GO TO 309	324
3030	RI(K)=TAB(M+1,2,K)+(TAB(M,2,K)-TAB(M+1,2,K))*(Z(II)-TAB(M+1,1,K))/	325
	1(TAB(M,1,K)-TAB(M+1,1,K))	326
	CALL DVCHK(NO)	327
	IF (NO.EQ.2) GO TO 3031	328
	NO=3030	329
	GO TO 940	330
3031	CONTINUE	331
	IF (M.EQ.JJJ) GO TO 3022	332
	IF (RI(K).GT.TAB(M+1,2,K).OR.RI(K).LT.TAB(M,2,K)) GO TO 309	333
3022	IF (MCOM.EQ.2) GO TO 305	334
	IF (KATCH.EQ.1) GO TO 304	335
	KATCH=1	336
	GO TO 3050	337
304	IF ((RX-RI(K)).GT.(RX-RM)) GO TO 309	338
3050	RM=RI(K)	339
	IF (K.EQ.2) GO TO 3040	340
	MPS=M	341
	KATCHP=1	342
	GO TO 309	343
3040	MTS=M	344
	KATCHT=1	345
	GO TO 309	346
305	CONTINUE	347

	IF (KATCH.EQ.1) GO TO 306	348
	KATCH=1	349
	GO TO 3050	350
306	IF ((RI(K)-RX).GT.(RM-RX)) GO TO 309	351
	GO TO 3050	352
309	CONTINUE	353
	RI(K)=RM	354
	IF (KATCH.NE.0) GO TO 310	355
	RI(K)=RMAX+1.	356
310	CONTINUE	357
	K=3	358
	IF (IRARF.EQ.1) RI(3)=RMAX+1.	359
	IF (IRARF.EQ.1) GO TO 315	360
	JJJ=NR-1	361
	KATCH=0	362
	DO 312 M=1, JJJ	363
	RI(3)=RARF(M+1,2)+(RARF(M,2)-RARF(M+1,2))*(Z(II)-RARF(M+1,2))/(RAR	364
	IF(M,1)-RARF(M+1,1))	365
	NO=3122	366
	CALL DVCHK(KQ)	367
	IF (KQ.EQ.1) GO TO 940	368
	IF (M.EQ.JJJ.OR.M.EQ.1) GO TO 3122	369
	IF (RI(K).GT.RARF(M+1,2).OR.RI(K).LT.RARF(M,2)) GO TO 312	370
3122	IF (MCOM.EQ.2) GO TO 316	371
	IF (KATCH.EQ.1) GO TO 317	372
	KATCH=1	373
	GO TO 3051	374
317	IF ((RX-RI(K)).GT.(RX-RM)) GO TO 312	375
3051	RM=RI(K)	376
	MR=M	377
	KATCHR=1	378
	GO TO 312	379
316	CONTINUE	380
	IF (KATCH.EQ.1) GO TO 318	381
	KATCH=1	382
	GO TO 3051	383



318	IF ((RI(K)-RX).GT.(RM-RX)) GO TO 312	384
	GO TO 3051	385
312	CONTINUE	386
	RI(K)=RM	387
	IF (KATCH.NE.0) GO TO 315	388
	RI(K)=RMAX+1.	389
315	CONTINUE	390
	KATCH=0	391
	JJJ=NP-1	392
	DO 3150 M=1,JJJ	393
	IF ((SURF(M,1)-SURF(M+1,1)).GT.1.E-6) GO TO 3130	394
	GO TO 3150	395
3130	RI(4)=SURF(M+1,2)+(SURF(M,2)-SURF(M+1,2))*(Z(11)-SURF(M+1,1))/(SURF(M,1)-SURF(M+1,1))	396
	NO=3130	397
	CALL DVCHK(KQ)	398
	IF (KQ.EQ.1) GO TO 940	399
	IF (M.EQ.JJJ) GO TO 3123	400
	IF (RI(4).GT.SURF(M+1,2).OR.RI(4).LT.SURF(M,2)) GO TO 3150	401
3123	IF (MCOM.EQ.2) GO TO 3105	402
	IF (KATCH.EQ.1) GO TO 3104	403
	KATCH=1	404
	GO TO 3109	405
3104	IF ((RX-RI(4)).GT.(RX-RM)) GO TO 3150	406
3109	RM=RI(4)	407
	MS=M	408
	KATCHS=1	409
	GO TO 3150	410
3105	IF (KATCH.EQ.1) GO TO 3106	411
	KATCH=1	412
	GO TO 3109	413
3106	IF ((RI(4)-RX).GT.(RM-RX)) GO TO 3150	414
	GO TO 3109	415
3150	CONTINUE	416
	RI(4)=RM	417
	IF (KATCH.NE.0) GO TO 3107	418
		419

	RI(4)=RMAX+1.	420
3107	CONTINUE	421
	IF (KATCHP+KATCHT+KATCHR+KATCHS.EQ.0) GO TO 485	422
	ZI(1)=Z(II)	423
	ZI(2)=Z(II)	424
	ZI(3)=Z(II)	425
	ZI(4)=Z(II)	426
C	J LOOP FOR LEFT AND RIGHT R GRID LINES	427
C		428
	DO 700 J=1,2	429
	IF (J.EQ.2) GO TO 350	430
C		431
C	LEFT R GRID LINE	432
C		433
	JJ=J1	434
	KEY=0	435
	DO 340 N=1,4	436
	IF (R(J1).GT.RI(N)) GO TO 340	437
	IF (RI(N).GT.RX) GO TO 340	438
	IF (KEY.EQ.1) GO TO 330	439
	KEY=1	440
	KEEP=N	441
	GO TO 340	442
C		443
C	FIND CLOSEST	444
C		445
330	DIF1=RX-RI(KEEP)	446
	DIF2=RX-RI(N)	447
	IF (DIF1.LE.DIF2) GO TO 340	448
	KEEP=N	449
340	CONTINUE	450
	GO TO 375	451
C		452
C	RIGHT R GRID LINE	453
C		454
350	JJ=J2	455

	KEY=0	456
	DO 360 N=1,4	457
	IF (R(J2).LT.RI(N)) GO TO 360	458
	IF (RI(N).LT.RX) GO TO 360	459
	IF (KEY.EQ.1) GO TO 355	460
	KEY=1	461
	KEEP=N	462
	GO TO 360	463
355	DIF1=RI(KEEP)-RX	464
	DIF2=RI(N)-RX	465
	IF (DIF1.LE.DIF2) GO TO 360	466
	KEEP=N	467
360	CONTINUE	468
375	IF (KEY.EQ.1) GO TO 400	469
C		470
C	NO POINTS BETWEEN RX AND GRID POINTS	471
C		472
	ANS2(J,1)=Z(II)	473
	ANS2(J,2)=R(JJ)	474
	ANS2(J,3)=XMESH(II,JJ,1)	475
	ANS2(J,4)=XMESH(II,JJ,2)	476
	ANS2(J,5)=XMESH(II,JJ,3)	477
	ANS2(J,6)=XMESH(II,JJ,4)	478
	ANS2(J,7)=XMESH(II,JJ,5)	479
	ANS2(J,8)=XMESH(II,JJ,6)	480
	GO TO 700	481
C		482
C	POINT FOUND BETWEEN RX AND GRID POINTS	483
C		484
400	GO TO (405,410,470,481),KEEP	485
C		486
C	INTERSECTION ON PROJECTILE SHOCK	487
C		488
405	N1=MPS	489
	RY=RI(KEEP)	490
	ZY=Z(III)	491

	GO TO 520	492
C		493
C	INTERSECTION ON TARGET SHOCK	494
C		495
410	N1=MTS	496
	RY=RI(KEEP)	497
	ZY=Z(II)	498
	GO TO 520	499
C		500
C	INTERSECTION ON RAREFACTION	501
C		502
470	N1=MR	503
	RY=RI(KEEP)	504
	ZY=Z(II)	505
	GO TO 520	506
C		507
C	INTERSECTION ON FREE SURFACE	508
C		509
481	N1=MS	510
	RY=RI(KEEP)	511
	ZY=Z(II)	512
	GO TO 520	513
C		514
C		515
485	WRITE (3,488) KEEP,II,JJ,ZX,RX	516
488	FORMAT (25HOERROR NEAR STATEMENT 485/1X5HKEEP=,I4,4X3HII=,I4,4X3HJ	517
	1J=,I4/1X3HZX=,E15.8,4X3HRX=,E15.8/1H1)	518
	CALL EXIT	519
C		520
C	FIND TABLE VALUES	521
C		522
520	IF (KEEP.EQ.3) GO TO 580	523
	IF (KEEP.EQ.4) GO TO 591	524
	DO 550 N=3,8	525
	ANS2(J,N)=TAB(N1,N,KEEP)+(TAB(N1+1,N,KEEP)-TAB(N1,N,KEEP))*SQRT(((	526
	1RY-TAB(N1,2,KEEP))*2+(ZY-TAB(N1,1,KEEP))*2)/((TAB(N1+1,2,KEEP)-T	527

	1AB(N1,2,KEEP))**2+(TAB(N1+1,1,KEEP)-TAB(N1,1,KEEP))**2))	528
550	CONTINUE	529
	IF (ZX.LT.0..AND.ABS(RX-RADIUS).LT.1.E-6) GO TO 552	530
	IF (RX.LT.RADIUS.OR.ABS(Z(II)).GT.1.E-6) GO TO 551	531
552	CONTINUE	532
	ANS2(J,3)=0.	533
	ANS2(J,6)=RHOSTR	534
	ANS2(J,7)=0.	535
	ANS2(J,8)=SQRT(BIGAPR/RHOSTR)	536
551	CONTINUE	537
	GO TO 600	538
580	DO 590 N=3,8	539
	ANS2(J,N)=RARF(N1,N)+(RARF(N1+1,N)-RARF(N1,N))*SQRT(((RY-RARF(N1,2	540
	1))**2+(ZY-RARF(N1,1))**2)/(((RARF(N1+1,2)-RARF(N1,2))**2+(RARF(N1+1	541
	1,1)-RARF(N1,1))**2))	542
590	CONTINUE	543
	GO TO 600	544
591	DO 592 N=3,8	545
	ANS2(J,N)=SURF(N1,N)+(SURF(N1+1,N)-SURF(N1,N))*SQRT(((RY-SURF(N1,2	546
	1))**2+(ZY-SURF(N1,1))**2)/(((SURF(N1+1,2)-SURF(N1,2))**2+(SURF(N1+1	547
	1,1)-SURF(N1,1))**2))	548
592	CONTINUE	549
600	CALL DVCHK(NO)	550
	IF (NO.EQ.2) GO TO 605	551
	NO=600	552
	GO TO 940	553
605	ANS2(J,1)=ZY	554
	ANS2(J,2)=RY	555
C		556
C	END OF LOOP FOR BOTH R GRID LINES	557
C		558
700	CONTINUE	559
C		560
C	INTERPOLATE FOR UPPER AND LOWER VALUES	561
C		562
	DO 720 J=3,8	563

	ANS1(I,J)=ANS2(1,J)+(ANS2(2,J)-ANS2(1,J))*(RX-ANS2(1,2))/(ANS2(2,2	564
	1)-ANS2(1,2))	565
720	CONTINUE	566
	CALL DVCHK(NO)	567
	IF (NO.EQ.2) GO TO 730	568
	NO=720	569
	GO TO 940	570
730	ANS1(I,1)=Z(II)	571
	ANS1(I,2)=RX	572
C		573
C	END OF LOOP FOR BOTH Z GRID LINES	574
C		575
800	CONTINUE	576
C		577
C	FIND FINAL VALUES	578
C		579
	DO 810 J=1,6	580
	ANS(J)=ANS1(1,J+2)+(ANS1(2,J+2)-ANS1(1,J+2))*(ZX-ANS1(1,1))/(ANS1(	581
	12,1)-ANS1(1,1))	582
810	CONTINUE	583
	CALL DVCHK(NO)	584
	IF (NO.EQ.2) GO TO 820	585
	NO=810	586
	GO TO 940	587
820	RETURN	588
C		589
940	WRITE (3,942)	590
942	FORMAT (35HODIVIDE CHECK ERROR IN SUBR. DBLTRP)	591
950	WRITE (3,952) NO,ZX,RX,I1,J1,KEEP,ZI,RI	592
952	FORMAT (19H NEAR STATEMENT NO.,I4/1X3HZX=,E15.8,4X3HRX=,E15.8/1X3H	593
	1I1=,I4,4X3HJ1=,I4,4X5HKEEP=,I4/1X3HZI=,4E18.8/1X3HRI=,4E18.8)	594
	WRITE (3,955) ((ANS1(I,J),J=1,8),I=1,2),((ANS2(I,J),J=1,8),I=1,2)	595
955	FORMAT (1X5HANS1=/8E16.8/8E16.8/1X5HANS2=/8E16.8/8E16.8/1H1)	596
	XYZ=-2.	597
	ZYX=SQRT(XYZ)	598
	CALL EXIT	599

	RETURN	600
	DEBUG SUBCHK	
	END	601
	SUBROUTINE SHOCK	1
C	COMPUTES SHOCK VALUES	2
	COMMON CASEID(14),ITS1,ITS2,ITS3,ITS4,ITI1,ITI2,ITI3,ITI4,EPS1,EPS	3
	12,EPS3,EPS4,EPS5,EPS6,EPI1,EPI2,EPI3,EPI4,EPI5,EPI6,EPI7,VP,AR,LEN	4
	1GTH,APR,BPR,BIGAPR,BIGBPR,ESTAR,ALPHA,BETA,RHOSTR,EPRS,RHOS	5
	COMMON XMESH(20,20,6),XMESH2(20,20,6),Z(20),R(20),SURF(15,8),SURF2	6
	1(15,8),TAB(15,14,2),TAB2(15,14,2),SPART(15,2,2),RARF(15,11),RARF2(	7
	115,4),RPART(15,2)	8
C		9
	COMMON ZO,RO,PO,UO,VO,LO,MO,RHOO,E0,A0,UBARO,VBARO	10
C		11
	COMMON NP,NT,NR,NI,NDEL,ISUB	12
C		13
	COMMON ZMIN,ZMAX,RMIN,RMAX,RADIUS,GZ,GR,DELTA,H	14
	COMMON DIRCOS	15
	COMMON TIME	16
	COMMON IRARF	17
	COMMON KSTOP	18
	COMMON TPSI	19
	COMMON KKK	20
C		21
	REAL LO,MO,LENGTH,MU,KO	22
C		23
	DIMENSION ANS(6)	24
	EXTERNAL FGOF1	25
	EPS=.0000001	26
C		27
C	BEGIN SHOCK POINT COMPUTATIONS	28
	DO 505 K=1,2	29
	GO TO (158,160),K	30
158	NN=NP	31
	GO TO 162	32
160	NN=NT	33

	VBARS=0.	34
162	DO 500 I=1,NN	35
	MPROJ=0	36
	IF (TAB(I,14,K).LT.0.) GO TO 500	37
164	CONTINUE	38
C		39
C	INITIALIZE TO ITERATE ON 1 SHOCK POINT	40
C		41
	NBIC=0	42
	ZO=TAB2(I,1,K)	43
	RO=TAB2(I,2,K)	44
	PO=TAB(I,3,K)	45
	UO=TAB(I,4,K)	46
	VO=TAB(I,5,K)	47
	RHOO=TAB(I,6,K)	48
	EO=TAB(I,7,K)	49
	AO=TAB(I,8,K)	50
	LO=TAB(I,9,K)	51
	MO=TAB(I,10,K)	52
	UBARO=TAB(I,11,K)	53
	VBARO=TAB(I,12,K)	54
	UTOH=TAB(I,13,K)	55
	UTO=UTOH	56
	ITS44=ITS4	57
	IF (IRARF.EQ.1) GO TO 170	58
	M=1-(NR-2)*(K-2)	59
	FF=RO-RARF2(M+1,2)-(RARF2(M,2)-RARF2(M+1,2))*(ZO-RARF2(M+1,1))/(RA	60
	IRF2(M,1)-RARF2(M+1,1))	61
169	CONTINUE	62
	IF (FF.LT..001) GO TO 350	63
170	IF (I.NE.1) GO TO 180	64
	MO=TAB(I,10,K)	65
	LO=0.	66
	GO TO 190	67
180	IF (I.LT.NN) GO TO 184	68
	UP=H*(TAB(I-1,13,K)-TAB(I,13,K))	69



	TMP=SQRT((TAB2(I-1,2,K)-R0)**2+(TAB2(I-1,1,K)-Z0)**2)	70
	DOMEG=UP/TMP	71
	GO TO 186	72
184	DR1=TAB2(I+1,2,K)-R0	73
	DR2=R0-TAB2(I-1,2,K)	74
	DZ1=TAB2(I+1,1,K)-Z0	75
	DZ2=Z0-TAB2(I-1,1,K)	76
	UP=H*(TAB(I-1,13,K)-TAB(I+1,13,K))	77
	TMP=SQRT(DR1**2+DZ1**2)+SQRT(DR2**2+DZ2**2)	78
	DOMEG=UP/TMP	79
	KICK=184	80
	CALL DVCHK(KQ)	81
	IF (KQ.EQ.1) GO TO 9980	82
C		83
C	COMPUTE NEW LO,M0	84
C		85
186	COMEG=COS(DOMEG)	86
	SOMEG=SIN(DOMEG)	87
	XLO=LO*COMEG+M0*SOMEG	88
	XMO=M0*COMEG-LO*SOMEG	89
	LO=XLO	90
	M0=XMO	91
	IF (P0.GT..0025) GO TO 190	92
	P0=0.	93
	U0=0.	94
	V0=VP*(1.-(-1.)**K)/2.	95
	RH00=RHOSTR	96
	E0=0.	97
	A0=SQRT(BIGAPR/RHOSTR)	98
	UBAR0=M0*V0	99
	VBAR0=VBARS	100
	UTO=UBAR0+A0*(-1.)**K	101
	GO TO 350	102
190	ITS33=ITS3	103
C		104
C	FIND GUESS TO START ITERATION	105

C		106
195	CALL GUESS(1,KOD2,ZO,RO,I,K,ZZ,RR,DZ,DR)	107
	IF (KOD2.EQ.1) GO TO 200	108
	WRITE (3,198) I,K,ZO,RO	109
	WRITE (3,7002) ZZ,RR,DZ,DR	110
198	FORMAT (31HONO GUESS FOUND FOR SHOCK POINT/3H0I=,I4,6X2HK=,I4,10X3	111
	1HZO=,E15.8,10X3HRO=,E15.8/1H1)	112
	CALL EXIT	113
200	CONTINUE	114
	KY=K	115
	NTW=0	116
	IF (K.EQ.2) GO TO 201	117
	VBAR=VP*LO	118
	DIRCOS=-MO	119
	GO TO 203	120
201	DIRCOS=MO	121
203	CONTINUE	122
	CALL NRIT2(Z1,R1,ZZ,DZ,RR,DR,EPS1,EPS2,FGOF1,ITS1,KODE)	123
	IF (KODE.EQ.0) GO TO 205	124
C		125
C	BICHAIRACTERISTIC SELECTION SCHEME	126
C		127
	IF (NBIC.EQ.0) GO TO 204	128
	IF (NTW.EQ.8)KY=KY+1	129
	IF (NTW.GT.21) GO TO 7000	130
	ANG1=ANG1+DTPSI*(-1.)**KY	131
	DIRCOS=SIN(ANG1)	132
	LO=COB(ANG1)	133
	NTW=NTW+1	134
	GO TO 203	135
204	CONTINUE	136
	NBIC=1	137
	CALL DBLTRP(ZZ,RR,ANS)	138
	UA=ANS(2)	139
	VA=ANS(3)	140
	AA=ANS(6)	141

	ZZZ=ZZ+DZ	142
	CALL DBLTRP(ZZZ,RR,ANS)	143
	UB=ANS(2)	144
	VB=ANS(3)	145
	AB=ANS(6)	146
	RRR=RR+DR	147
	CALL DBLTRP(ZZ,RRR,ANS)	148
	UC=ANS(2)	149
	VC=ANS(3)	150
	AC=ANS(6)	151
	MM=0	152
	TPSI=1.5708*(-1.)**K	153
	XB=ZZ	154
	YB=RR	155
	NOM=5	156
	CA=NOM	157
6201	DTPSI=.01745	158
	DTPSI=CA*DTPSI	159
	TPSI=TPSI+DTPSI*(-1.)**K	160
	A1=1.+H*(VB-VA+(AB-AA)*SIN(TPSI))/DZ	161
	B1=H*(VC-VA+(AC-AA)*SIN(TPSI))/DR	162
	C1=-(ZZ-ZO+H*(VA+AA*SIN(TPSI)))	163
	A2=H*(UB-UA+(AB-AA)*COS(TPSI))/DZ	164
	B2=1.+H*(UC-UA+(AC-AA)*COS(TPSI))/DR	165
	C2=-(RR-RO+H*(UA+AA*COS(TPSI)))	166
	DET=A1*B2-A2*B1	167
	DELX=(B2*C1-B1*C2)/DET	168
	DELY=(A1*C2-A2*C1)/DET	169
C		170
C	TEST FOR SAME REGION	171
C		172
	XB1=XB+DELX	173
	YB1=YB+DELY	174
	M=COMP(XB,YB,XB1,YB1)	175
	IF (M.EQ.1) GO TO 6203	176
	MM=MM+1	177

	IF (MM.LT.360/NOM) GO TO 6201	178
7000	WRITE (3,7001)	179
7001	FORMAT (41HOBICARACTERISTIC SELECTION SCHEME FAILED)	180
	WRITE (3,614) Z0,R0	181
614	FORMAT (1X5HZ0 =,E15.8,4X5HRO =,E15.8)	182
	WRITE (3,7002) UA,VA,AA,UB,VB,AB,UC,VC,AC,ZZ,DZ,RR,DR,ANG1	183
7002	FORMAT (4E16.8)	184
	CALL EXIT	185
6203	CONTINUE	186
	WRITE (3,6210)	187
6210	FORMAT (53HOBICARACTERISTIC SELECTION SCHEME EMPLOYED BY SHOCKX)	188
6204	ANG1=TPSI	189
	T1=DIRCOS	190
	T2=L0	191
	DIRCOS=SIN(ANG1)	192
	L0=COS(ANG1)	193
	GO TO 203	194
205	CONTINUE	195
	UBARS1=0.	196
	IF (K.EQ.1)UBARS1=M0*VP	197
	CALL DBLTRP(Z1,R1,ANS)	198
	P1=ANS(1)	199
	U1=ANS(2)	200
	V1=ANS(3)	201
	RH01=ANS(4)	202
	E1=ANS(5)	203
	A1=ANS(6)	204
206	CONTINUE	205
	KICK=205	206
	CALL DVCHK(KQ)	207
	IF (KQ.EQ.1) GO TO 9980	208
	IF (NBIC.EQ.0) GO TO 207	209
7003	SINTH=ABS(DIRCOS)	210
	COSTH=ABS(L0)	211
	DIRCOS=T1	212
	L0=T2	213

207	CONTINUE	214
	UBAR1=LO*U1+MO*V1	215
	IF (K.EQ.2) GO TO 208	216
	IF (UBAR1.LT.VP/2.) GO TO 208	217
	UBAR1=UBARS1-UBAR1	218
208	CONTINUE	219
218	CONTINUE	220
	M1=PART(1,Z1,R1,ZZ,RR,DELTA,NDEL)	221
	IF (M1.EQ.1) GO TO 210	222
	PUR=0.	223
	PVR=0.	224
	GO TO 215	225
210	CALL DBLTRP(ZZ,RR,ANS)	226
	DP=RR-R1	227
	PUR=(ANS(2)-U1)/DP	228
219	CONTINUE	229
	PVR=(ANS(3)-V1)/DP	230
215	M1=PART(2,Z1,R1,ZZ,RR,DELTA,NDEL)	231
	IF (M1.EQ.1) GO TO 220	232
	PUZ=0.	233
	PVZ=0.	234
	PAZ=0.	235
	GO TO 225	236
220	CALL DBLTRP(ZZ,RR,ANS)	237
	DP=ZZ-Z1	238
	PUZ=(ANS(2)-U1)/DP	239
	PVZ=(ANS(3)-V1)/DP	240
225	CONTINUE	241
	IF (NBIC.EQ.1) GO TO 7004	242
	PURB1=LO*PUR+MO*PVR	243
	PVRB1=LO*PVR-MO*PUR	244
	PVZB1=LO*PVZ-MO*PUZ	245
	PVEB1=-MO*PVRB1+LO*PVZB1	246
	SBAR1=PVEB1	247
226	CONTINUE	248
	IF (ABS(R1).LE.EPS) GO TO 235	249

	SBAR1=SBAR1+U1/R1	250
	GO TO 240	251
7004	CONTINUE	252
	IF (V1.GT.VP/2..AND.K.EQ.1)V1=VP-V1	253
	SBAR1=SINTH**2*PUR-SINTH*COSTH*(PUZ+PVR)+COSTH**2*PVZ	254
	GO TO 226	255
235	SBAR1=SBAR1+PUR	256
C		257
C		258
240	ITS22=ITS2	259
	MMM=0	260
250	CONTINUE	261
	CALL EQOSS(PFR,PFE)	262
	BIG1=RHO1*A1	263
	KICK=250	264
	CALL DVCHK(KQ)	265
	IF (KQ.EQ.1) GO TO 9980	266
	TEMP=1.-RHOSTR/RHOO	267
	TMP=SQRT(PO*TEMP/RHOSTR)	268
	IF (K.EQ.2) GO TO 251	269
	IF (TMP.LT.VP/2.) GO TO 251	270
	MPROJ=1	271
	TMP=UBARS1-TMP	272
251	CONTINUE	273
	TMP6=TMP	274
256	CONTINUE	275
	FNBIC=NBIC	276
	TMP1=P1+BIG1*UBAR1-RHO1*H*SBAR1*A1**2+BIG1*(-UBAR1+COSTH*U1+SINT	277
	1H*V1-SINTH*LO*VBARS+COSTH*MO*VBARS)*(FNBIC)	278
	TMP2=PFR*TEMP+PO*RHOSTR/RHOO**2	279
	TMP5=PFE*TEMP	280
	GTMP=-RHO1*A1	281
	IF (NBIC.EQ.0) GO TO 259	282
	GTMP=GTMP*(COSTH*LO+SINTH*MO)	283
259	CONTINUE	284
	BIGG=PO-(GTMP*TMP+TMP1)	285

	PGR=PFR-((GTMP*TMP2)/(2.*RHOSTR*TMP6))	286
	PGE=PFE-((GTMP*TMP5)/(2.*RHOSTR*TMP6))	287
265	TMP=.5*(1./RHOSTR-1./RH00)	288
	BIGH=E0-TMP*P0	289
	PHR=-TMP*PFR-.5*P0/RH00**2	290
	PHE=1.-TMP*PFE	291
	IF (ABS(BIGH).GT..0001) GO TO 267	292
	BIGH=0.	293
267	IF (ABS(BIGG).GT..0001) GO TO 269	294
	BIGG=0.	295
269	CONTINUE	296
C		297
C	COMPUTE DELTA E0,DELTA RH00	298
C		299
	DOWN=PGE*PHR-PGR*PHE	300
	DE0=(-BIGG*PHR+BIGH*PGR)/DOWN	301
	DRH00=(-BIGH*PGE+BIGG*PHE)/DOWN	302
C		303
	E02=E0+DE0	304
	IF (E02.LT.0.)E02=0.	305
	RH002=RH00+DRH00	306
	IF (RH002.LT.RHOSTR)RH002=RH00	307
	KICK=265	308
	CALL DVCHK(KQ)	309
	IF (KQ.EQ.1) GO TO 9980	310
	CALL EQOSP(RH002,E02,P02)	311
	UBAR02=(1.-RHOSTR/RH002)*(P02/RHOSTR)	312
	IF (UBAR02.GT.0.) GO TO 2669	313
	WRITE (3,2700) P02,RH002,E02,R0,Z0	314
	WRITE (3,7002) P1,U1,V1,RH01,E1,Z1TR1,SBAR1	315
2700	FORMAT (4E16.8)	316
2669	CONTINUE	317
	UBAR02=SQRT(UBAR02)	318
	IF (E02.LT.1.E-5) GO TO 273	319
	IF (ABS((E02-E0)/E02).LT.EPS4) GO TO 273	320
	IF (ABS(DE0).GT..01*EPS4) GO TO 275	321

273	IF (ABS((RHO02-RHO0)/RHO02).LE.EPS3) GO TO 285	322
	IF (ABS(DRHO0).LT.EPS3) GO TO 285	323
275	ITS22=ITS22-1	324
	IF (ITS22.GT.0) GO TO 280	325
	WRITE (3,278) ITS2	326
278	FORMAT (35HOE AND RHO FAILED TO CONVERGE AFTER,I4,6H TRIES)	327
	WRITE (3,279) I,K,ZO,RO,E0,RHO0,P0,E02,RHO02,P02	328
279	FORMAT (1X2HI=,I4,4X2HK=,I4/1X4HZO =,E15.8,4X4HRO =,E15.8,4X4HEO =	329
	1,E15.8,4X6HRHO0 =,E15.8,4X4HPO =,E15.8/1X4HE02=,E15.8,4X6HRHO02=,E	330
	115.8,4X4HP02=,E15.8/1H1)	331
	STOP	332
280	E0=E02	333
	RHO0=RHO02	334
	P0=P02	335
	UBARO=UBAR02	336
	GO TO 250	337
285	E0=E02	338
	RHO0=RHO02	339
	UBARO=UBAR02	340
	A0=SQRT(PFR+P02*PFE/RHO0**2)	341
C		342
C		343
	CALL DVCHK(KQ)	344
	KICK=285	345
	IF (KQ.EQ.1) GO TO 9980	346
	IF (K.EQ.2) GO TO 286	347
	VBARO=VP*LO	348
	GO TO 287	349
286	VBARO=0.	350
287	CONTINUE	351
295	P0=P02	352
	IF (K.EQ.2) GO TO 296	353
	UBARO=UBARS1-UBARO	354
296	CONTINUE	355
	UTO=(RHO0*UBARO-RHOSTR*UBARS1)/(RHO0-RHOSTR)	356
	VO=M0*UBARO+LO*VBARO	357



	UO=LO*UBARO-MO*VBARO	358
	UBAR=.5*(UTOH+UTO)	359
	IF (ABS((UBAR-UTOH)/UBAR).LE.EPS6) GO TO 350	360
	IF (ABS(UBAR-UTOH).LT.EPS6) GO TO 350	361
	ITS44=ITS44-1	362
	IF (ITS44.GT.0) GO TO 325	363
	WRITE (3,297) ITS4,UTOH,UTO	364
297	FORMAT (30HUBAR FAILED TO CONVERGE AFTER,I4,6H TRIES/1X5HUTOH=,E1	365
	15.8,4X4HUTO=,E15.8)	366
	CALL EXIT	367
	WRITE (3,279) I,K,ZO,RO,E0,RH00,P0,E02,RH002,P02	368
C		369
C	INIT. FOR MORE U BAR ITERATIONS	370
C		371
325	UTOH=UBAR	372
	AVMO=(TAB(I,10,K)+MO)*.5	373
	AVLO=(TAB(I,9,K)+LO)*.5	374
	ZO=TAB(I,1,K)+UBAR*H*AVMO-VBARS*AVLO*H	375
	RO=TAB(I,2,K)+UBAR*H*AVLO-VBARS*AVMO*H	376
	LO=AVLO	377
	MO=AVMO	378
	GO TO 195	379
C		380
C	ONE SHOCK POINT HAS CONVERGED	381
C		382
350	TAB2(I,1,K)=ZO	383
	TAB2(I,2,K)=RO	384
	TAB2(I,3,K)=P0	385
	TAB2(I,4,K)=UO	386
	TAB2(I,5,K)=VO	387
	TAB2(I,6,K)=RH00	388
	TAB2(I,7,K)=E0	389
	TAB2(I,8,K)=A0	390
	TAB2(I,9,K)=LO	391
	TAB2(I,10,K)=MO	392
	TAB2(I,11,K)=UBARO	393

	TAB2(I,12,K)=VBARO	394
	TAB2(I,13,K)=UTO	395
	KICK=500	396
	CALL DVCHK(KQ)	397
	IF (KQ.EQ.1) GO TO 9980	398
C		399
C		400
500	CONTINUE	401
505	CONTINUE	402
	RETURN	403
9980	WRITE (3,9985) KICK	404
9985	FORMAT (32HODIVIDE CHECK NEAR STATEMENT NO.,15,15H IN SUBR. SHOCK/	405
	11H1)	406
	CALL EXIT	407
	RETURN	408
	END	409
	SUBROUTINE FGOF1(ZX,RX,SS,QQ)	1
C		2
C	COMPUTES S1,Q1 FOR SHOCK LINE	3
C	ITERATION FOR Z1,R1	4
C		5
	COMMON CASEID(14),ITS1,ITS2,ITS3,ITS4,ITI1,ITI2,ITI3,ITI4,EPS1,EPS	6
	12,EPS3,EPS4,EPS5,EPS6,EPI1,EPI2,EPI3,EPI4,EPI5,EPI6,EPI7,VP,AR,LEN	7
	1GTH,APR,BPR,BIGAPR,BIGBPR,ESTAR,ALPHA,BETA,RHOSTR,EPRS,RHOS	8
	COMMON XMESH(20,20,6),XMESH2(20,20,6),Z(20),R(20),SURF(15,8),SURF2	9
	1(15,8),TAB(15,14,2),TAB2(15,14,2),SPART(15,2,2),RARF(15,11),RARF2(	10
	115,4),RPART(15,2)	11
		12
C		13
C		14
	COMMON ZO,RO,PO,UO,VO,LO,MO,RHOO,EQ,AO,UBARO,VBARO	15
C		16
	COMMON NP,NT,NR,NI,NDEL,ISUB	17
C		18
	COMMON ZMIN,ZMAX,RMIN,RMAX,RADIUS,GZ,GR,DELTA,H	19
	COMMON DIRCOS	20
	COMMON TIME	

	COMMON IRARF	21
	COMMON KSTOP	22
	COMMON TPSI	23
	COMMON KKK	24
	REAL LO,MO,LENGTH,MU,KO	25
C		26
	DIMENSION ANS(6)	27
C		28
	REAL LO,MO	29
	CALL DBLTRP(ZX,RX,ANS)	30
	U1=ANS(2)	31
	V1=ANS(3)	32
	A1=ANS(6)	33
	SS=ZX-ZO+H*(V1+A1*DIRCOS)	34
	QQ=RX-RO+H*(U1+A1*LO)	35
	RETURN	36
	END	37
	SUBROUTINE INTER(PHI,NMAX,MMAX)	
C	SUBROUTINE INTER	
C	COMPUTES INTERIOR REGION POINTS	2
	COMMON CASEID(14),ITS1,ITS2,ITS3,ITS4,ITI1,ITI2,ITI3,ITI4,EPS1,EPS	3
	12,EPS3,EPS4,EPS5,EPS6,EPI1,EPI2,EPI3,EPI4,EPI5,EPI6,EPI7,VP,AR,LEN	4
	1GTH,APR,BPR,BIGAPR,BIGBPR,ESTAR,ALPHA,BETA,RHOSTR,EPRS,RHOS	5
	COMMON XMESH(20,20,6),XMESH2(20,20,6),Z(20),R(20),SURF(15,8),SURF2	6
	1(15,8),TAB(15,14,2),TAB2(15,14,2),SPART(15,2,2),RARF(15,11),RARF2(	7
	115,4),RPART(15,2)	8
C		9
C		10
	COMMON ZO,RO,PO,UO,VO,LO,MO,RHOO,E0,A0,UBARO,VBARO	11
C		12
	COMMON NP,NT,NR,NI,NDEL,ISUB	13
C		14
	COMMON ZMIN,ZMAX,RMIN,RMAX,RADIUS,GZ,GR,DELTA,H	15
	COMMON DIRCOS	16
	COMMON TIME	17
	COMMON IRARF	18

	COMMON KSTOP	19
	COMMON TPSI	20
	COMMON KKK	21
C		22
C		23
	REAL LO,MO,LENGTH,MU,KO	24
	DOUBLE PRECISION PHI(20,20,6)	
	DIMENSION ANS(6),LL(3),ZI(11),RI(11),PI(11),UI(11),VI(11),RHOI(11)	25
	1,EI(11),AI(11),PUR(11),PVR(11),PAR(11),PUZ(11),PVZ(11),PAZ(11),PSI	26
	1(7),SPSI(11),CPSI(11),S(11)	27
C		28
	EXTERNAL FGOF1,FGOF5	29
	INTEGER CHECK,CHECK2	30
C		31
1	FORMAT (1H1)	32
	TSSS=1.1	
	EPS=.0000001	33
	DO 905 J=1,20	34
	DO 900 I=1,20	35
	M=TEST(Z(I),R(J))	36
	ZO=Z(I)	37
	RO=R(J)	38
	KICK=1	39
	CALL DVCHK(KQ)	40
	IF (KQ.EQ.1) GO TO 9980	41
	IF (M.EQ.3.AND.ZO.LT.EPS.AND.ABS(RO-RADIUS).LT.EPS)M=1	42
	IF (M.NE.1) GO TO 900	43
	DO 2 L=1,NP	44
	IF (TAB(L,14,1).LT.0.) GO TO 20	45
2	CONTINUE	46
	IF (IRARF.EQ.1) GO TO 20	47
	DO 3 N=1,NR	48
	IF (R(J).GT.RARF(N,2)) GO TO 5	49
3	CONTINUE	50
	GO TO 6	51
5	CONTINUE	52

	M=PICK(Z(I),R(J),3)	53
	FF=R(J)-RARF(M+1,2)-(RARF(M,2)-RARF(M+1,2))*(Z(I)-RARF(M+1,1))/(RA	54
	IRF(M,1)-RARF(M+1,1))	55
	IF (FF.GT.0.) GO TO 20	56
6	CONTINUE	57
	P02=RARF(1,3)	58
	U02=RARF(1,4)	59
	V02=RARF(1,5)	60
	RHO02=RARF(1,6)	61
	EO2=RARF(1,7)	62
	AO2=RARF(1,8)	63
	GO TO 870	64
20	CONTINUE	65
	CALL GUESS(2,KOD,Z0,R0,I,J,ZZ,RR,DZ,DR)	66
	IF (KOD.EQ.1) GO TO 580	67
	WRITE (3,575) I,J,Z0,R0	68
575	FORMAT (41HONO GUESS FOUND FOR INTERIOR REGION POINT/3H0I=I4,6X2HK	69
	1=,I4,10X3HZ0=,E15.8,10X3HR0=,E15.8/1H1)	70
	CALL EXIT	71
	580 IF(TIME.GT.TSSS) GO TO 150	
	CALL DBLTRP(ZZ,RR,ANS)	
	GO TO 151	
	150 CALL DSURFT(ZZ,RR,ANS,PHI,NMAX,MMAX)	
C		73
C	INITIALIZE FOR 1 POINT	74
C		75
C	PSI(1)=0.	
151	PSI(1)=0.	
	PSI(3)=1.0472	77
	PSI(4)=2.0944	78
	PSI(6)=4.18879	79
	PSI(7)=5.23599	80
	NBIC=0	81
	ITI22=ITI2	82
	P0=ANS(1)	83
	U0=ANS(2)	84

	V0=ANS(3)	85
	RH00=ANS(4)	86
	E0=ANS(5)	87
	A0=ANS(6)	88
	KICK=580	89
	CALL DVCHK(KQ)	90
	IF (KQ.EQ.1) GO TO 9980	91
590	IF (ABS(R0).GT.EPS) GO TO 594	92
	L1=1	93
	LL(1)=4	94
	LL(2)=6	95
	LLL=2	96
	GO TO 620	97
C		98
C		99
594	IF (ABS(R0-RADIUS).GT.EPS) GO TO 600	100
	IF (Z0.GT.EPS) GO TO 610	101
	L1=2	102
	LL(1)=3	103
	LL(2)=7	104
	LLL=2	105
	GO TO 620	106
600	IF (R0.LE.RADIUS.OR.ABS(Z0).GT.EPS) GO TO 610	107
	L1=3	108
	LL(1)=6	109
	LL(2)=7	110
	LLL=2	111
	GO TO 620	112
C		113
C		114
610	L1=4	115
	LL(1)=1	116
	LL(2)=4	117
	LL(3)=6	118
	LLL=3	119
C		120

C	ITERATE FOR I VALUES	121
C		122
619	CONTINUE	123
620	DO 630 KK=1,LLL	124
	LUMP=L1	125
	ISUB=LL(KK)	126
621	CONTINUE	127
	TPSI=PSI(ISUB)	128
	SPSI(ISUB)=SIN(TPSI)	129
	CPSI(ISUB)=COS(TPSI)	130
C	CALL NRIT2(ZI(ISUB),RI(ISUB),ZZ,DZ,RR,DR,EPI1,EPI2,FGOFI,ITI1,KODE	131
C	1)	
	CALL NRIT2(ZI(ISUB),RI(ISUB),ZZ,DZ,RR,DR,EPI1,EPI2,FGOFI,ITI1,KODE	131
	1,PHI,NMAX,MMAX)	
	IF (KODE.NE.0) GO TO 6200	133
625	IF(TIME.GT.TSSS) GO TO 125	
	CALL DBLTRP(ZI(ISUB),RI(ISUB),ANS)	
	GO TO 122	
125	CALL DSURFT(ZI(ISUB),RI(ISUB),ANS,PHI,NMAX,MMAX)	
122	PI(ISUB)=ANS(1)	
C	PI(ISUB)=ANS(1)	
	UI(ISUB)=ANS(2)	136
	VI(ISUB)=ANS(3)	137
	RHOI(ISUB)=ANS(4)	138
	EI(ISUB)=ANS(5)	139
	AI(ISUB)=ANS(6)	140
630	CONTINUE	141
C		142
C		143
	KICK=630	144
	CALL DVCHK(KQ)	145
	IF (KQ.EQ.1) GO TO 9980	146
	GO TO 6400	147
C		148
C	BICHARACTERISTIC SELECTION SCHEME	149
C		150

7000	WRITE (3,7001)	151
7001	FORMAT (41HOBIC CHARACTERISTIC SELECTION SCHEME FAILED)	152
	WRITE (3,614) ZO,R0	153
	WRITE (3,7002) (PSI(MNMN),MNMN=1,7),UA,VA,AA,UB,VB,AB,UC,VC,AC,ZZ,	154
	1DZ,RR,DR,ANG1,ANG2	155
	SUB=ISUB	156
	WRITE (3,7002) SUB,ZI(ISUB),RI(ISUB)	157
7002	FORMAT (4E16.8)	158
	CALL EXIT	159
6200	CONTINUE	160
	IF (NBIC.NE.0) GO TO 7000	161
	IF (L1.NE.2.OR.LL(1).EQ.1) GO TO 7300	162
	LL(1)=1	163
	GO TO 619	164
7300	CONTINUE	165
	IF (L1.NE.3) GO TO 7310	166
	IF (PSI(6).GT.4.2) GO TO 7310	167
	PSI(6)=5.75959	168
	GO TO 619	169
7310	CONTINUE	170
	IF (TIME.GT.TSSS) GO TO 222	
	CALL DBLTRP(ZZ,RR,ANS)	
	GO TO 223	
222	CALL DSURFT(ZZ,RR,ANS,PHI,NMAX,MMAX)	
223	UA=ANS(2)	
C	UA=ANS(2)	
	VA=ANS(3)	173
	AA=ANS(6)	174
	ZZZ=ZZ+DZ	175
	IF (TIME.GT.TSSS) GO TO 128	
	CALL DBLTRP(ZZZ,RR,ANS)	
	GO TO 129	
128	CALL DSURFT(ZZZ,RR,ANS,PHI,NMAX,MMAX)	
129	UB=ANS(2)	
C	UB=ANS(2)	
	VB=ANS(3)	178



	AB=ANS(6)	179
	RRR=RR+DR	180
	IF(TIME.GT.TSSS) GO TO 130	
	CALL DBLTRP(ZZ,RRR,ANS)	
	GO TO 131	
130	CALL DSURFT(ZZ,RRR,ANS,PHI,NMAX,MMAX)	
131	UC=ANS(2)	
C	UC=ANS(2)	
	VC=ANS(3)	183
	AC=ANS(6)	184
	MM=0	185
	TPSI=PSI(ISUB)	186
	XB=ZZ	187
	YB=RR	188
	NOM=5	189
	CA=NOM	190
	DO 6210 LM=1,2	191
6201	DTPSI=.01745	192
	DTPSI=CA*DTPSI	193
	TPSI=TPSI+DTPSI	194
	A1=1.+H*(VB-VA+(AB-AA)*SIN(TPSI))/DZ	195
	B1=H*(VC-VA+(AC-AA)*SIN(TPSI))/DR	196
	C1=-(ZZ-ZO+H*(VA+AA*SIN(TPSI)))	197
	A2=H*(UB-UA+(AB-AA)*COS(TPSI))/DZ	198
	B2=1.+H*(UC-UA+(AC-AA)*COS(TPSI))/DR	199
	C2=-(RR-RO+H*(UA+AA*COS(TPSI)))	200
	DET=A1*B2-A2*B1	201
	DELX=(B2*C1-B1*C2)/DET	202
	DELY=(A1*C2-A2*C1)/DET	203
C		204
C	TEST FOR SAME REGION	205
C		206
	XB1=XB+DELX	207
	YB1=YB+DELY	208
	M=COMP(XB,YB,XB1,YB1)	209
	IF (LM.EQ.2) GO TO 6700	210

	IF (M.EQ.1) GO TO 6203	211
	GO TO 6800	212
6700	CONTINUE	213
	IF (M.NE.1) GO TO 6203	214
6800	CONTINUE	215
	MM=MM+1	216
	IF (MM.LE.360/NOM) GO TO 6201	217
612	WRITE (3,613) ITI1	218
613	FORMAT (4H0FAILED TO FIND 2 POINTS IN THE SAME REGION 21H IN SUBR 1. NRIT2 AFTER,I4,6H TRIES)	219
	WRITE (3,614) Z0,R0	220
614	FORMAT (1X5HZ0 =,E15.8,4X5HRO =,E15.8)	221
	WRITE (3,6144) LM	222
	WRITE (3,6145) M	223
	WRITE (3,6146) KODE	224
	WRITE (3,7002) XB,YB,XB1,YB1	225
6144	FORMAT (4H LM=,I4)	226
6145	FORMAT (3H M=,I4)	227
6146	FORMAT (6H KODE=,I4)	228
	CALL EXIT	229
6203	GO TO (6204,6205),LM	230
6204	ANG1=TPSI	231
	MM=0	232
	GO TO 6210	233
6205	ANG2=TPSI-DTPSI	234
6210	CONTINUE	235
	AL=LLL+1	236
	DO 6300 KK=1,LLL	237
	ISUB=LL(KK)	238
	AK=KK	239
	PSI(ISUB)=ANG1+(ANG2-ANG1)*AK/AL	240
6300	CONTINUE	241
	NBIC=1	242
	GO TO 619	243
C		244
C		245
		246

6400	CONTINUE	247
	IF (L1.EQ.2.OR.L1.EQ.3) GO TO 642	248
C	CALL NRIT2(ZI(8),RI(8),ZZ,DZ,RR,DR,EPI1,EPI2,FGOF5,ITI1,KODE)	249
	CALL NRIT2(ZI(8),RI(8),ZZ,DZ,RR,DR,EPI1,EPI2,FGOF5,ITI1,KODE,	
	1 PHI,NMAX,MMAX)	
	IF (KODE.EQ.0) GO TO 635	250
	ISUB=8	251
	WRITE (3,622) ITI1,I,J,ISUB,ZO,RO,ZZ,RR,ZI(8),RI(8)	252
622	FORMAT (27HOF AILED TO FIND ZI,RI AFTER,I4,6H TRIES,3X2HI=,I4,3X2HJ	253
	1=,I4,3X5HISUB=,I4/1X3HZO=,E15.8,6X3HRO=,E15.8/1X3HZZ=,E15.8,6X3HRR	254
	1=,E15.8/1X3HZI=,E15.8,6X3HRI=,E15.8/1H1)	255
	CALL EXIT	256
C		257
C		258
	635 IF(TIME.GT.TSSS) GO TO 132	
	CALL DBLTRP(ZI(8),RI(8),ANS)	
	GO TO 133	
	132 CALL DSURFT(ZI(8),RI(8),ANS,PHI,NMAX,MMAX)	
	133 PI(8)=ANS(1)	
C	PI(8)=ANS(1)	
	UI(8)=ANS(2)	261
	VI(8)=ANS(3)	262
	RHOI(8)=ANS(4)	263
	EI(8)=ANS(5)	264
	AI(8)=ANS(6)	265
C		266
642	DO 670 IL=1,LLL	267
	NN=LL(IL)	268
	M=PART(1,ZI(NN),RI(NN),ZX,RX,DELTA,NDEL)	269
	IF (M.EQ.1) GO TO 645	270
	PUR(NN)=0.	271
	PVR(NN)=0.	272
	GO TO 648	273
	645 IF(TIME.GT.TSSS) GO TO 134	
	CALL DBLTRP(ZX,RX,ANS)	
	GO TO 135	

134	CALL DSURFT(ZX,RX,ANS,PHI,NMAX,MMAX)	
135	DEN=RX-RI(NN)	
C	DEN=RX-RI(NN)	
	PUR(NN)=(ANS(2)-UI(NN))/DEN	276
	PVR(NN)=(ANS(3)-VI(NN))/DEN	277
648	M=PART(2,ZI(NN),RI(NN),ZX,RX,DELTA,NDEL)	278
	IF (M.EQ.1) GO TO 650	279
	PUZ(NN)=0.	280
	PVZ(NN)=0.	281
	GO TO 655	282
650	IF(TIME.GT.TSSS) GO TO 136	
	CALL DBLTRP(ZX,RX,ANS)	
	GO TO 137	
136	CALL DSURFT(ZX,RX,ANS,PHI,NMAX,MMAX)	
137	DEN=ZX-ZI(NN)	
	PUZ(NN)=(ANS(2)-UI(NN))/DEN	285
	PVZ(NN)=(ANS(3)-VI(NN))/DEN	286
655	S(NN)=SPSI(NN)**2*PUR(NN)-CPSI(NN)*SPSI(NN)*(PVR(NN)+PUZ(NN))+CPSI	287
	1(NN)**2*PVZ(NN)	288
C		289
	IF (ABS(RI(NN)).GT.EPS) GO TO 660	290
	CON=PUR(NN)	291
	GO TO 662	292
660	CON=UI(NN)/RI(NN)	293
662	S(NN)=-RHOI(NN)*H*AI(NN)**2*(S(NN)+CON)+PI(NN)+RHOI(NN)*AI(NN)*CPS	294
	1I(NN)*UI(NN)+RHOI(NN)*AI(NN)*SPSI(NN)*VI(NN)	295
670	CONTINUE	296
1005	CONTINUE	297
1002	FORMAT (4E16.8)	298
	KICK=670	299
	CALL DVCHK(KQ)	300
	IF (KQ.EQ.1) GO TO 9980	301
C		302
C	COMPUTE NEW P,U,V	303
C		304
	GO TO (690,692,695,698),L1	305

690	DU0=0.	306
	U02=0.	307
	$V02=(S(4)-S(6))/(RHOI(4)*AI(4)*SPSI(4)-RHOI(6)*AI(6)*SPSI(6))$	308
	$P02=S(4)-RHOI(4)*AI(4)*SPSI(4)*V02$	309
	GO TO 700	310
C		311
C		312
692	DPO=0.	313
	P02=0.	314
	L=LL(1)	315
	$TMP1=RHOI(7)*RHOI(L)*AI(7)*AI(L)*(CPSI(7)*SPSI(L)-CPSI(L)*SPSI(7))$	316
	$V02=(S(L)*RHOI(7)*AI(7)*CPSI(7)-S(7)*RHOI(L)*AI(L)*CPSI(L))/TMP1$	317
	$U02=(S(L)-RHOI(L)*AI(L)*SPSI(L)*V02)/(RHOI(L)*AI(L)*CPSI(L))$	318
	GO TO 700	319
C		320
C		321
695	DPO=0.	322
	P02=0.	323
	$TMP1=RHOI(7)*RHOI(6)*AI(7)*AI(6)*(CPSI(7)*SPSI(6)-SPSI(7)*CPSI(6))$	324
	$V02=(S(6)*RHOI(7)*AI(7)*CPSI(7)-S(7)*RHOI(6)*AI(6)*CPSI(6))/TMP1$	325
	$U02=(S(6)-RHOI(6)*AI(6)*SPSI(6)*V02)/(RHOI(6)*AI(6)*CPSI(6))$	326
	GO TO 700	327
698	CONTINUE	328
	L=LL(1)	329
	$TMP1=RHOI(4)*AI(4)*CPSI(4)-RHOI(L)*AI(L)*CPSI(L)$	330
	$TMP2=RHOI(4)*AI(4)*SPSI(4)-RHOI(L)*AI(L)*SPSI(L)$	331
	$TMP3=RHOI(6)*AI(6)*CPSI(6)-RHOI(L)*AI(L)*CPSI(L)$	332
	$TMP4=RHOI(6)*AI(6)*SPSI(6)-RHOI(L)*AI(L)*SPSI(L)$	333
	$V02=((S(4)-S(L))*TMP3-(S(6)-S(L))*TMP1)/(TMP3*TMP2-TMP1*TMP4)$	334
	$U02=(S(4)-S(L)-TMP2*V02)/TMP1$	335
	$P02=S(6)-RHOI(6)*AI(6)*CPSI(6)*U02-RHOI(6)*AI(6)*SPSI(6)*V02$	336
700	KICK=700	337
	CALL DVCHK(KQ)	338
	IF (KQ.EQ.1) GO TO 9980	339
C		340
C		341

C	ITERATE FOR RH00,E0	342
C		343
705	ITI33=ITI3	344
	ITI44=ITI4	345
	KM=1	346
708	CONTINUE	347
	CALL EQOSI(P02,PGRHO,PGE,BIGG,CHECK,KRTT,A02,E02,RH002,KM,EPS)	348
	IF (KRTT.EQ.1) GO TO 871	349
725	T1=RH00-RHOI(8)	350
	T2=PI(8)/RHOI(8)**2	351
	BIGH=EI(8)+T2*T1-E0	352
	PHE=-1.	353
	PHRHO=T2	354
	KICK=725	355
	CALL DVCHK(KQ)	356
	IF (KQ.EQ.1) GO TO 9980	357
C		358
C	COMPUTE NEW E0,RH00	359
C		360
	DOWN=PGE*PHRHO-PGRHO*PHE	361
	DE0=(-BIGG*PHRHO+BIGH*PGRHO)/DOWN	362
	DRH00=(-BIGH*PGE+BIGG*PHE)/DOWN	363
	E02=E0+DE0	364
	RH002=RH00+DRH00	365
C		366
C	CHECK E02,RH002 FOR CONVERGENCE	367
	KICK=726	368
	CALL DVCHK(KQ)	369
	IF (KQ.EQ.1) GO TO 9980	370
C		371
	IF (ABS(DE0/E0).LT.EPI7) GO TO 726	372
	IF (ABS(DE0).GT..01*EPI7) GO TO 730	373
726	IF (ABS(DRH00/RH00).LE.EPI6) GO TO 740	374
	IF (ABS(DRH00).LT.EPI6) GO TO 740	375
730	ITI33=ITI33-1	376
	IF (ITI33.NE.0) GO TO 735	377

	WRITE (6,732) ITI3,I,J,ZO,RO,PO,UO,VO,RHOO,E0,P02,U02,V02,RH002,E0	378
	12	379
732	FORMAT (33H0EO,RH00 FAILED TO CONVERGE AFTER,I4,6H TRIES/1X2HI=,I4	380
	1,4X2HJ=,I4,4X2HZ=,E15.8,4X2HR=,E15.8/5X2HP018X2HU018X2HV018X4HRH00	381
	116X2HE0/5X3HP0217X3HU0217X3HV0217X5HRH00215X3HE02//(5E20.8))	382
	WRITE (3,1)	383
	CALL EXIT	384
735	E0=E02	385
	RH00=RH002	386
	KM=0	387
	GO TO 708	388
C		389
C	CHECK FOR PROPER EQUATIONS	390
C		391
740	CONTINUE	392
	PGE=-PGE	393
	PGRHO=-PGRHO	394
	IF (RH002.GE.RH0STR) GO TO 750	395
	IF (E02.LT.EPRS) GO TO 750	396
742	CHECK2=0	397
	GO TO 752	398
750	CHECK2=1	399
752	A02=SQRT(+PGRHO+P02*PGE/RH002**2)	400
	IF (CHECK.EQ.CHECK2) GO TO 870	401
	ITI44=ITI44-1	402
	IF (ITI44.NE.0) GO TO 770	403
	WRITE (3,755) ITI4,I,J,ZO,RO,PO,UO,VO,RHOO,E0,A0,P02,U02,V02,RH002	404
	1,E02,A02	405
755	FORMAT (38H0FAILED TO USE CORRECT EQUATIONS AFTER,I4,6H TRIES/1X2H	406
	1I=,I4,4X2HJ=,I4,4X2HZ=,E15.8,4X2HR=,E15.8/5X2HP018X2HU018X2HV018X4	407
	1HRH0016X2HE018X2HA0/5X3HP0217X3HU0217X3HV0217X5HRH00215X3HE0217X3H	408
	1A02//(6E20.8))	409
	WRITE (3,1)	410
	CALL EXIT	411
770	KICK=770	412
	CALL DVCHK(KQ)	413

	IF (KQ.EQ.1) GO TO 9980	414
	ITI33=ITI3	415
	GO TO 735	416
C		417
C	ALL VALUES HAVE CONVERGED FOR 1 INTERIOR POINT	418
C		419
871	KRTT=0	420
870	XMESH2(I,J,1)=P02	421
	XMESH2(I,J,2)=U02	422
	XMESH2(I,J,3)=V02	423
	XMESH2(I,J,4)=RHO02	424
	XMESH2(I,J,5)=E02	425
	XMESH2(I,J,6)=A02	426
	KICK=900	427
	CALL DVCHK(KQ)	428
	IF (KQ.EQ.1) GO TO 9980	429
900	CONTINUE	430
905	CONTINUE	431
	IF (ITS3.EQ.1) GO TO 950	432
	CALL ITRP	433
	RETURN	434
950	CONTINUE	435
9980	WRITE (3,9985) KICK	436
	WRITE (3,614) Z0,R0	437
9985	FORMAT (32HODIVIDE CHECK NEAR STATEMENT NO.,15,15H IN SUBR. INTER/	438
	11H1)	439
	CALL EXIT	440
	RETURN	441
	DEBUG SUBCHK	
	END	442
	SUBROUTINE EQOS1(PRHO,PPP,PVV,PEE,TEE,TRHO,KICK)	1
	COMMON CASEID(14),ITS1,ITS2,ITS3,ITS4,ITI1,ITI2,ITI3,ITI4,EPS1,EPS	2
	12,EPS3,EPS4,EPS5,EPS6,EPI1,EPI2,EPI3,EPI4,EPI5,EPI6,EPI7,VP,AR,LEN	3
	1GTH,APR,BPR,BIGAPR,BIGBPR,ESTAR,ALPHA,BETA,RHOSTR,EPRS,RHOS	4
	COMMON XMESH(20,20,6),XMESH2(20,20,6),Z(20),R(20),SURF(15,8),SURF2	5
	1(15,8),TAB(15,14,2),TAB2(15,14,2),SPART(15,2,2),RARF(15,11),RARF2(	6



	115,4),RPART(15,2)	7
C		8
C		9
	COMMON ZO,RO,PO,UO,VO,LO,MO,RHOO,E0,A0,UBARO,VBARO	10
C		11
	COMMON NP,NT,NR,NI,NDEL,ISUB	12
C		13
	COMMON ZMIN,ZMAX,RMIN,RMAX,RADIUS,GZ,GR,DELTA,H	14
	COMMON DIRCOS	15
	COMMON TIME	16
	COMMON IRARF	17
	COMMON KSTOP	18
	COMMON TPSI	19
	COMMON KKK	20
C		21
C		22
	REAL LO,MO,LENGTH,MU,KO	23
	RHO=RHOSTR	24
	E=VP**2/8.	25
	DO 100 M=1,100	26
	ETA=RHO/RHOSTR	27
	MU=ETA-1.	28
	G=-RHOSTR*(VP/2. )**2+((APR+BPR/(E/(ESTAR*ETA**2)+1. ))*E*RHO+BIGAPR	29
	1*MU+BIGBPR*MU**2)*(1.-RHOSTR/RHO)	30
	DERIVG=((APR+BPR/(E/(ESTAR*ETA**2)+1. ))*E+BIGAPR/RHOSTR+2.*BIGBPR*	31
	1MU/RHOSTR+2.*E**2*BPR/(ESTAR*ETA**2*(E/(ESTAR*ETA**2)+1. )**2))*(1.	32
	1-RHOSTR/RHO)+((APR+BPR/(E/(ESTAR*ETA**2)+1. ))*E*RHO+BIGAPR*MU+BIGB	33
	1PR*MU**2)*RHOSTR/RHO**2	34
	DLTRHO=-G/DERIVG	35
	RHO=RHO+DLTRHO	36
C	IF(ABS(DLTRHO).LT.1.E-07) GO TO 101	37
	IF (ABS(DLTRHO).LT.1.E-06) GO TO 101	38
100	CONTINUE	39
	KICK=2200	40
	GO TO 9980	41
101	CONTINUE	42

	PRHO=RHO	43
	TRHO=RHO	44
	PEE=E	45
	TEE=E	46
	PVV=VP/2.	47
	PPP=(APR+BPR/(E/(ESTAR*ETA**2)+1.))*E*RHO+BIGAPR*MU+BIGBPR*MU**2	48
9980	RETURN	49
	DEBUG SUBCHK	
	END	50
	SUBROUTINE EQOS2(PPP,PRHO,PEE)	1
	COMMON CASEID(14),ITS1,ITS2,ITS3,ITS4,ITI1,ITI2,ITI3,ITI4,EPS1,EPS	2
	12,EPS3,EPS4,EPS5,EPS6,EPI1,EPI2,EPI3,EPI4,EPI5,EPI6,EPI7,VP,AR,LEN	3
	1GTH,APR,BPR,BIGAPR,BIGBPR,ESTAR,ALPHA,BETA,RHOSTR,EPRS,RHOS	4
	COMMON XMESH(20,20,6),XMESH2(20,20,6),Z(20),R(20),SURF(15,8),SURF2	5
	1(15,8),TAB(15,14,2),TAB2(15,14,2),SPART(15,2,2),RARF(15,11),RARF2(	6
	115,4),RPART(15,2)	7
C		8
C		9
	COMMON ZO,RO,PO,UO,VO,LO,MO,RHOO,E0,A0,UBARO,VBARO	10
C		11
	COMMON NP,NT,NR,NI,NDEL,ISUB	12
C		13
	COMMON ZMIN,ZMAX,RMIN,RMAX,RADIUS,GZ,GR,DELTA,H	14
	COMMON DIRCOS	15
	COMMON TIME	16
	COMMON IRARF	17
	COMMON KSTOP	18
C		19
	COMMON TPSI	20
	COMMON KKK	21
C		22
	REAL LO,MO,LENGTH,MU,KO	23
	P=PPP	24
	RHO=PRHO	25
	E=PEE	26
	ETA=RHO/RHOSTR	27

	MU=ETA-1.	28
	EE=E/(ESTAR*ETA**2)+1.	29
	PGRHO=E*(APR+BPR/EE)+BIGAPR/RHOSTR+(2.*BIGBPR*MU)/RHOSTR+(2.*E**2*	30
	1BPR)/(ESTAR*ETA**2*EE**2)	31
	PGE=(APR+BPR/EE)*RHO-(E*BPR*RHO)/(ESTAR*ETA**2*EE**2)	32
	AR=SQRT(PGRHO+PGE*P/RHO**2)	33
	RETURN	34
	DEBUG SUBCHK	
	END	35
	SUBROUTINE EQOS3(RHO,AA,E,P)	1
	COMMON CASEID(14),ITS1,ITS2,ITS3,ITS4,ITI1,ITI2,ITI3,ITI4,EPS1,EPS	2
	12,EPS3,EPS4,EPS5,EPS6,EPI1,EPI2,EPI3,EPI4,EPI5,EPI6,EPI7,VP,AR,LEN	3
	1GTH,APR,BPR,BIGAPR,BIGBPR,ESTAR,ALPHA,BETA,RHOSTR,EPRS,RHOS	4
	COMMON XMESH(20,20,6),XMESH2(20,20,6),Z(20),R(20),SURF(15,8),SURF2	5
	1(15,8),TAB(15,14,2),TAB2(15,14,2),SPART(15,2,2),RARF(15,11),RARF2(	6
	115,4),RPART(15,2)	7
C		8
C		9
	COMMON ZO,RO,PO,UO,VO,LO,MO,RHOO,E0,A0,UBARO,VBARO	10
C		11
	COMMON NP,NT,NR,NI,NDEL,ISUB	12
C		13
	COMMON ZMIN,ZMAX,RMIN,RMAX,RADIUS,GZ,GR,DELTA,H	14
	COMMON DIRCOS	15
	COMMON TIME	16
	COMMON IRARF	17
	COMMON KSTOP	18
	COMMON TPSI	19
	COMMON KKK	20
C		21
C		22
	REAL LO,MO,LENGTH,MU,KO	23
70	ETA=RHO/RHOSTR	24
	MU=ETA-1.	25
	EE=E/(ESTAR*ETA**2)+1.	26
	IF (RHO.GT.RHOSTR) GO TO 72	27

	IF (E.GE.EPRS) GO TO 74	28
72	PGRHO=E*(APR+BPR/EE)+BIGAPR/RHOSTR+{(2.*BIGBPR*MU)/RHOSTR+(2.*E**2*1BPR)/(ESTAR*ETA**2*EE**2)}	29
	PGE=(APR+BPR/EE)*RHO-(E*BPR*RHO)/(ESTAR*ETA**2*EE**2)	30
	GO TO 75	31
74	C1=RHOSTR/RHO-1.	32
	C2=EXP(-BETA*C1)	33
	C3=EXP(-ALPHA*C1**2)	34
	T1=(BPR*E*RHO)/EE+BIGAPR*MU*C2	35
	T2=2.*ALPHA*C1*(RHOSTR/(RHO**2))	36
	T3=BPR*E/EE	37
	T4=(2.*E)/(ESTAR*ETA**2*EE)	38
	T4=T3*T4	39
	T5=(BIGAPR*C2)/RHOSTR	40
	T6=(BIGAPR*MU*BETA*RHOSTR*C2)/(RHO**2)	41
	PGRHO=APR*E+C3*(T1*T2+T3+T4+T5+T6)	42
	T7=(BPR*RHO)/EE	43
	PGE=APR*RHO+C3*(T7-T7*(E/(ESTAR*ETA**2*EE)))	44
75	AA=SQRT(PGRHO+PGE*P/RHO**2)	45
	RETURN	46
	DEBUG SUBCHK	47
	END	48
	SUBROUTINE EQOSS(PFR,PFE)	1
	COMMON CASEID(14),ITS1,ITS2,ITS3,ITS4,ITI1,ITI2,ITI3,ITI4,EPS1,EPS	2
	12,EPS3,EPS4,EPS5,EPS6,EPI1,EPI2,EPI3,EPI4,EPI5,EPI6,EPI7,VP,AR,LEN	3
	1GTH,APR,BPR,BIGAPR,BIGBPR,ESTAR,ALPHA,BETA,RHOSTR,EPRS,RHOS	4
	COMMON XMESH(20,20,6),XMESH2(20,20,6),Z(20),R(20),SURF(15,8),SURF2	5
	1(15,8),TAB(15,14,2),TAB2(15,14,2),SPART(15,2,2),RARF(15,11),RARF2(	6
	115,4),RPART(15,2)	7
C		8
C		9
	COMMON ZO,RO,PO,UO,VO,LO,MO,RHOO,E0,A0,UBARO,VBARO	10
C		11
	COMMON NP,NT,NR,NI,NDEL,ISUB	12
C		13
	COMMON ZMIN,ZMAX,RMIN,RMAX,RADIUS,GZ,GR,DELTA,H	14

	COMMON DIRCOS	15
	COMMON TIME	16
	COMMON IRARF	17
	COMMON KSTOP	18
	COMMON TPSI	19
	COMMON KKK	20
C		21
C		22
250	REAL LO,MO,LENGTH,MU,KO	23
	ETA=RHO0/RHOSTR	24
	MU=ETA-1.	25
C		26
C		27
	EPP=EO/(ESTAR*ETA**2)+1.	28
	TMP=APR+BPR/EPP	29
	TMP1=BPR/(ESTAR*ETA**2+EPP**2)	30
	PFR=TMP*EO+(BIGAPR+2.*BIGBPR*MU)/RHOSTR+2.*EO**2*TMP1	31
	PFE=TMP*RHO0-EO*RHO0*TMP1	32
	RETURN	33
	DEBUG SUBCHK	
	END	34
	SUBROUTINE EQDSP(RHO02,E02,P02)	1
	COMMON CASEID(14),ITS1,ITS2,ITS3,ITS4,ITI1,ITI2,ITI3,ITI4,EPS1,EPS	2
	12,EPS3,EPS4,EPS5,EPS6,EPI1,EPI2,EPI3,EPI4,EPI5,EPI6,EPI7,VP,AR,LEN	3
	1GTH,APR,BPR,BIGAPR,BIGBPR,ESTAR,ALPHA,BETA,RHOSTR,EPRS,RHOS	4
	COMMON XMESH(20,20,6),XMESH2(20,20,6),Z(20),R(20),SURF(15,8),SURF2	5
	1(15,8),TAB(15,14,2),TAB2(15,14,2),SPART(15,2,2),RARF(15,11),RARF2(	6
	115,4),RPART(15,2)	7
C		8
C		9
	COMMON ZO,RO,PO,UO,VO,LO,MO,RHO0,E0,A0,UBARO,VBARO	10
C		11
	COMMON NP,NT,NR,NI,NDEL,ISUB	12
C		13
	COMMON ZMIN,ZMAX,RMIN,RMAX,RADIUS,GZ,GR,DELTA,H	14
	COMMON DIRCOS	15

	COMMON TIME	16
	COMMON IRARF	17
	COMMON KSTOP	18
	COMMON TPSI	19
	COMMON KKK	20
C		21
C		22
	REAL LO,MO,LENGTH,MU,KO	23
	ETA=RHO02/RHOSTR	24
	MU=ETA-1.	25
	P02=E02*RHO02*(APR+(BPR*ESTAR*ETA**2)/(E02+ESTAR*ETA**2))+BIGAPR*M	26
	1U+BIGBPR*MU**2	27
	RETURN	28
	DEBUG SUBCHK	
	END	29
	SUBROUTINE EQOSI(P02,PGRHO,PGE,BIGG,CHECK,KRTT,A02,E02,RHO02,KM,EP	1
	1S)	2
	COMMON CASEID(14),ITS1,ITS2,ITS3,ITS4,ITI1,ITI2,ITI3,ITI4,EPS1,EP	3
	12,EPS3,EPS4,EPS5,EPS6,EPI1,EPI2,EPI3,EPI4,EPI5,EPI6,EPI7,VP,AR,LEN	4
	1GTH,APR,BPR,BIGAPR,BIGBPR,ESTAR,ALPHA,BETA,RHOSTR,EPRS,RHOS	5
	COMMON XMESH(20,20,6),XMESH2(20,20,6),Z(20),R(20),SURF(15,8),SURF2	6
	1(15,8),TAB(15,14,2),TAB2(15,14,2),SPART(15,2,2),RARF(15,11),RARF2(	7
	115,4),RPART(15,2)	8
C		9
C		10
	COMMON ZO,RO,PO,UO,VO,LO,MO,RHOO,E0,A0,UBARO,VBARO	11
C		12
	COMMON NP,NT,NR,NI,NDEL,ISUB	13
C		14
	COMMON ZMIN,ZMAX,RMIN,RMAX,RADIUS,GZ,GR,DELTA,H	15
	COMMON DIRCOS	16
	COMMON TIME	17
	COMMON IRARF	18
	COMMON KSTOP	19
	COMMON TPSI	20
	COMMON KKK	21

C		22
C		23
	REAL LO,MO,LENGTH,MU,KO	24
	INTEGER CHECK,CHECK2	25
	IF (KM.EQ.0) GO TO 708	26
	RH00=RHOSTR	27
	TMP1=(APR+BPR)*RHOSTR-P02/ESTAR	28
	TMP2=SQRT(TMP1**2+4.*P02*APR*RHOSTR/ESTAR)	29
	E0=(-TMP1+TMP2)/(2.*APR*RHOSTR/ESTAR)	30
	IF (P02.GT.EPS) GO TO 708	31
	P02=0.	32
	E02=0.	33
	RH002=RHOSTR	34
	A02=SQRT(BIGAPR/RHOSTR)	35
	KRTT=1	36
	GO TO 870	37
708	KRTT=0	38
	ETA=RH00/RHOSTR	39
	MU=ETA-1.	40
	EE=E0/(ESTAR*ETA**2)+1.	41
	IF (RH00.GT.RHOSTR) GO TO 720	42
	IF (E0.LT.EPRS) GO TO 720	43
715	C1=RHOSTR/RH00-1.	44
	BEC1=BETA*C1	45
	IF (BEC1.LT.10.E10) GO TO 716	46
	C2=0.0	47
	GO TO 717	48
716	C2=EXP(-BEC1)	49
717	C3AL=ALPHA*C1**2	50
	IF (C3AL.LT.10.E12) GO TO 718	51
	C3=0.0	52
	GO TO 719	53
718	C3=EXP(-C3AL)	54
719	CONTINUE	55
	T1=(BPR*E0*RH00)/EE+BIGAPR*MU*C2	56
	T2=2.*ALPHA*C1*(RHOSTR/(RH00**2))	57

	T3=BPR*EO/EE	58
	T4=(2.*EO)/(ESTAR*ETA**2*EE)	59
	T4=T3*T4	60
	T5=(BIGAPR*C2)/RHOSTR	61
	T6=(BIGAPR*MU*BETA*RHOSTR*C2)/(RHOO**2)	62
	T7=(BPR*RHOO)/EE	63
	PGRHO=APR*EO+C3*(T1*T2+T3+T4+T5+T6)	64
	PGE=APR*RHOO+C3*(T7-T7*(EO/(ESTAR*ETA**2*EE)))	65
	BIGG=P02-APR*EO*RHOO-T1*C3	66
	CHECK=0	67
	GO TO 725	68
720	T1=APR+BPR/EE	69
	T2=(BPR*EO)/(ESTAR*ETA**2*EE**2)	70
	BIGG=P02-T1*EO*RHOO-BIGAPR*MU-BIGBPR*MU**2	71
	PGRHO=T1*EO+BIGAPR/RHOSTR+2.*BIGBPR*MU/RHOSTR+T2*2.*EO	72
	PGRHO=-PGRHO	73
	PGE=T1*RHOO-RHOO*T2	74
	PGE=-PGE	75
	CHECK=1	76
725	CONTINUE	77
870	CONTINUE	78
	RETURN	79
	DEBUG SUBCHK	
	END	80
	SUBROUTINE SOUT2	1
C		2
C	PRINTS 6 LINES OF DISCONTINUITY AT TO	3
C		4
	COMMON CASEID(14),ITS1,ITS2,ITS3,ITS4,ITI1,ITI2,ITI3,ITI4,EPS1,EPS	5
	12,EPS3,EPS4,EPS5,EPS6,EPI1,EPI2,EPI3,EPI4,EPI5,EPI6,EPI7,VP,AR,LEN	6
	1GTH,APR,BPR,BIGAPR,BIGBPR,ESTAR,ALPHA,BETA,RHOSTR,EPRS,RHOS	7
	COMMON XMESH(20,20,6),XMESH2(20,20,6),Z(20),R(20),SURF(15,8),SURF2	8
	1(15,8),TAB(15,14,2),TAB2(15,14,2),SPART(15,2,2),RARF(15,11),RARF2(	9
	115,4),RPART(15,2)	10
C		11
C		12



	COMMON ZO,RO,PO,UO,VO,LO,MO,RHOO,E0,A0,UBARO,VBARO	13
C		14
	COMMON NP,NT,NR,NI,NDEL,ISUB	15
C		16
	COMMON ZMIN,ZMAX,RMIN,RMAX,RADIUS,GZ,GR,DELTA,H	17
	COMMON DIRCOS	18
	COMMON TIME	19
	COMMON IRARF	20
	COMMON KSTOP	21
	COMMON TPSI	22
	COMMON KKK	23
	REAL LO,MO,LENGTH,MU,KO	24
C		25
4	FORMAT (///30H CURVES OF DISCONTINUITY AT TO//40X20H--PROJECTILE S	26
	1HOCK--//)	27
6	FORMAT (//35X29H--PROJECTILE PARTICLE CURVE--//)	28
8	FORMAT (//42X16H--TARGET SHOCK--//)	29
10	FORMAT (//38X25H--TARGET PARTICLE CURVE--//)	30
12	FORMAT (//42X15H--RAREFACTION--//)	31
14	FORMAT (//35X30H--RAREFACTION PARTICLE CURVE--//)	32
16	FORMAT (7X1HZ19X1HR19X1HP19X1HU19X1HV/7X3HRHO17X1HE19X1HA19X1HL19X	33
	11HM//)	34
18	FORMAT (7X1HZ19X1HR//)	35
20	FORMAT (7X1HZ19X1HR19X1HL19X1HM//)	36
30	FORMAT (5E20.8/5E20.8//)	37
35	FORMAT (2E20.8)	38
38	FORMAT (4E20.8)	39
39	FORMAT (//35X16H--FREE SURFACE--//)	40
40	FORMAT (1H1)	41
	WRITE (3,4)	42
	WRITE (3,16)	43
	WRITE (3,30) ((TAB2(I,J,1),J=1,10),I=1,NP)	44
	WRITE (3,6)	45
	WRITE (3,18)	46
	WRITE (3,35) ((SPART(I,J,1),J=1,2),I=1,NP)	47
	WRITE (3,8)	48

	WRITE (3,16)	49
	WRITE (3,30) ((TAB2(I,J,2),J=1,10),I=1,NT)	50
	WRITE (3,10)	51
	WRITE (3,18)	52
	WRITE (3,35) ((SPART(I,J,2),J=1,2),I=1,NT)	53
	WRITE (3,12)	54
	WRITE (3,20)	55
	WRITE (3,38) ((RARF2(I,J),J=1,4),I=1,NR)	56
	WRITE (3,14)	57
	WRITE (3,39)	58
	WRITE (3,35) ((SURF2(I,J),J=1,2),I=1,NP)	59
	WRITE (3,40)	60
	RETURN	61
	DEBUG SUBCHK	
	END	62
	SUBROUTINE SOUT	1
C		2
C	PRINTS 4 LINES OF DISCONTINUITY AT TO-H	3
C		4
	COMMON CASEID(14),ITS1,ITS2,ITS3,ITS4,ITI1,ITI2,ITI3,ITI4,EPS1,EPS	5
	12,EPS3,EPS4,EPS5,EPS6,EPI1,EPI2,EPI3,EPI4,EPI5,EPI6,EPI7,VP,AR,LEN	6
	1GTH,APR,BPR,BIGAPR,BIGBPR,ESTAR,ALPHA,BETA,RHOSTR,EPRS,RHOS	7
	COMMON XMESH(20,20,6),XMESH2(20,20,6),Z(20),R(20),SURF(15,8),SURF2	8
	1(15,8),TAB(15,14,2),TAB2(15,14,2),SPART(15,2,2),RARF(15,11),RARF2(	9
	115,4),RPART(15,2)	10
C		11
C		12
	COMMON ZO,RO,PO,UO,VO,LO,MO,RHOO,E0,AO,UBARO,VBARO	13
C		14
	COMMON NP,NT,NR,NI,NDEL,ISUB	15
C		16
	COMMON ZMIN,ZMAX,RMIN,RMAX,RADIUS,GZ,GR,DELTA,H	17
	COMMON DIRCOS	18
	COMMON TIME	19
	COMMON IRARF	20
	COMMON KSTOP	21

	COMMON TPSI	22
	COMMON KKK	23
	REAL LO,MO,LENGTH,MU,KO	24
C		25
4	FORMAT (///32H CURVES OF DISCONTINUITY AT TO-H//40X20H--PROJECTILE	26
	1 SHOCK--//)	27
6	FORMAT (//42X16H--TARGET SHOCK--//)	28
8	FORMAT (//42X15H--RAREFACTION--//)	29
10	FORMAT (7X1HZ19X1HR19X1HP19X1HU19X1HV/7X3HRHO17X1HE19X1HA19X1HL19X	30
	11HM//)	31
15	FORMAT (5E20.8/5E20.8//)	32
18	FORMAT (1H1)	33
21	FORMAT (//35X16H--FREE SURFACE--//)	34
25	FORMAT (2E20.8)	35
	WRITE (3,4)	36
	WRITE (3,10)	37
	WRITE (3,15) ((TAB(I,J,1),J=1,10),I=1,NP)	38
	WRITE (3,6)	39
	WRITE (3,10)	40
	WRITE (3,15) ((TAB(I,J,2),J=1,10),I=1,NT)	41
	WRITE (3,8)	42
	WRITE (3,10)	43
	WRITE (3,15) ((RARF(I,J),J=1,10),I=1,NR)	44
	WRITE (3,21)	45
	WRITE (3,25) ((SURF(I,J),J=1,2),I=1,NP)	46
	WRITE (3,18)	47
	RETURN	48
	DEBUG SUBCHK	
	END	49
	SUBROUTINE PRINT(BL,ZTAB,RTAB,KK,PHI,NMAX,MMAX)	
C	SUBROUTINE PRINT(BL,ZTAB,RTAB,KK)	
	DOUBLE PRECISION XS(20),RU(20),ZU(20,20,6),UU(20),WW(20),	
	1ZCOMP(20,20,6),PHI(20,20,6),CETA(20,20),DENC,POLY	
C	PRINTS INTERIOR REGION	2
C		3
	COMMON CASEID(14),ITS1,ITS2,ITS3,ITS4,ITI1,ITI2,ITI3,ITI4,EPS1,EPS	4

	12, EPS3, EPS4, EPS5, EPS6, EPI1, EPI2, EPI3, EPI4, EPI5, EPI6, EPI7, VP, AR, LEN	5
	1GTH, APR, BPR, BIGAPR, BIGBPR, ESTAR, ALPHA, BETA, RHOSTR, EPRS, RHOS	6
	COMMON XMESH(20,20,6), XMESH2(20,20,6), Z(20), R(20), SURF(15,8), SURF2	7
	1(15,8), TAB(15,14,2), TAB2(15,14,2), SPART(15,2,2), RARF(15,11), RARF2(	8
	115,4), RPART(15,2)	9
C		10
C		11
	COMMON ZO, RO, PO, UO, VO, LO, MO, RHOO, EO, AO, UBARO, VBARO	12
C		13
	COMMON NP, NT, NR, NI, NDEL, ISUB	14
C		15
	COMMON ZMIN, ZMAX, RMIN, RMAX, RADIUS, GZ, GR, DELTA, H	16
	COMMON DIRCOS	17
	COMMON TIME	18
	COMMON IRARF	19
	COMMON KSTOP	20
	COMMON TPSI	21
	COMMON KKK	22
	REAL LO, MO, LENGTH, MU, KO	23
C		24
	DIMENSION BL(20,20,6), ZTAB(20), RTAB(20)	25
C		26
	TSSS=1.1	
	M=0	
	N=0	
	DO 15 I=1,20	27
	DO 15 J=1,20	28
	IF (ABS(BL(I,J,1))+ABS(BL(I,J,2))+ABS(BL(I,J,3))) 20,15,20	29
15	CONTINUE	30
	WRITE (3,18)	31
18	FORMAT (15H1TABLES ALL = 0/1H1)	32
	CALL EXIT	33
20	I1=I	34
	DO 30 I=I1,20	35
	IF (ABS(BL(I,1,1))+ABS(BL(I,1,2))+ABS(BL(I,1,3))) 30,22,30	36
22	DO 25 J=1,20	37

	IF (ABS(BL(I,J,1))+ABS(BL(I,J,2))+ABS(BL(I,J,3))) 30,25,30	38
25	CONTINUE	39
	I2=I-1	40
	GO TO 35	41
30	CONTINUE	42
	I2=20	43
35	DO 45 J=1,20	44
	IF (ABS(BL(I1,J,1))+ABS(BL(I1,J,2))+ABS(BL(I1,J,3))) 45,37,45	45
37	DO 40 I=I1,I2	46
	IF (ABS(BL(I,J,1))+ABS(BL(I,J,2))+ABS(BL(I,J,3))) 45,40,45	47
40	CONTINUE	48
	J2=J-1	49
	GO TO 50	50
45	CONTINUE	51
	J2=20	52
50	J1=1	53
C		54
C	PRINT TABLE	55
C		56
	GO TO (52,56),KK	57
52	WRITE (3,53)	58
53	FORMAT (//24H0INTERIOR REGION AT T0-H//)	59
	GO TO 62	60
56	WRITE (3,57)	61
57	FORMAT (//22H0INTERIOR REGION AT T0//)	62
62	DO 70 I=I1,I2	63
	WRITE (3,64) ZTAB(I)	64
64	FORMAT (///7H0ZTAB =,F10.4//7X1HR9X1HP17X1HU17X1HV17X3HRH015X1HE17	65
	1X1HA//)	66
	M=M+1	
	XS(M)=ZTAB(I)	
	UU(M)=1.0	
	DO 69 J=J1,J2	67
	WRITE (3,68) RTAB(J),(BL(I,J,K),K=1,6)	68
	N=N+1	
	RU(N)=RTAB(J)	

	WW(N)=1.0	
	DO 156 IK=1,6	
C	ZU(M,N)=BL(I,J,4)	
C	ZZ(M,N)=BL(I,J,1)	
156	ZU(M,N,IK)=BL(I,J,IK)	
68	FORMAT (F12.4,6E18.8)	69
69	CONTINUE	70
	MMA=N	
	N=0	
70	CONTINUE	71
	NMAX=M	
C	IF(TIME.LT.TSSS) GO TO 80	
333	IMAX=I2+1-I1	
	JMAX=J2+1-J1	
	CALL SURFIT(XS,UU,RU,WW,ZU,NMAX,MMA,IMAX,JMAX,CETA,PHI,ZCOMP,	
	1SQD,SQDC,SDC,DFC)	
	WRITE(3,100)	
100	FORMAT(' *** ')	
	DO 88 IK=1,6	
	DO 48 I=1,IMAX	
	DO 48 J=1,JMAX	
	DENC=0.00	
	DO 43 IS=1,NMAX	
	K=NMAX-IS+1	
	POLY=PHI(K,MMA,IK)	
	IF(MMA-1)43,43,46	
46	DO 42 IT=2,MMA	
	L=MMA-IT+1	
42	POLY=POLY*RU(J)+PHI(K,L,IK)	
43	DENC=DENC*XS(I)+POLY	
	ZCOMP(I,J,IK)=DENC	
48	CONTINUE	
88	CONTINUE	
80	WRITE (3,82)	72
82	FORMAT (1H1)	73
	RETURN	74

	DEBUG SUBCHK	
	END	75
	SUBROUTINE NRIT2(X,Y,X0,DX,Y0,DY,EX,EY,FGOF,IT,KODE,	
	1PHI,NMAX,MMAX)	
C	SUBROUTINE NRIT2(X,Y,X0,DX,Y0,DY,EX,EY,FGOF,IT,KODE)	1
C		2
C	NEWTON-RAPHSON METHOD FOR SOLUTION OF	3
C	TWO NON LINEAR EQUATIONS IN TWO UNKNOWNNS	4
C		5
	COMMON CASEID(14),ITS1,ITS2,ITS3,ITS4,ITI1,ITI2,ITI3,ITI4,EPS1,EPS	6
	12,EPS3,EPS4,EPS5,EPS6,EPI1,EPI2,EPI3,EPI4,EPI5,EPI6,EPI7,VP,AR,LEN	7
	1GTH,APR,BPR,BIGAPR,BIGBPR,ESTAR,ALPHA,BETA,RHOSTR,EPRS,RHOS	8
	COMMON XMESH(20,20,6),XMESH2(20,20,6),Z(20),R(20),SURF(15,8),SURF2	9
	1(15,8),TAB(15,14,2),TAB2(15,14,2),SPART(15,2,2),RARF(15,11),RARF2(	10
	115,4),RPART(15,2)	11
C		12
C		13
	COMMON ZO,RO,PO,UO,VO,LO,MO,RHOO,E0,A0,UBARO,VBARO	14
C		15
	COMMON NP,NT,NR,NI,NDEL,ISUB	16
C		17
	COMMON ZMIN,ZMAX,RMIN,RMAX,RADIUS,GZ,GR,DELTA,H	18
	COMMON DIRCOS	19
	COMMON TIME	20
	COMMON IRARF	21
	COMMON KSTOP	22
	COMMON TPSI	23
	COMMON KKK	24
	REAL LO,MO,LENGTH,MU,KO	25
	DOUBLE PRECISION PHI(20,20,6)	
C		26
	TSSS=1.1	
	XB=X0	27
	YB=Y0	28
	OXX=DX	29
	OYY=DY	30

	DELX1=0	31
	DELY1=0	32
	KODE=0	33
1	CONTINUE	34
	DO 50 I=1, IT	35
	KK=0	36
	XX=XB+DXX	37
	YY=YB+DYY	38
C		39
C		40
	IF (TIME.LT.TSSS) GO TO 266	
	CALL FGOF(XB,YY,F2,G2,PHI,NMAX,MMAX)	
	CALL FGOF(XX,YB,F1,G1,PHI,NMAX,MMAX)	
	CALL FGOF(XB,YB,F0,G0,PHI,NMAX,MMAX)	
	GO TO 267	
266	CALL FGOF(XB,YY,F2,G2)	
	CALL FGOF(XX,YB,F1,G1)	
	CALL FGOF(XB,YB,F0,G0)	
267	A1=(F1-F0)/DXX	
	B1=(F2-F0)/DYY	45
	C1=-F0	46
	A2=(G1-G0)/DXX	47
	B2=(G2-G0)/DYY	48
	C2=-G0	49
	DET=A1*B2-A2*B1	50
	IF (DET.EQ.0.) GO TO 920	51
	DELX=(B2*C1-B1*C2)/DET	52
	DELY=(A1*C2-A2*C1)/DET	53
	IF (ABS(DELX).GT..001) GO TO 8	54
	DELX=0.	55
8	IF (ABS(DELY).GT..001) GO TO 9	56
	DELY=0.	57
9	CONTINUE	58
	SDEL=ABS(DELX+DELX1)+ABS(DELY+DELY1)	59
	DELX1=DELX	60
	DELY1=DELY	61



C		62
C	TEST FOR SAME REGION	63
C		64
	DO 10 J=1,IT	65
	XB1=XB+DELX	66
	YB1=YB+DELY	67
	IF (YB1.LE.0.)YB1=0.	68
	M=COMP(XB,YB,XB1,YB1)	69
	IF (M.EQ.1) GO TO 15	70
11	CONTINUE	71
	KK=1	72
	DELX=.5*DELX	73
	DELY=.5*DELY	74
10	CONTINUE	75
	GO TO 930	76
15	IF (ABS(XB-XB1).GT.EX) GO TO 45	77
	IF (ABS(YB-YB1).GT.EY) GO TO 45	78
	IF (KK.NE.0) GO TO 45	79
	X=XB1	80
	Y=YB1	81
	KODE=0	82
	RETURN	83
45	CONTINUE	84
	IF (KODE.NE.1) GO TO 46	85
	IF (SDEL.GT.EPI1) GO TO 46	86
	DELX=.5*DELX	87
	DELY=.5*DELY	88
	GO TO 9	89
46	XB=XB1	90
	YB=YB1	91
	DEL=DELTA	92
	DO 70 N=1,NDEL	93
	XB2=XB+DEL	94
	M=COMP(XB,YB,XB2,YB)	95
	IF (M.NE.1) GO TO 55	96
	DXX=DEL	97

	GO TO 80	98
55	XB2=XB-DEL	99
	M=COMP(XB,YB,XB2,YB)	100
	IF (M.NE.1) GO TO 60	101
	DXX=-DEL	102
	GO TO 80	103
60	DEL=.5*DEL	104
70	CONTINUE	105
	GO TO 980	106
80	DEL=DELTA	107
	DO 100 N=1,NDEL	108
	YB2=YB+DEL	109
	M=COMP(XB,YB,XB,YB2)	110
	IF (M.NE.1) GO TO 85	111
	DYY=DEL	112
	GO TO 50	113
85	YB2=YB-DEL	114
	M=COMP(XB,YB,XB,YB2)	115
	IF (M.NE.1) GO TO 90	116
	DYY=-DEL	117
	GO TO 50	118
90	DEL=.5*DEL	119
100	CONTINUE	120
	GO TO 990	121
50	CONTINUE	122
	X=XB1	123
	Y=YB1	124
	IF (KODE.EQ.1) RETURN	125
	KODE=1	126
	GO TO 1	127
920	WRITE (3,922) I	128
922	FORMAT (46HODETERMINANT IS 0 IN SUBR. NRIT2 FOR ITERATION,I4)	129
	GO TO 950	130
930	KODE=2	131
	RETURN	132
950	WRITE (3,952) X0,Y0,XB,YB,XB1,YB1,DELX,DELY	133

952	FORMAT (1X5HZO =,E15.8,4X5HRO =,E15.8/1X5HZB =,E15.8,4X5HRB =,	134
	1E15.8/1X5HZB1 =,E15.8,4X5HRB1 =,E15.8/1X5HDELZ=,E15.8,4X5HDELR=,E1	135
	15.8/1H1)	136
	CALL EXIT	137
	RETURN	138
980	KODE=3	139
	RETURN	140
990	KODE=4	141
	RETURN	142
	DEBUG SUBCHK	
	END	143
	FUNCTION COMP(ZP,RP,ZP1,RP1)	1
C		2
C	DETERMINES IF 2 POINTS ARE IN THE SAME REGION	3
	COMMON CASEID(14),ITS1,ITS2,ITS3,ITS4,ITI1,ITI2,ITI3,ITI4,EPS1,EPS	4
	12,EPS3,EPS4,EPS5,EPS6,EPI1,EPI2,EPI3,EPI4,EPI5,EPI6,EPI7,VP,AR,LEN	5
	1GTH,APR,BPR,BIGAPR,BIGBPR,ESTAR,ALPHA,BETA,RHOSTR,EPRS,RHOS	6
	COMMON XMESH(20,20,6),XMESH2(20,20,6),Z(20),R(20),SURF(15,8),SURF2	7
	1(15,8),TAB(15,14,2),TAB2(15,14,2),SPART(15,2,2),RARF(15,11),RARF2(	8
	115,4),RPART(15,2)	9
C		10
	COMMON ZO,RO,PO,UO,VO,LO,MO,RHOO,E0,A0,UBARO,VBARO	11
C		12
	COMMON NP,NT,NR,NI,NDEL,ISUB	13
C		14
	COMMON ZMIN,ZMAX,RMIN,RMAX,RADIUS,GZ,GR,DELTA,H	15
	COMMON DIRCOS	16
	COMMON TIME	17
	COMMON IRARF	18
	COMMON KSTOP	19
	COMMON TPSI	20
	COMMON KKK	21
	REAL LO,MO,LENGTH,MU,KO	22
	EPS=.0000001	23
	IF (RP1.LT.0.) GO TO 80	24
	IF (ZP1.GE.0.) GO TO 4	25

	IF (RP1.GT.RADIUS) GO TO 80	26
C		27
C	FIND CONTROL CONSTANTS FOR ZP,RP	28
C		29
4	CONTINUE	30
	IF (ITS3.EQ.1) GO TO 33	31
	IF (IRARF.EQ.1) GO TO 13	32
	M=PICK(ZP,RP,3)	33
	IF (ZP.GT.RARF(M,1).AND.M.NE.1)M=M-1	34
	FF=RP-RARF(M+1,2)-(RARF(M,2)-RARF(M+1,2))*(ZP-RARF(M+1,1))/(RARF(M	35
	1,1)-RARF(M+1,1))	36
	IF (FF.LT.0.) GO TO 11	37
10	NN=1	38
	GO TO 13	39
11	NN=0	40
13	CONTINUE	41
	DO 22 K=1,2	42
	M=PICK(ZP1,RP1,K)	43
	IF (RP1.LT.TAB(M,2,K).AND.M.NE.1)M=M-1	44
5	CONTINUE	45
	FF=ZP1-TAB(M+1,1,K)-(TAB(M,1,K)-TAB(M+1,1,K))*(RP1-TAB(M+1,2,K))/(	46
	1TAB(M,2,K)-TAB(M+1,2,K))	47
	IF (K.EQ.2) GO TO 17	48
	IF (RP1.GT.RADIUS) GO TO 21	49
	IF (FF.LT.-EPS) GO TO 90	50
	GO TO 21	51
17	IF (FF.GT.EPS) GO TO 100	52
21	IF (RP.GT.RADIUS) GO TO 22	53
	M=PICK(ZP1,RP1,4)	54
	FF=ZP1-SURF(M+1,1)-(SURF(M,1)-SURF(M+1,1))*(RP1-SURF(M+1,2))/(SURF	55
	1(M,2)-SURF(M+1,2))	56
	IF (FF) 80,22,22	57
22	CONTINUE	58
	IF (IRARF.EQ.1) GO TO 33	59
	M=PICK(ZP1,RP1,3)	60
	IF (ZP1.GT.RARF(M,1).AND.M.NE.1)M=M-1	61

	FF=RP1-RARF(M+1,2)-(RARF(M,2)-RARF(M+1,2))*(ZP1-RARF(M+1,1))/(RARF	62
	1(M,1)-RARF(M+1,1))	63
	IF (FF.LT.0.) GO TO 31	64
30	NN1=1	65
	GO TO 32	66
31	NN1=0	67
32	IF (NN1.NE.NN) GO TO 110	68
33	CONTINUE	69
	COMP=1	70
	COMP=COMP+.2	71
	RETURN	72
80	COMP=2	73
	COMP=COMP+.2	74
	RETURN	75
90	COMP=3.	76
	COMP=COMP+.2	77
	RETURN	78
100	COMP=4.	79
	COMP=COMP+.2	80
	RETURN	81
110	COMP=5.	82
	COMP=COMP+.2	83
	RETURN	84
	DEBUG SUBCHK	
	END	85
	FUNCTION PICK(ZP,RP,KODE)	1
C		2
C	DETERMINES 2 CLOSEST CONSECUTIVE POINTS ON SPECIFIED	3
C	LINE OF DISCONTINUITY TO A GIVEN POINT	4
C		5
	COMMON CASEID(14),ITS1,ITS2,ITS3,ITS4,ITI1,ITI2,ITI3,ITI4,EPS1,EPS	6
	12,EPS3,EPS4,EPS5,EPS6,EPI1,EPI2,EPI3,EPI4,EPI5,EPI6,EPI7,VP,AR,LEN	7
	1GTH,APR,BPR,BIGAPR,BIGBPR,ESTAR,ALPHA,BETA,RHOSTR,EPRS,RHOS	8
	COMMON XMESH(20,20,6),XMESH2(20,20,6),Z(20),R(20),SURF(15,8),SURF2	9
	1(15,8),TAB(15,14,2),TAB2(15,14,2),SPART(15,2,2),RARF(15,11),RARF2(	10
	115,4),RPART(15,2)	11

C		12
C		13
	COMMON ZO,RO,PO,UO,VO,LO,MO,RHOO,E0,A0,UBARO,VBARO	14
C		15
	COMMON NP,NT,NR,NI,NDEL,ISUB	16
C		17
	COMMON ZMIN,ZMAX,RMIN,RMAX,RADIUS,GZ,GR,DELTA,H	18
	COMMON DIRCOS	19
	COMMON TIME	20
	COMMON IRARF	21
	COMMON KSTOP	22
	COMMON TPSI	23
	COMMON KKK	24
	REAL LO,MO,LENGTH,MU,KO	25
C		26
	GO TO (5,10,100,300),KODE	27
5	NN=NP	28
	K=1	29
	GO TO 15	30
10	NN=NT	31
	K=2	32
15	AA=(TAB(1,1,K)-ZP)**2+(TAB(1,2,K)-RP)**2	33
C		34
C	SEARCH SHOCK TABLES	35
C		36
	DO 60 N=2,NN	37
	A=(TAB(N,1,K)-ZP)**2+(TAB(N,2,K)-RP)**2	38
	IF (A.GE.AA) GO TO 23	39
	AA=A	40
60	CONTINUE	41
	PICK=NN-1	42
	PICK=PICK+.2	43
	RETURN	44
23	PICK=N-1	45
	PICK=PICK+.2	46
	RETURN	47

100	AA=(RARF(1,1)-ZP)**2+(RARF(1,2)-RP)**2	48
C		49
C	SEARCH RAREFACTION TABLE	50
C		51
	DO 200 N=2,NR	52
	A=(RARF(N,1)-ZP)**2+(RARF(N,2)-RP)**2	53
	IF (A.GE.AA) GO TO 203	54
	AA=A	55
200	CONTINUE	56
	PICK=NR-1	57
	PICK=PICK+.2	58
	RETURN	59
203	PICK=N-1	60
	PICK=PICK+.2	61
	RETURN	62
300	AA=(SURF(1,1)-ZP)**2+(SURF(1,2)-RP)**2	63
C		64
C	SEARCH FREE SURFACE TABLE	65
C		66
	DO 400 N=2,NP	67
	A=(SURF(N,1)-ZP)**2+(SURF(N,2)-RP)**2	68
	IF (A.GE.AA) GO TO 303	69
	AA=A	70
400	CONTINUE	71
	PICK=NP-1	72
	PICK=PICK+.2	73
	RETURN	74
303	PICK=N-1	75
	PICK=PICK+.2	76
304	CONTINUE	77
	RETURN	78
	DEBUG SUBCHK	
	END	79
	SUBROUTINE GUESS(KOD1,KOD2,ZP,RP,I2,K2,ZG,RG,DZ,DR)	1
C		2
C	DETERMINES STARTING POINT AND DELTAS	3

C	FOR NEWTON-RAPHSON ITERATION	4
C		5
	COMMON CASEID(14),ITS1,ITS2,ITS3,ITS4,ITI1,ITI2,ITI3,ITI4,EPS1,EPS	6
	12,EPS3,EPS4,EPS5,EPS6,EPI1,EPI2,EPI3,EPI4,EPI5,EPI6,EPI7,VP,AR,LEN	7
	1GTH,APR,BPR,BIGAPR,BIGBPR,ESTAR,ALPHA,BETA,RHOSTR,EPRS,RHOS	8
	COMMON XMESH(20,20,6),XMESH2(20,20,6),Z(20),R(20),SURF(15,8),SURF2	9
	1(15,8),TAB(15,14,2),TAB2(15,14,2),SPART(15,2,2),RARF(15,11),RARF2(	10
	115,4),RPART(15,2)	11
C		12
C		13
	COMMON ZO,RO,PO,UO,VO,LO,MO,RHOO,E0,A0,UBARO,VBARO	14
C		15
	COMMON NP,NT,NR,NI,NDEL,ISUB	16
C		17
	COMMON ZMIN,ZMAX,RMIN,RMAX,RADIUS,GZ,GR,DELTA,H	18
	COMMON DIRCOS	19
	COMMON TIME	20
	COMMON IRARF	21
	COMMON KSTOP	22
	COMMON TPSI	23
	COMMON KKK	24
	REAL LO,MO,LENGTH,MU,KO	25
C		26
	KS=0	27
	IF (KOD1.EQ.2) GO TO 10	28
	ZG=TAB(I2,1,K2)	29
	RG=TAB(I2,2,K2)	30
	IF (IRARF.EQ.1) GO TO 9	31
2	M=1-(NR-2)*(K2-2)	32
	FF=RG-RARF(M+1,2)-(RARF(M,2)-RARF(M+1,2))*(ZG-RARF(M+1,1))/(RARF(M	33
	1,1)-RARF(M+1,1))	34
	IF (FF.GT.0.) GO TO 9	35
	ZG=(1.-.02/(RADIUS-RG))*ZG	36
	RG=RG+.02	37
	IF (RG.GT.(RADIUS-.01)) GO TO 110	38
	GO TO 2	39



9	CONTINUE	40
	GO TO 50	41
10	JJJ=NT-1	42
	IF (ITS3.EQ.1) GO TO 26	43
	DO 24 M=1,JJJ	44
	IF (RP.GT.TAB(M+1,2,2).OR.RP.LT.TAB(M,2,2)) GO TO 24	45
	GO TO 25	46
24	CONTINUE	47
25	CONTINUE	48
	FF=ZP-TAB(M+1,1,2)-(TAB(M,1,2)-TAB(M+1,1,2))*(RP-TAB(M+1,2,2))/(TA	49
	1B(M,2,2)-TAB(M+1,2,2))	50
	IF (FF.GT.0.) GO TO 20	51
26	CONTINUE	52
	ZG=ZP	53
	RG=RP	54
	GO TO 50	55
20	IK=M	56
	M=CROSS(TAB(IK,1,2),TAB(IK,2,2),TAB(IK+1,1,2),TAB(IK+1,2,2),0.,0.,	57
	1ZP,RP,ZG,RG)	58
	GO TO (50,920,930),M	59
C		60
C	COMPUTE DELTAS	61
C		62
50	DEL=DELTA	63
C		64
C	Z DELTA	65
C		66
	LL=0	67
52	DO 70 N=1,NDEL	68
	ZZ=ZG+DEL	69
	M=COMP(ZG,RG,ZZ,RG)	70
	IF (M.NE.1) GO TO 55	71
	DZ=DEL	72
	GO TO 80	73
55	ZZ=ZG-DEL	74
	M=COMP(ZG,RG,ZZ,RG)	75

	IF (M.NE.1) GO TO 60	76
	DZ=-DEL	77
	GO TO 80	78
60	DEL=.5*DEL	79
70	CONTINUE	80
	LL=LL+1	81
	IF (LL.EQ.3) GO TO 75	82
	RG=RG-DELTA/5.	83
	DEL=DELTA	84
	GO TO 52	85
75	KOD2=2	86
	RETURN	87
80	DEL=DELTA	88
	IF (KS.EQ.1) GO TO 120	89
C		90
C	R DELTA	91
C		92
	LL=0	93
82	DO 100 N=1,NDEL	94
	RR=RG+DEL	95
	M=COMP(ZG,RG,ZG,RR)	96
	IF (M.NE.1) GO TO 85	97
	DR=DEL	98
	IF (KS.EQ.1) GO TO 50	99
	GO TO 120	100
85	RR=RG-DEL	101
	M=COMP(ZG,RG,ZG,RR)	102
	IF (M.NE.1) GO TO 90	103
	DR=-DEL	104
	IF (KS.EQ.1) GO TO 50	105
	GO TO 120	106
90	DEL=.5*DEL	107
100	CONTINUE	108
108	CONTINUE	109
	LL=LL+1	110
	FLL=LL	111

	IF (LL.EQ.5) GO TO 110	112
C		113
104	ZG1=ZG+DELTA/5.*FLL*(-1.)**LL	114
	M=COMP(ZG, RG, ZG1, RG)	115
	ZG=ZG1	116
	IF (M.NE.1) GO TO 108	117
	KS=1	118
	GO TO 82	119
110	KOD2=2	120
	RETURN	121
120	KOD2=1	122
	RETURN	123
920	WRITE (3,922)	124
922	FORMAT (42HOERROR FOR COINCIDENT LINES IN SUBR. GUESS)	125
	GO TO 950	126
C		127
930	WRITE (3,932)	128
932	FORMAT (40HOERROR FOR PARALLEL LINES IN SUBR. GUESS)	129
C		130
950	WRITE (3,952) KOD1,I2,K2,ZP,RP	131
952	FORMAT (1X5HKOD1=,I4,4X3HI2=,I4,4X3HK2=,I4/1X3HZP=,E15.8,4X3HRP=,E	132
	115.8/1H1)	133
	XYZ=-2.	134
	ZYX=SQRT(XYZ)	135
	CALL EXIT	136
	RETURN	137
	END	138
	FUNCTION CROSS(X1,Y1,X2,Y2,X3,Y3,X4,Y4,X,Y)	1
C		2
C	FINDS INTERSECTION OF TWO STRAIGHT LINES	3
C		4
	EPS=.0000001	5
	A1=Y2-Y1	6
	B1=X1-X2	7
	C1=X1*A1+Y1*B1	8
	A2=Y4-Y3	9

	B2=X3-X4	10
	C2=X3*A2+Y3*B2	11
	DET=A1*B2-A2*B1	12
	D1=C1*B2-C2*B1	13
	D2=A1*C2-A2*C1	14
	IF (ABS(DET).LE.EPS) GO TO 10	15
	X=D1/DET	16
	Y=D2/DET	17
	CROSS=1	18
	CROSS=CROSS+.2	19
	RETURN	20
10	IF (ABS(D1).GT.EPS) GO TO 20	21
	IF (ABS(D2).LE.EPS) GO TO 30	22
20	CROSS=3	23
	CROSS=CROSS+.2	24
	RETURN	25
30	X=X1	26
	Y=Y1	27
	CROSS=2	28
	CROSS=CROSS+.2	29
316	CONTINUE	30
	RETURN	31
	DEBUG SUBCHK	
	END	32
	FUNCTION PART(MODE,ZP,RP,ZX,RX,DELTA,NDEL)	1
C		2
C	LOCATES A POINT IN THE SAME REGION AS A GIVEN POINT	3
C	TO BE USED IN COMPUTING A PARTIAL	4
C	MODE=1,WITH RESPECT TO R	5
C	MODE=2,WITH RESPECT TO Z	6
C		7
	GO TO (2,4),MODE	8
2	DR=DELTA	9
	DZ=0.	10
	GO TO 8	11
4	DR=0.	12

	DZ=DELTA	13
8	DO 50 NN=1,NDEL	14
	RR=RP+DR	15
	ZZ=ZP+DZ	16
	M=COMP(ZP,RP,ZZ,RR)	17
	IF (M.EQ.1) GO TO 60	18
	RR=RP-DR	19
	ZZ=ZP-DZ	20
	M=COMP(ZP,RP,ZZ,RR)	21
	IF (M.EQ.1) GO TO 60	22
	DZ=DZ*.5	23
	DR=DR*.5	24
50	CONTINUE	25
	PART=2	26
	PART=PART+.2	27
	RETURN	28
60	ZX=ZZ	29
	RX=RR	30
	PART=1	31
	PART=PART+.2	32
	RETURN	33
	DEBUG SUBCHK	
	END	34
	FUNCTION PICK2(ZP,RP,KODE)	1
C		2
C	DETERMINES 2 CLOSEST CONSECUTIVE POINTS ON SPECIFIED	3
C	LINE OF DISCONTINUITY TO A GIVEN POINT	4
	COMMON CASEID(14),ITS1,ITS2,ITS3,ITS4,ITI1,ITI2,ITI3,ITI4,EPS1,EPS	5
	12,EPS3,EPS4,EPS5,EPS6,EPI1,EPI2,EPI3,EPI4,EPI5,EPI6,EPI7,VP,AR,LEN	6
	1GTH,APR,BPR,BIGAPR,BIGBPR,ESTAR,ALPHA,BETA,RHOSTR,EPRS,RHOS	7
	COMMON XMESH(20,20,6),XMESH2(20,20,6),Z(20),R(20),SURF(15,8),SURF2	8
	1(15,8),TAB(15,14,2),TAB2(15,14,2),SPART(15,2,2),RARF(15,11),RARF2(	9
	115,4),RPART(15,2)	10
C		11
	COMMON ZO,RO,PO,UO,VO,LO,MO,RHOO,E0,A0,UBARO,VBARO	12
	COMMON NP,NT,NR,NI,NDEL,ISUB	13

///

C	COMMON ZMIN,ZMAX,RMIN,RMAX,RADIUS,GZ,GR,DELTA,H	14
	COMMON DIRCOS	15
	COMMON TIME	16
	COMMON IRARF	17
	COMMON KSTOP	18
	COMMON TPSI	19
	COMMON KKK	20
	REAL LO,M0,LENGTH,MU,KO	21
C		22
	GO TO (5,10,100,205,210,300,500),KODE	23
5	NN=NP	24
	K=1	25
	GO TO 15	26
10	NN=NT	27
	K=2	28
15	AA=(TAB2(1,1,K)-ZP)**2+(TAB2(1,2,K)-RP)**2	29
C		30
C	SEARCH SHOCK TABLES	31
C		32
	DO 60 N=2,NN	33
	A=(TAB2(N,1,K)-ZP)**2+(TAB2(N,2,K)-RP)**2	34
	IF (A.GE.AA) GO TO 23	35
	AA=A	36
60	CONTINUE	37
	PICK2=NN-1	38
	PICK2=PICK2+.2	39
	RETURN	40
23	PICK2=N-1	41
	PICK2=PICK2+.2	42
	RETURN	43
100	AA=(RARF2(1,1)-ZP)**2+(RARF2(1,2)-RP)**2	44
C		45
C	SEARCH RAREFACTION TABLE	46
C		47
	DO 200 N=2,NR	48
		49

	A=(RARF2(N,1)-ZP)**2+(RARF2(N,2)-RP)**2	50
	IF (A.GE.AA) GO TO 203	51
	AA=A	52
200	CONTINUE	53
	PICK2=NR-1	54
	PICK2=PICK2+.2	55
	RETURN	56
203	PICK2=N-1	57
	PICK2=PICK2+.2	58
	RETURN	59
205	NN=NP	60
	K=1	61
	GO TO 215	62
210	NN=NT	63
	K=2	64
215	AA=(SPART(1,1,K)-ZP)**2+(SPART(1,2,K)-RP)**2	65
C		66
C	SEARCH SHOCK PARTICLE TABLES	67
C		68
	DO 260 N=2,NN	69
	A=(SPART(N,1,K)-ZP)**2+(SPART(N,2,K)-RP)**2	70
	IF (A.GE.AA) GO TO 223	71
	AA=A	72
260	CONTINUE	73
	PICK2=NN-1	74
	PICK2=PICK2+.2	75
	RETURN	76
223	PICK2=N-1	77
	PICK2=PICK2+.2	78
	RETURN	79
300	AA=(RPART(1,1)-ZP)**2+(RPART(1,2)-RP)**2	80
C		81
C	SEARCH RAREFACTION PARTICLE TABLE	82
C		83
	DO 400 N=2,NR	84
	A=(RPART(N,1)-ZP)**2+(RPART(N,2)-RP)**2	85

	IF (A.GE.AA) GO TO 403	86
	AA=A	87
400	CONTINUE	88
	PICK2=NR-1	89
	PICK2=PICK2+.2	90
	RETURN	91
403	PICK2=N-1	92
	PICK2=PICK2+.2	93
	RETURN	94
500	AA=(SURF2(1,1)-ZP)**2+(SURF2(1,2)-RP)**2	95
C		96
C	SEARCH FREE SURFACE TABLE	97
C		98
	DO 520 N=2,NP	99
	A=(SURF2(N,1)-ZP)**2+(SURF2(N,2)-RP)**2	100
	IF (A.GE.AA) GO TO 523	101
	AA=A	102
520	CONTINUE	103
	PICK2=NP-1	104
	PICK2=PICK2+.2	105
	RETURN	106
523	PICK2=N-1	107
	PICK2=PICK2+.2	108
	RETURN	109
	DEBUG SUBCHK	
	END	110
	FUNCTION TEST(ZP,RP)	1
C		2
C		3
C	DETERMINES IF A GIVEN INTERIOR POINT IS IN	4
C	THE REGION TO BE CONSIDERED	5
C		6
	COMMON CASEID(14),ITS1,ITS2,ITS3,ITS4,ITI1,ITI2,ITI3,ITI4,EPS1,EPS	7
	12,EPS3,EPS4,EPS5,EPS6,EPI1,EPI2,EPI3,EPI4,EPI5,EPI6,EPI7,VP,AR,LEN	8
	1GTH,APR,BPR,BIGAPR,BIGBPR,ESTAR,ALPHA,BETA,RHOSTR,EPRS,RHOS	9
	COMMON XMesh(20,20,6),XMesh2(20,20,6),Z(20),R(20),SURF(15,8),SURF2	10



	1(15,8),TAB(15,14,2),TAB2(15,14,2),SPART(15,2,2),RARF(15,11),RARF2(	11
	115,4),RPART(15,2)	12
C		13
C		14
	COMMON ZO,RO,PO,UO,VO,LO,MO,RHOO,E0,A0,UBARO,VBARO	15
C		16
	COMMON NP,NT,NR,NI,NDEL,ISUB	17
C		18
	COMMON ZMIN,ZMAX,RMIN,RMAX,RADIUS,GZ,GR,DELTA,H	19
	COMMON DIRCOS	20
	COMMON TIME	21
	COMMON IRARF	22
	COMMON KSTOP	23
	COMMON TPSI	24
	COMMON KKK	25
	REAL LO,MO,LENGTH,MU,KO	26
C		27
	EPS=.0001	28
	IF (ITS3.EQ.1) GO TO 5	29
	IF (RP.GT.(RADIUS+EPS)) GO TO 5	30
	M=PICK2(ZP,RP,7)	31
	FF=ZP-SURF2(M+1,1)-(SURF2(M,1)-SURF2(M+1,1))*(RP-SURF2(M,2))/(SURF	32
	12(M,2)-SURF2(M+1,2))	33
	KICK=5	34
	CALL DVCHK(KQ)	35
	IF (KQ.EQ.1) GO TO 9980	36
	IF (FF) 200,5,5	37
5	CONTINUE	38
	IF (ZP.GT.-EPS) GO TO 1	39
	IF (RP.GT.(RADIUS+EPS)) GO TO 200	40
1	DO 10 K=1,2	41
	IF (ITS3.EQ.1) GO TO 100	42
	M=PICK2(ZP,RP,K)	43
	IF (TAB2(M,2,K).GT.RP.AND.M.NE.1)M=M-1	44
	FF=ZP-TAB2(M+1,1,K)-(TAB2(M,1,K)-TAB2(M+1,1,K))*(RP-TAB2(M+1,2,K))	45
	1/(TAB2(M,2,K)-TAB2(M+1,2,K))	46

	KICK=50	47
	CALL DVCHK(KQ)	48
	IF (KQ.EQ.1) GO TO 9980	49
	IF (K.EQ.2) GO TO 50	50
	IF (RP.GT.RADIUS) GO TO 10	51
	IF (FF) 200,10,10	52
50	IF (FF) 10,10,200	53
10	CONTINUE	54
	DO 20 K=1,2	55
	J=K+3	56
	M=PICK2(ZP,RP,J)	57
	IF (SPART(M,2,K).GT.RP.AND.M.NE.1)M=M-1	58
	FF=ZP-SPART(M+1,1,K)-(SPART(M,1,K)-SPART(M+1,1,K))*(RP-SPART(M+1,2	59
	1,K))/(SPART(M,2,K)-SPART(M+1,2,K))	60
	KICK=15	61
	CALL DVCHK(KQ)	62
	IF (KQ.EQ.1) GO TO 9980	63
	IF (K.EQ.2) GO TO 15	64
	IF (RP.GT.RADIUS) GO TO 20	65
	IF (FF.LT..001) GO TO 300	66
	GO TO 20	67
15	IF (FF.GT.-.001) GO TO 400	68
20	CONTINUE	69
	IF (IRARF.EQ.1) GO TO 100	70
	M=PICK2(ZP,RP,3)	71
	FF=RP-RARF2(M+1,2)-(RARF2(M,2)-RARF2(M+1,2))*(ZP-RARF2(M+1,1))/(RA	72
	1RF2(M,1)-RARF2(M+1,1))	73
	KICK=20	74
	CALL DVCHK(KQ)	75
	IF (KQ.EQ.1) GO TO 9980	76
	IF (FF.LT.0.) GO TO 100	77
	M=PICK2(ZP,RP,6)	78
	FF=RP-RPART(M+1,2)-(RPART(M,2)-RPART(M+1,2))*(ZP-RPART(M+1,1))/(RP	79
	1ART(M,1)-RPART(M+1,1))	80
	KICK=100	81
	CALL DVCHK(KQ)	82

	IF (KQ.EQ.1) GO TO 9980	83
	IF (FF.LT.0.) GO TO 500	84
100	TEST=1	85
	TEST=TEST+.2	86
	RETURN	87
200	TEST=2	88
	TEST=TEST+.2	89
	RETURN	90
300	TEST=3	91
	TEST=TEST+.2	92
	RETURN	93
400	TEST=4	94
	TEST=TEST+.2	95
	RETURN	96
500	TEST=5	97
	TEST=TEST+.2	98
	RETURN	99
9980	WRITE (3,9985) KICK	100
9985	FORMAT (32HODIVIDE CHECK NEAR STATEMENT NO.,I5,14H IN SUBR. TEST/I	101
	1H1)	102
	RETURN	103
	DEBUG SUBCHK	
	END	104
	SUBROUTINE FGOF5(Z5,R5,SS,QQ,PHI,NMAX,MMAX)	
C	SUBROUTINE FGOF5(Z5,R5,SS,QQ)	
C		2
C	COMPUTES S5,Q5 FOR INTERIOR REGION	3
C	ITERATION FOR Z5,R5	4
C		5
	COMMON CASEID(14),ITS1,ITS2,ITS3,ITS4,ITI1,ITI2,ITI3,ITI4,EPS1,EPS	6
	12,EPS3,EPS4,EPS5,EPS6,EPI1,EPI2,EPI3,EPI4,EPI5,EPI6,EPI7,VP,AR,LEN	7
	1GTH,APR,BPR,BIGAPR,BIGBPR,ESTAR,ALPHA,BETA,RHOSTR,EPRS,RHOS	8
	COMMON XMESH(20,20,6),XMESH2(20,20,6),Z(20),R(20),SURF(15,8),SURF2	9
	1(15,8),TAB(15,14,2),TAB2(15,14,2),SPART(15,2,2),RARF(15,11),RARF2(	10
	115,4),RPART(15,2)	11
C		12

C	COMMON ZO,RO,PO,UO,VO,LO,MO,RHOO,EQ,AO,UBARO,VBARO	13
		14
C	COMMON NP,NT,NR,NI,NDEL,ISUB	15
		16
C	COMMON ZMIN,ZMAX,RMIN,RMAX,RADIUS,GZ,GR,DELTA,H	17
	COMMON DIRCOS	18
	COMMON TIME	19
	COMMON IRARF	20
	COMMON KSTOP	21
	COMMON TPSI	22
	COMMON KKK	23
	REAL LO,MO,LENGTH,MU,KO	24
	DOUBLE PRECISION PHI(20,20,6)	25
C		26
	DIMENSION ANS(6)	27
C		28
	TSSS=1.1	
	IF(TIME.GT.TSSS) GO TO 100	
	CALL DBLTRP(Z5,R5,ANS)	
	GO TO 101	
100	CALL DSURFT(Z5,R5,ANS,PHI,NMAX,MMAX)	
101	U5=ANS(2)	
C	U5=ANS(2)	31
	V5=ANS(3)	32
	SS=Z5-ZO+H*V5	33
	QQ=R5-RO+H*U5	34
	RETURN	
	DEBUG SUBCHK	
	END	35
	SUBROUTINE ITRP	1
	COMMON CASEID(14),ITS1,ITS2,ITS3,ITS4,ITI1,ITI2,ITI3,ITI4,EPS1,EPS	2
	12,EPS3,EPS4,EPS5,EPS6,EPI1,EPI2,EPI3,EPI4,EPI5,EPI6,EPI7,VP,AR,LEN	3
	1GTH,APR,BPR,BIGAPR,BIGBPR,ESTAR,ALPHA,BETA,RHOSTR,EPRS,RHOS	4
	COMMON XMESH(20,20,6),XMESH2(20,20,6),Z(20),R(20),SURF(15,8),SURF2	5
	1(15,8),TAB(15,14,2),TAB2(15,14,2),SPART(15,2,2),RARF(15,11),RARF2(	6

118

	115,4),RPART(15,2)	7
C		8
C		9
	COMMON ZO,RO,PO,UO,VO,LO,MO,RHOO,E0,A0,UBARO,VBARO	10
C		11
	COMMON NP,NT,NR,NI,NDEL,ISUB	12
C		13
	COMMON ZMIN,ZMAX,RMIN,RMAX,RADIUS,GZ,GR,DELTA,H	14
	COMMON DIRCOS	15
	COMMON TIME	16
	COMMON IRARF	17
	COMMON KSTOP	18
	COMMON TPSI	19
	COMMON KKK	20
C		21
C		22
	REAL LO,MO,LENGTH,MU,KO	23
C		24
C	INTERPOLATION SCHEME FOR POINTS BETWEEN PARTICLE CURVES	25
C	AND DISCONTINUITIES	26
C		27
	EPS=.0000001	28
	KOD1=0	29
	KOD2=0	30
	DO 1000 J=1,20	31
	DO 1000 I=1,20	32
	M=TEST(Z(I),R(J))	33
	IF (M.NE.5) GO TO 906	34
	IF (IRARF.EQ.1) GO TO 906	35
	NR1=NR-1	36
	DO 907 JJ=1,NR1	37
	IF (RARF2(JJ,1).LT.Z(I).AND.RARF2(JJ+1,1).GT.Z(I)) GO TO 908	38
907	CONTINUE	39
908	CONTINUE	40
	FF=R(J)-RARF2(JJ+1,2)+(RARF2(JJ,2)-RARF2(JJ+1,2))*(Z(I)-RARF2(JJ+1,1))/(RARF2(JJ,1)-RARF2(JJ+1,1))	41
		42

	IF (FF.LT.0.) GO TO 1000	43
906	CONTINUE	44
	IF (M.EQ.3.AND.Z(I).LT.EPS.AND.ABS(R(J)-RADIUS).LT.EPS) GO TO 1000	45
	IF (M.LT.3) GO TO 8051	46
	WRITE (3,8050)	47
8050	FORMAT (30H0INTERPOLATION SCHEME EMPLOYED)	48
614	FORMAT (1X5HZ0 =,E15.8,4X5HRO =,E15.8)	49
	Z0=Z(I)	50
	RO=R(J)	51
	WRITE (3,614) Z0,RO	52
	WRITE (3,8888) M	53
8888	FORMAT (1X4HM =,I4)	54
8051	CONTINUE	55
	GO TO (1000,1000,1001,1010,1100),M	56
1001	IF (IRARF.EQ.1) GO TO 1003	57
	M=PICK2(Z(I),R(J),3)	58
	FF=R(J)-RARF2(M+1,2)+(RARF2(M,2)-RARF2(M+1,2))*(Z(I)-RARF2(M+1,1))	59
	1/(RARF2(M,1)-RARF2(M+1,1))	60
	IF (FF.GT.0.) GO TO 1003	61
	DO 8002 K=1,6	62
	L=K+2	63
8002	XMESH2(I,J,K)=RARF(1,L)	64
	GO TO 1000	65
1003	L=1+1	66
	N=TEST(Z(L),R(J))	67
	GO TO (1004,1007,1030,1030,1050),N	68
1004	M=PICK2(Z(I),R(J),1)	69
	DO 1006 K=1,8	70
	ANS=TAB2(M,K,1)+(TAB2(M+1,K,1)-TAB2(M,K,1))*(R(J)-TAB2(M,2,1))/(TA	71
	1B2(M+1,2,1)-TAB2(M,2,1))	72
	IF (K.NE.1) GO TO 8005	73
	ANS1=ANS	74
	GO TO 1006	75
8005	CONTINUE	76
	IF (K.EQ.2) GO TO 1006	77
	KX=K-2	78

	IF (ABS(R(J)-RADIUS).GT.EPS) GO TO 9024	79
	IF (K.GT.5.OR.K.LT.4) GO TO 9024	80
	ANS=TAB2(M+1,K,1)	81
9024	CONTINUE	82
	XMESH2(I,J,KX)=ANS+(XMESH2(L,J,KX)-ANS)*(Z(I)-ANS1)/(Z(L)-ANS1)	83
	IF (ABS(R(J)-RADIUS).GT.EPS) GO TO 1006	84
	XMESH2(I,J,1)=0.	85
	XMESH2(I,J,4)=RHOSTR	86
	XMESH2(I,J,5)=0.	87
	XMESH2(I,J,6)=SQRT(BIGAPR/RHOSTR)	88
1006	CONTINUE	89
	GO TO 1000	90
1007	MM=PICK2(Z(I),R(J),2)	91
	M=PICK2(Z(I),R(J),1)	92
	DO 1009 K=1,8	93
	ANS=TAB2(M,K,1)+(TAB2(M+1,K,1)-TAB2(M,K,1))*(R(J)-TAB2(M,2,1))/(TAB2(M+1,2,1)-TAB2(M,2,1))	94
	ANSW=TAB2(MM,K,2)+(TAB2(MM+1,K,2)-TAB2(MM,K,2))*(R(J)-TAB2(MM,2,2))/(TAB2(MM+1,2,2)-TAB2(MM,2,1))	95
	IF (K.NE.1) GO TO 1008	96
	ANS1=ANS	97
	ANS2=ANSW	98
	GO TO 1009	99
1008	CONTINUE	100
	IF (K.EQ.2) GO TO 1009	101
	KX=K-2	102
	XMESH2(I,J,KX)=ANS+(ANSW-ANS)*(Z(I)-ANS1)/(ANS2-ANS1)	103
1009	CONTINUE	104
	GO TO 1000	105
1010	IF (IRARF.EQ.1) GO TO 1013	106
	M=PICK2(Z(I),R(J),3)	107
	FF=R(J)-RARF2(M+1,2)+(RARF2(M,2)-RARF2(M+1,2))*(Z(I)-RARF2(M+1,1))/(RARF2(M,1)-RARF2(M+1,1))	108
	IF (FF.GT.0.) GO TO 1013	109
	DO 1012 K=1,6	110
	L=K+2	111
		112
		113
		114

121

1012	XMESH2(I,J,K)=RARF(1,L)	115
	GO TO 1000	116
1013	L=I-1	117
	IF (ABS(Z(I)).LT.EPS) GO TO 1017	118
	N=TEST(Z(L),R(J))	119
	GO TO (1014,1017,1030,1017,1051),N	120
1014	M=PICK2(Z(I),R(J),2)	121
	DO 1016 K=1,8	122
	ANS=TAB2(M,K,2)+(TAB2(M+1,K,2)-TAB2(M,K,2))*(R(J)-TAB2(M,2,2))/(TAB2(M+1,2,2)-TAB2(M,2,2))	123
	IF (K.NE.1) GO TO 1015	124
	ANS1=ANS	125
	GO TO 1016	126
1015	CONTINUE	127
	IF (K.EQ.2) GO TO 1016	128
	KX=K-2	129
	XMESH2(I,J,KX)=ANS+(XMESH2(L,J,KX)-ANS)*(Z(I)-ANS1)/(Z(L)-ANS1)	130
1016	CONTINUE	131
	GO TO 1000	132
1017	L=J-1	133
	N=TEST(Z(I),R(L))	134
	GO TO (1024,1030,1030,1030,1051),N	135
1024	M=PICK2(Z(I),R(J),2)	136
	DO 1026 K=2,8	137
	ANS=TAB2(M,K,2)+(TAB2(M+1,K,2)-TAB2(M,K,2))*(Z(I)-TAB2(M,1,2))/(TAB2(M+1,1,2)-TAB2(M,1,2))	138
	IF (K.NE.2) GO TO 1025	139
	ANS1=ANS	140
	GO TO 1026	141
1025	CONTINUE	142
	KX=K-2	143
	IF (ABS(Z(I)).GT.EPS) GO TO 9125	144
	IF (K.GT.5.OR.K.LT.4) GO TO 9125	145
	ANS=TAB2(M+1,K,2)	146
9125	CONTINUE	147
	XMESH2(I,J,KX)=ANS+(XMESH2(I,L,KX)-ANS)*(R(J)-ANS1)/(R(L)-ANS1)	148
		149
		150



	IF (ABS(Z(I)).GT.EPS) GO TO 1026	151
	XMESH2(I,J,1)=0.	152
	XMESH2(I,J,4)=RHOSTR	153
	XMESH2(I,J,5)=0.	154
	XMESH2(I,J,6)=SQRT(BIGAPR/RHOSTR)	155
1026	CONTINUE	156
	GO TO 1000	157
1100	M=PICK2(Z(I),R(J),3)	158
	ANS1=RARF2(M+1,2)+(RARF2(M,2)-RARF2(M+1,2))*(Z(I)-RARF2(M+1,1))/(R	159
	1ARF2(M,1)-RARF2(M+1,1))	160
	L=J+1	161
	M=TEST(Z(I),R(L))	162
	GO TO (1101,1030,1051,1030),M	163
1101	CONTINUE	164
	DO 1106 K=1,6	165
	LL=K+2	166
	XMESH2(I,J,K)=RARF(1,LL)+(XMESH2(I,L,K)-RARF(1,LL))*(R(J)-ANS1)/(R	167
	1(L)-ANS1)	168
1106	CONTINUE	169
	GO TO 1000	170
1050	JJ1=J	171
	II1=I	172
	KOD1=1	173
	GO TO 1000	174
1051	JJ2=J	175
	II2=I	176
	KOD2=1	177
1000	CONTINUE	178
	IF (KOD1.EQ.0) GO TO 2000	179
	M=PICK2(Z(II1),R(JJ1),1)	180
	DO 2016 K=1,8	181
	ANS=TAB2(M,K,1)+(TAB2(M+1,K,1)-TAB2(M,K,1))*(R(JJ1)-TAB2(M,2,1))/(	182
	1TAB2(M+1,2,1)-TAB2(M,2,1))	183
	IF (K.NE.1) GO TO 2005	184
	ANS1=ANS	185
	GO TO 2016	186

2005	CONTINUE	187
	I=II1	188
	J=JJ1	189
	L=II1+1	190
	IF (K.EQ.2) GO TO 2016	191
	KX=K-2	192
	XMESH2(I,J,KX)=ANS+(XMESH2(L,J,KX)-ANS)*(Z(I)-ANS1)/(Z(L)-ANS1)	193
2016	CONTINUE	194
2000	IF (KOD2.EQ.0) GO TO 3000	195
	M=PICK2(Z(II2),R(JJ2),2)	196
	DO 3016 K=1,8	197
	ANS=TAB2(M,K,2)+(TAB2(M+1,K,2)-TAB2(M,K,2))*(R(JJ2)-TAB2(M,2,2))/(	198
	1TAB2(M+1,2,2)-TAB2(M,2,2))	199
	IF (K.NE.1) GO TO 3015	200
	ANS1=ANS	201
	GO TO 3016	202
3015	CONTINUE	203
	I=II2	204
	J=JJ2	205
	L=II2-1	206
	IF (K.EQ.2) GO TO 3016	207
	KX=K-2	208
	XMESH2(I,J,KX)=ANS+(XMESH2(L,J,KX)-ANS)*(Z(I)-ANS1)/(Z(L)-ANS1)	209
3016	CONTINUE	210
3000	CONTINUE	211
	GO TO 3017	212
1030	WRITE (3,1040) I,J	213
1040	FORMAT (27H0 TIME STEP TOO LARGE AT I=,I4,2HJ=,I4,///)	214
	CALL EXIT	215
3017	CONTINUE	216
C		217
C		218
	RETURN	219
	DEBUG SUBCHK	
	END	220
	SUBROUTINE EXIT	1

C	COMMON CASEID(14), ITS1, ITS2, ITS3, ITS4, ITI1, ITI2, ITI3, ITI4, EPS1, EPS	2
	12, EPS3, EPS4, EPS5, EPS6, EPI1, EPI2, EPI3, EPI4, EPI5, EPI6, EPI7, VP, AR, LEN	3
	1GTH, APR, BPR, BIGAPR, BIGBPR, ESTAR, ALPHA, BETA, RHOSTR, EPRS, RHOS	4
	COMMON XMESH(20,20,6), XMESH2(20,20,6), Z(20), R(20), SURF(15,8), SURF2	5
	1(15,8), TAB(15,14,2), TAB2(15,14,2), SPART(15,2,2), RARF(15,11), RARF2(	6
	115,4), RPART(15,2)	7
		8
C		9
C	COMMON ZO, RO, PO, UO, VO, LO, MO, RHOO, EO, AO, UBARO, VBARO	10
		11
C	COMMON NP, NT, NR, NI, NDEL, ISUB	12
		13
C	COMMON ZMIN, ZMAX, RMIN, RMAX, RADIUS, GZ, GR, DELTA, H	14
	COMMON DIRCOS	15
	COMMON TIME	16
	COMMON IRARF	17
	COMMON KSTOP	18
	COMMON TPSI	19
	COMMON KKK	20
	REAL LO, MO, LENGTH, MU, KO	21
	KSTOP=1	22
	STOP	23
	END	24
	SUBROUTINE FGOFI(ZX, RX, SS, QQ, PHI, NMAX, MMAX)	25
	SUBROUTINE FGOFI(ZX, RX, SS, QQ)	
C		2
C	COMPUTES SI, QI FOR INTERIOR REGION	3
C	ITERATION FOR ZI, RI	4
C		5
	COMMON CASEID(14), ITS1, ITS2, ITS3, ITS4, ITI1, ITI2, ITI3, ITI4, EPS1, EPS	6
	12, EPS3, EPS4, EPS5, EPS6, EPI1, EPI2, EPI3, EPI4, EPI5, EPI6, EPI7, VP, AR, LEN	7
	1GTH, APR, BPR, BIGAPR, BIGBPR, ESTAR, ALPHA, BETA, RHOSTR, EPRS, RHOS	8
	COMMON XMESH(20,20,6), XMESH2(20,20,6), Z(20), R(20), SURF(15,8), SURF2	9
	1(15,8), TAB(15,14,2), TAB2(15,14,2), SPART(15,2,2), RARF(15,11), RARF2(	10
	115,4), RPART(15,2)	11

C		12
C		13
	COMMON ZO,RO,PO,UO,VO,LO,MO,RHOO,E0,A0,UBARO,VBARO	14
C		15
	COMMON NP,NT,NR,NI,NDEL,ISUB	16
C		17
	COMMON ZMIN,ZMAX,RMIN,RMAX,RADIUS,GZ,GR,DELTA,H	18
	COMMON DIRCOS	19
	COMMON TIME	20
	COMMON IRARF	21
	COMMON KSTOP	22
	COMMON TPSI	23
	COMMON KKK	24
	REAL LO,MO,LENGTH,MU,KO	25
C		26
	DIMENSION ANS(6),PSI(4),SPSI(11),CPSI(11)	27
	DOUBLE PRECISION PHI(20,20,6)	
C		28
C		29
C		30
C		31
C		32
	TSSS=1.1	
	IF(TIME.GT.TSSS) GO TO 100	
	CALL DBLTRP(ZX,RX,ANS)	
	GO TO 101	
100	CALL DSURFT(ZX,RX,ANS,PHI,NMAX,MMAX)	
101	UI=ANS(2)	
C	UI=ANS(2)	35
	VI=ANS(3)	36
	AI=ANS(6)	37
	SS=ZX-ZO+H*(VI+AI*SIN(TPSI))	38
	QQ=RX-RO+H*(UI+AI*COS(TPSI))	39
	RETURN	

II.2. Method of Characteristics Calculations and the Computer Code  
for Materials with Arbitrary Equations of State.

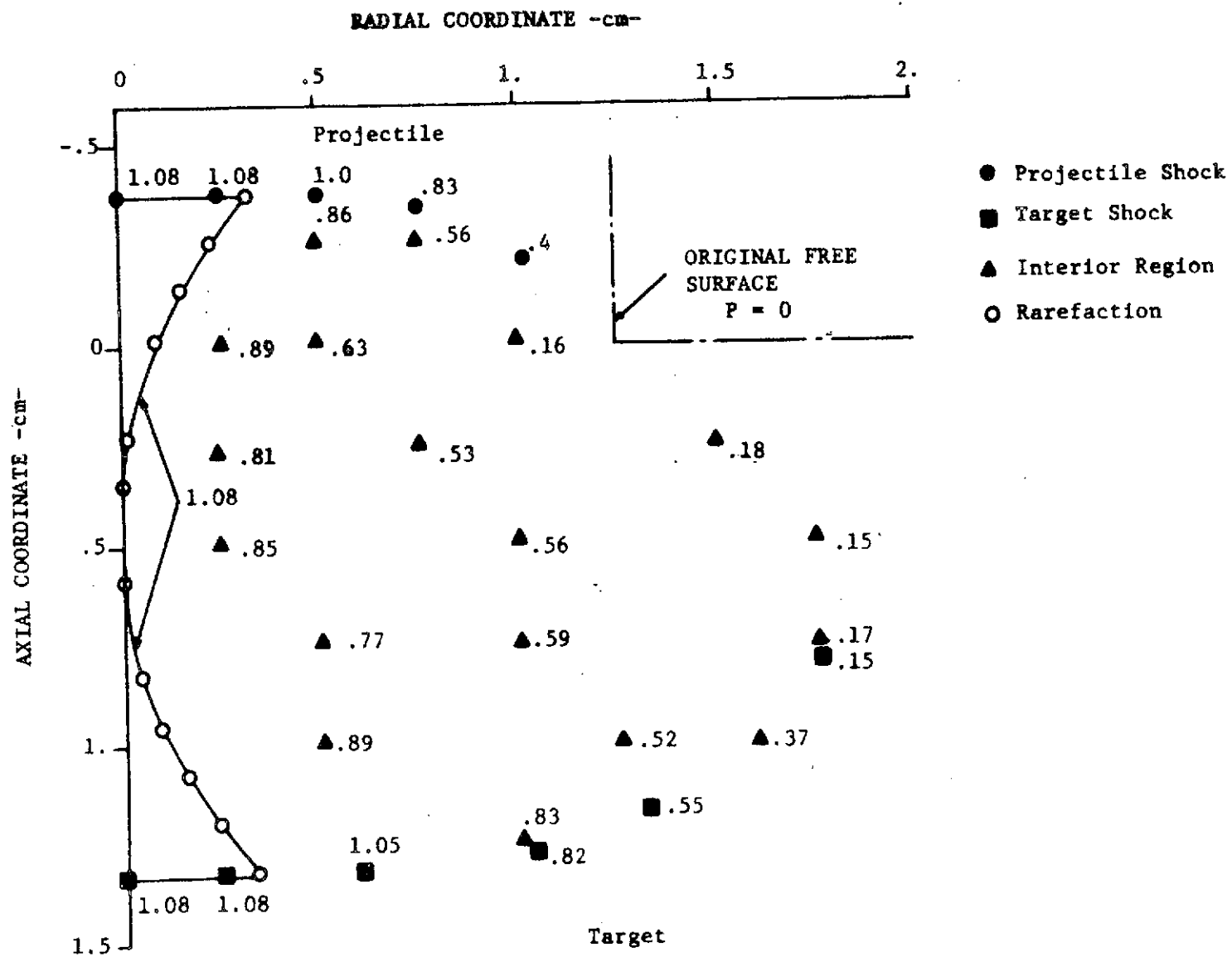


Fig. 1. Pressure distribution from the characteristic solution at  $t = 1.25 \mu\text{sec}$  after impact of a 2.5 -cm- diameter projectile at 0.76 cm/ $\mu\text{sec}$  on an aluminum half-space.

128

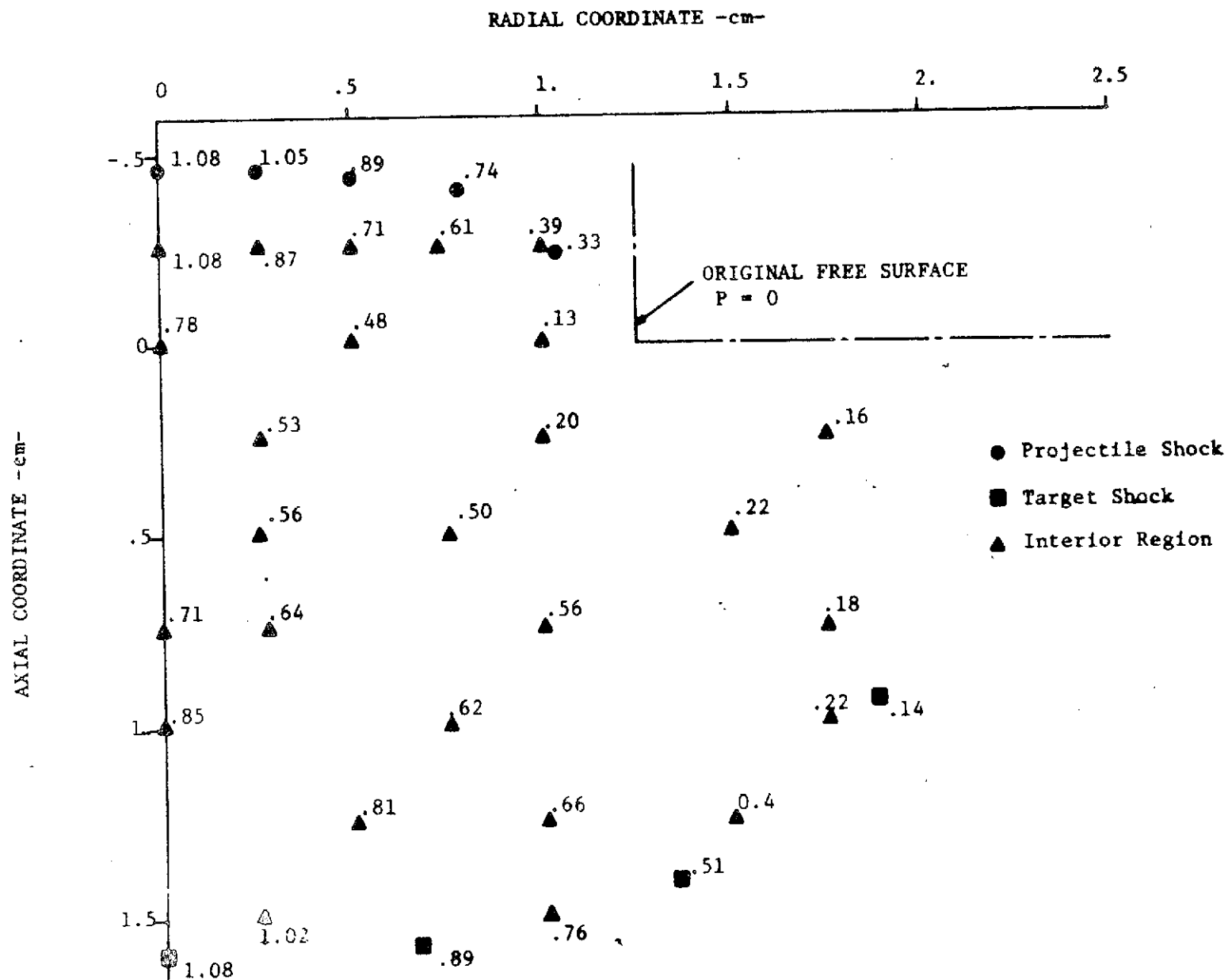


Fig. 2. Pressure distribution from the characteristic solution at  $t = 1.52 \mu\text{sec}$  after impact of a 2.5 -cm- diameter projectile at 0.76 cm/ $\mu\text{sec}$  on an aluminum half-space.

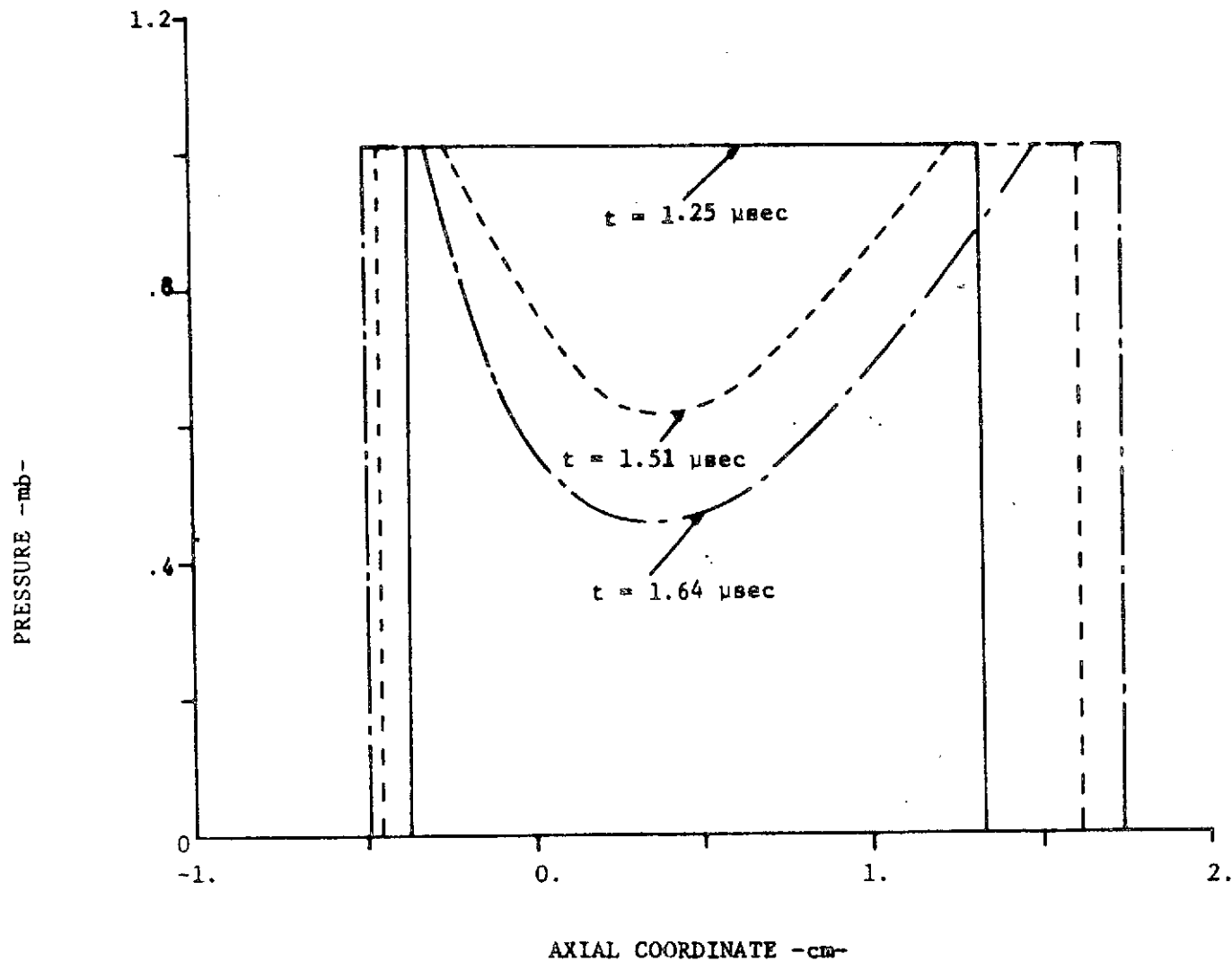


Fig 3. Axial pressure profiles at various times as predicted by the characteristic method for a 2.5 -cm- diameter aluminum projectile impacting on aluminum half-space at 0.76 cm/ $\mu\text{sec}$ .



	COMMON CASEID(14), ITS1, ITS2, ITS3, ITS4, ITI1, ITI2, ITI3, ITI4, EPS1, EPSMAIN	1
	12, EPS3, EPS4, EPS5, EPS6, EPI1, EPI2, EPI3, EPI4, EPI5, EPI6, EPI7, VP, AR, LENMAIN	2
	1GTH, APR, BPR, BIGAPR, BIGBPR, ESTAR, ALPHA, BETA, RHOSTR, EPRS, RHDS	MAIN 3
	COMMON XMESH(20,20,6), XMESH2(20,20,6), Z(20), R(20), SURF(15,8), SURF2MAIN	4
	1(15,8), TAB(15,14,2), TAB2(15,14,2), SPART(15,2,2), RARF(15,11), RARF2(	MAIN 5
	115,4), RPART(15,2)	MAIN 6
C		MAIN 7
C		MAIN 8
	COMMON ZO, RO, PO, UO, VO, LO, MO, RHOO, EO, AO, UBARO, VBARO	MAIN 9
C		MAIN 10
	COMMON NP, NT, NR, NI, NDEL, ISUB	MAIN 11
C		MAIN 12
	COMMON ZMIN, ZMAX, RMIN, RMAX, RADIUS, GZ, GR, DELTA, H	MAIN 13
	COMMON DIRCOS	MAIN 14
	COMMON TIME	MAIN 15
	COMMON IRARF	MAIN 16
	COMMON KSTOP	MAIN 17
	COMMON TPSI	MAIN 18
	COMMON KKK	MAIN 19
C		MAIN 20
C		MAIN 21
	REAL LO, MO, LENGTH, MU, KO	MAIN 22
	KR=10	MAIN 23
	EPS=.0000001	MAIN 24
	KSTOP=0	MAIN 25
1	FORMAT (1H1)	MAIN 26
	CALL DVCHK(KEY)	MAIN 27
	KICK=0	MAIN 28
	IF (KEY.EQ.1) GO TO 9980	MAIN 29
C		MAIN 30
	DO 2 K=1,6	MAIN 31
	DO 2 J=1,20	MAIN 32
	DO 2 I=1,20	MAIN 33
	XMESH(I,J,K)=0.	MAIN 34
	XMESH2(I,J,K)=0.	MAIN 35
2	CONTINUE	MAIN 36

C	KRW=0	MAIN	37
	NUZON=0	MAIN	38
C		MAIN	39
C		MAIN	40
	WRITE (3,4)	MAIN	41
C		MAIN	42
C	DATA INPUT SECTION	MAIN	43
C		MAIN	44
4	FORMAT (52H1HYPERVELOCITY IMPACT METHOD OF CHARACTERISTICS CODE///	MAIN	45
	1)	MAIN	46
C	ID AND FX. PT. CONSTANTS	MAIN	47
C		MAIN	48
	READ (1,8) CASEID,ITS1,ITS2,ITS3,ITS4,ITI1,ITI2,ITI3,ITI4,NDEL	MAIN	49
8	FORMAT (13A6,A2/9I3)	MAIN	50
	IRARF=ITI2	MAIN	51
C		MAIN	52
C	FL. PT. CONSTANTS	MAIN	53
C		MAIN	54
	READ (1,15) EPS1,EPS2,EPS3,EPS4,EPS5,EPS6,EPI1,EPI2,EPI3,EPI4,EPI5	MAIN	55
	1,EPI6,EPI7	MAIN	56
	READ (1,14) NP,NT,NR	MAIN	57
14	FORMAT (3I3)	MAIN	58
	READ (1,15) APR,BPR,BIGAPR,BIGBPR,ESTAR,ALPHA,BETA,RHOSTR,EPRS,REF	MAIN	59
	1L	MAIN	60
	READ (1,15) ZMIN,ZMAX,RMIN,RMAX,GR,GZ,DELTA,VP,LENGTH,RADIUS,HSTAR	MAIN	61
15	FORMAT (6E12.8)	MAIN	62
	READ (1,15) RST	MAIN	63
	IF (RST.GT.0.) GO TO 16	MAIN	64
	REWIND 9	MAIN	65
C	DO 1529 JTP=1,200	MAIN	66
	READ (9)TIME	MAIN	67
C	IF (ABS(RST+TIME).LT..001) GO TO 1530	MAIN	68
C	READ(9)BLOB	MAIN	69
C1529	CONTINUE	MAIN	70
1530	CONTINUE	MAIN	71
C	KRW=1	MAIN	72

	READ (9)((X(MESH(I,J,K),I=1,20),J=1,20),K=1,6),(Z(I),I=1,20),(R(I)MAIN	73
	1,I=1,20),(SURF(I,J),I=1,15),J=1,8),((TAB(I,J,K),I=1,15),J=1,14),MAIN	74
	1K=1,2),(RARF(I,J),I=1,15),J=1,11),TIME,ZMIN,ZMAX,RMIN,RMAX,GR,GZ,MAIN	75
	1AR	MAIN 76
	DO 1500 J=1,20	MAIN 77
	DO 1500 I=1,20	MAIN 78
	DO 1500 K=1,6	MAIN 79
1500	XMESH2(I,J,K)=XMESH(I,J,K)	MAIN 80
	DO 1501 I=1,15	MAIN 81
	DO 1501 J=1,8	MAIN 82
1501	SURF2(I,J)=SURF(I,J)	MAIN 83
	WRITE (3,145) TIME	MAIN 84
	CALL SOUT	MAIN 85
	CALL PRINT(XMESH2,Z,R,1)	MAIN 86
	KREFL=0	MAIN 87
16	CONTINUE	MAIN 88
	WRITE (3,10) CASEID,ITS1,ITS2,ITS3,ITS4,ITI1,ITI2,ITI3,ITI4,NDEL	MAIN 89
10	FORMAT (1X13A6,A2//17H SHOCK ITERATIONS6X,4I4//20H INTERIOR ITERATMAIN	90
	1IONS3X,4I4//7H NDEL =,14//)	MAIN 91
	WRITE (3,18) EPS1,EPS2,EPS3,EPS4,EPS5,EPS6,EPI1,EPI2,EPI3,EPI4,EPIMAIN	92
	15,EPI6,EPI7,ZMIN,ZMAX,RMIN,RMAX,DELTA,VP,LENGTH,RADIUS,APR,BPR,BIGMAIN	93
	1APR,BIGBPR,ESTAR,ALPHA,BETA,RHOSTR,EPRS,REFL	MAIN 94
18	FORMAT (///38H ERROR CRITERIA FOR SHOCK COMPUTATIONS//5X8HDELTA Z1MAIN	95
	18X8HDELTA R18X9HDELTA RHO7X7HDELTA E9X7HDELTA P9X7HDELTA U/6E16.6/MAIN	96
	1//41H ERROR CRITERIA FOR INTERIOR COMPUTATIONS//5X8HDELTA Z18X8HDEMAIN	97
	1LTA R18X7HDELTA P9X7HDELTA U9X7HDELTA V9X9HDELTA RHO7X7HDELTA E/7EMAIN	98
	116.6///5X4HZMIN12X4HZMAX12X4HRMIN12X4HRMAX12X5HDELTA11X2HV14X6HLEMAIN	99
	1NGTH10X6HRADIUS/8E16.6///5X2HA*14X2HB*14X6HBIG A*10X6HBIG B*10X2HEMAIN	100
	1*14X5HALPHA11X4HBETA12X4HRHO*/8E16.6//5X3HE*S13X4HREFL/2E16.6///) MAIN	101
	IF (RST.LT.0.) GO TO 140	MAIN 102
C		MAIN 103
C	STORE RHO* IN ALL XMESH	MAIN 104
C		MAIN 105
	DO 22 J=1,20	MAIN 106
	DO 22 I=1,20	MAIN 107
22	XMESH(I,J,4)=RHOSTR	MAIN 108

40	FORMAT (5E12.8)	MAIN 109
C		MAIN 110
C	PROJECTILE SHOCK	MAIN 111
C		MAIN 112
	CALL EQOS1(PRHO,PPP,PVV,PEE,TEE,TRHO,KICK)	MAIN 113
	IF (KICK.EQ.2200) GO TO 9980	MAIN 114
	DO 230 N=1,NP	MAIN 115
	TAB(N,1,1)=(PRHO*PVV-RHOSTR*VP)*HSTAR/(PRHO-RHOSTR)	MAIN 116
	EE=N-1	MAIN 117
	FNP=NP	MAIN 118
	TAB(N,2,1)=RMIN+EE*(RADIUS-RMIN)/FNP	MAIN 119
	TAB(N,3,1)=PPP	MAIN 120
	TAB(N,4,1)=0.0	MAIN 121
	TAB(N,5,1)=PVV	MAIN 122
	TAB(N,6,1)=PRHO	MAIN 123
	TAB(N,7,1)=PEE	MAIN 124
	TAB(N,9,1)=0.0	MAIN 125
	TAB(N,10,1)=1.0	MAIN 126
230	CONTINUE	MAIN 127
C		MAIN 128
C	TARGET SHOCK	MAIN 129
C		MAIN 130
	M=0	MAIN 131
	DO 240 N=1,NT	MAIN 132
	EE=N-1	MAIN 133
	FNT=NT-4	MAIN 134
	TAB(N,2,2)=RMIN+EE*(RADIUS-RMIN)/FNT	MAIN 135
	TAB(N,7,2)=TEE	MAIN 136
	TAB(N,6,2)=TRHO	MAIN 137
	TAB(N,3,2)=PPP	MAIN 138
	IF (TAB(N,2,2).GT.RADIUS) GO TO 250	MAIN 139
	TAB(N,1,2)=TRHO*PVV*HSTAR/(TRHO-RHOSTR)	MAIN 140
	TAB(N,4,2)=0.0	MAIN 141
	TAB(N,5,2)=PVV	MAIN 142
	TAB(N,9,2)=0.0	MAIN 143
	TAB(N,10,2)=1.0	MAIN 144

	GO TO 240	MAIN 145
250	EF=M	MAIN 146
	TAB(N,9,2)=SIN(.5236+EF*.2618)	MAIN 147
	TAB(N,10,2)=COS(.5236+EF*.2618)	MAIN 148
	TAB(N,4,2)=PVV*TAB(N,9,2)	MAIN 149
	TAB(N,5,2)=PVV*TAB(N,10,2)	MAIN 150
	TAB(N,1,2)=TAB(1,1,2)*TAB(N,10,2)	MAIN 151
	TAB(N,2,2)=RADIUS+TAB(1,1,2)*TAB(N,9,2)	MAIN 152
	M=M+1	MAIN 153
240	CONTINUE	MAIN 154
C		MAIN 155
C	RAREFACTION	MAIN 156
C		MAIN 157
	CALL EQOS2(PPP,PRHO,PEE)	MAIN 158
	EE=NR-1	MAIN 159
	ADEL=(TAB(1,1,2)-TAB(1,1,1))/EE	MAIN 160
	RARF(1,1)=TAB(1,1,2)	MAIN 161
	DO 205 N=2, NR	MAIN 162
	RARF(N,1)=RARF(N-1,1)-ADEL	MAIN 163
205	CONTINUE	MAIN 164
	DO 210 N=1, NR	MAIN 165
	RARF(N,10)=(RARF(N,1)/HSTAR-.5*VP1)/AR	MAIN 166
	RARF(N,9)=-SQRT(1.-RARF(N,10)**2)	MAIN 167
	RARF(N,2)=RADIUS+HSTAR*AR*RARF(N,9)	MAIN 168
210	CONTINUE	MAIN 169
	DO 220 N=1, NR	MAIN 170
	RARF(N,3)=TAB(1,3,1)	MAIN 171
	RARF(N,4)=0.	MAIN 172
	RARF(N,5)=TAB(1,5,1)	MAIN 173
	RARF(N,6)=TAB(1,6,1)	MAIN 174
	RARF(N,7)=TAB(1,7,1)	MAIN 175
220	CONTINUE	MAIN 176
C	REGION INTERIOR TO SHOCKS	MAIN 177
	I=-ZMIN/GZ+1.2	MAIN 178
	J=0	MAIN 179
260	J=J+1	MAIN 180

	XMESH(I,J,1)=PPP	MAIN 181
	XMESH(I,J,3)=PVV	MAIN 182
	XMESH(I,J,4)=PRHO	MAIN 183
	XMESH(I,J,5)=PEE	MAIN 184
	EE=(J-1)	MAIN 185
	IF ((EE*GR-RADIUS).LT.-EPS) GO TO 260	MAIN 186
	XMESH(I,J,1)=0.	MAIN 187
	XMESH(I,J,4)=RHOSTR	MAIN 188
	XMESH(I,J,5)=0.	MAIN 189
C		MAIN 190
C	FREE SURFACE	MAIN 191
C		MAIN 192
	DO 50 I=1,NP	MAIN 193
	SURF(I,1)=-LENGTH+VP*HSTAR	MAIN 194
	SURF(I,2)=TAB(I,2,1)	MAIN 195
	SURF(I,3)=0.	MAIN 196
	SURF(I,4)=0.	MAIN 197
	SURF(I,5)=VP	MAIN 198
	SURF(I,6)=RHOSTR	MAIN 199
	SURF(I,7)=0.	MAIN 200
	SURF(I,8)=SQRT(8IGAPR/RHOSTR)	MAIN 201
50	CONTINUE	MAIN 202
	DO 51 I=1,NP	MAIN 203
	DO 51 J=1,8	MAIN 204
51	SURF2(I,J)=SURF(I,J)	MAIN 205
	IF (NUZON.EQ.0) GO TO 5001	MAIN 206
5000	GR=GR*2.	MAIN 207
	GZ=GZ*2.	MAIN 208
	ZMAX=ZMAX*2.-ZMIN	MAIN 209
	RMAX=RMAX*2.	MAIN 210
	NUZON=1	MAIN 211
	WRITE (3,5003)	MAIN 212
5003	FORMAT (7H REZONE///)	MAIN 213
5001	CONTINUE	MAIN 214
C		MAIN 215
C		MAIN 216

```

      DO 55 I=1,20
      EE=I-1
      Z(I)=ZMIN+EE*GZ
      R(I)=RMIN+EE*GR
55    CONTINUE
      IF (NUZON.EQ.0) GO TO 5101
      DO 5100 I=1,10
      DO 5100 J=1,10
      DO 5100 K=1,6
      L=2*I-1
      M=2*J-1
      XMESH(I,J,K)=XMESH(L,M,K)
5100  CONTINUE
      GO TO 157
5101  CONTINUE
C
C      COMPUTE A FOR 2 SHOCKS AND MESH
C
      DO 86 K=1,3
      GO TO (57,59,61),K
57    NN=NP
      JJ=1
      GO TO 63
59    NN=NT
      JJ=1
      GO TO 63
61    NN=20
      JJ=20
63    DO 84 N=1,NN
      DO 82 J=1,JJ
      GO TO (65,65,68),K
65    P=TAB(N,3,K)
      RHO=TAB(N,6,K)
      E=TAB(N,7,K)
      GO TO 70
68    P=XMESH(J,N,1)

```

```

MAIN 217
MAIN 218
MAIN 219
MAIN 220
MAIN 221
MAIN 222
MAIN 223
MAIN 224
MAIN 225
MAIN 226
MAIN 227
MAIN 228
MAIN 229
MAIN 230
MAIN 231
MAIN 232
MAIN 233
MAIN 234
MAIN 235
MAIN 236
MAIN 237
MAIN 238
MAIN 239
MAIN 240
MAIN 241
MAIN 242
MAIN 243
MAIN 244
MAIN 245
MAIN 246
MAIN 247
MAIN 248
MAIN 249
MAIN 250
MAIN 251
MAIN 252

```

	RHO=XMESH(J,N,4)	MAIN 253
	E=XMESH(J,N,5)	MAIN 254
70	CONTINUE	MAIN 255
	CALL EQOS3(RHO,AA,E,P)	MAIN 256
	GO TO (76,76,78),K	MAIN 257
76	TAB(N,8,K)=AA	MAIN 258
	GO TO 82	MAIN 259
78	XMESH(J,N,6)=AA	MAIN 260
82	CONTINUE	MAIN 261
84	CONTINUE	MAIN 262
86	CONTINUE	MAIN 263
	KICK=86	MAIN 264
	CALL DVCHK(KQ)	MAIN 265
	IF (KQ.EQ.1) GO TO 9980	MAIN 266
C		MAIN 267
C	STORE A FOR RAREFACTION	MAIN 268
C		MAIN 269
	DO 90 I=1,NR	MAIN 270
90	RARF(I,8)=AR	MAIN 271
C		MAIN 272
C	COMPLETE SHOCK TABLES	MAIN 273
C		MAIN 274
	DO 99 K=1,2	MAIN 275
	GO TO (92,94),K	MAIN 276
92	NN=NP	MAIN 277
	GO TO 95	MAIN 278
94	NN=NT	MAIN 279
	US=0.	MAIN 280
95	DO 97 N=1,NN	MAIN 281
	GO TO (93,96),K	MAIN 282
93	CONTINUE	MAIN 283
	US=VP*TAB(N,10,1)	MAIN 284
96	CONTINUE	MAIN 285
	TAB(N,11,K)=TAB(N,9,K)*TAB(N,4,K)+TAB(N,10,K)*TAB(N,5,K)	MAIN 286
	TAB(N,12,K)=TAB(N,9,K)*TAB(N,5,K)-TAB(N,10,K)*TAB(N,4,K)	MAIN 287
	TAB(N,13,K)=((TAB(N,6,K)*ABS(TAB(N,11,K)))/(TAB(N,6,K)-RHOSTR)-US)	MAIN 288



1*(-1.)**K	MAIN 289
TAB(N,14,K)=1.	MAIN 290
97 CONTINUE	MAIN 291
99 CONTINUE	MAIN 292
C	MAIN 293
C	MAIN 294
C STORE ALL XMESH IN XMESH2	MAIN 295
C	MAIN 296
130 DO 135 K=1,6	MAIN 297
DO 135 J=1,20	MAIN 298
DO 135 I=1,20	MAIN 299
XMESH2(I,J,K)=XMESH(I,J,K)	MAIN 300
135 CONTINUE	MAIN 301
TIME=HSTAR	MAIN 302
WRITE (3,145) TIME	MAIN 303
CALL SOUT	MAIN 304
CALL PRINT(XMESH2,Z,R,1)	MAIN 305
C	MAIN 306
KREFL=0	MAIN 307
139 IF (KREFL.NE.0) GO TO 143	MAIN 308
C ENTRY FOR TIME STEP	MAIN 309
C	MAIN 310
140 READ (1,142) H	MAIN 311
142 FORMAT (E12.8)	MAIN 312
143 CONTINUE	MAIN 313
TIME=TIME+H	MAIN 314
WRITE (3,145) TIME	MAIN 315
145 FORMAT (1H1///6H TIME=,E15.8///)	MAIN 316
WRITE (3,999) KR	MAIN 317
999 FORMAT (5X,4H KR=,I5)	MAIN 318
C	MAIN 319
C	MAIN 320
C ADVANCE SHOCK POINTS	MAIN 321
C	MAIN 322
DO 159 N=1,NP	MAIN 323
IF (TAB(N,14,1).LT.0.) GO TO 156	MAIN 324

	IF ((TAB(N,1,1)-SURF(N,1)).GT.EPS) GO TO 154	MAIN 325
156	TAB2(N,1,1)=TAB(N,1,1)	MAIN 326
	TAB2(N,2,1)=TAB(N,2,1)	MAIN 327
	TAB(N,14,1)=-1.	MAIN 328
	GO TO 159	MAIN 329
154	TAB2(N,1,1)=TAB(N,1,1)+TAB(N,13,1)*H*TAB(N,10,1)-VP*TAB(N,9,1)*TAB(N,10,1)*H	MAIN 330
	TAB2(N,2,1)=TAB(N,2,1)+TAB(N,13,1)*H*TAB(N,9,1)-VP*TAB(N,9,1)**2*H	MAIN 331
150	CONTINUE	MAIN 332
159	DO 155 N=1,NT	MAIN 333
	TAB2(N,1,2)=TAB(N,1,2)+TAB(N,13,2)*H*TAB(N,10,2)	MAIN 334
155	TAB2(N,2,2)=TAB(N,2,2)+TAB(N,13,2)*H*TAB(N,9,2)	MAIN 335
	DO 158 M=1,NT	MAIN 336
	IF (TAB2(M,1,2).GT.ZMAX) GO TO 5000	MAIN 337
	IF (TAB2(M,2,2).GT.RMAX) GO TO 5000	MAIN 338
158	CONTINUE	MAIN 339
157	NUZON=0	MAIN 340
C	ADVANCE RAREFACTION	MAIN 341
C		MAIN 342
	IF (RARF(1,2).LT.0.)IRARF=1	MAIN 343
	IF (IRARF.EQ.1) GO TO 516	MAIN 344
	ENR=NR-1	MAIN 345
	ADEL=(TAB2(1,1,2)-TAB2(1,1,1))/ENR	MAIN 346
	RARF2(1,1)=TAB2(1,1,2)	MAIN 347
	DO 510 N=2,NR	MAIN 348
	RARF2(N,1)=RARF2(N-1,1)-ADEL	MAIN 349
510	CONTINUE	MAIN 350
	DO 515 N=1,NR	MAIN 351
	RARF2(N,3)=(RARF2(N,1)/TIME-.5*VP)/AR	MAIN 352
	RARF2(N,4)=-SQRT(1.-RARF2(N,3)**2)	MAIN 353
	RARF2(N,2)=RADIUS+TIME*AR*RARF2(N,4)	MAIN 354
515	CONTINUE	MAIN 355
516	CONTINUE	MAIN 356
	CALL SHOCK	MAIN 357
C		MAIN 358
C		MAIN 359
		MAIN 360

	IF (ITS3.EQ.1) GO TO 569	MAIN 361
C	SHOCK COMPUTATIONS COMPLETED	MAIN 362
C	COMPUTE PARTICLE CURVES	MAIN 363
C		MAIN 364
	TMP=.5*VP*H	MAIN 365
	DO 520 N=1,NP	MAIN 366
	SPART(N,1,1)=TAB(N,1,1)+TAB(N,5,1)*H	MAIN 367
520	SPART(N,2,1)=TAB(N,2,1)+TAB(N,4,1)*H	MAIN 368
	DO 525 N=1,NT	MAIN 369
	SPART(N,1,2)=TAB(N,1,2)+TAB(N,5,2)*H	MAIN 370
525	SPART(N,2,2)=TAB(N,2,2)+TAB(N,4,2)*H	MAIN 371
	IF (IRARF.EQ.1) GO TO 531	MAIN 372
	DO 530 N=1,NR	MAIN 373
	RPART(N,1)=RARF(N,1)+TMP	MAIN 374
530	RPART(N,2)=RARF(N,2)	MAIN 375
531	CONTINUE	MAIN 376
C		MAIN 377
C		MAIN 378
568	CALL SOUT2	MAIN 379
569	CONTINUE	MAIN 380
C	ADVANCE PROJECTILE REAR SURFACE	MAIN 381
	DO 5300 I=1,NP	MAIN 382
	DO 5300 J=1,8	MAIN 383
5300	SURF2(I,J)=SURF(I,J)	MAIN 384
	KICK=568	MAIN 385
	CALL DVCHK(KQ)	MAIN 386
	IF (KQ.EQ.1) GO TO 9980	MAIN 387
C		MAIN 388
C	START INTERIOR REGION COMPUTATIONS	MAIN 389
C		MAIN 390
	CALL INTER	MAIN 391
C		MAIN 392
C	INTERIOR REGION COMPUTATIONS COMPLETED	MAIN 393
C		MAIN 394
	CALL PRINT(XMESH2,Z,R,2)	MAIN 395
570	CONTINUE	MAIN 396

C		MAIN 397
C	INITIALIZE FOR NEXT TIME STEP	MAIN 398
C		MAIN 399
	DO 920 K=1,6	MAIN 400
	DO 920 J=1,20	MAIN 401
	DO 920 I=1,20	MAIN 402
	XMESH(I,J,K)=XMESH2(I,J,K)	MAIN 403
920	CONTINUE	MAIN 404
	DO 930 J=1,13	MAIN 405
	DO 930 I=1,NP	MAIN 406
	TAB(I,J,1)=TAB2(I,J,1)	MAIN 407
930	CONTINUE	MAIN 408
	DO 940 J=1,13	MAIN 409
	DO 940 I=1,NT	MAIN 410
	TAB(I,J,2)=TAB2(I,J,2)	MAIN 411
940	CONTINUE	MAIN 412
	IF (IRARF.EQ.1) GO TO 951	MAIN 413
	DO 950 I=1,NR	MAIN 414
	RARF(I,1)=RARF2(I,1)	MAIN 415
	RARF(I,2)=RARF2(I,2)	MAIN 416
950	CONTINUE	MAIN 417
951	CONTINUE	MAIN 418
	DO 960 I=1,NP	MAIN 419
	DO 959 J=1,5	MAIN 420
	SURF(I,J)=SURF2(I,J)	MAIN 421
959	CONTINUE	MAIN 422
960	CONTINUE	MAIN 423
	IF (KR.EQ.10) GO TO 888	MAIN 424
	REWIND 4	MAIN 425
	WRITE (4)TIME	MAIN 426
	WRITE (4)((XMESH(I,J,K),I=1,20),J=1,20),K=1,6),(Z(I),I=1,20),(R(I	MAIN 427
	1),I=1,20),((SURF(I,J),I=1,15),J=1,8),(((TAB(I,J,K),I=1,15),J=1,14)	MAIN 428
	1,K=1,2),((RARF(I,J),I=1,15),J=1,11),TIME,ZMIN,ZMAX,RMIN,RMAX,GR,GZ	MAIN 429
	1,AR	MAIN 430
	KR=10	MAIN 431
	GO TO 777	MAIN 432

888	REWIND 10	MAIN	433
C	IF(KRW.EQ.1)REWIND10	MAIN	434
C	KRW=0	MAIN	435
	WRITE (10)TIME	MAIN	436
	WRITE (10)((X(MESH(I,J,K),I=1,20),J=1,20),K=1,6),(Z(I),I=1,20),(R(I	MAIN	437
	11),I=1,20),(SURF(I,J),I=1,15),J=1,8),(((TAB(I,J,K),I=1,15),J=1,14	MAIN	438
	1),K=1,2),(RARF(I,J),I=1,15),J=1,11),TIME,ZMIN,ZMAX,RMIN,RMAX,GR,G	MAIN	439
	1Z,AR	MAIN	440
	KR=4	MAIN	441
777	IF (KREFL.EQ.0) GO TO 980	MAIN	442
	KREFL=0	MAIN	443
	H=H1	MAIN	444
	GO TO 143	MAIN	445
980	CONTINUE	MAIN	446
	CALL DVCHK(KICK)	MAIN	447
	IF (KICK.EQ.2) GO TO 140	MAIN	448
	WRITE (3,970)	MAIN	449
970	FORMAT (28HODIVIDE CHECK AT END OF CASE/1H1)	MAIN	450
	CALL EXIT	MAIN	451
C		MAIN	452
C	DIVIDE CHECK	MAIN	453
C		MAIN	454
9980	WRITE (3,9985) KICK	MAIN	455
9985	FORMAT (32HODIVIDE CHECK NEAR STATEMENT NO.,15/1H1)	MAIN	456
	RETURN	MAIN	457
	END	MAIN	458
	SUBROUTINE DBLTRP(ZX,RX,ANS)	SUB1	1
C		SUB1	2
C	1ST ORDER DOUBLE INTERPOLATION THAT CONSIDERS	SUB1	3
C	LINES OF DISCONTINUITY IF IN CONSIDERED REGION	SUB1	4
C		SUB1	5
	COMMON CASEID(14),ITS1,ITS2,ITS3,ITS4,ITI1,ITI2,ITI3,ITI4,EPS1,EPSS	SUB1	6
	12,EPS3,EPS4,EPSS5,EPS6,EPI1,EPI2,EPI3,EPI4,EPI5,EPI6,EPI7,VP,AR,LENS	SUB1	7
	1GTH,APR,BPR,BIGAPR,BIGBPR,ESTAR,ALPHA,BETA,RHOSTR,EPRS,RHOS	SUB1	8
	COMMON XMESH(20,20,6),XMESH2(20,20,6),Z(20),R(20),SURF(15,8),SURF2	SUB1	9
	1(15,8),TAB(15,14,2),TAB2(15,14,2),SPART(15,2,2),RARF(15,11),RARF2	SUB1	10

	115,4),RPART(15,2)	SUB1	11
C		SUB1	12
C	COMMON ZO,RO,PO,UO,VO,LO,MO,RHOO,EO,AO,UBARO,VBARO	SUB1	13
C	COMMON NP,NT,NR,NI,NDEL,ISUB	SUB1	14
C	COMMON ZMIN,ZMAX,RMIN,RMAX,RADIUS,GZ,GR,DELTA,H	SUB1	15
	COMMON DIRCOS	SUB1	16
	COMMON TIME	SUB1	17
	COMMON IRARF	SUB1	18
	COMMON KSTOP	SUB1	19
	COMMON TPSI	SUB1	20
	COMMON KKK	SUB1	21
	REAL LO,MO,LENGTH,MU,KO	SUB1	22
C		SUB1	23
	DIMENSION ANS(6),ANS1(2,8),ANS2(2,8),ZI(4),RI(4),IK(4)	SUB1	24
	CALL OVCHK(KEY)	SUB1	25
	IF (KEY.EQ.2) GO TO 4	SUB1	26
	NO=0	SUB1	27
	GO TO 940	SUB1	28
C		SUB1	29
C	FIND SUBSCRIPTS FOR GRID	SUB1	30
C		SUB1	31
4	I1=(ZX-ZMIN)/GZ+1.000001	SUB1	32
	I2=I1+1	SUB1	33
	J1=(RX-RMIN)/GR+1.000001	SUB1	34
	J2=J1+1	SUB1	35
	NN=NP	SUB1	36
	IF (ITS3.EQ.1) GO TO 3	SUB1	37
	DO 1 K=1,2	SUB1	38
	IF (K.EQ.2)NN=NT	SUB1	39
	DO 1 I=1,NN	SUB1	40
	ALF=SQRT((TAB(I,1,K)-ZX)**2+(TAB(I,2,K)-RX)**2)	SUB1	41
	IF (ALF.GT.EPS1) GO TO 1	SUB1	42
	ANS(1)=TAB(I,3,K)	SUB1	43
		SUB1	44
		SUB1	45
		SUB1	46

	ANS(2)=TAB(I,4,K)	SUB1	47
	ANS(3)=TAB(I,5,K)	SUB1	48
	ANS(4)=TAB(I,6,K)	SUB1	49
	ANS(5)=TAB(I,7,K)	SUB1	50
	ANS(6)=TAB(I,8,K)	SUB1	51
	RETURN	SUB1	52
1	CONTINUE	SUB1	53
	IF (IRARF.EQ.1) GO TO 3	SUB1	54
	DO 2 I=1,NR	SUB1	55
	ALF=SQRT((RARF(I,1)-ZX)**2+(RARF(I,2)-RX)**2)	SUB1	56
	IF (ALF.GT.EPI1) GO TO 2	SUB1	57
	ANS(1)=RARF(I,3)	SUB1	58
	ANS(2)=RARF(I,4)	SUB1	59
	ANS(3)=RARF(I,5)	SUB1	60
	ANS(4)=RARF(I,6)	SUB1	61
	ANS(5)=RARF(I,7)	SUB1	62
	ANS(6)=RARF(I,8)	SUB1	63
	RETURN	SUB1	64
2	CONTINUE	SUB1	65
3	CONTINUE	SUB1	66
C		SUB1	67
C		SUB1	68
	ZXX=ZX+.01	SUB1	69
	RXX=RX+.01	SUB1	70
C		SUB1	71
C	I LOOP FOR UPPER AND LOWER Z GRID LINES	SUB1	72
C		SUB1	73
	DO 800 I=1,2	SUB1	74
	IF (ITS3.EQ.1) GO TO 14	SUB1	75
	IF (I.EQ.2) GO TO 8	SUB1	76
	II=I1	SUB1	77
	GO TO 12	SUB1	78
8	II=I2	SUB1	79
12	M=COMP(ZX,RX,Z(II),R(J1))	SUB1	80
	IF (M.EQ.1) GO TO 13	SUB1	81
	MCOM=1	SUB1	82

	GO TO 20	SUB1 83
13	M=COMP(ZX,RX,Z(II),R(J2))	SUB1 84
	IF (M.EQ.1) GO TO 14	SUB1 85
	MCOM=2	SUB1 86
	GO TO 20	SUB1 87
C		SUB1 88
C	GET 6 VALUES ON GRID LINES	SUB1 89
C		SUB1 90
14	DO 15 K=1,6	SUB1 91
	ANS1(I,K+2)=XMESH(II,J1,K)+(XMESH(II,J2,K)-XMESH(II,J1,K))*(RX-R(J	SUB1 92
	11))/(R(J2)-R(J1))	SUB1 93
15	CONTINUE	SUB1 94
	CALL DVCHK(NO)	SUB1 95
	IF (NO.EQ.2) GO TO 17	SUB1 96
	NO=15	SUB1 97
	GO TO 940	SUB1 98
17	ANS1(I,1)=Z(II)	SUB1 99
	ANS1(I,2)=RX	SUB1 100
	GO TO 800	SUB1 101
C		SUB1 102
C		SUB1 103
20	ZZ=Z(III)	SUB1 104
	RR=RX	SUB1 105
	M=COMP(ZX,RX,ZZ,RR)	SUB1 106
	IF (M.EQ.1) GO TO 300	SUB1 107
C		SUB1 108
C		SUB1 109
	DO 25 K=1,2	SUB1 110
	KATCH=0	SUB1 111
	GO TO (21,22),K	SUB1 112
21	NN=NP	SUB1 113
	GO TO 23	SUB1 114
22	NN=NT	SUB1 115
23	JJJ=NN-1	SUB1 116
	DO 24 M=1,JJJ	SUB1 117
	IF (M.EQ.JJJ) GO TO 210	SUB1 118



	IF (RX.GT.TAB(M+1,2,K).OR.RX.LT.TAB(M,2,K)) GO TO 24	SUB1 119
210	ZI(K)=TAB(M+1,1,K)+(TAB(M,1,K)-TAB(M+1,1,K))*(RX-TAB(M+1,2,K))/(TAB(M,2,K)-TAB(M+1,2,K))	SUB1 120
	NO=210	SUB1 121
	CALL DVCHK(KQ)	SUB1 122
	IF (KQ.EQ.1) GO TO 940	SUB1 123
	IF (I.EQ.2) GO TO 211	SUB1 124
	IF (KATCH.EQ.1) GO TO 212	SUB1 125
	KATCH=1	SUB1 126
	GO TO 213	SUB1 127
212	IF ((ZX-ZI(K)).GT.(ZX-ZM)) GO TO 24	SUB1 128
	IF (ZI(K).GT.ZX) GO TO 24	SUB1 129
213	ZM=ZI(K)	SUB1 130
	IF (K.EQ.2) GO TO 215	SUB1 131
	NPS=M	SUB1 132
	GO TO 24	SUB1 133
215	NTS=M	SUB1 134
	GO TO 24	SUB1 135
211	CONTINUE	SUB1 136
	IF (KATCH.EQ.1) GO TO 26	SUB1 137
	KATCH=1	SUB1 138
	GO TO 213	SUB1 139
26	IF ((ZI(K)-ZX).GT.(ZM-ZX)) GO TO 24	SUB1 140
	IF (ZI(K).LT.ZX) GO TO 24	SUB1 141
	GO TO 213	SUB1 142
24	CONTINUE	SUB1 143
	ZI(K)=ZM	SUB1 144
	IF (KATCH.NE.0) GO TO 25	SUB1 145
	ZI(K)=ZMAX+1.	SUB1 146
25	CONTINUE	SUB1 147
	IF (IRARF.EQ.1) ZI(3)=ZMAX+1.	SUB1 148
	IF (IRARF.EQ.1) GO TO 2504	SUB1 149
	KATCH=0	SUB1 150
	JJJ=NR-1	SUB1 151
	DO 27 M=1, JJJ	SUB1 152
	ZI(3)=RARF(M+1,1)+(RARF(M,1)-RARF(M+1,1))*(RX-RARF(M+1,2))/(RARF(M,2)-RARF(M+1,2))	SUB1 153
		SUB1 154

1,2)-RARF(M+1,2))	SUB1 155
NO=25	SUB1 156
CALL DVCHK(KQ)	SUB1 157
IF (KQ.EQ.1) GO TO 940	SUB1 158
IF (ABS(ZI(3)-ZX).GT.1.E-5) GO TO 279	SUB1 159
DO 2799 LN=1,6	SUB1 160
LNN=LN+2	SUB1 161
ANS(LN)=RARF(1,LNN)	SUB1 162
2799 CONTINUE	SUB1 163
GO TO 820	SUB1 164
279 CONTINUE	SUB1 165
IF (I.EQ.2) GO TO 28	SUB1 166
IF (ZI(3).GT.ZX) GO TO 27	SUB1 167
IF (KATCH.EQ.1) GO TO 280	SUB1 168
KATCH=1	SUB1 169
GO TO 281	SUB1 170
280 IF ((ZX-ZI(3)).GT.(ZX-ZM)) GO TO 27	SUB1 171
281 ZM=ZI(3)	SUB1 172
MR=M	SUB1 173
GO TO 27	SUB1 174
28 IF (ZI(3).LT.ZX) GO TO 27	SUB1 175
IF (KATCH.EQ.1) GO TO 282	SUB1 176
KATCH=1	SUB1 177
GO TO 281	SUB1 178
282 IF ((ZI(3)-ZX).GT.(ZM-ZX)) GO TO 27	SUB1 179
GO TO 281	SUB1 180
27 CONTINUE	SUB1 181
ZI(3)=ZM	SUB1 182
2504 CONTINUE	SUB1 183
KATCH=0	SUB1 184
K=4	SUB1 185
JJJ=NP-1	SUB1 186
DO 2700 M=1,JJJ	SUB1 187
IF (M.EQ.JJJ) GO TO 2710	SUB1 188
IF (RX.GT.SURF(M+1,2).OR.RX.LT.SURF(M,2)) GO TO 2700	SUB1 189
2710 ZI(4)=SURF(M+1,1)+(SURF(M,1)-SURF(M+1,1))*(RX-SURF(M+1,2))/(SURF(M	SUB1 190

1,2)-SURF(M+1,2))	SUB1 191
IF (KQ.EQ.1) GO TO 940	SUB1 192
CALL DVCHK(KQ)	SUB1 193
NO=2710	SUB1 194
IF (I.EQ.2) GO TO 2711	SUB1 195
IF (KATCH.EQ.1) GO TO 2712	SUB1 196
KATCH=1	SUB1 197
GO TO 2713	SUB1 198
2712 IF ((ZX-ZI(K)).GT.(ZX-ZM)) GO TO 2700	SUB1 199
2713 ZM=ZI(4)	SUB1 200
MS=M	SUB1 201
GO TO 2700	SUB1 202
2711 CONTINUE	SUB1 203
IF (KATCH.EQ.1) GO TO 2726	SUB1 204
KATCH=1	SUB1 205
GO TO 2713	SUB1 206
2726 IF ((ZI(K)-ZX).GT.(ZM-ZX)) GO TO 2700	SUB1 207
GO TO 2713	SUB1 208
2700 CONTINUE	SUB1 209
ZI(4)=ZM	SUB1 210
IF (KATCH.NE.0) GO TO 2701	SUB1 211
ZI(4)=ZMAX+1.	SUB1 212
2701 CONTINUE	SUB1 213
RI(1)=RX	SUB1 214
RI(2)=RX	SUB1 215
RI(3)=RX	SUB1 216
RI(4)=RX	SUB1 217
C FIND INTERSECTION TO USE	SUB1 218
C	SUB1 219
30 KEY=0	SUB1 220
IF (I.EQ.2) GO TO 50	SUB1 221
C	SUB1 222
C UPPER GRID LINE	SUB1 223
C	SUB1 224
DO 40 KK=1,4	SUB1 225
IF (Z(II).GT.ZI(KK)) GO TO 40	SUB1 226

	IF (ABS(ZI(KK)-ZX).LT.1.E-5) GO TO 35	SUB1 227
	IF (ZI(KK).GT.ZX) GO TO 40	SUB1 228
	IF (KEY.EQ.0) GO TO 35	SUB1 229
	IF (ZI(KK).LE.ZI(KEEP)) GO TO 40	SUB1 230
	KEEP=KK	SUB1 231
	GO TO 40	SUB1 232
35	KEEP=KK	SUB1 233
	KEY=1	SUB1 234
40	CONTINUE	SUB1 235
	GO TO 65	SUB1 236
C		SUB1 237
C	LOWER GRID LINE	SUB1 238
C		SUB1 239
50	DO 60 KK=1,4	SUB1 240
	IF (ZI(KK).LT.ZI(KEEP)) GO TO 60	SUB1 241
	IF (ABS(ZI(KK)-ZX).LT.1.E-5) GO TO 55	SUB1 242
	IF (ZI(KK).LT.ZX) GO TO 60	SUB1 243
	IF (KEY.EQ.0) GO TO 55	SUB1 244
	IF (ZI(KK).GE.ZI(KEEP)) GO TO 60	SUB1 245
	KEEP=KK	SUB1 246
	GO TO 60	SUB1 247
55	KEEP=KK	SUB1 248
	KEY=1	SUB1 249
60	CONTINUE	SUB1 250
C		SUB1 251
65	IF (KEY.NE.0) GO TO 70	SUB1 252
	WRITE (6,67) ZX,RX,I,(ZI(KEY),KEY=1,4),(RI(KEY),KEY=1,4)	SUB1 253
67	FORMAT (34HOERROR NEAR STATEMENT 65 IN DBLTRP/1X3HZX=,E15.8,4X3HRX	SUB1 254
	I=,F15.8,4X2HI=,[3/1X3HZI=,4E20.8/1X3HRI=,4E20.8/1HI)	SUB1 255
	XYZ=-2.	SUB1 256
	ZYX=SQRT(XYZ)	SUB1 257
	CALL EXIT	SUB1 258
C		SUB1 259
C	FIND 6 VALUES ON SELECTED DISCONTINUITY	SUB1 260
C		SUB1 261
70	IF (KEEP.EQ.3) GO TO 80	SUB1 262

	IF (KEEP.EQ.4) GO TO 81	SUB1 263
	IF (KEEP.EQ.2) GO TO 71	SUB1 264
	N=NPS	SUB1 265
	GO TO 72	SUB1 266
71	N=NTS	SUB1 267
72	CONTINUE	SUB1 268
	ZY=ZI(KEEP)	SUB1 269
	RY=RX	SUB1 270
	DO 75 K=3,8	SUB1 271
	ANS1(I,K)=TAB(N,K,KEEP)+(TAB(N+1,K,KEEP)-TAB(N,K,KEEP))*SQRT(((RY-SUB1 272	
	1TAB(N,2,KEEP))*2+(ZY-TAB(N,1,KEEP))*2)/((TAB(N+1,2,KEEP)-TAB(N,2SUB1 273	
	1,KEEP))*2+(TAB(N+1,1,KEEP)-TAB(N,1,KEEP))*2))	SUB1 274
	NO=75	SUB1 275
	CALL DVCHK(KQ)	SUB1 276
	IF (KQ.EQ.1) GO TO 940	SUB1 277
75	CONTINUE	SUB1 278
	GO TO 90	SUB1 279
80	N=MR	SUB1 280
	ZY=ZI(3)	SUB1 281
	RY=RX	SUB1 282
	DO 85 K=3,8	SUB1 283
	ANS1(I,K)=RARF(N,K)+(RARF(N+1,K)-RARF(N,K))*SQRT(((RY-RARF(N,2))*SUB1 284	
	12+(ZY-RARF(N,1))*2)/((RARF(N+1,2)-RARF(N,2))*2+(RARF(N+1,1)-RARFSUB1 285	
	1(N,1))*2))	SUB1 286
	NO=85	SUB1 287
	CALL DVCHK(KQ)	SUB1 288
	IF (KQ.EQ.1) GO TO 940	SUB1 289
85	CONTINUE	SUB1 290
	GO TO 90	SUB1 291
81	N=MS	SUB1 292
	ZY=ZI(4)	SUB1 293
	RY=RX	SUB1 294
	DO 86 K=3,8	SUB1 295
	ANS1(I,K)=SURF(N,K)+(SURF(N+1,K)-SURF(N,K))*SQRT(((RY-SURF(N,2))*SUB1 296	
	12+(ZY-SURF(N,1))*2)/((SURF(N+1,2)-SURF(N,2))*2+(SURF(N+1,1)-SURFSUB1 297	
	1(N,1))*2))	SUB1 298

86	CONTINUE	SUB1 299
90	CALL DVCHK(NO)	SUB1 300
	IF (NO.EQ.2) GO TO 92	SUB1 301
	NO=90	SUB1 302
	GO TO 940	SUB1 303
92	ANSI(1,1)=ZY	SUB1 304
	ANSI(1,2)=RY	SUB1 305
	GO TO 800	SUB1 306
C		SUB1 307
C	FIND INTERSECTIONS OF 3 DISCONTINUITIES AND 2 GRID LINE	SUB1 308
C		SUB1 309
300	CONTINUE	SUB1 310
	KATCHP=0	SUB1 311
	KATCHR=0	SUB1 312
	KACHT=0	SUB1 313
	KATCHS=0	SUB1 314
	DO 310 K=1,2	SUB1 315
	KATCH=0	SUB1 316
	GO TO (303,301),K	SUB1 317
303	NN=NP	SUB1 318
	GO TO 302	SUB1 319
301	NN=NT	SUB1 320
302	JJJ=NN-1	SUB1 321
	DO 309 M=1,JJJ	SUB1 322
	IF ((TAB(M,1,K)-TAB(M+1,1,K)).GT.1.E-6) GO TO 3030	SUB1 323
	GO TO 309	SUB1 324
3030	RI(K)=TAB(M+1,2,K)+(TAB(M,2,K)-TAB(M+1,2,K))*(Z(11)-TAB(M+1,1,K))/	SUB1 325
	1(TAB(M,1,K)-TAB(M+1,1,K))	SUB1 326
	CALL DVCHK(NO)	SUB1 327
	IF (NO.EQ.2) GO TO 3031	SUB1 328
	NO=3030	SUB1 329
	GO TO 940	SUB1 330
3031	CONTINUE	SUB1 331
	IF (M.EQ.JJJ) GO TO 3022	SUB1 332
	IF (RI(K).GT.TAB(M+1,2,K).OR.RI(K).LT.TAB(M,2,K)) GO TO 309	SUB1 333
3022	IF (MCOM.EQ.2) GO TO 305	SUB1 334

IF (KATCH.EQ.1) GO TO 304	SUB1 335
KATCH=1	SUB1 336
GO TO 3050	SUB1 337
304 IF ((RX-RI(K)).GT.(RX-RM)) GO TO 309	SUB1 338
3050 RM=RI(K)	SUB1 339
IF (K.EQ.2) GO TO 3040	SUB1 340
MPS=M	SUB1 341
KATCHP=1	SUB1 342
GO TO 309	SUB1 343
3040 MTS=M	SUB1 344
KATCHT=1	SUB1 345
GO TO 309	SUB1 346
305 CONTINUE	SUB1 347
IF (KATCH.EQ.1) GO TO 306	SUB1 348
KATCH=1	SUB1 349
GO TO 3050	SUB1 350
306 IF ((RI(K)-RX).GT.(RM-RX)) GO TO 309	SUB1 351
GO TO 3050	SUB1 352
309 CONTINUE	SUB1 353
RI(K)=RM	SUB1 354
IF (KATCH.NE.0) GO TO 310	SUB1 355
RI(K)=RMAX+1.	SUB1 356
310 CONTINUE	SUB1 357
K=3	SUB1 358
IF (IRARF.EQ.1) RI(3)=RMAX+1.	SUB1 359
IF (IRARF.EQ.1) GO TO 315	SUB1 360
JJJ=NR-1	SUB1 361
KATCH=0	SUB1 362
DO 312 M=1,JJJ	SUB1 363
RI(3)=RARF(M+1,2)+(RARF(M,2)-RARF(M+1,2))*(Z(11)-RARF(M+1,2))/(RARF(M,1)-RARF(M+1,1))	SUB1 364
NO=3122	SUB1 365
CALL DVCHK(KQ)	SUB1 366
IF (KQ.EQ.1) GO TO 940	SUB1 367
IF (M.EQ.JJJ.OR.M.EQ.1) GO TO 3122	SUB1 368
IF (RI(K).GT.RARF(M+1,2).OR.RI(K).LT.RARF(M,2)) GO TO 312	SUB1 369
	SUB1 370

3122	IF (MCOM.EQ.2) GO TO 316	SUB1 371
	IF (KATCH.EQ.1) GO TO 317	SUB1 372
	KATCH=1	SUB1 373
	GO TO 3051	SUB1 374
317	IF ((RX-RI(K)).GT.(RX-RM)) GO TO 312	SUB1 375
3051	RM=RI(K)	SUB1 376
	MR=M	SUB1 377
	KATCHR=1	SUB1 378
	GO TO 312	SUB1 379
316	CONTINUE	SUB1 380
	IF (KATCH.EQ.1) GO TO 318	SUB1 381
	KATCH=1	SUB1 382
	GO TO 3051	SUB1 383
318	IF ((RI(K)-RX).GT.(RM-RX)) GO TO 312	SUB1 384
	GO TO 3051	SUB1 385
312	CONTINUE	SUB1 386
	RI(K)=RM	SUB1 387
	IF (KATCH.NE.0) GO TO 315	SUB1 388
	RI(K)=RMAX+1.	SUB1 389
315	CONTINUE	SUB1 390
	KATCH=0	SUB1 391
	JJJ=NP-1	SUB1 392
	DO 3150 M=1, JJJ	SUB1 393
	IF ((SURF(M,1)-SURF(M+1,1)).GT.1.E-6) GO TO 3130	SUB1 394
	GO TO 3150	SUB1 395
3130	RI(4)=SURF(M+1,2)+(SURF(M,2)-SURF(M+1,2))*(Z(11)-SURF(M+1,1))/(SURF(M,1)-SURF(M+1,1))	SUB1 396
	NO=3130	SUB1 397
	CALL DVCHK(KQ)	SUB1 398
	IF (KQ.EQ.1) GO TO 940	SUB1 399
	IF (M.EQ.JJJ) GO TO 3123	SUB1 400
	IF (RI(4).GT.SURF(M+1,2).OR.RI(4).LT.SURF(M,2)) GO TO 3150	SUB1 401
3123	IF (MCOM.EQ.2) GO TO 3105	SUB1 402
	IF (KATCH.EQ.1) GO TO 3104	SUB1 403
	KATCH=1	SUB1 404
	GO TO 3109	SUB1 405
		SUB1 406



3104	IF ((RX-RI(4)).GT.(RX-RM)) GO TO 3150	SUB1 407
3109	RM=RI(4)	SUB1 408
	MS=M	SUB1 409
	KATCHS=1	SUB1 410
	GO TO 3150	SUB1 411
3105	IF (KATCH.EQ.1) GO TO 3106	SUB1 412
	KATCH=1	SUB1 413
	GO TO 3109	SUB1 414
3106	IF ((RI(4)-RX).GT.(RM-RX)) GO TO 3150	SUB1 415
	GO TO 3109	SUB1 416
3150	CONTINUE	SUB1 417
	RI(4)=RM	SUB1 418
	IF (KATCH.NE.0) GO TO 3107	SUB1 419
	RI(4)=RMAX+1.	SUB1 420
3107	CONTINUE	SUB1 421
	IF (KATCHP+KATCHT+KATCHR+KATCHS.EQ.0) GO TO 485	SUB1 422
	ZI(1)=Z(11)	SUB1 423
	ZI(2)=Z(11)	SUB1 424
	ZI(3)=Z(11)	SUB1 425
	ZI(4)=Z(11)	SUB1 426
C	J LOOP FOR LEFT AND RIGHT R GRID LINES	SUB1 427
C		SUB1 428
	DO 700 J=1,2	SUB1 429
	IF (J.EQ.2) GO TO 350	SUB1 430
C		SUB1 431
C	LEFT R GRID LINE	SUB1 432
C		SUB1 433
	JJ=J1	SUB1 434
	KEY=0	SUB1 435
	DO 340 N=1,4	SUB1 436
	IF (R(J1).GT.RI(N)) GO TO 340	SUB1 437
	IF (RI(N).GT.RX) GO TO 340	SUB1 438
	IF (KEY.EQ.1) GO TO 330	SUB1 439
	KEY=1	SUB1 440
	KEEP=N	SUB1 441
	GO TO 340	SUB1 442

C		SUB1 443
C	FIND CLOSEST	SUB1 444
C		SUB1 445
330	DIF1=RX-RI(KEEP)	SUB1 446
	DIF2=RX-RI(N)	SUB1 447
	IF (DIF1.LE.DIF2) GO TO 340	SUB1 448
	KEEP=N	SUB1 449
340	CONTINUE	SUB1 450
	GO TO 375	SUB1 451
C		SUB1 452
C	RIGHT R GRID LINE	SUB1 453
C		SUB1 454
350	JJ=J2	SUB1 455
	KEY=0	SUB1 456
	DO 360 N=1,4	SUB1 457
	IF (R(J2).LT.RI(N)) GO TO 360	SUB1 458
	IF (RI(N).LT.RX) GO TO 360	SUB1 459
	IF (KEY.EQ.1) GO TO 355	SUB1 460
	KEY=1	SUB1 461
	KEEP=N	SUB1 462
	GO TO 360	SUB1 463
355	DIF1=RI(KEEP)-RX	SUB1 464
	DIF2=RI(N)-RX	SUB1 465
	IF (DIF1.LE.DIF2) GO TO 360	SUB1 466
	KEEP=N	SUB1 467
360	CONTINUE	SUB1 468
375	IF (KEY.EQ.1) GO TO 400	SUB1 469
C		SUB1 470
C	NO POINTS BETWEEN RX AND GRID POINTS	SUB1 471
C		SUB1 472
	ANS2(J,1)=Z(II)	SUB1 473
	ANS2(J,2)=R(JJ)	SUB1 474
	ANS2(J,3)=XMESH(II,JJ,1)	SUB1 475
	ANS2(J,4)=XMESH(II,JJ,2)	SUB1 476
	ANS2(J,5)=XMESH(II,JJ,3)	SUB1 477
	ANS2(J,6)=XMESH(II,JJ,4)	SUB1 478

ANS2(J,7)=XMESH(II,JJ,5)	SUB1 479
ANS2(J,8)=XMESH(II,JJ,6)	SUB1 480
GO TO 700	SUB1 481
C	SUB1 482
C POINT FOUND BETWEEN RX AND GRID POINTS	SUB1 483
C	SUB1 484
400 GO TO (405,410,470,481),KEEP	SUB1 485
C	SUB1 486
C INTERSECTION ON PROJECTILE SHOCK	SUB1 487
C	SUB1 488
405 NI=MPS	SUB1 489
RY=RI(KEEP)	SUB1 490
ZY=Z(III)	SUB1 491
GO TO 520	SUB1 492
C	SUB1 493
C INTERSECTION ON TARGET SHOCK	SUB1 494
C	SUB1 495
410 NI=MTS	SUB1 496
RY=RI(KEEP)	SUB1 497
ZY=Z(III)	SUB1 498
GO TO 520	SUB1 499
C	SUB1 500
C INTERSECTION ON RAREFACTION	SUB1 501
C	SUB1 502
470 NI=MR	SUB1 503
RY=RI(KEEP)	SUB1 504
ZY=Z(III)	SUB1 505
GO TO 520	SUB1 506
C	SUB1 507
C INTERSECTION ON FREE SURFACE	SUB1 508
C	SUB1 509
481 NI=MS	SUB1 510
RY=RI(KEEP)	SUB1 511
ZY=Z(III)	SUB1 512
GO TO 520	SUB1 513
C	SUB1 514

C		SUB1 515
485	WRITE (3,488) KEEP,I1,JJ,ZX,RX	SUB1 516
488	FORMAT (25HOERROR NEAR STATEMENT 485/1X5HKEEP=,I4,4X3HII=,I4,4X3HJSUB1 517	
	1J=,I4/1X3HZX=,E15.8,4X3HRX=,E15.8/1H1)	SUB1 518
	CALL EXIT	SUB1 519
C		SUB1 520
C	FIND TABLE VALUES	SUB1 521
C		SUB1 522
520	IF (KEEP.EQ.3) GO TO 580	SUB1 523
	IF (KEEP.EQ.4) GO TO 591	SUB1 524
	DO 550 N=3,8	SUB1 525
	ANS2(J,N)=TAB(N1,N,KEEP)+(TAB(N1+1,N,KEEP)-TAB(N1,N,KEEP))*SQRT(((SUB1 526	
	1RY-TAB(N1,2,KEEP))*2+(ZY-TAB(N1,1,KEEP))*2)/((TAB(N1+1,2,KEEP)-TSUB1 527	
	1AB(N1,2,KEEP))*2+(TAB(N1+1,1,KEEP)-TAB(N1,1,KEEP))*2))	SUB1 528
550	CONTINUE	SUB1 529
	IF (ZX.LT.0..AND.ABS(RX-RADIUS).LT.1.E-6) GO TO 552	SUB1 530
	IF (RX.LT.RADIUS.OR.ABS(Z(11)).GT.1.E-6) GO TO 551	SUB1 531
552	CONTINUE	SUB1 532
	ANS2(J,3)=0.	SUB1 533
	ANS2(J,6)=RHOSTR	SUB1 534
	ANS2(J,7)=0.	SUB1 535
	ANS2(J,8)=SQRT(BIGAPR/RHOSTR)	SUB1 536
551	CONTINUE	SUB1 537
	GO TO 600	SUB1 538
580	DO 590 N=3,8	SUB1 539
	ANS2(J,N)=RARF(N1,N)+(RARF(N1+1,N)-RARF(N1,N))*SQRT(((RY-RARF(N1,2SUB1 540	
	1))*2+(ZY-RARF(N1,1))*2)/((RARF(N1+1,2)-RARF(N1,2))*2+(RARF(N1+1SUB1 541	
	1,1)-RARF(N1,1))*2))	SUB1 542
590	CONTINUE	SUB1 543
	GO TO 600	SUB1 544
591	DO 592 N=3,8	SUB1 545
	ANS2(J,N)=SURF(N1,N)+(SURF(N1+1,N)-SURF(N1,N))*SQRT(((RY-SURF(N1,2SUB1 546	
	1))*2+(ZY-SURF(N1,1))*2)/((SURF(N1+1,2)-SURF(N1,2))*2+(SURF(N1+1SUB1 547	
	1,1)-SURF(N1,1))*2))	SUB1 548
592	CONTINUE	SUB1 549
600	CALL DVCHK(NO)	SUB1 550

	IF (NO.EQ.2) GO TO 605	SUB1 551
	NO=600	SUB1 552
	GO TO 940	SUB1 553
605	ANS2(J,1)=ZY	SUB1 554
	ANS2(J,2)=RY	SUB1 555
C		SUB1 556
C	END OF LOOP FOR BOTH R GRID LINES	SUB1 557
C		SUB1 558
700	CONTINUE	SUB1 559
C		SUB1 560
C	INTERPOLATE FOR UPPER AND LOWER VALUES	SUB1 561
C		SUB1 562
	DO 720 J=3,8	SUB1 563
	ANS1(I,J)=ANS2(1,J)+(ANS2(2,J)-ANS2(1,J))*(RX-ANS2(1,2))/(ANS2(2,2)	SUB1 564
	1)-ANS2(1,2))	SUB1 565
720	CONTINUE	SUB1 566
	CALL DVCHK(NO)	SUB1 567
	IF (NO.EQ.2) GO TO 730	SUB1 568
	NO=720	SUB1 569
	GO TO 940	SUB1 570
730	ANS1(I,1)=Z(11)	SUB1 571
	ANS1(I,2)=RX	SUB1 572
C		SUB1 573
C	END OF LOOP FOR BOTH Z GRID LINES	SUB1 574
C		SUB1 575
800	CONTINUE	SUB1 576
C		SUB1 577
C	FIND FINAL VALUES	SUB1 578
C		SUB1 579
	DO 810 J=1,6	SUB1 580
	ANS(J)=ANS1(1,J+2)+(ANS1(2,J+2)-ANS1(1,J+2))*(ZX-ANS1(1,1))/(ANS1(	SUB1 581
	12,1)-ANS1(1,1))	SUB1 582
810	CONTINUE	SUB1 583
	CALL DVCHK(NO)	SUB1 584
	IF (NO.EQ.2) GO TO 820	SUB1 585
	NO=810	SUB1 586

	GO TO 940	SUB1 587
820	RETURN	SUB1 588
C		SUB1 589
940	WRITE (3,942)	SUB1 590
942	FORMAT (35HODIVIDE CHECK ERROR IN SUBR. DBLTRP)	SUB1 591
950	WRITE (3,952) NO,ZX,RX,I1,J1,KEEP,ZI,RI	SUB1 592
952	FORMAT (19H NEAR STATEMENT NO.,I4/1X3HZX=,E15.8,4X3HRX=,E15.8/1X3HSUB1 593	
	I11=,I4,4X3HJ1=,I4,4X5HKEEP=,I4/1X3HZI=,4E18.8/1X3HRI=,4E18.8)	SUB1 594
	WRITE (3,955) ((ANS1(I,J),J=1,8),I=1,2),((ANS2(I,J),J=1,8),I=1,2)	SUB1 595
955	FORMAT (1X5HANS1=/8E16.8/8E16.8/1X5HANS2=/8E16.8/8E16.8/1H1)	SUB1 596
	XYZ=-2.	SUB1 597
	ZYX=SQRT(XYZ)	SUB1 598
	CALL EXIT	SUB1 599
	RETURN	SUB1 600
	END	SUB1 601
	SUBROUTINE SHOCK	SUB2 1
C	COMPUTES SHOCK VALUES	SUB2 2
	COMMON CASEID(14),ITS1,ITS2,ITS3,ITS4,ITI1,ITI2,ITI3,ITI4,EPS1,EPSSUB2 3	
	12,EPS3,EPS4,EPS5,EPS6,EPI1,EPI2,EPI3,EPI4,EPI5,EPI6,EPI7,VP,AR,LENSUB2 4	
	1GTH,APR,BPR,BIGAPR,BIGBPR,ESTAR,ALPHA,BETA,RHOSTR,EPRS,RHOS	SUB2 5
	COMMON XMESH(20,20,6),XMESH2(20,20,6),Z(20),R(20),SURF(15,8),SURF2SUB2 6	
	1(15,8),TAB(15,14,2),TAB2(15,14,2),SPART(15,2,20),RARF(15,11),RARF2(SUB2 7	
	115,4),RPART(15,2)	SUB2 8
C		SUB2 9
	COMMON ZO,RO,PO,UO,VO,LO,MO,RHOO,E0,A0,UBARO,VBARO	SUB2 10
C		SUB2 11
	COMMON NP,NT,NR,NI,NDEL,ISUB	SUB2 12
C		SUB2 13
	COMMON ZMIN,ZMAX,RMIN,RMAX,RADIUS,GZ,GR,DELTA,H	SUB2 14
	COMMON DIRCOS	SUB2 15
	COMMON TIME	SUB2 16
	COMMON IRARF	SUB2 17
	COMMON KSTOP	SUB2 18
	COMMON TPSI	SUB2 19
	COMMON KKK	SUB2 20
C		SUB2 21

C	REAL LO,MO,LENGTH,MU,KO	SUB2	22
		SUB2	23
	DIMENSION ANS(6)	SUB2	24
	EXTERNAL FGOF1	SUB2	25
	EPS=.0000001	SUB2	26
C		SUB2	27
C	BEGIN SHOCK POINT COMPUTATIONS	SUB2	28
	DO 505 K=1,2	SUB2	29
	GO TO (158,160),K	SUB2	30
158	NN=NP	SUB2	31
	GO TO 162	SUB2	32
160	NN=NT	SUB2	33
	VBAR=0.	SUB2	34
162	DO 500 I=1,NN	SUB2	35
	MPROJ=0	SUB2	36
	IF (TAB(I,14,K).LT.0.) GO TO 500	SUB2	37
164	CONTINUE	SUB2	38
C		SUB2	39
C	INITIALIZE TO ITERATE ON 1 SHOCK POINT	SUB2	40
C		SUB2	41
	NBIC=0	SUB2	42
	ZO=TAB2(1,1,K)	SUB2	43
	RO=TAB2(1,2,K)	SUB2	44
	PO=TAB(1,3,K)	SUB2	45
	UO=TAB(1,4,K)	SUB2	46
	VO=TAB(1,5,K)	SUB2	47
	RHOO=TAB(1,6,K)	SUB2	48
	EO=TAB(1,7,K)	SUB2	49
	AO=TAB(1,8,K)	SUB2	50
	LO=TAB(1,9,K)	SUB2	51
	MO=TAB(1,10,K)	SUB2	52
	UBARO=TAB(1,11,K)	SUB2	53
	VBARO=TAB(1,12,K)	SUB2	54
	UTOH=TAB(1,13,K)	SUB2	55
	UTO=UTOH	SUB2	56
	ITS44=ITS4	SUB2	57

	IF (IRARF.EQ.1) GO TO 170	SUB2	58
	M=1-(NR-2)*(K-2)	SUB2	59
	FF=RO-RARF2(M+1,2)-(RARF2(M,2)-RARF2(M+1,2))*(ZO-RARF2(M+1,1))/(R	SUB2	60
	IRF2(M,1)-RARF2(M+1,1))	SUB2	61
169	CONTINUE	SUB2	62
	IF (FF.LT..001) GO TO 350	SUB2	63
170	IF (I.NF.1) GO TO 180	SUB2	64
	MO=TAB(I,10,K)	SUB2	65
	LO=0.	SUB2	66
	GO TO 190	SUB2	67
180	IF (I.LT.NN) GO TO 184	SUB2	68
	UP=H*(TAB(I-1,13,K)-TAB(I,13,K))	SUB2	69
	TMP=SQRT((TAB2(I-1,2,K)-RO)**2+(TAB2(I-1,1,K)-ZO)**2)	SUB2	70
	DOMEG=UP/TMP	SUB2	71
	GO TO 186	SUB2	72
184	DR1=TAB2(I+1,2,K)-RO	SUB2	73
	DR2=RO-TAB2(I-1,2,K)	SUB2	74
	DZ1=TAB2(I+1,1,K)-ZO	SUB2	75
	DZ2=ZO-TAB2(I-1,1,K)	SUB2	76
	UP=H*(TAB(I-1,13,K)-TAB(I+1,13,K))	SUB2	77
	TMP=SQRT(DR1**2+DZ1**2)+SQRT(DR2**2+DZ2**2)	SUB2	78
	DOMEG=UP/TMP	SUB2	79
	KICK=184	SUB2	80
	CALL DVCHK(KQ)	SUB2	81
	IF (KQ.EQ.1) GO TO 9980	SUB2	82
C		SUB2	83
C	COMPUTE NEW LO,MO	SUB2	84
C		SUB2	85
186	COMEG=COS(DOMEG)	SUB2	86
	SOMEG=SIN(DOMEG)	SUB2	87
	XLO=LO*COMEG+MO*SOMEG	SUB2	88
	XMO=MO*COMEG-LO*SOMEG	SUB2	89
	LO=XLO	SUB2	90
	MO=XMO	SUB2	91
	IF (PO.GT..0025) GO TO 190	SUB2	92
	PO=0.	SUB2	93



	UO=0.	SUB2 94
	VO=VP*(1.-(-1.)**K)/2.	SUB2 95
	RHOO=RHOSTR	SUB2 96
	EO=0.	SUB2 97
	AO=SQRT(BIGAPR/RHOSTR)	SUB2 98
	UBARO=MO*VO	SUB2 99
	VBARO=VBARS	SUB2 100
	UTO=UBARO+AO*(-1.)**K	SUB2 101
	GO TO 350	SUB2 102
190	ITS33=ITS3	SUB2 103
C		SUB2 104
C	FIND GUESS TO START ITERATION	SUB2 105
C		SUB2 106
195	CALL GUESS(1,KOD2,ZO,RO,I,K,ZZ,RR,DZ,DR)	SUB2 107
	IF (KOD2.EQ.1) GO TO 200	SUB2 108
	WRITE (3,198) I,K,ZO,RO	SUB2 109
	WRITE (3,7002) ZZ,RR,DZ,DR	SUB2 110
198	FORMAT (31HONO GUESS FOUND FOR SHOCK POINT/3H0I=,I4,6X2HK=,I4,10X3	SUB2 111
	1HZO=,E15.8,10X3HRO=,E15.8/1H1)	SUB2 112
	CALL EXIT	SUB2 113
200	CONTINUE	SUB2 114
	KY=K	SUB2 115
	NTW=0	SUB2 116
	IF (K.EQ.2) GO TO 201	SUB2 117
	VBARO=VP*LO	SUB2 118
	DIRCOS=-MO	SUB2 119
	GO TO 203	SUB2 120
201	DIRCOS=MO	SUB2 121
203	CONTINUE	SUB2 122
	CALL NRIT2(Z1,R1,ZZ,DZ,RR,DR,EPS1,EPS2,FGOF1,ITS1,KODE)	SUB2 123
	IF (KODE.EQ.0) GO TO 205	SUB2 124
C		SUB2 125
C	BICARACTERISTIC SELECTION SCHEME	SUB2 126
C		SUB2 127
	IF (NBIC.EQ.0) GO TO 204	SUB2 128
	IF (NTW.EQ.8)KY=KY+1	SUB2 129

	IF (NTW.GT.21) GO TO 7000	SUB2 130
	ANG1=ANG1+DTPSI*(-1.)**KY	SUB2 131
	DIRCOS=SIN(ANG1)	SUB2 132
	LO=COS(ANG1)	SUB2 133
	NTW=NTW+1	SUB2 134
	GO TO 203	SUB2 135
204	CONTINUE	SUB2 136
	NBIC=1	SUB2 137
	CALL DBLTRP(ZZ,RR,ANS)	SUB2 138
	UA=ANS(2)	SUB2 139
	VA=ANS(3)	SUB2 140
	AA=ANS(6)	SUB2 141
	ZZZ=ZZ+DZ	SUB2 142
	CALL DBLTRP(ZZZ,RR,ANS)	SUB2 143
	UB=ANS(2)	SUB2 144
	VB=ANS(3)	SUB2 145
	AB=ANS(6)	SUB2 146
	RRR=RR+DR	SUB2 147
	CALL DBLTRP(ZZ,RRR,ANS)	SUB2 148
	UC=ANS(2)	SUB2 149
	VC=ANS(3)	SUB2 150
	AC=ANS(6)	SUB2 151
	MM=0	SUB2 152
	TPSI=1.5708*(-1.)**K	SUB2 153
	XB=ZZ	SUB2 154
	YB=RR	SUB2 155
	NOM=5	SUB2 156
	CA=NOM	SUB2 157
6201	DTPSI=.01745	SUB2 158
	DTPSI=CA*DTPSI	SUB2 159
	TPSI=TPSI+DTPSI*(-1.)**K	SUB2 160
	A1=1.+H*(VB-VA+(AB-AA)*SIN(TPSI))/DZ	SUB2 161
	B1=H*(VC-VA+(AC-AA)*SIN(TPSI))/DR	SUB2 162
	C1=-(ZZ-ZO+H*(VA+AA*SIN(TPSI)))	SUB2 163
	A2=H*(UB-UA+(AB-AA)*COS(TPSI))/DZ	SUB2 164
	B2=1.+H*(UC-UA+(AC-AA)*COS(TPSI))/DR	SUB2 165

	C2=-(RR-RO+H*(UA+AA*COS(TPSI)))	SUB2 166
	DET=A1*B2-A2*B1	SUB2 167
	DELX=(R2*C1-B1*C2)/DET	SUB2 168
	DELY=(A1*C2-A2*C1)/DET	SUB2 169
C		SUB2 170
C	TEST FOR SAME REGION	SUB2 171
C		SUB2 172
	XB1=XB+DELX	SUB2 173
	YB1=YB+DELY	SUB2 174
	M=COMP(XB,YB,XB1,YB1)	SUB2 175
	IF (M.EQ.1) GO TO 6203	SUB2 176
	MM=MM+1	SUB2 177
	IF (MM.LT.360/NOM) GO TO 6201	SUB2 178
7000	WRITE (3,7001)	SUB2 179
7001	FORMAT (41HOBICARACTERISTIC SELECTION SCHEME FAILED)	SUB2 180
	WRITE (3,614) ZO,RO	SUB2 181
614	FORMAT (1X5H2O =,E15.8,4X5HRO =,E15.8)	SUB2 182
	WRITE (3,7002) UA,VA,AA,UB,VB,AB,UC,VC,AC,ZZ,DZ,RR,DR,ANG1	SUB2 183
7002	FORMAT (4E16.8)	SUB2 184
	CALL EXIT	SUB2 185
6203	CONTINUE	SUB2 186
	WRITE (3,6210)	SUB2 187
6210	FORMAT (53HOBICARACTERISTIC SELECTION SCHEME EMPLOYED BY SHOCKX)	SUB2 188
6204	ANG1=TPSI	SUB2 189
	T1=DIRCOS	SUB2 190
	T2=LO	SUB2 191
	DIRCOS=SIN(ANG1)	SUB2 192
	LO=COS(ANG1)	SUB2 193
	GO TO 203	SUB2 194
205	CONTINUE	SUB2 195
	UBARS1=0.	SUB2 196
	IF (K.EQ.1)UBARS1=MO*VP	SUB2 197
	CALL DBLTRP(Z1,R1,ANS)	SUB2 198
	P1=ANS(1)	SUB2 199
	U1=ANS(2)	SUB2 200
	V1=ANS(3)	SUB2 201

	RHO1=ANS(4)	SUB2 202
	E1=ANS(5)	SUB2 203
	A1=ANS(6)	SUB2 204
206	CONTINUE	SUB2 205
	KICK=205	SUB2 206
	CALL DVCHK(KQ)	SUB2 207
	IF (KQ.EQ.1) GO TO 9980	SUB2 208
	IF (NBIC.EQ.0) GO TO 207	SUB2 209
7003	SINTH=ABS(DIRCOS)	SUB2 210
	COSTH=ABS(LO)	SUB2 211
	DIRCOS=T1	SUB2 212
	LO=T2	SUB2 213
207	CONTINUE	SUB2 214
	UBAR1=LO*U1+MO*V1	SUB2 215
	IF (K.EQ.2) GO TO 208	SUB2 216
	IF (UBAR1.LT.VP/2.) GO TO 208	SUB2 217
	UBAR1=UBARS1-UBAR1	SUB2 218
208	CONTINUE	SUB2 219
218	CONTINUE	SUB2 220
	M1=PART(1,Z1,R1,ZZ,RR,DELTA,NDEL)	SUB2 221
	IF (M1.EQ.1) GO TO 210	SUB2 222
	PUR=0.	SUB2 223
	PVR=0.	SUB2 224
	GO TO 215	SUB2 225
210	CALL DBLTRP(ZZ,RR,ANS)	SUB2 226
	DP=RR-R1	SUB2 227
	PUR=(ANS(2)-U1)/DP	SUB2 228
219	CONTINUE	SUB2 229
	PVR=(ANS(3)-V1)/DP	SUB2 230
215	M1=PART(2,Z1,R1,ZZ,RR,DELTA,NDEL)	SUB2 231
	IF (M1.EQ.1) GO TO 220	SUB2 232
	PUZ=0.	SUB2 233
	PVZ=0.	SUB2 234
	PAZ=0.	SUB2 235
	GO TO 225	SUB2 236
220	CALL DBLTRP(ZZ,RR,ANS)	SUB2 237

	DP=Z7-Z1	SUB2 238
	PUZ=(ANS(2)-U1)/DP	SUB2 239
	PVZ=(ANS(3)-V1)/DP	SUB2 240
225	CONTINUE	SUB2 241
	IF (NBIC.EQ.1) GO TO 7004	SUB2 242
	PURB1=LO*PUR+MO*PVR	SUB2 243
	PVRB1=LO*PVR-MO*PUR	SUB2 244
	PVZB1=LO*PVZ-MO*PUZ	SUB2 245
	PVEB1=-MO*PVRB1+LO*PVZB1	SUB2 246
	SBAR1=PVEB1	SUB2 247
226	CONTINUE	SUB2 248
	IF (ABS(R1).LE.EPS) GO TO 235	SUB2 249
	SBAR1=SBAR1+U1/R1	SUB2 250
	GO TO 240	SUB2 251
7004	CONTINUE	SUB2 252
	IF (V1.GT.VP/2..AND.K.EQ.1)V1=VP-V1	SUB2 253
	SBAR1=SINTH**2*PUR-SINTH*COSTH*(PUZ+PVR)+COSTH**2*PVZ	SUB2 254
	GO TO 226	SUB2 255
235	SBAR1=SBAR1+PUR	SUB2 256
C		SUB2 257
C		SUB2 258
240	ITS22=ITS2	SUB2 259
	MMM=0	SUB2 260
250	CONTINUE	SUB2 261
	CALL EQOSS(PFR,PFE)	SUB2 262
	BIG1=RHO1*A1	SUB2 263
	KICK=250	SUB2 264
	CALL DVCHK(KQ)	SUB2 265
	IF (KQ.EQ.1) GO TO 9980	SUB2 266
	TEMP=1.-RHOSTR/RHOO	SUB2 267
	TMP=SQRT(P0*TEMP/RHOSTR)	SUB2 268
	IF (K.EQ.2) GO TO 251	SUB2 269
	IF (TMP.LT.VP/2.) GO TO 251	SUB2 270
	MPROJ=1	SUB2 271
	TMP=UBARS1-TMP	SUB2 272
251	CONTINUE	SUB2 273

	TMP6=TMP	SUB2 274
256	CONTINUE	SUB2 275
	FNBIC=NBIC	SUB2 276
	TMP1=P1+BIGA1*UBAR1-RHO1*H*SBAR1*A1**2+BIGA1*(-UBAR1+COSTH*U1+SINT	SUB2 277
	1H*V1-SINTH*LO*VBARS+COSTH*MO*VBARS)*(FNBIC)	SUB2 278
	TMP2=PFR*TEMP+PO*RHOSTR/RHOO**2	SUB2 279
	TMP5=PFE*TEMP	SUB2 280
	GTMP=-RHO1*A1	SUB2 281
	IF (NBIC.EQ.0) GO TO 259	SUB2 282
	GTMP=GTMP*(COSTH*LO+SINTH*MO)	SUB2 283
259	CONTINUE	SUB2 284
	BIGG=PO-(GTMP*TMP+TMP1)	SUB2 285
	PGR=PFR-((GTMP*TMP2)/(2.*RHOSTR*TMP6))	SUB2 286
	PGE=PFE-((GTMP*TMP5)/(2.*RHOSTR*TMP6))	SUB2 287
265	TMP=.5*(1./RHOSTR-1./RHOO)	SUB2 288
	BIGH=EO-TMP*PO	SUB2 289
	PHR=-TMP*PFR-.5*PO/RHOO**2	SUB2 290
	PHE=1.-TMP*PFE	SUB2 291
	IF (ABS(BIGH).GT..0001) GO TO 267	SUB2 292
	BIGH=0.	SUB2 293
267	IF (ABS(BIGG).GT..0001) GO TO 269	SUB2 294
	BIGG=0.	SUB2 295
269	CONTINUE	SUB2 296
C		SUB2 297
C	COMPUTE DELTA EO,DELTA RHOO	SUB2 298
C		SUB2 299
	DOWN=PGE*PHR-PGR*PHE	SUB2 300
	DEO=(-BIGG*PHR+BIGH*PGR)/DOWN	SUB2 301
	DRHOO=(-BIGH*PGE+BIGG*PHE)/DOWN	SUB2 302
C		SUB2 303
	EO2=EO+DEO	SUB2 304
	IF (EO2.LT.0.)EO2=0.	SUB2 305
	RHOO2=RHOO+DRHOO	SUB2 306
	IF (RHOO2.LT.RHOSTR)RHOO2=RHOO	SUB2 307
	KICK=265	SUB2 308
	CALL DVCHK(KQ)	SUB2 309

	IF (KQ.EQ.1) GO TO 9980	SUB2 310
	CALL EQOSP(RH002,E02,P02)	SUB2 311
	UBAR02=(1.-RHOSTR/RH002)*(P02/RHOSTR)	SUB2 312
	IF (UBAR02.GT.0.) GO TO 2669	SUB2 313
	WRITE (3,2700) P02,RH002,E02,R0,Z0	SUB2 314
	WRITE (3,7002) P1,U1,V1,RH01,E1,Z1TR1,SBAR1	SUB2 315
2700	FORMAT (4E16.8)	SUB2 316
2669	CONTINUE	SUB2 317
	UBAR02=SQRT(UBAR02)	SUB2 318
	IF (E02.LT.1.E-5) GO TO 273	SUB2 319
	IF (ABS((E02-E01)/E02).LT.EPS4) GO TO 273	SUB2 320
	IF (ABS(DE0).GT..01*EPS4) GO TO 275	SUB2 321
273	IF (ABS((RH002-RH00)/RH002).LE.EPS3) GO TO 285	SUB2 322
	IF (ABS(DRH00).LT.EPS3) GO TO 285	SUB2 323
275	ITS22=ITS22-1	SUB2 324
	IF (ITS22.GT.0) GO TO 280	SUB2 325
	WRITE (3,278) ITS2	SUB2 326
278	FORMAT (35H0E AND RHO FAILED TO CONVERGE AFTER,14,6H TRIES)	SUB2 327
	WRITE (3,279) I,K,Z0,R0,E0,RH00,P0,E02,RH002,P02	SUB2 328
279	FORMAT (1X2H1=,14,4X2HK=,14/1X4HZ0 =,E15.8,4X4HRO =,E15.8,4X4HE0 =	SUB2 329
	1,E15.8,4X6HRH00 =,E15.8,4X4HPO =,E15.8/1X4HE02=,E15.8,4X6HRH002=,E	SUB2 330
	115.8,4X4HP02=,E15.8/1H1)	SUB2 331
	STOP	SUB2 332
280	E0=E02	SUB2 333
	RH00=RH002	SUB2 334
	P0=P02	SUB2 335
	UBAR0=UBAR02	SUB2 336
	GO TO 250	SUB2 337
285	E0=E02	SUB2 338
	RH00=RH002	SUB2 339
	UBAR0=UBAR02	SUB2 340
	A0=SQRT(PFR+P02*PFE/RH00**2)	SUB2 341
C		SUB2 342
C		SUB2 343
	CALL DVCHK(KQ)	SUB2 344
	KICK=285	SUB2 345

	IF (KQ.EQ.1) GO TO 9980	SUB2 346
	IF (K.EQ.2) GO TO 286	SUB2 347
	VBARO=VP*LO	SUB2 348
	GO TO 287	SUB2 349
286	VBARO=0.	SUB2 350
287	CONTINUE	SUB2 351
295	P0=P02	SUB2 352
	IF (K.EQ.2) GO TO 296	SUB2 353
	UBARO=UBARS1-UBARO	SUB2 354
296	CONTINUE	SUB2 355
	UTO=(RH00*UBARO-RHOSTR*UBARS1)/(RH00-RHOSTR)	SUB2 356
	VO=MO*UBARO+LO*VBARO	SUB2 357
	UO=LO*UBARO-MO*VBARO	SUB2 358
	UBAR=.5*(UTOH+UTO)	SUB2 359
	IF (ABS((UBAR-UTOH)/UBAR).LE.EPS6) GO TO 350	SUB2 360
	IF (ABS(UBAR-UTOH).LT.EPS6) GO TO 350	SUB2 361
	ITS44=ITS44-1	SUB2 362
	IF (ITS44.GT.0) GO TO 325	SUB2 363
	WRITE (3,297) ITS4,UTOH,UTO	SUB2 364
297	FORMAT (30H0UBAR FAILED TO CONVERGE AFTER,I4,6H TRIES/1X5HUTOH=,E15.8,4X4HUTO=,E15.8)	SUB2 365
	CALL EXIT	SUB2 366
	WRITE (3,279) I,K,ZO,RO,E0,RH00,P0,E02,RH002,P02	SUB2 367
C		SUB2 368
C	INIT. FOR MORE U BAR ITERATIONS	SUB2 369
C		SUB2 370
325	UTOH=UBAR	SUB2 371
	AVMO=(TAB(I,10,K)+MO)*.5	SUB2 372
	AVLO=(TAB(I,9,K)+LO)*.5	SUB2 373
	ZO=TAB(I,1,K)+UBAR*H*AVMO-VBARS*AVLO*M	SUB2 374
	RO=TAB(I,2,K)+UBAR*H*AVLO-VBARS*AVMO*M	SUB2 375
	LO=AVLO	SUB2 376
	MO=AVMO	SUB2 377
	GO TO 195	SUB2 378
C		SUB2 379
C	ONE SHOCK POINT HAS CONVERGED	SUB2 380
		SUB2 381



C		SUB2 382
350	TAB2(I,1,K)=Z0	SUB2 383
	TAB2(I,2,K)=R0	SUB2 384
	TAB2(I,3,K)=P0	SUB2 385
	TAB2(I,4,K)=U0	SUB2 386
	TAB2(I,5,K)=V0	SUB2 387
	TAB2(I,6,K)=RH00	SUB2 388
	TAB2(I,7,K)=E0	SUB2 389
	TAB2(I,8,K)=A0	SUB2 390
	TAB2(I,9,K)=L0	SUB2 391
	TAB2(I,10,K)=M0	SUB2 392
	TAB2(I,11,K)=UBARO	SUB2 393
	TAB2(I,12,K)=VBARO	SUB2 394
	TAB2(I,13,K)=UTO	SUB2 395
	KICK=500	SUB2 396
	CALL DVCHK(KQ)	SUB2 397
	IF (KQ.EQ.1) GO TO 9980	SUB2 398
C		SUB2 399
C		SUB2 400
500	CONTINUE	SUB2 401
505	CONTINUE	SUB2 402
	RETURN	SUB2 403
9980	WRITE (3,9985) KICK	SUB2 404
9985	FORMAT (32HODIVIDE CHECK NEAR STATEMENT NO.,15,15H IN SUBR. SHOCK/	SUB2 405
	11H1)	SUB2 406
	CALL EXIT	SUB2 407
	RETURN	SUB2 408
	END	SUB2 409
	SUBROUTINE FGOF1(ZX,RX,SS,QQ)	SUB3 1
C		SUB3 2
C	COMPUTES S1,Q1 FOR SHOCK LINE	SUB3 3
C	ITERATION FOR Z1,R1	SUB3 4
C		SUB3 5
	COMMON CASEID(14),ITS1,ITS2,ITS3,ITS4,ITI1,ITI2,ITI3,ITI4,EPSSUB3	6
	12,EPS3,EPS4,EPS5,EPS6,EPI1,EPI2,EPI3,EPI4,EPI5,EPI6,EPI7,VP,AR,LENSUB3	7
	1GTH,APR,BPR,BIGAPR,BIGBPR,ESTAR,ALPHA,BETA,RHOSTR,EPRS,RHOS	SUB3 8

	COMMON XMESH(20,20,6),XMESH2(20,20,6),Z(20),R(20),SURF(15,8),SURF2SUB3	9
	1(15,8),TAB(15,14,2),TAB2(15,14,2),SPART(15,2,2),RARF(15,11),RARF2(SUB3	10
	115,4),RPART(15,2)	SUB3 11
C		SUB3 12
C		SUB3 13
	COMMON ZO,RO,PO,UO,VO,LO,MO,RHOO,EO,AO,UBARO,VBARO	SUB3 14
C		SUB3 15
	COMMON NP,NT,NR,NI,NDEL,ISUB	SUB3 16
C		SUB3 17
	COMMON ZMIN,ZMAX,RMIN,RMAX,RADIUS,GZ,GR,DELTA,H	SUB3 18
	COMMON DIRCOS	SUB3 19
	COMMON TIME	SUB3 20
	COMMON IRARF	SUB3 21
	COMMON KSTOP	SUB3 22
	COMMON TPSI	SUB3 23
	COMMON KKK	SUB3 24
	REAL LO,MO,LENGTH,MU,KO	SUB3 25
C		SUB3 26
	DIMENSION ANS(6)	SUB3 27
C		SUB3 28
	REAL LO,MO	SUB3 29
	CALL DBLTRP(ZX,RX,ANS)	SUB3 30
	U1=ANS(2)	SUB3 31
	V1=ANS(3)	SUB3 32
	A1=ANS(6)	SUB3 33
	SS=ZX-ZO+H*(V1+A1*DIRCOS)	SUB3 34
	QQ=RX-RO+H*(U1+A1*LO)	SUB3 35
	RETURN	SUB3 36
	END	SUB3 37
	SUBROUTINE INTER	SUB4 1
C	COMPUTES INTERIOR REGION POINTS	SUB4 2
	COMMON CASEID(14),ITS1,ITS2,ITS3,ITS4,ITI1,ITI2,ITI3,ITI4,EPS1,EPSSUB4	3
	12,EPS3,EPS4,EPS5,EPS6,EPI1,EPI2,EPI3,EPI4,EPI5,EPI6,EPI7,VP,AR,LENSUB4	4
	1GTH,APR,BPR,BIGAPR,BIGBPR,ESTAR,ALPHA,BETA,RHOSTR,EPRS,RHDS	SUB4 5
	COMMON XMESH(20,20,6),XMESH2(20,20,6),Z(20),R(20),SURF(15,8),SURF2SUB4	6
	1(15,8),TAB(15,14,2),TAB2(15,14,2),SPART(15,2,2),RARF(15,11),RARF2(SUB4	7

	115,4),RPART(15,2)	SUB4	8
C		SUB4	9
C		SUB4	10
	COMMON ZO,RO,PO,UO,VO,LO,MO,RHOO,EO,AO,UBARO,VBARO	SUB4	11
C		SUB4	12
	COMMON NP,NT,NR,NI,NDEL,ISUB	SUB4	13
C		SUB4	14
	COMMON ZMIN,ZMAX,RMIN,RMAX,RADIUS,GZ,GR,DELTA,H	SUB4	15
	COMMON DIRCOS	SUB4	16
	COMMON TIME	SUB4	17
	COMMON IRARF	SUB4	18
	COMMON KSTOP	SUB4	19
	COMMON TPSI	SUB4	20
	COMMON KKK	SUB4	21
C		SUB4	22
C		SUB4	23
	REAL LO,MO,LENGTH,MU,KO	SUB4	24
	DIMENSION ANS(6),LL(3),ZI(11),RI(11),PI(11),UI(11),VI(11),RHOI(11)	SUB4	25
	1,EI(11),AI(11),PUR(11),PVR(11),PAR(11),PUZ(11),PVZ(11),PAZ(11),PSI	SUB4	26
	1(7),SPSI(11),CPSI(11),S(11)	SUB4	27
C		SUB4	28
	EXTERNAL FGOF1,FGOF5	SUB4	29
	INTEGER CHECK,CHECK2	SUB4	30
C		SUB4	31
1	FORMAT (1H1)	SUB4	32
	EPS=.0000001	SUB4	33
	DO 905 J=1,20	SUB4	34
	DO 900 I=1,20	SUB4	35
	M=TEST(Z(I),R(J))	SUB4	36
	ZO=Z(I)	SUB4	37
	RO=R(J)	SUB4	38
	KICK=1	SUB4	39
	CALL DVCHK(KQ)	SUB4	40
	IF (KQ.EQ.1) GO TO 9980	SUB4	41
	IF (M.EQ.3.AND.ZO.LT.EPS.AND.ABS(RO-RADIUS).LT.EPS)M=1	SUB4	42
	IF (M.NE.1) GO TO 900	SUB4	43

	DO 2 L=1,NP	SUB4	44
	IF (TAB(L,14,1).LT.0.) GO TO 20	SUB4	45
2	CONTINUE	SUB4	46
	IF (IRARF.EQ.1) GO TO 20	SUB4	47
	DO 3 N=1,NR	SUB4	48
	IF (R(J).GT.RARF(N,2)) GO TO 5	SUB4	49
3	CONTINUE	SUB4	50
	GO TO 6	SUB4	51
5	CONTINUE	SUB4	52
	M=PICK(Z(I),R(J),3)	SUB4	53
	FF=R(J)-RARF(M+1,2)-(RARF(M,2)-RARF(M+1,2))*(Z(I)-RARF(M+1,1))/(R(SUB4	SUB4	54
	IRF(M,1)-RARF(M+1,1))	SUB4	55
	IF (FF.GT.0.) GO TO 20	SUB4	56
6	CONTINUE	SUB4	57
	P02=RARF(1,3)	SUB4	58
	U02=RARF(1,4)	SUB4	59
	V02=RARF(1,5)	SUB4	60
	RH002=RARF(1,6)	SUB4	61
	E02=RARF(1,7)	SUB4	62
	A02=RARF(1,8)	SUB4	63
	GO TO 870	SUB4	64
20	CONTINUE	SUB4	65
	CALL GUESS(2,KOD,Z0,R0,I,J,ZZ,RR,DZ,DR)	SUB4	66
	IF (KOD.EQ.1) GO TO 580	SUB4	67
	WRITE (3,575) I,J,Z0,R0	SUB4	68
575	FORMAT (41HONO GUESS FOUND FOR INTERIOR POINT/3H0I=14,6X2HK	SUB4	69
	1=,14,10X3HZ0=,E15.8,10X3HRO=,E15.8/1H1)	SUB4	70
	CALL EXIT	SUB4	71
580	CALL DBLTRP(ZZ,RR,ANS)	SUB4	72
C		SUB4	73
C	INITIALIZE FOR 1. POINT	SUB4	74
C		SUB4	75
	PSI(1)=0.	SUB4	76
	PSI(3)=1.0472	SUB4	77
	PSI(4)=2.0944	SUB4	78
	PSI(6)=4.18879	SUB4	79

PSI(7)=5.23599	SUB4	80
NBIC=0	SUB4	81
ITI22=ITI2	SUB4	82
PO=ANS(1)	SUB4	83
UO=ANS(2)	SUB4	84
VO=ANS(3)	SUB4	85
RHOO=ANS(4)	SUB4	86
EO=ANS(5)	SUB4	87
AO=ANS(6)	SUB4	88
KICK=580	SUB4	89
CALL DVCHK(KQ)	SUB4	90
IF (KQ.EQ.1) GO TO 9980	SUB4	91
590 IF (ABS(RO).GT.EPS) GO TO 594	SUB4	92
L1=1	SUB4	93
LL(1)=4	SUB4	94
LL(2)=6	SUB4	95
LLL=2	SUB4	96
GO TO 620	SUB4	97
C	SUB4	98
C	SUB4	99
594 IF (ABS(RO-RADIUS).GT.EPS) GO TO 600	SUB4	100
IF (ZO.GT.EPS) GO TO 610	SUB4	101
L1=2	SUB4	102
LL(1)=3	SUB4	103
LL(2)=7	SUB4	104
LLL=2	SUB4	105
GO TO 620	SUB4	106
600 IF (RO.LE.RADIUS.OR.ABS(ZO).GT.EPS) GO TO 610	SUB4	107
L1=3	SUB4	108
LL(1)=6	SUB4	109
LL(2)=7	SUB4	110
LLL=2	SUB4	111
GO TO 620	SUB4	112
C	SUB4	113
C	SUB4	114
610 L1=4	SUB4	115

LL(1)=1	SUB4 116
LL(2)=4	SUB4 117
LL(3)=6	SUB4 118
LLL=3	SUB4 119
C	SUB4 120
C       ITERATE FOR I VALUES	SUB4 121
C	SUB4 122
619   CONTINUE	SUB4 123
620   DO 630 KK=1,LLL	SUB4 124
LUMP=L1	SUB4 125
ISUB=LL(KK)	SUB4 126
621   CONTINUE	SUB4 127
TPSI=PSI(ISUB)	SUB4 128
SPSI(ISUB)=SIN(TPSI)	SUB4 129
CPSI(ISUB)=COS(TPSI)	SUB4 130
CALL NRIT2(ZI(ISUB),RI(ISUB),ZZ,DZ,RR,DR,EPI1,EPI2,FGOFI,ITI1,KODE	SUB4 131
1)	SUB4 132
IF (KODE.NE.0) GO TO 6200	SUB4 133
625   CALL DBLTRP(ZI(ISUB),RI(ISUB),ANS)	SUB4 134
PI(ISUB)=ANS(1)	SUB4 135
UI(ISUB)=ANS(2)	SUB4 136
VI(ISUB)=ANS(3)	SUB4 137
RHOI(ISUB)=ANS(4)	SUB4 138
EI(ISUB)=ANS(5)	SUB4 139
AI(ISUB)=ANS(6)	SUB4 140
630   CONTINUE	SUB4 141
C	SUB4 142
C	SUB4 143
KICK=630	SUB4 144
CALL DVCHK(KQ)	SUB4 145
IF (KQ.EQ.1) GO TO 9980	SUB4 146
GO TO 6400	SUB4 147
C	SUB4 148
C   BICHARACTERISTIC SELECTION SCHEME	SUB4 149
C	SUB4 150
7000   WRITE (3,7001)	SUB4 151

7001	FORMAT (41HOBICARACTERISTIC SELECTION SCHEME FAILED)	SUB4 152
	WRITE (3,614) ZO,RO	SUB4 153
	WRITE (3,7002) (PSI(MNMN),MNMN=1,7),UA,VA,AA,UB,VB,AB,UC,VC,AC,ZZ,	SUB4 154
	1DZ,RR,DR,ANG1,ANG2	SUB4 155
	SUB=ISUB	SUB4 156
	WRITE (3,7002) SUB,ZI(ISUB),RI(ISUB)	SUB4 157
7002	FORMAT (4E16.8)	SUB4 158
	CALL EXIT	SUB4 159
6200	CONTINUE	SUB4 160
	IF (NBIC.NE.0) GO TO 7000	SUB4 161
	IF (L1.NE.2.OR.LL(1).EQ.1) GO TO 7300	SUB4 162
	LL(1)=1	SUB4 163
	GO TO 619	SUB4 164
7300	CONTINUE	SUB4 165
	IF (L1.NE.3) GO TO 7310	SUB4 166
	IF (PSI(6).GT.4.2) GO TO 7310	SUB4 167
	PSI(6)=5.75959	SUB4 168
	GO TO 619	SUB4 169
7310	CONTINUE	SUB4 170
	CALL DBLTRP(ZZ,RR,ANS)	SUB4 171
	UA=ANS(2)	SUB4 172
	VA=ANS(3)	SUB4 173
	AA=ANS(6)	SUB4 174
	ZZZ=ZZ+DZ	SUB4 175
	CALL DBLTRP(ZZZ,RR,ANS)	SUB4 176
	UB=ANS(2)	SUB4 177
	VB=ANS(3)	SUB4 178
	AB=ANS(6)	SUB4 179
	RRR=RR+DR	SUB4 180
	CALL DBLTRP(ZZ,RRR,ANS)	SUB4 181
	UC=ANS(2)	SUB4 182
	VC=ANS(3)	SUB4 183
	AC=ANS(6)	SUB4 184
	MM=0	SUB4 185
	TPSI=PSI(ISUB)	SUB4 186
	XB=ZZ	SUB4 187

	YB=RR	SUB4 188
	NOM=5	SUB4 189
	CA=NOM	SUB4 190
	DO 6210 LM=1,2	SUB4 191
6201	DTPSI=.01745	SUB4 192
	DTPSI=CA*DTPSI	SUB4 193
	TPSI=TPSI+DTPSI	SUB4 194
	A1=1.+H*(VB-VA+(AB-AA)*SIN(TPSI))/DZ	SUB4 195
	B1=H*(VC-VA+(AC-AA)*SIN(TPSI))/DR	SUB4 196
	C1=-(ZZ-ZO+H*(VA+AA*SIN(TPSI)))	SUB4 197
	A2=H*(UB-UA+(AB-AA)*COS(TPSI))/DZ	SUB4 198
	B2=1.+H*(UC-UA+(AC-AA)*COS(TPSI))/DR	SUB4 199
	C2=-(RR-RO+H*(UA+AA*COS(TPSI)))	SUB4 200
	DET=A1*B2-A2*B1	SUB4 201
	DELX=(B2*C1-B1*C2)/DET	SUB4 202
	DELY=(A1*C2-A2*C1)/DET	SUB4 203
C		SUB4 204
C	TEST FOR SAME REGION	SUB4 205
C		SUB4 206
	XB1=XB+DELX	SUB4 207
	YB1=YB+DELY	SUB4 208
	M=COMP(XB,YB,XB1,YB1)	SUB4 209
	IF (LM.EQ.2) GO TO 6700	SUB4 210
	IF (M.EQ.1) GO TO 6203	SUB4 211
	GO TO 6800	SUB4 212
6700	CONTINUE	SUB4 213
	IF (M.NE.1) GO TO 6203	SUB4 214
6800	CONTINUE	SUB4 215
	MM=MM+1	SUB4 216
	IF (MM.LE.360/NOM) GO TO 6201	SUB4 217
612	WRITE (3,613) ITI1	SUB4 218
613	FORMAT (44HOF AILED TO FIND 2 POINTS IN THE SAME REGION 21H IN SUBR	SUB4 219
	1. NRIT2 AFTER,14,6H TRIES)	SUB4 220
	WRITE (3,614) ZO,RO	SUB4 221
614	FORMAT (1X5HZO =,E15.8,4X5HRO =,E15.8)	SUB4 222
	WRITE (3,6144) LM	SUB4 223



	WRITE (3,6145) M	SUB4 224
	WRITE (3,6146) KODE	SUB4 225
	WRITE (3,7002) XB,YB,XB1,YB1	SUB4 226
6144	FORMAT (4H LM=,I4)	SUB4 227
6145	FORMAT (3H M=,I4)	SUB4 228
6146	FORMAT (6H KODE=,I4)	SUB4 229
	CALL EXIT	SUB4 230
6203	GO TO (6204,6205),LM	SUB4 231
6204	ANG1=TPSI	SUB4 232
	MM=0	SUB4 233
	GO TO 6210	SUB4 234
6205	ANG2=TPSI-DTPSI	SUB4 235
6210	CONTINUE	SUB4 236
	AL=LLL+1	SUB4 237
	DO 6300 KK=1,LLL	SUB4 238
	ISUB=LL(KK)	SUB4 239
	AK=KK	SUB4 240
	PSI(ISUB)=ANG1+(ANG2-ANG1)*AK/AL	SUB4 241
6300	CONTINUE	SUB4 242
	NBIC=1	SUB4 243
	GO TO 619	SUB4 244
C		SUB4 245
C		SUB4 246
6400	CONTINUE	SUB4 247
	IF (L1.EQ.2.OR.L1.EQ.3) GO TO 642	SUB4 248
	CALL NRIT2(ZI(8),RI(8),ZZ,DZ,RR,DR,EPI1,EPI2,FGOF5,ITI1,KODE)	SUB4 249
	IF (KODE.EQ.0) GO TO 635	SUB4 250
	ISUB=8	SUB4 251
	WRITE (3,622) ITI1,I,J,ISUB,ZO,RO,ZZ,RR,ZI(8),RI(8)	SUB4 252
622	FORMAT (27HOF AILED TO FIND ZI,RI AFTER,14,6H TRIES,3X2HI=,I4,3X2HJSUB4 253	
	1=,I4,3X5HISUB=,I4/1X3HZO=,E15.8,6X3HRO=,E15.8/1X3HZZ=,E15.8,6X3HRRSUB4 254	
	1=,E15.8/1X3HZI=,E15.8,6X3HRI=,E15.8/1H1)	SUB4 255
	CALL EXIT	SUB4 256
C		SUB4 257
C		SUB4 258
635	CALL OBLTRP(ZI(8),RI(8),ANS)	SUB4 259

	PI(8)=ANS(1)	SUB4 260
	UI(8)=ANS(2)	SUB4 261
	VI(8)=ANS(3)	SUB4 262
	RHOI(8)=ANS(4)	SUB4 263
	EI(8)=ANS(5)	SUB4 264
	AI(8)=ANS(6)	SUB4 265
C		SUB4 266
642	DO 670 IL=1,LLL	SUB4 267
	NN=LL(IL)	SUB4 268
	M=PART(1,ZI(NN),RI(NN),ZX,RX,DELTA,NDEL)	SUB4 269
	IF (M.EQ.1) GO TO 645	SUB4 270
	PUR(NN)=0.	SUB4 271
	PVR(NN)=0.	SUB4 272
	GO TO 648	SUB4 273
645	CALL DBLTRP(ZX,RX,ANS)	SUB4 274
	DEN=RX-RI(NN)	SUB4 275
	PUR(NN)=(ANS(2)-UI(NN))/DEN	SUB4 276
	PVR(NN)=(ANS(3)-VI(NN))/DEN	SUB4 277
648	M=PART(2,ZI(NN),RI(NN),ZX,RX,DELTA,NDEL)	SUB4 278
	IF (M.EQ.1) GO TO 650	SUB4 279
	PUZ(NN)=0.	SUB4 280
	PVZ(NN)=0.	SUB4 281
	GO TO 655	SUB4 282
650	CALL DBLTRP(ZX,RX,ANS)	SUB4 283
	DEN=ZX-ZI(NN)	SUB4 284
	PUZ(NN)=(ANS(2)-UI(NN))/DEN	SUB4 285
	PVZ(NN)=(ANS(3)-VI(NN))/DEN	SUB4 286
655	S(NN)=SPSI(NN)**2*PUR(NN)-CPSI(NN)*SPSI(NN)*(PVR(NN)+PUZ(NN))+CPSI	SUB4 287
	I(NN)**2*PVZ(NN)	SUB4 288
C		SUB4 289
	IF (ABS(RI(NN)).GT.EPS) GO TO 660	SUB4 290
	CON=PUR(NN)	SUB4 291
	GO TO 662	SUB4 292
660	CON=UI(NN)/RI(NN)	SUB4 293
662	S(NN)=-RHOI(NN)*H*AI(NN)**2*(S(NN)+CON)+PI(NN)+RHOI(NN)*AI(NN)*CPS	SUB4 294
	II(NN)*UI(NN)+RHOI(NN)*AI(NN)*SPSI(NN)*VI(NN)	SUB4 295

670	CONTINUE	SUB4 296
1005	CONTINUE	SUB4 297
1002	FORMAT (4E16.8)	SUB4 298
	KICK=670	SUB4 299
	CALL DVCHK(KQ)	SUB4 300
	IF (KQ.EQ.1) GO TO 9980	SUB4 301
C		SUB4 302
C	COMPUTE NEW P,U,V	SUB4 303
C		SUB4 304
	GO TO (690,692,695,698),L1	SUB4 305
690	DU0=0.	SUB4 306
	U02=0.	SUB4 307
	V02=(S(4)-S(6))/(RHOI(4)*AI(4)*SPSI(4)-RHOI(6)*AI(6)*SPSI(6))	SUB4 308
	P02=S(4)-RHOI(4)*AI(4)*SPSI(4)*V02	SUB4 309
	GO TO 700	SUB4 310
C		SUB4 311
C		SUB4 312
692	DP0=0.	SUB4 313
	P02=0.	SUB4 314
	L=LL(1)	SUB4 315
	TMP1=RHOI(7)*RHOI(L)*AI(7)*AI(L)*(CPSI(7)*SPSI(L)-CPSI(L)*SPSI(7))	SUB4 316
	V02=(S(L)*RHOI(7)*AI(7)*CPSI(7)-S(7)*RHOI(L)*AI(L)*CPSI(L))/TMP1	SUB4 317
	U02=(S(L)-RHOI(L)*AI(L)*SPSI(L)*V02)/(RHOI(L)*AI(L)*CPSI(L))	SUB4 318
	GO TO 700	SUB4 319
C		SUB4 320
C		SUB4 321
695	DP0=0.	SUB4 322
	P02=0.	SUB4 323
	TMP1=RHOI(7)*RHOI(6)*AI(7)*AI(6)*(CPSI(7)*SPSI(6)-SPSI(7)*CPSI(6))	SUB4 324
	V02=(S(6)*RHOI(7)*AI(7)*CPSI(7)-S(7)*RHOI(6)*AI(6)*CPSI(6))/TMP1	SUB4 325
	U02=(S(6)-RHOI(6)*AI(6)*SPSI(6)*V02)/(RHOI(6)*AI(6)*CPSI(6))	SUB4 326
	GO TO 700	SUB4 327
698	CONTINUE	SUB4 328
	L=LL(1)	SUB4 329
	TMP1=RHOI(4)*AI(4)*CPSI(4)-RHOI(L)*AI(L)*CPSI(L)	SUB4 330
	TMP2=RHOI(4)*AI(4)*SPSI(4)-RHOI(L)*AI(L)*SPSI(L)	SUB4 331

	TMP3=RHOI(6)*AI(6)*CPSI(6)-RHOI(L)*AI(L)*CPSI(L)	SUB4 332
	TMP4=RHOI(6)*AI(6)*SPSI(6)-RHOI(L)*AI(L)*SPSI(L)	SUB4 333
	V02=((S(4)-S(L))*TMP3-(S(6)-S(L))*TMP1)/(TMP3*TMP2-TMP1*TMP4)	SUB4 334
	U02=(S(4)-S(L)-TMP2*V02)/TMP1	SUB4 335
	P02=S(6)-RHOI(6)*AI(6)*CPSI(6)*U02-RHOI(6)*AI(6)*SPSI(6)*V02	SUB4 336
700	KICK=700	SUB4 337
	CALL DVCHK(KQ)	SUB4 338
	IF (KQ.EQ.1) GO TO 9980	SUB4 339
C		SUB4 340
C		SUB4 341
C	ITERATE FOR RHO0,E0	SUB4 342
C		SUB4 343
705	IT133=IT13	SUB4 344
	IT144=IT14	SUB4 345
	KM=1	SUB4 346
708	CONTINUE	SUB4 347
	CALL EQDSI(P02,PGRHO,PGE,BIGG,CHECK,KRTT,A02,E02,RHO02,KM,EPS)	SUB4 348
	IF (KRTT.EQ.1) GO TO 871	SUB4 349
725	T1=RHO0-RHOI(8)	SUB4 350
	T2=PI(8)/RHOI(8)**2	SUB4 351
	BIGH=EI(8)+T2*T1-E0	SUB4 352
	PHE=-1.	SUB4 353
	PHRHO=T2	SUB4 354
	KICK=725	SUB4 355
	CALL DVCHK(KQ)	SUB4 356
	IF (KQ.EQ.1) GO TO 9980	SUB4 357
C		SUB4 358
C	COMPUTE NEW E0,RHO0	SUB4 359
C		SUB4 360
	DOWN=PGE*PHRHO-PGRHO*PHE	SUB4 361
	DE0=(-BIGG*PHRHO+BIGH*PGRHO)/DOWN	SUB4 362
	DRHO0=(-BIGH*PGE+BIGG*PHE)/DOWN	SUB4 363
	E02=E0+DE0	SUB4 364
	RHO02=RHO0+DRHO0	SUB4 365
C		SUB4 366
C	CHECK E02,RHO02 FOR CONVERGENCE	SUB4 367

	KICK=726	SUB4 368
	CALL DVCHK(KQ)	SUB4 369
	IF (KQ.EQ.1) GO TO 9980	SUB4 370
C		SUB4 371
	IF (ABS(DE0/E0).LT.EPI7) GO TO 726	SUB4 372
	IF (ABS(DE0).GT..01*EPI7) GO TO 730	SUB4 373
726	IF (ABS(DRH00/RH00).LE.EPI6) GO TO 740	SUB4 374
	IF (ABS(DRH00).LT.EPI6) GO TO 740	SUB4 375
730	ITI33=ITI33-1	SUB4 376
	IF (ITI33.NE.0) GO TO 735	SUB4 377
	WRITE (6,732) ITI3,I,J,Z0,RO,PO,UO,VO,RH00,E0,P02,U02,V02,RH002,E0	SUB4 378
	12	SUB4 379
732	FORMAT (33H0E0,RH00 FAILED TO CONVERGE AFTER,I4,6H TRIES/1X2HI=,I4	SUB4 380
	1,4X2HJ=,I4,4X2HZ=,E15.8,4X2HR=,E15.8/5X2HP018X2HU018X2HV018X4HRH00	SUB4 381
	116X2HE0/5X3HP0217X3HU0217X3HV0217X5HRH00215X3HE02// (5E20.8))	SUB4 382
	WRITE (3,1)	SUB4 383
	CALL EXIT	SUB4 384
735	E0=E02	SUB4 385
	RH00=RH002	SUB4 386
	KM=0	SUB4 387
	GO TO 708	SUB4 388
C		SUB4 389
C	CHECK FOR PROPER EQUATIONS	SUB4 390
C		SUB4 391
740	CONTINUE	SUB4 392
	PGE=-PGE	SUB4 393
	PGRHO=-PGRHO	SUB4 394
	IF (RH002.GE.RHOSTR) GO TO 750	SUB4 395
	IF (E02.LT.EPRS) GO TO 750	SUB4 396
742	CHECK2=0	SUB4 397
	GO TO 752	SUB4 398
750	CHECK2=1	SUB4 399
752	A02=SQRT(+PGRHO+P02*PGE/RH002**2)	SUB4 400
	IF (CHECK.EQ.CHECK2) GO TO 870	SUB4 401
	ITI44=ITI44-1	SUB4 402
	IF (ITI44.NE.0) GO TO 770	SUB4 403

	WRITE (3,755) ITI4,I,J,ZO,RO,PO,UO,VO,RHOO,E0,A0,PO2,U02,V02,RH002SUB4	404
	1,E02,A02	SUB4 405
755	FORMAT (38H0FAILED TO USE CORRECT EQUATIONS AFTER,14,6H TRIES/1X2HSUB4	406
	1I=,I4,4X2HJ=,I4,4X2HZ=,E15.8,4X2HR=,E15.8/5X2HP018X2HU018X2HV018X4SUB4	407
	1HRH0016X2HE018X2HA0/5X3HP0217X3HU0217X3HV0217X5HRH00215X3HE0217X3HSUB4	408
	1A02/(6E20.8))	SUB4 409
	WRITE (3,1)	SUB4 410
	CALL EXIT	SUB4 411
770	KICK=770	SUB4 412
	CALL DVCHK(KQ)	SUB4 413
	IF (KQ.EQ.1) GO TO 9980	SUB4 414
	ITI33=ITI3	SUB4 415
	GO TO 735	SUB4 416
C		SUB4 417
C	ALL VALUES HAVE CONVERGED FOR 1 INTERIOR POINT	SUB4 418
C		SUB4 419
871	KRTT=0	SUB4 420
870	XMESH2(I,J,1)=P02	SUB4 421
	XMESH2(I,J,2)=U02	SUB4 422
	XMESH2(I,J,3)=V02	SUB4 423
	XMESH2(I,J,4)=RH002	SUB4 424
	XMESH2(I,J,5)=E02	SUB4 425
	XMESH2(I,J,6)=A02	SUB4 426
	KICK=900	SUB4 427
	CALL DVCHK(KQ)	SUB4 428
	IF (KQ.EQ.1) GO TO 9980	SUB4 429
900	CONTINUE	SUB4 430
905	CONTINUE	SUB4 431
	IF (ITS3.EQ.1) GO TO 950	SUB4 432
	CALL ITRP	SUB4 433
	RETURN	SUB4 434
950	CONTINUE	SUB4 435
9980	WRITE (3,9985) KICK	SUB4 436
	WRITE (3,614) ZO,RO	SUB4 437
9985	FORMAT (32H00IVIDE CHECK NEAR STATEMENT NO.,15,15H IN SUBR. INTER/SUB4	438
	11H1)	SUB4 439

CALL EXIT	SUB4 440
RETURN	SUB4 441
END	SUB4 442
SUBROUTINE EQOS1(PRHO,PPP,PVV,PEE,TEE,TRHO,KICK)	SUB5 1
COMMON CASEID(14),ITS1,ITS2,ITS3,ITS4,ITI1,ITI2,ITI3,ITI4,EPS1,EPSSUB5 2	
12,EPS3,EPS4,EPS5,EPS6,EPI1,EPI2,EPI3,EPI4,EPI5,EPI6,EPI7,VP,AR,LENSUB5 3	
1GTH,APR,BPR,BIGAPR,BIGBPR,ESTAR,ALPHA,BETA,RHOSTR,EPRS,RHOS SUB5 4	
COMMON XMESH(20,20,6),XMESH2(20,20,6),Z(20),R(20),SURF(15,8),SURF2SUB5 5	
1(15,8),TAB(15,14,2),TAB2(15,14,2),SPART(15,2,2),RARF(15,11),RARF2(SUB5 6	
115,4),RPART(15,2)	SUB5 7
	SUB5 8
	SUB5 9
COMMON ZO,RO,PO,UO,VO,LO,MO,RHOO,EO,AO,UBARO,VBARO	SUB5 10
	SUB5 11
COMMON NP,NT,NR,NI,NDEL,ISUB	SUB5 12
	SUB5 13
COMMON ZMIN,ZMAX,RMIN,RMAX,RADIUS,GZ,GR,DELTA,H	SUB5 14
COMMON DIRCOS	SUB5 15
COMMON TIME	SUB5 16
COMMON IRARF	SUB5 17
COMMON KSTOP	SUB5 18
COMMON TPSI	SUB5 19
COMMON KKK	SUB5 20
	SUB5 21
	SUB5 22
REAL LO,MO,LENGTH,MU,KO	SUB5 23
RHO=RHOSTR	SUB5 24
E=VP**2/8.	SUB5 25
DO 100 M=1,100	SUB5 26
ETA=RHO/RHOSTR	SUB5 27
MU=ETA-1.	SUB5 28
G=-RHOSTR*(VP/2.)*2+((APR+BPR/(E/(ESTAR*ETA**2)+1.))*E*RHO+BIGAPRSUB5 29	
1*MU+BIGBPR*MU**2)*(1.-RHOSTR/RHO)	SUB5 30
DERIVG=((APR+BPR/(E/(ESTAR*ETA**2)+1.))*E+BIGAPR/RHOSTR+2.*BIGBPR*SUB5 31	
1MU/RHOSTR+2.*E**2*BPR/(ESTAR*ETA**2*(E/(ESTAR*ETA**2)+1.)*2))*1.SUB5 32	
1-RHOSTR/RHO)+((APR+BPR/(E/(ESTAR*ETA**2)+1.))*E*RHO+BIGAPR*MU+BIGBSUB5 33	

	1PR*MU**2)*RHOSTR/RHO**2	SUB5	34
	DLTRHO=-G/DERIVG	SUB5	35
	RHO=RHO+DLTRHO	SUB5	36
	IF (ABS(DLTRHO).LT.1.E-07) GO TO 101	SUB5	37
C	IF (ABS(DLTRHO).LT.1.E-06) GO TO 101	SUB5	38
100	CONTINUE	SUB5	39
	KICK=2200	SUB5	40
	GO TO 9980	SUB5	41
101	CONTINUE	SUB5	42
	PRHO=RHO	SUB5	43
	TRHO=RHO	SUB5	44
	PEE=E	SUB5	45
	TEE=E	SUB5	46
	PVV=VP/2.	SUB5	47
	PPP=(APR+BPR/(E/(ESTAR*ETA**2)+1.))*E*RHO+BIGAPR*MU+BIGBPR*MU**2	SUB5	48
9980	RETURN	SUB5	49
	END	SUB5	50
	SUBROUTINE EQDS2(PPP,PRHO,PEE)	SUB6	1
	COMMON CASEID(14),ITS1,ITS2,ITS3,ITS4,ITI1,ITI2,ITI3,ITI4,EPS1,EPSSUB6	SUB6	2
	12,EPS3,EPS4,EPS5,EPS6,EPI1,EPI2,EPI3,EPI4,EPI5,EPI6,EPI7,VP,AR,LENSUB6	SUB6	3
	1GTH,APR,BPR,BIGAPR,BIGBPR,ESTAR,ALPHA,BETA,RHOSTR,EPRS,RHOS	SUB6	4
	COMMON XMESH(20,20,6),XMESH2(20,20,6),Z(20),R(20),SURF(15,8),SURF2SUB6	SUB6	5
	1(15,8),TAB(15,14,2),TAB2(15,14,2),SPART(15,2,2),RARF(15,11),RARF2(SUB6	SUB6	6
	115,4),RPART(15,2).	SUB6	7
C		SUB6	8
C		SUB6	9
	COMMON ZO,RO,PO,UO,VO,LO,MO,RHOO,EQ,AO,UBARO,VBARO	SUB6	10
C		SUB6	11
	COMMON NP,NT,NR,NI,NOEL,ISUB	SUB6	12
C		SUB6	13
	COMMON ZMIN,ZMAX,RMIN,RMAX,RADIUS,GZ,GR,DELTA,H	SUB6	14
	COMMON DIRCOS	SUB6	15
	COMMON TIME	SUB6	16
	COMMON IRARF	SUB6	17
	COMMON KSTOP	SUB6	18
C		SUB6	19



	COMMON TPSI	SUB6	20
	COMMON KKK	SUB6	21
C	REAL LO,MO,LENGTH,MU,KO	SUB6	22
	P=PPP	SUB6	23
	RHO=PRHO	SUB6	24
	E=PEE	SUB6	25
	ETA=RHO/RHOSTR	SUB6	26
	MU=ETA-1.	SUB6	27
	EE=E/(ESTAR*ETA**2)+1.	SUB6	28
	PGRHO=E*(APR+BPR/EE)+BIGAPR/RHOSTR+(2.*BIGBPR*MU)/RHOSTR+(2.*E**2*	SUB6	29
	1BPR)/(ESTAR*ETA**2*EE**2)	SUB6	30
	PGE=(APR+BPR/EE)*RHO-(E*BPR*RHO)/(ESTAR*ETA**2*EE**2)	SUB6	31
	AR=SQRT(PGRHO+PGE*P/RHO**2)	SUB6	32
	RETURN	SUB6	33
	END	SUB6	34
	SUBROUTINE EQDS3(RHO,AA,E,P)	SUB6	35
	COMMON CASEID(14),ITS1,ITS2,ITS3,ITS4,ITI1,ITI2,ITI3,ITI4,EPS1,EPSSUB7	SUB7	1
	12,EPS3,EPS4,EPS5,EPS6,EPI1,EPI2,EPI3,EPI4,EPI5,EPI6,EPI7,VP,AR,LENSUB7	SUB7	2
	1GTH,APR,BPR,BIGAPR,BIGBPR,ESTAR,ALPHA,BETA,RHOSTR,EPRS,RHOS	SUB7	3
	COMMON XMESH(20,20,6),XMESH2(20,20,6),Z(20),R(20),SURF(15,8),SURF2SUB7	SUB7	4
	1(15,8),TAB(15,14,2),TAB2(15,14,2),SPART(15,2,2),RARF(15,11),RARF2(SUB7	SUB7	5
	115,4),RPART(15,2)	SUB7	6
C		SUB7	7
C		SUB7	8
	COMMON ZO,RO,PO,UO,VO,LO,MO,RHOO,EO,AO,UBARO,VBARO	SUB7	9
C		SUB7	10
	COMMON NP,NT,NR,NI,NOEL,ISUB	SUB7	11
		SUB7	12
C		SUB7	13
	COMMON ZMIN,ZMAX,RMIN,RMAX,RADIUS,GZ,GR,DELTA,H	SUB7	14
	COMMON DIRCOS	SUB7	15
	COMMON TIME	SUB7	16
	COMMON IRARF	SUB7	17
	COMMON KSTOP	SUB7	18
	COMMON TPSI	SUB7	19
	COMMON KKK	SUB7	20

C		SUB7	21
C		SUB7	22
	REAL LO,MO,LENGTH,MU,KO	SUB7	23
70	ETA=RHO/RHOSTR	SUB7	24
	MU=ETA-1.	SUB7	25
	EE=E/(ESTAR*ETA**2)+1.	SUB7	26
	IF (RHO.GT.RHOSTR) GO TO 72	SUB7	27
	IF (E.GE.EPRS) GO TO 74	SUB7	28
72	PGRHO=E*(APR+BPR/EE)+BIGAPR/RHOSTR+(2.*B(GBPR*MU)/RHOSTR+(2.*E**2*	SUB7	29
	IBPR)/(ESTAR*ETA**2*EE**2)	SUB7	30
	PGE=(APR+BPR/EE)*RHO-(E*BPR*RHO)/(ESTAR*ETA**2*EE**2)	SUB7	31
	GO TO 75	SUB7	32
74	C1=RHOSTR/RHO-1.	SUB7	33
	C2=EXP(-BETA*C1)	SUB7	34
	C3=EXP(-ALPHA*C1**2)	SUB7	35
	T1=(BPR*E*RHO)/EE+BIGAPR*MU*C2	SUB7	36
	T2=2.*ALPHA*C1*(RHOSTR/(RHO**2))	SUB7	37
	T3=BPR*E/EE	SUB7	38
	T4=(2.*E)/(ESTAR*ETA**2*EE)	SUB7	39
	T4=T3*T4	SUB7	40
	T5=(BIGAPR*C2)/RHOSTR	SUB7	41
	T6=(BIGAPR*MU*BETA*RHOSTR*C2)/(RHO**2)	SUB7	42
	PGRHO=APR*E+C3*(T1*T2+T3+T4+T5+T6)	SUB7	43
	T7=(BPR*RHO)/EE	SUB7	44
	PGE=APR*RHO+C3*(T7-T7*(E/(ESTAR*ETA**2*EE)))	SUB7	45
75	AA=SQRT(PGRHO+PGE*P/RHO**2)	SUB7	46
	RETURN	SUB7	47
	END	SUB7	48
	SUBROUTINE EQOSS(PFR,PFE)	SUB8	1
	COMMON CASEID(14),ITS1,ITS2,ITS3,ITS4,ITI1,ITI2,ITI3,ITI4,EPS1,EPSSUB8		2
	12,EPS3,EPS4,EPS5,EPS6,EPI1,EPI2,EPI3,EPI4,EPI5,EPI6,EPI7,VP,AR,LENSUB8		3
	LGTH,APR,BPR,BIGAPR,BIGBPR,ESTAR,ALPHA,BETA,RHOSTR,EPRS,RHOS	SUB8	4
	COMMON XMESH(20,20,6),XMESH2(20,20,6),Z(20),R(20),SURF(15,8),SURF2SUB8		5
	1(15,8),TAB(15,14,2),TAB2(15,14,2),SPART(15,2,2),RARF(15,11),RARF2(SUB8		6
	115,4),RPART(15,2)	SUB8	7
C		SUB8	8

C		SUB8	9
	COMMON ZO,RO,PO,UO,VO,LO,MO,RHOO,E0,A0,UBARO,VBARO	SUB8	10
C		SUB8	11
	COMMON NP,NT,NR,NI,NDEL,ISUB	SUB8	12
C		SUB8	13
	COMMON ZMIN,ZMAX,RMIN,RMAX,RADIUS,GZ,GR,DELTA,H	SUB8	14
	COMMON DIRCOS	SUB8	15
	COMMON TIME	SUB8	16
	COMMON IRARF	SUB8	17
	COMMON KSTOP	SUB8	18
	COMMON TPSI	SUB8	19
	COMMON KKK	SUB8	20
C		SUB8	21
C		SUB8	22
	REAL LO,MO,LENGTH,MU,KO	SUB8	23
250	ETA=RHOO/RHOSTR	SUB8	24
	MU=ETA-1.	SUB8	25
C		SUB8	26
C		SUB8	27
	EPP=E0/(ESTAR*ETA**2)+1.	SUB8	28
	TMP=APR+BPR/EPP	SUB8	29
	TMP1=BPR/(ESTAR*ETA**2+EPP**2)	SUB8	30
	PFR=TMP*E0+(BIGAPR+2.*BIGBPR*MU)/RHOSTR+2.*E0**2*TMP1	SUB8	31
	PFE=TMP*RHOO-E0*RHOO*TMP1	SUB8	32
	RETURN	SUB8	33
	END	SUB8	34
	SUBROUTINE EQOSP(RHOO2,E02,P02)	SUB9	1
	COMMON CASEID(14),ITS1,ITS2,ITS3,ITS4,ITI1,ITI2,ITI3,ITI4,EPS1,EPSSUB9	SUB9	2
	12,EPS3,EPS4,EPSS,EPS6,EPI1,EPI2,EPI3,EPI4,EPI5,EPI6,EPI7,VP,AR,LENSUB9	SUB9	3
	1GTH,APR,BPR,BIGAPR,BIGBPR,ESTAR,ALPHA,BETA,RHOSTR,EPRS,RHOS	SUB9	4
	COMMON XMESH(20,20,6),XMESH2(20,20,6),Z(20),R(20),SURF(15,8),SURF2SUB9	SUB9	5
	1(15,8),TAB(15,14,2),TAB2(15,14,2),SPART(15,2,2),RARF(15,11),RARF2(SUB9	SUB9	6
	115,4),RPART(15,2)	SUB9	7
C		SUB9	8
C		SUB9	9
	COMMON ZO,RO,PO,UO,VO,LO,MO,RHOO,E0,A0,UBARO,VBARO	SUB9	10

C		SUB9	11
	COMMON NP,NT,NR,NI,NDEL,ISUB	SUB9	12
C		SUB9	13
	COMMON ZMIN,ZMAX,RMIN,RMAX,RADIUS,GZ,GR,DELTA,H	SUB9	14
	COMMON DIRCOS	SUB9	15
	COMMON TIME	SUB9	16
	COMMON IRARF	SUB9	17
	COMMON KSTOP	SUB9	18
	COMMON TPSI	SUB9	19
	COMMON KKK	SUB9	20
C		SUB9	21
C		SUB9	22
	REAL LO,MO,LENGTH,MU,KO	SUB9	23
	ETA=RHO02/RHOSTR	SUB9	24
	MU=ETA-1.	SUB9	25
	PO2=E02*RHO02*(APR+(BPR*ESTAR*ETA**2)/(E02+ESTAR*ETA**2))+BIGAPR*MSUB9	SUB9	26
	1U+BIGBPR*MU**2	SUB9	27
	RETURN	SUB9	28
	END	SUB9	29
	SUBROUTINE EQOSI(PO2,PGRHO,PGE,BIGG,CHECK,KRTT,A02,E02,RHO02,KM,EPSSU10	SU10	1
	1S)	SU10	2
	COMMON CASEID(14),ITS1,ITS2,ITS3,ITS4,ITI1,ITI2,ITI3,ITI4,EPS1,EPSSU10	SU10	3
	12,EPS3,EPS4,EPSS5,EPSS6,EPI1,EPI2,EPI3,EPI4,EPI5,EPI6,EPI7,VP,AR,LENSU10	SU10	4
	1GTH,APR,BPR,BIGAPR,BIGBPR,ESTAR,ALPHA,BETA,RHOSTR,EPRS,RHOS	SU10	5
	COMMON XMESH(20,20,6),XMESH2(20,20,6),Z(20),R(20),SURF(15,8),SURF2SU10	SU10	6
	1(15,8),TAB(15,14,2),TAB2(15,14,2),SPART(15,2,2),RARF(15,11),RARF2(SU10	SU10	7
	115,4),RPART(15,2)	SU10	8
C		SU10	9
C		SU10	10
	COMMON ZO,RO,PO,UO,VO,LO,MO,RHOO,E0,AO,UBARO,VBARO	SU10	11
C		SU10	12
	COMMON NP,NT,NR,NI,NDEL,ISUB	SU10	13
C		SU10	14
	COMMON ZMIN,ZMAX,RMIN,RMAX,RADIUS,GZ,GR,DELTA,H	SU10	15
	COMMON DIRCOS	SU10	16
	COMMON TIME	SU10	17

	COMMON IRARF	SU10	18
	COMMON KSTOP	SU10	19
	COMMON TPSI	SU10	20
	COMMON KKK	SU10	21
C		SU10	22
C		SU10	23
	REAL LO,MO,LENGTH,MU,KO	SU10	24
	INTEGER CHECK,CHECK2	SU10	25
	IF (KM.EQ.0) GO TO 708	SU10	26
	RH00=RH0STR	SU10	27
	TMP1=(APR+BPR)*RH0STR-P02/ESTAR	SU10	28
	TMP2=SQRT(TMP1**2+4.*P02*APR*RH0STR/ESTAR)	SU10	29
	EO=(-TMP1+TMP2)/(2.*APR*RH0STR/ESTAR)	SU10	30
	IF (P02.GT.EPS) GO TO 708	SU10	31
	P02=0.	SU10	32
	E02=0.	SU10	33
	RH002=RH0STR	SU10	34
	A02=SQRT(8IGAPR/RH0STR)	SU10	35
	KRTT=1	SU10	36
	GO TO 870	SU10	37
708	KRTT=0	SU10	38
	ETA=RH00/RH0STR	SU10	39
	MU=ETA-1.	SU10	40
	EE=EO/(ESTAR*ETA**2)+1.	SU10	41
	IF (RH00.GT.RH0STR) GO TO 720	SU10	42
	IF (EO.LT.EPRS) GO TO 720	SU10	43
715	C1=RH0STR/RH00-1.	SU10	44
	BEC1=BETA*C1	SU10	45
	IF (BEC1.LT.10.E10) GO TO 716	SU10	46
	C2=0.0	SU10	47
	GO TO 717	SU10	48
716	C2=EXP(-BEC1)	SU10	49
717	C3AL=ALPHA*C1**2	SU10	50
	IF (C3AL.LT.10.E12) GO TO 718	SU10	51
	C3=0.0	SU10	52
	GO TO 719	SU10	53

718	C3=EXP(-C3AL)	SU10	54
719	CONTINUE	SU10	55
	T1=(BPR*EO*RHO0)/EE+BIGAPR*MU*C2	SU10	56
	T2=2.*ALPHA*C1*(RHOSTR/(RHO0**2))	SU10	57
	T3=BPR*EO/EE	SU10	58
	T4=(2.*EO)/(ESTAR*ETA**2*EE)	SU10	59
	T4=T3*T4	SU10	60
	T5=(BIGAPR*C2)/RHOSTR	SU10	61
	T6=(BIGAPR*MU*BETA*RHOSTR*C2)/(RHO0**2)	SU10	62
	T7=(BPR*RHO0)/EE	SU10	63
	PGRHO=APR*EO+C3*(T1*T2+T3+T4+T5+T6)	SU10	64
	PGE=APR*RHO0+C3*(T7-T7*(EO/(ESTAR*ETA**2*EE)))	SU10	65
	BIGG=P02-APR*EO*RHO0-T1*C3	SU10	66
	CHECK=0	SU10	67
	GO TO 725	SU10	68
720	T1=APR+BPR/EE	SU10	69
	T2=(BPR*EO)/(ESTAR*ETA**2*EE**2)	SU10	70
	BIGG=P02-T1*EO*RHO0-BIGAPR*MU-BIGBPR*MU**2	SU10	71
	PGRHO=T1*EO+BIGAPR/RHOSTR+2.*BIGBPR*MU/RHOSTR+T2*2.*EO	SU10	72
	PGRHO=-PGRHO	SU10	73
	PGE=T1*RHO0-RHO0*T2	SU10	74
	PGE=-PGE	SU10	75
	CHECK=1	SU10	76
725	CONTINUE	SU10	77
870	CONTINUE	SU10	78
	RETURN	SU10	79
	END	SU10	80
	SUBROUTINE SOUT2	SU11	1
C		SU11	2
C	PRINTS 6 LINES OF DISCONTINUITY AT TO	SU11	3
C		SU11	4
	COMMON CASEID(14),ITS1,ITS2,ITS3,ITS4,ITI1,ITI2,ITI3,ITI4,EPS1,EPSSU11	SU11	5
	12,EPS3,EPS4,EPS5,EPS6,EPI1,EPI2,EPI3,EPI4,EPI5,EPI6,EPI7,VP,AR,LENSU11	SU11	6
	1GTH,APR,BPR,BIGAPR,BIGBPR,ESTAR,ALPHA,BETA,RHOSTR,EPRS,RHOS	SU11	7
	COMMON XMESH(20,20,6),XMESH2(20,20,6),Z(20),R(20),SURF(15,8),SURF2SU11	SU11	8
	1(15,8),TAB(15,14,2),TAB2(15,14,2),SPART(15,2,2),RARF(15,11),RARF2(SU11	SU11	9

	115,4),RPART(15,2)	SU11	10
C		SU11	11
C		SU11	12
	COMMON ZO,RO,PO,UO,VO,LO,MO,RHOO,E0,A0,UBARO,VBARO	SU11	13
C		SU11	14
	COMMON NP,NT,NR,NI,NDEL,ISUB	SU11	15
C		SU11	16
	COMMON ZMIN,ZMAX,RMIN,RMAX,RADIUS,GZ,GR,DELTA,H	SU11	17
	COMMON DIRCOS	SU11	18
	COMMON TIME	SU11	19
	COMMON IRARF	SU11	20
	COMMON KSTOP	SU11	21
	COMMON TPSI	SU11	22
	COMMON KKK	SU11	23
	REAL LO,MO,LENGTH,MU,KO	SU11	24
C		SU11	25
4	FORMAT (///30H CURVES OF DISCONTINUITY AT T0//40X20H--PROJECTILE SHOCK--//)	SU11	26
6	FORMAT (///35X29H--PROJECTILE PARTICLE CURVE--//)	SU11	27
8	FORMAT (///42X16H--TARGET SHOCK--//)	SU11	28
10	FORMAT (///38X25H--TARGET PARTICLE CURVE--//)	SU11	29
12	FORMAT (///42X15H--RAREFACTION--//)	SU11	30
14	FORMAT (///35X30H--RAREFACTION PARTICLE CURVE--//)	SU11	31
16	FORMAT (7X1HZ19X1HR19X1HP19X1HU19X1HV/7X3HRHO17X1HE19X1HA19X1HL19X1HM//)	SU11	32
18	FORMAT (7X1HZ19X1HR//)	SU11	33
20	FORMAT (7X1HZ19X1HR19X1HL19X1HM//)	SU11	34
30	FORMAT (5E20.8/5E20.8//)	SU11	35
35	FORMAT (2E20.8)	SU11	36
38	FORMAT (4E20.8)	SU11	37
39	FORMAT (///35X16H--FREE SURFACE--//)	SU11	38
40	FORMAT (1H1)	SU11	39
	WRITE (3,4)	SU11	40
	WRITE (3,16)	SU11	41
	WRITE (3,30) ((TAB2(I,J,1),J=1,10),I=1,NP)	SU11	42
	WRITE (3,6)	SU11	43
		SU11	44
		SU11	45

WRITE (3,18)	SU11	46
WRITE (3,35) ((SPART(I,J,1),J=1,2),I=1,NP)	SU11	47
WRITE (3,8)	SU11	48
WRITE (3,16)	SU11	49
WRITE (3,30) ((TAB2(I,J,2),J=1,10),I=1,NT)	SU11	50
WRITE (3,10)	SU11	51
WRITE (3,18)	SU11	52
WRITE (3,35) ((SPART(I,J,2),J=1,2),I=1,NT)	SU11	53
WRITE (3,12)	SU11	54
WRITE (3,20)	SU11	55
WRITE (3,38) ((RARF2(I,J),J=1,4),I=1,NR)	SU11	56
WRITE (3,14)	SU11	57
WRITE (3,39)	SU11	58
WRITE (3,35) ((SURF2(I,J),J=1,2),I=1,NP)	SU11	59
WRITE (3,40)	SU11	60
RETURN	SU11	61
END	SU11	62
SUBROUTINE SOUT	SU12	1
	SU12	2
PRINTS 4 LINES OF DISCONTINUITY AT TO-H	SU12	3
	SU12	4
COMMON CASEID(14),ITS1,ITS2,ITS3,ITS4,ITI1,ITI2,ITI3,ITI4,EPS1,EPSSU12		5
12,EPS3,EPS4,EPSS5,EPS6,EPI1,EPI2,EPI3,EPI4,EPI5,EPI6,EPI7,VP,AR,LENSU12		6
1GTH,APR,BPR,BIGAPR,BIGBPR,ESTAR,ALPHA,BETA,RHOSTR,EPRS,RHOS	SU12	7
COMMON XMESH(20,20,6),XMESH2(20,20,6),Z(20),R(20),SURF(15,8),SURF2SU12		8
1(15,8),TAB(15,14,2),TAB2(15,14,2),SPART(15,2,2),RARF(15,11),RARF21SU12		9
115,4),RPART(15,2)	SU12	10
	SU12	11
	SU12	12
COMMON ZO,RO,PO,UO,VO,LO,MO,RHOO,E0,AO,UBARO,VBARO	SU12	13
	SU12	14
COMMON NP,NT,NR,NI,NDEL,ISUB	SU12	15
	SU12	16
COMMON ZMIN,ZMAX,RMIN,RMAX,RADIUS,GZ,GR,DELTA,H	SU12	17
COMMON DIRCOS	SU12	18
COMMON TIME	SU12	19



COMMON IRARF SU12 20  
COMMON KSTOP SU12 21  
COMMON TPSI SU12 22  
COMMON KKK SU12 23  
REAL LO,MO,LENGTH,MU,KO SU12 24  
C SU12 25  
4 FORMAT (///32H CURVES OF DISCONTINUITY AT TO-H//40X20H--PROJECTILE SU12 26  
1 SHOCK--//) SU12 27  
6 FORMAT (//42X16H--TARGET SHOCK--//) SU12 28  
8 FORMAT (//42X15H--RAREFACTION--//) SU12 29  
10 FORMAT (7X1HZ19X1HR19X1HP19X1HU19X1HV/7X3HRHO17X1HE19X1HA19X1HL19XSU12 30  
11HM//) SU12 31  
15 FORMAT (5E20.8/5E20.8//) SU12 32  
18 FORMAT (1H1) SU12 33  
21 FORMAT (//35X16H--FREE SURFACE--//) SU12 34  
25 FORMAT (2E20.8) SU12 35  
WRITE (3,4) SU12 36  
WRITE (3,10) SU12 37  
WRITE (3,15) ((TAB(I,J,1),J=1,10),I=1,NP) SU12 38  
WRITE (3,6) SU12 39  
WRITE (3,10) SU12 40  
WRITE (3,15) ((TAB(I,J,2),J=1,10),I=1,NT) SU12 41  
WRITE (3,8) SU12 42  
WRITE (3,10) SU12 43  
WRITE (3,15) ((RARF(I,J),J=1,10),I=1,NR) SU12 44  
WRITE (3,21) SU12 45  
WRITE (3,25) ((SURF(I,J),J=1,2),I=1,NP) SU12 46  
WRITE (3,18) SU12 47  
RETURN SU12 48  
END SU12 49  
SUBROUTINE PRINT(BL,ZTAB,RTAB,KK) SU13 1  
C PRINTS INTERIOR REGION SU13 2  
C SU13 3  
COMMON CASEID(14),ITS1,ITS2,ITS3,ITS4,ITI1,ITI2,ITI3,ITI4,EPS1,EPSSU13 4  
12,EPS3,EPS4,EPSS,EPSS,EPSS,EPSS,EPI1,EPI2,EPI3,EPI4,EPI5,EPI6,EPI7,VP,AR,LENSU13 5  
1GTH,APR,BPR,BIGAPR,BIGBPR,ESTAR,ALPHA,BETA,RHOSTR,EPRS,RHOS SU13 6

	COMMON XMESH(20,20,6),XMESH2(20,20,6),Z(20),R(20),SURF(15,8),SURF2	SU13	7
	1(15,8),TAB(15,14,2),TAB2(15,14,2),SPART(15,2,2),RARF(15,11),RARF2	SU13	8
	115,4),RPART(15,2)	SU13	9
C		SU13	10
C		SU13	11
	COMMON ZO,RO,PO,UO,VO,LO,MO,RHOO,EO,AO,UBARO,VBARO	SU13	12
C		SU13	13
	COMMON NP,NT,NR,NI,NDEL,ISUB	SU13	14
C		SU13	15
	COMMON ZMIN,ZMAX,RMIN,RMAX,RADIUS,GZ,GR,DELTA,H	SU13	16
	COMMON DIRCOS	SU13	17
	COMMON TIME	SU13	18
	COMMON IRARF	SU13	19
	COMMON KSTOP	SU13	20
	COMMON TPSI	SU13	21
	COMMON KKK	SU13	22
	REAL LO,MO,LENGTH,MU,KO	SU13	23
C		SU13	24
	DIMENSION BL(20,20,6),ZTAB(20),RTAB(20)	SU13	25
C		SU13	26
	DO 15 I=1,20	SU13	27
	DO 15 J=1,20	SU13	28
	IF (ABS(BL(I,J,1))+ABS(BL(I,J,2))+ABS(BL(I,J,3))) 20,15,20	SU13	29
15	CONTINUE	SU13	30
	WRITE (3,18)	SU13	31
18	FORMAT (15H1TABLES ALL = 0/1H1)	SU13	32
	CALL EXIT	SU13	33
20	I1=I	SU13	34
	DO 30 I=I1,20	SU13	35
	IF (ABS(BL(I,1,1))+ABS(BL(I,1,2))+ABS(BL(I,1,3))) 30,22,30	SU13	36
22	DO 25 J=1,20	SU13	37
	IF (ABS(BL(I,J,1))+ABS(BL(I,J,2))+ABS(BL(I,J,3))) 30,25,30	SU13	38
25	CONTINUE	SU13	39
	I2=I-1	SU13	40
	GO TO 35	SU13	41
30	CONTINUE	SU13	42

	I2=20	SU13	43
35	DO 45 J=1,20	SU13	44
	IF (ABS(BL(I1,J,1))+ABS(BL(I1,J,2))+ABS(BL(I1,J,3))) 45,37,45	SU13	45
37	DO 40 I=I1,I2	SU13	46
	IF (ABS(BL(I,J,1))+ABS(BL(I,J,2))+ABS(BL(I,J,3))) 45,40,45	SU13	47
40	CONTINUE	SU13	48
	J2=J-1	SU13	49
	GO TO 50	SU13	50
45	CONTINUE	SU13	51
	J2=20	SU13	52
50	J1=1	SU13	53
C		SU13	54
C	PRINT TABLE	SU13	55
C		SU13	56
	GO TO (52,56),KK	SU13	57
52	WRITE (3,53)	SU13	58
53	FORMAT (//24H0INTERIOR REGION AT TO-H//)	SU13	59
	GO TO 62	SU13	60
56	WRITE (3,57)	SU13	61
57	FORMAT (//22H0INTERIOR REGION AT TO//)	SU13	62
62	DO 70 I=I1,I2	SU13	63
	WRITE (3,64) ZTAB(I)	SU13	64
64	FORMAT (///7H0ZTAB =,F10.4//7X1HR9X1HP17X1HU17X1HV17X3HRHO15X1HE17	SU13	65
	1X1HA//)	SU13	66
	DO 69 J=J1,J2	SU13	67
	WRITE (3,68) RTAB(J),(BL(I,J,K),K=1,6)	SU13	68
68	FORMAT (F12.4,6E18.8)	SU13	69
69	CONTINUE	SU13	70
70	CONTINUE	SU13	71
80	WRITE (3,82)	SU13	72
82	FORMAT (1H1)	SU13	73
	RETURN	SU13	74
	END	SU13	75
	SUBROUTINE NRIT2(X,Y,XO,OX,YO,DY,EX,EY,FGOF,IT,KODE)	SU14	1
C		SU14	2
C	NEWTON-RAPHSON METHOD FOR SOLUTION OF	SU14	3

C	TWO NON LINEAR EQUATIONS IN TWO UNKNOWNNS	SU14	4
C		SU14	5
	COMMON CASEID(14),ITS1,ITS2,ITS3,ITS4,ITI1,ITI2,ITI3,ITI4,EPS1,EPSSU14		6
	12,EPS3,EPS4,EPS5,EPS6,EPI1,EPI2,EPI3,EPI4,EPI5,EPI6,EPI7,VP,AR,LENSU14		7
	1GTH,APR,BPR,BIGAPR,BIGBPR,ESTAR,ALPHA,BETA,RHOSTR,EPRS,RHOS	SU14	8
	COMMON XMESH(20,20,6),XMESH2(20,20,6),Z(20),R(20),SURF(15,8),SURF2SU14		9
	1(15,8),TAB(15,14,2),TAB2(15,14,2),SPART(15,2,2),RARF(15,11),RARF2(SU14		10
	115,4),RPART(15,2)	SU14	11
C		SU14	12
C		SU14	13
	COMMON ZO,RO,PO,UO,VO,LO,MO,RHOO,E0,AO,UBARO,VBARO	SU14	14
C		SU14	15
	COMMON NP,NT,NR,NI,NDEL,ISUB	SU14	16
C		SU14	17
	COMMON ZMIN,ZMAX,RMIN,RMAX,RADIUS,GZ,GR,DELTA,H	SU14	18
	COMMON DIRCOS	SU14	19
	COMMON TIME	SU14	20
	COMMON IRARF	SU14	21
	COMMON KSTOP	SU14	22
	COMMON TPSI	SU14	23
	COMMON KKK	SU14	24
	REAL LO,MO,LENGTH,MU,KO	SU14	25
C		SU14	26
	XB=X0	SU14	27
	YB=Y0	SU14	28
	DXX=DX	SU14	29
	DYY=DY	SU14	30
	DELX1=0	SU14	31
	DELY1=0	SU14	32
	KODE=0	SU14	33
1	CONTINUE	SU14	34
	DO 50 I=1,IT	SU14	35
	KK=0	SU14	36
	XX=XB+DXX	SU14	37
	YY=YB+DYY	SU14	38
C		SU14	39

C	CALL FGOF(XB,YY,F2,G2)	SU14	40
	CALL FGOF(XX,YB,F1,G1)	SU14	41
	CALL FGOF(XB,YB,F0,G0)	SU14	42
	A1=(F1-F0)/DXX	SU14	43
	B1=(F2-F0)/DYY	SU14	44
	C1=-F0	SU14	45
	A2=(G1-G0)/DXX	SU14	46
	B2=(G2-G0)/DYY	SU14	47
	C2=-G0	SU14	48
	DET=A1*B2-A2*B1	SU14	49
	IF (DET.EQ.0.) GO TO 920	SU14	50
	DELX=(B2*C1-B1*C2)/DET	SU14	51
	DELY=(A1*C2-A2*C1)/DET	SU14	52
	IF (ABS(DELX).GT..001) GO TO 8	SU14	53
	DELX=0.	SU14	54
8	IF (ABS(DELY).GT..001) GO TO 9	SU14	55
	DELY=0.	SU14	56
9	CONTINUE	SU14	57
	SDEL=ABS(DELX+DELX1)+ABS(DELY+DELY1)	SU14	58
	DELX1=DELX	SU14	59
	DELY1=DELY	SU14	60
C		SU14	61
C	TEST FOR SAME REGION	SU14	62
C		SU14	63
	DO 10 J=1,IT	SU14	64
	XB1=XB+DELX	SU14	65
	YB1=YB+DELY	SU14	66
	IF (YB1.LE.0.)YB1=0.	SU14	67
	M=COMP(XB,YB,XB1,YB1)	SU14	68
	IF (M.EQ.1) GO TO 15	SU14	69
11	CONTINUE	SU14	70
	KK=1	SU14	71
	DELX=.5*DELX	SU14	72
	DELY=.5*DELY	SU14	73
10	CONTINUE	SU14	74
		SU14	75

```

      GO TO 930
15  IF (ABS(XB-XB1).GT.EX) GO TO 45
      IF (ABS(YB-YB1).GT.EY) GO TO 45
      IF (KK.NE.0) GO TO 45
      X=XB1
      Y=YB1
      KODE=0
      RETURN
45  CONTINUE
      IF (KODE.NE.1) GO TO 46
      IF (SDEL.GT.EPI1) GO TO 46
      DELX=.5*DELX
      DELY=.5*DELY
      GO TO 9
46  XB=XB1
      YB=YB1
      DEL=DELTA
      DO 70 N=1,NDEL
      XB2=XB+DEL
      M=COMP(XB,YB,XB2,YB)
      IF (M.NE.1) GO TO 55
      OXX=DEL
      GO TO 80
55  XB2=XB-DEL
      M=COMP(XB,YB,XB2,YB)
      IF (M.NE.1) GO TO 60
      OXX=-DEL
      GO TO 80
60  DEL=.5*DEL
70  CONTINUE
      GO TO 980
80  DEL=DELTA
      DO 100 N=1,NDEL
      YB2=YB+DEL
      M=COMP(XB,YB,XB,YB2)
      IF (M.NE.1) GO TO 85

```

SU14	76
SU14	77
SU14	78
SU14	79
SU14	80
SU14	81
SU14	82
SU14	83
SU14	84
SU14	85
SU14	86
SU14	87
SU14	88
SU14	89
SU14	90
SU14	91
SU14	92
SU14	93
SU14	94
SU14	95
SU14	96
SU14	97
SU14	98
SU14	99
SU14	100
SU14	101
SU14	102
SU14	103
SU14	104
SU14	105
SU14	106
SU14	107
SU14	108
SU14	109
SU14	110
SU14	111

	DYY=DEL	SU14 112
	GO TO 50	SU14 113
85	YB2=YB-DEL	SU14 114
	M=COMP(XB,YB,XB,YB2)	SU14 115
	IF (M.NE.1) GO TO 90	SU14 116
	DYY=-DEL	SU14 117
	GO TO 50	SU14 118
90	DEL=.5*DEL	SU14 119
100	CONTINUE	SU14 120
	GO TO 990	SU14 121
50	CONTINUE	SU14 122
	X=XB1	SU14 123
	Y=YB1	SU14 124
	IF (KODE.EQ.1) RETURN	SU14 125
	KODE=1	SU14 126
	GO TO 1	SU14 127
920	WRITE (3,922) 1	SU14 128
922	FORMAT (46HODETERMINANT IS 0 IN SUBR. NRIT2 FOR ITERATION,14)	SU14 129
	GO TO 950	SU14 130
930	KODE=2	SU14 131
	RETURN	SU14 132
950	WRITE (3,952) X0,Y0,XB,YB,XB1,YB1,DELX,DELY	SU14 133
952	FORMAT (1X5HZ0 =,E15.8,4X5HRO =,E15.8/1X5HZB =,E15.8,4X5HRB =,SU14 134	
	1E15.8/1X5HZB1 =,E15.8,4X5HRB1 =,E15.8/1X5HDELZ=,E15.8,4X5HDELR=,E1SU14 135	
	15.8/1H1)	SU14 136
	CALL EXIT	SU14 137
	RETURN	SU14 138
980	KODE=3	SU14 139
	RETURN	SU14 140
990	KODE=4	SU14 141
	RETURN	SU14 142
	END	SU14 143
	FUNCTION COMP(ZP,RP,ZP1,RP1)	SU15 1
C		SU15 2
C	DETERMINES IF 2 POINTS ARE IN THE SAME REGION	SU15 3
	COMMON CASEID(14),ITS1,ITS2,ITS3,ITS4,ITI1,ITI2,ITI3,ITI4,EPS1,EPSSU15 4	

	12, EPS3, EPS4, EPS5, EPS6, EPI1, EPI2, EPI3, EPI4, EPI5, EPI6, EPI7, VP, AR, LENS	SU15	5
	1GTH, APR, BPR, BIGAPR, BIGBPR, ESTAR, ALPHA, BETA, RHOSTR, EPRS, RHOS	SU15	6
	COMMON XMESH(20,20,6), XMESH2(20,20,6), Z(20), R(20), SURF(15,8), SURF2	SU15	7
	1(15,8), TAB(15,14,2), TAB2(15,14,2), SPART(15,2,2), RARF(15,11), RARF2	SU15	8
	115,4), RPART(15,2)	SU15	9
C		SU15	10
	COMMON ZO, RO, PO, UO, VO, LO, MO, RHOO, EO, AO, UBARO, VBARO	SU15	11
C		SU15	12
	COMMON NP, NT, NR, NI, NDEL, ISUB	SU15	13
C		SU15	14
	COMMON ZMIN, ZMAX, RMIN, RMAX, RADIUS, GZ, GR, DELTA, H	SU15	15
	COMMON DIRCOS	SU15	16
	COMMON TIME	SU15	17
	COMMON IRARF	SU15	18
	COMMON KSTOP	SU15	19
	COMMON TPSI	SU15	20
	COMMON KKK	SU15	21
	REAL LO, MO, LENGTH, MU, KO	SU15	22
	EPS=.0000001	SU15	23
	IF (RP1.LT.0.) GO TO 80	SU15	24
	IF (ZP1.GE.0.) GO TO 4	SU15	25
	IF (RP1.GT.RADIUS) GO TO 80	SU15	26
C		SU15	27
C	FIND CONTROL CONSTANTS FOR ZP, RP	SU15	28
C		SU15	29
4	CONTINUE	SU15	30
	IF (ITS3.EQ.1) GO TO 33	SU15	31
	IF (IRARF.EQ.1) GO TO 13	SU15	32
	M=PICK(ZP, RP, 3)	SU15	33
	IF (ZP.GT.RARF(M,1).AND.M.NE.1) M=M-1	SU15	34
	FF=RP-RARF(M+1,2)-(RARF(M,2)-RARF(M+1,2))*(ZP-RARF(M+1,1))/(RARF(M	SU15	35
	1,1)-RARF(M+1,1))	SU15	36
	IF (FF.LT.0.) GO TO 11	SU15	37
10	NN=1	SU15	38
	GO TO 13	SU15	39
11	NN=0	SU15	40



13	CONTINUE	SU15	41
	DO 22 K=1,2	SU15	42
	M=PICK(ZP1,RP1,K)	SU15	43
	IF (RP1.LT.TAB(M,2,K).AND.M.NE.1)M=M-1	SU15	44
5	CONTINUE	SU15	45
	FF=ZP1-TAB(M+1,1,K)-(TAB(M,1,K)-TAB(M+1,1,K))*(RP1-TAB(M+1,2,K))/(	SU15	46
	1TAB(M,2,K)-TAB(M+1,2,K))	SU15	47
	IF (K.EQ.2) GO TO 17	SU15	48
	IF (RP1.GT.RADIUS) GO TO 21	SU15	49
	IF (FF.LT.-EPS) GO TO 90	SU15	50
	GO TO 21	SU15	51
17	IF (FF.GT.EPS) GO TO 100	SU15	52
21	IF (RP.GT.RADIUS) GO TO 22	SU15	53
	M=PICK(ZP1,RP1,4)	SU15	54
	FF=ZP1-SURF(M+1,1)-(SURF(M,1)-SURF(M+1,1))*(RP1-SURF(M+1,2))/(SURF	SU15	55
	1(M,2)-SURF(M+1,2))	SU15	56
	IF (FF) 80,22,22	SU15	57
22	CONTINUE	SU15	58
	IF (IRARF.EQ.1) GO TO 33	SU15	59
	M=PICK(ZP1,RP1,3)	SU15	60
	IF (ZP1.GT.RARF(M,1).AND.M.NE.1)M=M-1	SU15	61
	FF=RP1-RARF(M+1,2)-(RARF(M,2)-RARF(M+1,2))*(ZP1-RARF(M+1,1))/(RARF	SU15	62
	1(M,1)-RARF(M+1,1))	SU15	63
	IF (FF.LT.0.) GO TO 31	SU15	64
30	NN1=1	SU15	65
	GO TO 32	SU15	66
31	NN1=0	SU15	67
32	IF (NN1.NE.NN) GO TO 110	SU15	68
33	CONTINUE	SU15	69
	COMP=1	SU15	70
	COMP=COMP+.2	SU15	71
	RETURN	SU15	72
80	COMP=2	SU15	73
	COMP=COMP+.2	SU15	74
	RETURN	SU15	75
90	COMP=3.	SU15	76

	COMP=COMP+.2	SU15	77
	RETURN	SU15	78
100	COMP=4.	SU15	79
	COMP=COMP+.2	SU15	80
	RETURN	SU15	81
110	COMP=5.	SU15	82
	COMP=COMP+.2	SU15	83
	RETURN	SU15	84
	END	SU15	85
	FUNCTION PICK(ZP,RP,KODE)	SU16	1
C		SU16	2
C	DETERMINES 2 CLOSEST CONSECUTIVE POINTS ON SPECIFIED	SU16	3
C	LINE OF DISCONTINUITY TO A GIVEN POINT	SU16	4
C		SU16	5
	COMMON CASEID(14),ITS1,ITS2,ITS3,ITS4,ITI1,ITI2,ITI3,ITI4,EPS1,EPSSU16	SU16	6
	12,EPS3,EPS4,EPS5,EPS6,EPI1,EPI2,EPI3,EPI4,EPI5,EPI6,EPI7,VP,AR,LENSU16	SU16	7
	1GTH,APR,BPR,BIGAPR,BIGBPR,ESTAR,ALPHA,BETA,RHOSTR,EPRS,RHOS	SU16	8
	COMMON XMESH(20,20,6),XMESH2(20,20,6),Z(20),R(20),SURF(15,8),SURF2SU16	SU16	9
	1(15,8),TAB(15,14,2),TAB2(15,14,2),SPART(15,2,2),RARF(15,11),RARF2(SU16	SU16	10
	115,4),RPART(15,2)	SU16	11
C		SU16	12
C		SU16	13
	COMMON ZO,RO,PO,UO,VO,LO,MO,RHOO,EO,AO,UBARO,VBARO	SU16	14
C		SU16	15
	COMMON NP,NT,NR,NI,NDEL,ISUB	SU16	16
C		SU16	17
	COMMON ZMIN,ZMAX,RMIN,RMAX,RADIUS,GZ,GR,DELTA,H	SU16	18
	COMMON DIRCOS	SU16	19
	COMMON TIME	SU16	20
	COMMON IRARF	SU16	21
	COMMON KSTOP	SU16	22
	COMMON TPSI	SU16	23
	COMMON KKK	SU16	24
	REAL LO,MO,LENGTH,MU,KO	SU16	25
C		SU16	26
	GO TO (5,10,100,300),KODE	SU16	27

5	NN=NP	SU16	28
	K=1	SU16	29
	GO TO 15	SU16	30
10	NN=NT	SU16	31
	K=2	SU16	32
15	AA=(TAB(1,1,K)-ZP)**2+(TAB(1,2,K)-RP)**2	SU16	33
C		SU16	34
C	SEARCH SHOCK TABLES	SU16	35
C		SU16	36
	DO 60 N=2,NN	SU16	37
	A=(TAB(N,1,K)-ZP)**2+(TAB(N,2,K)-RP)**2	SU16	38
	IF (A.GE.AA) GO TO 23	SU16	39
	AA=A	SU16	40
60	CONTINUE	SU16	41
	PICK=NN-1	SU16	42
	PICK=PICK+.2	SU16	43
	RETURN	SU16	44
23	PICK=N-1	SU16	45
	PICK=PICK+.2	SU16	46
	RETURN	SU16	47
100	AA=(RARF(1,1)-ZP)**2+(RARF(1,2)-RP)**2	SU16	48
C		SU16	49
C	SEARCH RAREFACTION TABLE	SU16	50
C		SU16	51
	DO 200 N=2,NR	SU16	52
	A=(RARF(N,1)-ZP)**2+(RARF(N,2)-RP)**2	SU16	53
	IF (A.GE.AA) GO TO 203	SU16	54
	AA=A	SU16	55
200	CONTINUE	SU16	56
	PICK=NR-1	SU16	57
	PICK=PICK+.2	SU16	58
	RETURN	SU16	59
203	PICK=N-1	SU16	60
	PICK=PICK+.2	SU16	61
	RETURN	SU16	62
300	AA=(SURF(1,1)-ZP)**2+(SURF(1,2)-RP)**2	SU16	63

C		SU16	64
C	SEARCH FREE SURFACE TABLE	SU16	65
C		SU16	66
	DD 400 N=2,NP	SU16	67
	A=(SURF(N,1)-ZP)**2+(SURF(N,2)-RP)**2	SU16	68
	IF (A.GE.AA) GO TO 303	SU16	69
	AA=A	SU16	70
400	CONTINUE	SU16	71
	PICK=NP-1	SU16	72
	PICK=PICK+.2	SU16	73
	RETURN	SU16	74
303	PICK=N-1	SU16	75
	PICK=PICK+.2	SU16	76
304	CONTINUE	SU16	77
	RETURN	SU16	78
	END	SU16	79
	SUBROUTINE GUESS(KOD1,KOD2,ZP,RP,I2,K2,ZG,RG,DZ,DR)	SU17	1
C		SU17	2
C	DETERMINES STARTING POINT AND DELTAS	SU17	3
C	FOR NEWTON-RAPHSON ITERATION	SU17	4
C		SU17	5
	COMMON CASEID(14),ITS1,ITS2,ITS3,ITS4,ITI1,ITI2,ITI3,ITI4,EPS1,EPSSU17	SU17	6
	I2,EPS3,EPS4,EPS5,EPS6,EPI1,EPI2,EPI3,EPI4,EPI5,EPI6,EPI7,VP,AR,LENSU17	SU17	7
	IGTH,APR,BPR,BIGAPR,BIGBPR,ESTAR,ALPHA,BETA,RHOSTR,EPRS,RHOS	SU17	8
	COMMON XMESH(20,20,6),XMESH2(20,20,6),Z(20),R(20),SURF(15,8),SURF2SU17	SU17	9
	I(15,8),TAB(15,14,2),TAB2(15,14,2),SPART(15,2,2),RARF(15,11),RARF2(SU17	SU17	10
	115,4),RPART(15,2)	SU17	11
C		SU17	12
C		SU17	13
	COMMON ZO,RO,PO,UO,VO,LO,MO,RHOO,EO,AO,UBARO,VBARO	SU17	14
C		SU17	15
	COMMON NP,NT,NR,NI,NDEL,ISUB	SU17	16
C		SU17	17
	COMMON ZMIN,ZMAX,RMIN,RMAX,RADIUS,GZ,GR,DELTA,H	SU17	18
	COMMON DIRCOS	SU17	19
	COMMON TIME	SU17	20

	COMMON IRARF	SU17	21
	COMMON KSTOP	SU17	22
	COMMON TPSI	SU17	23
	COMMON KKK	SU17	24
	REAL LO,MO,LENGTH,MU,KO	SU17	25
C		SU17	26
	KS=0	SU17	27
	IF (KOD1.EQ.2) GO TO 10	SU17	28
	ZG=TAB(I2,1,K2)	SU17	29
	RG=TAB(I2,2,K2)	SU17	30
	IF (IRARF.EQ.1) GO TO 9	SU17	31
2	M=1-(NR-2)*(K2-2)	SU17	32
	FF=RG-RARF(M+1,2)-(RARF(M,2)-RARF(M+1,2))*{ZG-RARF(M+1,1)}/(RARF(M	SU17	33
	1,1)-RARF(M+1,1))	SU17	34
	IF (FF.GT.0.) GO TO 9	SU17	35
	ZG=(1.-.02/(RADIUS-RG))*ZG	SU17	36
	RG=RG+.02	SU17	37
	IF (RG.GT.(RADIUS-.01)) GO TO 110	SU17	38
	GO TO 2	SU17	39
9	CONTINUE	SU17	40
	GO TO 50	SU17	41
10	JJJ=NT-1	SU17	42
	IF (ITS3.EQ.1) GO TO 26	SU17	43
	DO 24 M=1,JJJ	SU17	44
	IF (RP.GT.TAB(M+1,2,2).OR.RP.LT.TAB(M,2,2)) GO TO 24	SU17	45
	GO TO 25	SU17	46
24	CONTINUE	SU17	47
25	CONTINUE	SU17	48
	FF=ZP-TAB(M+1,1,2)-(TAB(M,1,2)-TAB(M+1,1,2))*{RP-TAB(M+1,2,2)}/(TASU17	49	
	1B(M,2,2)-TAB(M+1,2,2))	SU17	50
	IF (FF.GT.0.) GO TO 20	SU17	51
26	CONTINUE	SU17	52
	ZG=ZP	SU17	53
	RG=RP	SU17	54
	GO TO 50	SU17	55
20	IK=M	SU17	56

	M=CROSS(TAB(IK,1,2),TAB(IK,2,2),TAB(IK+1,1,2),TAB(IK+1,2,2),0.,0.,	SU17	57
	1ZP,RP,ZG,RG)	SU17	58
	GO TO (50,920,930),M	SU17	59
C		SU17	60
C	COMPUTE DELTAS	SU17	61
C		SU17	62
50	DEL=DELTA	SU17	63
C		SU17	64
C	Z DELTA	SU17	65
C		SU17	66
	LL=0	SU17	67
52	DO 70 N=1,NDEL	SU17	68
	ZZ=ZG+DEL	SU17	69
	M=COMP(ZG,RG,ZZ,RG)	SU17	70
	IF (M.NE.1) GO TO 55	SU17	71
	DZ=DEL	SU17	72
	GO TO 80	SU17	73
55	ZZ=ZG-DEL	SU17	74
	M=COMP(ZG,RG,ZZ,RG)	SU17	75
	IF (M.NE.1) GO TO 60	SU17	76
	DZ=-DEL	SU17	77
	GO TO 80	SU17	78
60	DEL=.5*DEL	SU17	79
70	CONTINUE	SU17	80
	LL=LL+1	SU17	81
	IF (LL.EQ.3) GO TO 75	SU17	82
	RG=RG-DELTA/5.	SU17	83
	DEL=DELTA	SU17	84
	GO TO 52	SU17	85
75	KOD2=2	SU17	86
	RETURN	SU17	87
80	DEL=DELTA	SU17	88
	IF (KS.EQ.1) GO TO 120	SU17	89
C		SU17	90
C	R DELTA	SU17	91
C		SU17	92

	LL=0	SU17 93
82	DO 100 N=1,NDEL	SU17 94
	RR=RG+DEL	SU17 95
	M=COMP(ZG,RG,ZG,RR)	SU17 96
	IF (M.NE.1) GO TO 85	SU17 97
	OR=DEL	SU17 98
	IF (KS.EQ.1) GO TO 50	SU17 99
	GO TO 120	SU17 100
85	RR=RG-DEL	SU17 101
	M=COMP(ZG,RG,ZG,RR)	SU17 102
	IF (M.NE.1) GO TO 90	SU17 103
	OR=-DEL	SU17 104
	IF (KS.EQ.1) GO TO 50	SU17 105
	GO TO 120	SU17 106
90	DEL=.5*DEL	SU17 107
100	CONTINUE	SU17 108
108	CONTINUE	SU17 109
	LL=LL+1	SU17 110
	FLL=LL	SU17 111
	IF (LL.EQ.5) GO TO 110	SU17 112
C		SU17 113
104	ZG1=ZG+DELTA/5.*FLL*(-1.)*LL	SU17 114
	M=COMP(ZG,RG,ZG1,RG)	SU17 115
	ZG=ZG1	SU17 116
	IF (M.NE.1) GO TO 108	SU17 117
	KS=1	SU17 118
	GO TO 82	SU17 119
110	KOD2=2	SU17 120
	RETURN	SU17 121
120	KOD2=1	SU17 122
	RETURN	SU17 123
920	WRITE (3,922)	SU17 124
922	FORMAT (42HOERROR FOR COINCIDENT LINES IN SUBR. GUESS)	SU17 125
	GO TO 950	SU17 126
C		SU17 127
930	WRITE (3,932)	SU17 128

932	FORMAT (40HOERROR FOR PARALLEL LINES IN SUBR. GUESS)	SU17	129
C		SU17	130
950	WRITE (3,952) KOD1,I2,K2,ZP,RP	SU17	131
952	FORMAT (1X5HKOD1=,I4,4X3HI2=,I4,4X3HK2=,I4/1X3HZP=,E15.8,4X3HRP=,E	SU17	132
	115.8/1H1)	SU17	133
	XYZ=-2.	SU17	134
	ZYX=SQRT(XYZ)	SU17	135
	CALL EXIT	SU17	136
	RETURN	SU17	137
	END	SU17	138
	FUNCTION CROSS(X1,Y1,X2,Y2,X3,Y3,X4,Y4,X,Y)	SU18	1
C		SU18	2
C	FINDS INTERSECTION OF TWO STRAIGHT LINES	SU18	3
C		SU18	4
	EPS=.0000001	SU18	5
	A1=Y2-Y1	SU18	6
	B1=X1-X2	SU18	7
	C1=X1*A1+Y1*B1	SU18	8
	A2=Y4-Y3	SU18	9
	B2=X3-X4	SU18	10
	C2=X3*A2+Y3*B2	SU18	11
	DET=A1*B2-A2*B1	SU18	12
	D1=C1*B2-C2*B1	SU18	13
	D2=A1*C2-A2*C1	SU18	14
	IF (ABS(DET).LE.EPS) GO TO 10	SU18	15
	X=D1/DET	SU18	16
	Y=D2/DET	SU18	17
	CROSS=1	SU18	18
	CROSS=CROSS+.2	SU18	19
	RETURN	SU18	20
10	IF (ABS(D1).GT.EPS) GO TO 20	SU18	21
	IF (ABS(D2).LE.EPS) GO TO 30	SU18	22
20	CROSS=3	SU18	23
	CROSS=CROSS+.2	SU18	24
	RETURN	SU18	25
30	X=X1	SU18	26



```

      Y=Y1
      CROSS=2
      CROSS=CROSS+.2
316  CONTINUE
      RETURN
      END
      FUNCTION PART(MODE,ZP,RP,ZX,RX,DELTA,NDEL)
C
C      LOCATES A POINT IN THE SAME REGION AS A GIVEN POINT
C      TO BE USED IN COMPUTING A PARTIAL
C      MODE=1, WITH RESPECT TO R
C      MODE=2, WITH RESPECT TO Z
C
      GO TO (2,4),MODE
2      DR=DELTA
      DZ=0.
      GO TO 8
4      DR=0.
      DZ=DELTA
8      DO 50 NN=1,NDEL
      RR=RP+DR
      ZZ=ZP+DZ
      M=COMP(ZP,RP,ZZ,RR)
      IF (M.EQ.1) GO TO 60
      RR=RP-DR
      ZZ=ZP-DZ
      M=COMP(ZP,RP,ZZ,RR)
      IF (M.EQ.1) GO TO 60
      DZ=DZ*.5
      DR=DR*.5
50     CONTINUE
      PART=2
      PART=PART+.2
      RETURN
60     ZX=ZZ
      RX=RR

```

SU18	27
SU18	28
SU18	29
SU18	30
SU18	31
SU18	32
SU19	1
SU19	2
SU19	3
SU19	4
SU19	5
SU19	6
SU19	7
SU19	8
SU19	9
SU19	10
SU19	11
SU19	12
SU19	13
SU19	14
SU19	15
SU19	16
SU19	17
SU19	18
SU19	19
SU19	20
SU19	21
SU19	22
SU19	23
SU19	24
SU19	25
SU19	26
SU19	27
SU19	28
SU19	29
SU19	30

	PART=1	SU19	31
	PART=PART+.2	SU19	32
	RETURN	SU19	33
	END	SU19	34
	FUNCTION PICK2(ZP,RP,KODE)	SU20	1
C		SU20	2
C	DETERMINES 2 CLOSEST CONSECUTIVE POINTS ON SPECIFIED	SU20	3
C	LINE OF DISCONTINUITY TO A GIVEN POINT	SU20	4
	COMMON CASEID(14),ITS1,ITS2,ITS3,ITS4,ITI1,ITI2,ITI3,ITI4,EPSSU20	SU20	5
	12,EPS3,EPS4,EPS5,EPS6,EPI1,EPI2,EPI3,EPI4,EPI5,EPI6,EPI7,VP,AR,LENSU20	SU20	6
	1GTH,APR,BPR,BIGAPR,BIGBPR,ESTAR,ALPHA,BETA,RHOSTR,EPRS,RHDS	SU20	7
	COMMON XMESH(20,20,6),XMESH2(20,20,6),Z(20),R(20),SURF(15,8),SURF2SU20	SU20	8
	1(15,8),TAB(15,14,2),TAB2(15,14,2),SPART(15,2,2),RARF(15,11),RARF2(SU20	SU20	9
	115,4),RPART(15,2)	SU20	10
C		SU20	11
	COMMON ZO,RO,PO,UO,VO,LO,MO,RHOO,EO,AO,UBARO,VBARO	SU20	12
	COMMON NP,NT,NR,NI,NDEL,ISUB	SU20	13
C		SU20	14
	COMMON ZMIN,ZMAX,RMIN,RMAX,RADIUS,GZ,GR,DELTA,H	SU20	15
	COMMON DIRCOS	SU20	16
	COMMON TIME	SU20	17
	COMMON IRARF	SU20	18
	COMMON KSTOP	SU20	19
	COMMON TPSI	SU20	20
	COMMON KKK	SU20	21
	REAL LO,MO,LENGTH,MU,KO	SU20	22
C		SU20	23
	GO TO (5,10,100,205,210,300,500),KODE	SU20	24
5	NN=NP	SU20	25
	K=1	SU20	26
	GO TO 15	SU20	27
10	NN=NT	SU20	28
	K=2	SU20	29
15	AA=(TAB2(1,1,KI)-ZP)**2+(TAB2(1,2,KI)-RP)**2	SU20	30
C		SU20	31
C	SEARCH SHOCK TABLES	SU20	32

C	DO 60 N=2,NN	SU20	33
	A=(TAB2(N,1,K)-ZP)**2+(TAB2(N,2,K)-RP)**2	SU20	34
	IF (A.GE.AA) GO TO 23	SU20	35
	AA=A	SU20	36
60	CONTINUE	SU20	37
	PICK2=NN-1	SU20	38
	PICK2=PICK2+.2	SU20	39
	RETURN	SU20	40
23	PICK2=N-1	SU20	41
	PICK2=PICK2+.2	SU20	42
	RETURN	SU20	43
100	AA=(RARF2(1,1)-ZP)**2+(RARF2(1,2)-RP)**2	SU20	44
C		SU20	45
C	SEARCH RAREFACTION TABLE	SU20	46
C		SU20	47
	DO 200 N=2,NR	SU20	48
	A=(RARF2(N,1)-ZP)**2+(RARF2(N,2)-RP)**2	SU20	49
	IF (A.GE.AA) GO TO 203	SU20	50
	AA=A	SU20	51
200	CONTINUE	SU20	52
	PICK2=NR-1	SU20	53
	PICK2=PICK2+.2	SU20	54
	RETURN	SU20	55
203	PICK2=N-1	SU20	56
	PICK2=PICK2+.2	SU20	57
	RETURN	SU20	58
205	NN=NP	SU20	59
	K=1	SU20	60
	GO TO 215	SU20	61
210	NN=NT	SU20	62
	K=2	SU20	63
215	AA=(SPART(1,1,K)-ZP)**2+(SPART(1,2,K)-RP)**2	SU20	64
C		SU20	65
C	SEARCH SHOCK PARTICLE TABLES	SU20	66
C		SU20	67
		SU20	68

	DO 260 N=2,NN	SU20	69
	A=(SPART(N,1,K)-ZP)**2+(SPART(N,2,K)-RP)**2	SU20	70
	IF (A.GE.AA) GO TO 223	SU20	71
	AA=A	SU20	72
260	CONTINUE	SU20	73
	PICK2=NN-1	SU20	74
	PICK2=PICK2+.2	SU20	75
	RETURN	SU20	76
223	PICK2=N-1	SU20	77
	PICK2=PICK2+.2	SU20	78
	RETURN	SU20	79
300	AA=(RPART(1,1)-ZP)**2+(RPART(1,2)-RP)**2	SU20	80
C		SU20	81
C	SEARCH RAREFACTION PARTICLE TABLE	SU20	82
C		SU20	83
	DO 400 N=2,NR	SU20	84
	A=(RPART(N,1)-ZP)**2+(RPART(N,2)-RP)**2	SU20	85
	IF (A.GE.AA) GO TO 403	SU20	86
	AA=A	SU20	87
400	CONTINUE	SU20	88
	PICK2=NR-1	SU20	89
	PICK2=PICK2+.2	SU20	90
	RETURN	SU20	91
403	PICK2=N-1	SU20	92
	PICK2=PICK2+.2	SU20	93
	RETURN	SU20	94
500	AA=(SURF2(1,1)-ZP)**2+(SURF2(1,2)-RP)**2	SU20	95
C		SU20	96
C	SEARCH FREE SURFACE TABLE	SU20	97
C		SU20	98
	DO 520 N=2,NP	SU20	99
	A=(SURF2(N,1)-ZP)**2+(SURF2(N,2)-RP)**2	SU20	100
	IF (A.GE.AA) GO TO 523	SU20	101
	AA=A	SU20	102
520	CONTINUE	SU20	103
	PICK2=NP-1	SU20	104

	PICK2=PICK2+.2	SU20 105
	RETURN	SU20 106
523	PICK2=N-1	SU20 107
	PICK2=PICK2+.2	SU20 108
	RETURN	SU20 109
	END	SU20 110
	FUNCTION TEST(ZP,RP)	SU21 1
C		SU21 2
C		SU21 3
C	DETERMINES IF A GIVEN INTERIOR POINT IS IN	SU21 4
C	THE REGION TO BE CONSIDERED	SU21 5
C		SU21 6
	COMMON CASEID(14),ITS1,ITS2,ITS3,ITS4,IT11,IT12,IT13,IT14,EPS1,EPSSU21	7
	12,EPS3,EPS4,EPS5,EPS6,EPI1,EPI2,EPI3,EPI4,EPI5,EPI6,EPI7,VP,AR,LENSU21	8
	1GTH,APR,BPR,BIGAPR,BIGBPR,ESTAR,ALPHA,BETA,RHOSTR,EPRS,RHDS	SU21 9
	COMMON XMESH(20,20,6),XMESH2(20,20,6),Z(20),R(20),SURF(15,8),SURF2SU21	10
	1(15,8),TAB(15,14,2),TAB2(15,14,2),SPART(15,2,2),RARF(15,11),RARF2(SU21	11
	115,4),RPART(15,2)	SU21 12
C		SU21 13
C		SU21 14
	COMMON ZO,RO,PO,UO,VO,LO,MO,RHOO,EO,AO,UBARO,VBARO	SU21 15
C		SU21 16
	COMMON NP,NT,NR,NI,NDEL,ISUB	SU21 17
C		SU21 18
	COMMON ZMIN,ZMAX,RMIN,RMAX,RADIUS,GZ,GR,DELTA,H	SU21 19
	COMMON DIRCOS	SU21 20
	COMMON TIME	SU21 21
	COMMON IRARF	SU21 22
	COMMON KSTOP	SU21 23
	COMMON TPSI	SU21 24
	COMMON KKK	SU21 25
	REAL LO,MO,LENGTH,MU,KO	SU21 26
C		SU21 27
	EPS=.0001	SU21 28
	IF (ITS3.EQ.1) GO TO 5	SU21 29
	IF (RP.GT.(RADIUS+EPS)) GO TO 5	SU21 30

	M=PICK2(ZP,RP,7)	SU21	31
	FF=ZP-SURF2(M+1,1)-(SURF2(M,1)-SURF2(M+1,1))*(RP-SURF2(M,2))/(SURF2(M,2)-SURF2(M+1,2))	SU21	32
	KICK=5	SU21	33
	CALL DVCHK(KQ)	SU21	34
	IF (KQ.EQ.1) GO TO 9980	SU21	35
	IF (FF) 200,5,5	SU21	36
5	CONTINUE	SU21	37
	IF (ZP.GT.-EPS) GO TO 1	SU21	38
	IF (RP.GT.(RADIUS+EPS)) GO TO 200	SU21	39
1	DO 10 K=1,2	SU21	40
	IF (ITS3.EQ.1) GO TO 100	SU21	41
	M=PICK2(ZP,RP,K)	SU21	42
	IF (TAB2(M,2,K).GT.RP.AND.M.NE.1) M=M-1	SU21	43
	FF=ZP-TAB2(M+1,1,K)-(TAB2(M,1,K)-TAB2(M+1,1,K))*(RP-TAB2(M+1,2,K))/	SU21	44
	1/(TAB2(M,2,K)-TAB2(M+1,2,K))	SU21	45
	KICK=50	SU21	46
	CALL DVCHK(KQ)	SU21	47
	IF (KQ.EQ.1) GO TO 9980	SU21	48
	IF (K.EQ.2) GO TO 50	SU21	49
	IF (RP.GT.RADIUS) GO TO 10	SU21	50
	IF (FF) 200,10,10	SU21	51
50	IF (FF) 10,10,200	SU21	52
10	CONTINUE	SU21	53
	DO 20 K=1,2	SU21	54
	J=K+3	SU21	55
	M=PICK2(ZP,RP,J)	SU21	56
	IF (SPART(M,2,K).GT.RP.AND.M.NE.1) M=M-1	SU21	57
	FF=ZP-SPART(M+1,1,K)-(SPART(M,1,K)-SPART(M+1,1,K))*(RP-SPART(M+1,2,K))/	SU21	58
	1,K)/(SPART(M,2,K)-SPART(M+1,2,K))	SU21	59
	KICK=15	SU21	60
	CALL DVCHK(KQ)	SU21	61
	IF (KQ.EQ.1) GO TO 9980	SU21	62
	IF (K.EQ.2) GO TO 15	SU21	63
	IF (RP.GT.RADIUS) GO TO 20	SU21	64
	IF (FF.LT..001) GO TO 300	SU21	65
		SU21	66

	GO TO 20	SU21	67
15	IF (FF.GT.-.001) GO TO 400	SU21	68
20	CONTINUE	SU21	69
	IF (IRARF.EQ.1) GO TO 100	SU21	70
	M=PICK2(ZP,RP,3)	SU21	71
	FF=RP-RARF2(M+1,2)-(RARF2(M,2)-RARF2(M+1,2))*(ZP-RARF2(M+1,1))/(RASU21	SU21	72
	IRF2(M,1)-RARF2(M+1,1))	SU21	73
	KICK=20	SU21	74
	CALL DVCHK(KQ)	SU21	75
	IF (KQ.EQ.1) GO TO 9980	SU21	76
	IF (FF.LT.0.) GO TO 100	SU21	77
	M=PICK2(ZP,RP,6)	SU21	78
	FF=RP-RPART(M+1,2)-(RPART(M,2)-RPART(M+1,2))*(ZP-RPART(M+1,1))/(RPSU21	SU21	79
	IPART(M,1)-RPART(M+1,1))	SU21	80
	KICK=100	SU21	81
	CALL DVCHK(KQ)	SU21	82
	IF (KQ.EQ.1) GO TO 9980	SU21	83
	IF (FF.LT.0.) GO TO 500	SU21	84
100	TEST=1	SU21	85
	TEST=TEST+.2	SU21	86
	RETURN	SU21	87
200	TEST=2	SU21	88
	TEST=TEST+.2	SU21	89
	RETURN	SU21	90
300	TEST=3	SU21	91
	TEST=TEST+.2	SU21	92
	RETURN	SU21	93
400	TEST=4	SU21	94
	TEST=TEST+.2	SU21	95
	RETURN	SU21	96
500	TEST=5	SU21	97
	TEST=TEST+.2	SU21	98
	RETURN	SU21	99
9980	WRITE (3,9985) KICK	SU21	100
9985	FORMAT (32HODIVIDE CHECK NEAR STATEMENT NO.,I5,I4H IN SUBR. TEST/1SU21	SU21	101
	1H1)	SU21	102

	RETURN	SU21	103
	END	SU21	104
	SUBROUTINE FGOF5(Z5,R5,SS,QQ)	SU22	1
C		SU22	2
C	COMPUTES SS,QQ FOR INTERIOR REGION	SU22	3
C	ITERATION FOR Z5,R5	SU22	4
C		SU22	5
	COMMON CASEID(14),ITS1,ITS2,ITS3,ITS4,ITI1,ITI2,ITI3,ITI4,EPS1,EPSSU22	SU22	6
	12,EPS3,EPS4,EPS5,EPS6,EPI1,EPI2,EPI3,EPI4,EPI5,EPI6,EPI7,VP,AR,LENSU22	SU22	7
	1GTH,APR,BPR,BIGAPR,BIGBPR,ESTAR,ALPHA,BETA,RHOSTR,EPRS,RHOS	SU22	8
	COMMON XMESH(20,20,6),XMESH2(20,20,6),Z(20),R(20),SURF(15,8),SURF2SU22	SU22	9
	1(15,8),TAB(15,14,2),TAB2(15,14,2),SPART(15,2,2),RARF(15,11),RARF2(SU22	SU22	10
	115,4),RPART(15,2)	SU22	11
C		SU22	12
C		SU22	13
	COMMON Z0,R0,P0,U0,V0,L0,M0,RH00,E0,A0,UBARO,VBARO	SU22	14
C		SU22	15
	COMMON NP,NT,NR,NI,NDEL,ISUB	SU22	16
C		SU22	17
	COMMON ZMIN,ZMAX,RMIN,RMAX,RADIUS,GZ,GR,DELTA,H	SU22	18
	COMMON DIRCOS	SU22	19
	COMMON TIME	SU22	20
	COMMON IRARF	SU22	21
	COMMON KSTOP	SU22	22
	COMMON TPSI	SU22	23
	COMMON KKK	SU22	24
	REAL L0,M0,LENGTH,MU,KO	SU22	25
C		SU22	26
	DIMENSION ANS(6)	SU22	27
C		SU22	28
	CALL DBLTRP(Z5,R5,ANS)	SU22	29
	U5=ANS(2)	SU22	30
	V5=ANS(3)	SU22	31
	SS=Z5-Z0+H*V5	SU22	32
	QQ=R5-R0+H*U5	SU22	33
	RETURN	SU22	34



END	SU22	35
SUBROUTINE ITRP	SU23	1
COMMON CASEID(14),ITS1,ITS2,ITS3,ITS4,ITI1,ITI2,ITI3,ITI4,EPS1,EPSSU23		2
12,EPS3,EPS4,EPS5,EPS6,EPI1,EPI2,EPI3,EPI4,EPI5,EPI6,EPI7,VP,AR,LENSU23		3
1GTH,APR,BPR,BIGAPR,BIGBPR,ESTAR,ALPHA,BETA,RHOSTR,EPRS,RHOS	SU23	4
COMMON XMESH(20,20,6),XMESH2(20,20,6),Z(20),R(20),SURF(15,8),SURF2SU23		5
1(15,8),TAB(15,14,2),TAB2(15,14,2),SPART(15,2,2),RARF(15,11),RARF2(SU23		6
115,4),RPART(15,2)	SU23	7
C	SU23	8
C	SU23	9
COMMON ZO,RO,PO,UO,VO,LO,MO,RHOO,E0,A0,UBARO,VBARO	SU23	10
C	SU23	11
COMMON NP,NT,NR,NI,NDEL,ISUB	SU23	12
C	SU23	13
COMMON ZMIN,ZMAX,RMIN,RMAX,RADIUS,GZ,GR,DELTA,H	SU23	14
COMMON DIRCOS	SU23	15
COMMON TIME	SU23	16
COMMON IRARF	SU23	17
COMMON KSTOP	SU23	18
COMMON TPSI	SU23	19
COMMON KKK	SU23	20
C	SU23	21
C	SU23	22
REAL LO,MO,LENGTH,MU,KO	SU23	23
C	SU23	24
C INTERPOLATION SCHEME FOR POINTS BETWEEN PARTICLE CURVES	SU23	25
C AND DISCONTINUITIES	SU23	26
C	SU23	27
EPS=.0000001	SU23	28
KOD1=0	SU23	29
KOD2=0	SU23	30
DO 1000 J=1,20	SU23	31
DO 1000 I=1,20	SU23	32
M=TEST(Z(I),R(J))	SU23	33
IF (M.NE.5) GO TO 906	SU23	34
IF (IRARF.EQ.1) GO TO 906	SU23	35

	NR1=NR-1	SU23	36
	DO 907 JJ=1,NR1	SU23	37
	IF (RARF2(JJ,1).LT.Z(I).AND.RARF2(JJ+1,1).GT.Z(I)) GO TO 908	SU23	38
907	CONTINUE	SU23	39
908	CONTINUE	SU23	40
	FF=R(J)-RARF2(JJ+1,2)+(RARF2(JJ,2)-RARF2(JJ+1,2))*(Z(I)-RARF2(JJ+1,1,1))/(RARF2(JJ,1)-RARF2(JJ+1,1))	SU23	41
	IF (FF.LT.0.) GO TO 1000	SU23	42
906	CONTINUE	SU23	43
	IF (M.EQ.3.AND.Z(I).LT.EPS.AND.ABS(R(J)-RADIUS).LT.EPS) GO TO 1000	SU23	44
	IF (M.LT.3) GO TO 8051	SU23	45
	WRITE (3,8050)	SU23	46
8050	FORMAT (30H0INTERPOLATION SCHEME EMPLOYED)	SU23	47
614	FORMAT (1X5H20 =,E15.8,4X5HRO =,E15.8)	SU23	48
	Z0=Z(I)	SU23	49
	RO=R(J)	SU23	50
	WRITE (3,614) Z0,RO	SU23	51
	WRITE (3,8888) M	SU23	52
8888	FORMAT (1X4HM =,I4)	SU23	53
8051	CONTINUE	SU23	54
	GO TO (1000,1000,1001,1010,1100),M	SU23	55
1001	IF (IRARF.EQ.1) GO TO 1003	SU23	56
	M=PICK2(Z(I),R(J),3)	SU23	57
	FF=R(J)-RARF2(M+1,2)+(RARF2(M,2)-RARF2(M+1,2))*(Z(I)-RARF2(M+1,1,1))/(RARF2(M,1)-RARF2(M+1,1))	SU23	58
	IF (FF.GT.0.) GO TO 1003	SU23	59
	DO 8002 K=1,6	SU23	60
	L=K+2	SU23	61
8002	XMESH2(I,J,K)=RARF(I,L)	SU23	62
	GO TO 1000	SU23	63
1003	L=I+1	SU23	64
	N=TEST(Z(L),R(J))	SU23	65
	GO TO (1004,1007,1030,1030,1050),N	SU23	66
1004	M=PICK2(Z(I),R(J),1)	SU23	67
	DO 1006 K=1,8	SU23	68
	ANS=TAB2(M,K,1)+(TAB2(M+1,K,1)-TAB2(M,K,1))*(R(J)-TAB2(M,2,1))/(TASU23	70	71

	1B2(M+1,2,1)-TAB2(M,2,1))	SU23	72
	IF (K.NE.1) GO TO 8005	SU23	73
	ANS1=ANS	SU23	74
	GO TO 1006	SU23	75
8005	CONTINUE	SU23	76
	IF (K.EQ.2) GO TO 1006	SU23	77
	KX=K-2	SU23	78
	IF (ABS(R(J)-RADIUS).GT.EPS) GO TO 9024	SU23	79
	IF (K.GT.5.OR.K.LT.4) GO TO 9024	SU23	80
	ANS=TAB2(M+1,K,1)	SU23	81
9024	CONTINUE	SU23	82
	XMESH2(I,J,KX)=ANS+(XMESH2(L,J,KX)-ANS)*(Z(I)-ANS1)/(Z(L)-ANS1)	SU23	83
	IF (ABS(R(J)-RADIUS).GT.EPS) GO TO 1006	SU23	84
	XMESH2(I,J,1)=0.	SU23	85
	XMESH2(I,J,4)=RHOSTR	SU23	86
	XMESH2(I,J,5)=0.	SU23	87
	XMESH2(I,J,6)=SQRT(BIGAPR/RHOSTR)	SU23	88
1006	CONTINUE	SU23	89
	GO TO 1000	SU23	90
1007	MM=PICK2(Z(I),R(J),2)	SU23	91
	M=PICK2(Z(I),R(J),1)	SU23	92
	DO 1009 K=1,8	SU23	93
	ANS=TAB2(M,K,1)+(TAB2(M+1,K,1)-TAB2(M,K,1))*(R(J)-TAB2(M,2,1))/(TASU23	SU23	94
	1B2(M+1,2,1)-TAB2(M,2,1))	SU23	95
	ANSW=TAB2(MM,K,2)+(TAB2(MM+1,K,2)-TAB2(MM,K,2))*(R(J)-TAB2(MM,2,2)	SU23	96
	1)/(TAB2(MM+1,2,2)-TAB2(MM,2,1))	SU23	97
	IF (K.NE.1) GO TO 1008	SU23	98
	ANS1=ANS	SU23	99
	ANS2=ANSW	SU23	100
	GO TO 1009	SU23	101
1008	CONTINUE	SU23	102
	IF (K.EQ.2) GO TO 1009	SU23	103
	KX=K-2	SU23	104
	XMESH2(I,J,KX)=ANS+(ANSW-ANS)*(Z(I)-ANS1)/(ANS2-ANS1)	SU23	105
1009	CONTINUE	SU23	106
	GO TO 1000	SU23	107

1010	IF (IRARF.EQ.1) GO TO 1013	SU23 108
	M=PICK2(Z(I),R(J),3)	SU23 109
	FF=R(J)-RARF2(M+1,2)+(RARF2(M,2)-RARF2(M+1,2))*(Z(I)-RARF2(M+1,1))	SU23 110
	1/(RARF2(M,1)-RARF2(M+1,1))	SU23 111
	IF (FF.GT.0.) GO TO 1013	SU23 112
	DO 1012 K=1,6	SU23 113
	L=K+2	SU23 114
1012	XMESH2(I,J,K)=RARF(1,L)	SU23 115
	GO TO 1000	SU23 116
1013	L=I-1	SU23 117
	IF (ABS(Z(I)).LT.EPS) GO TO 1017	SU23 118
	N=TEST(Z(L),R(J))	SU23 119
	GO TO (1014,1017,1030,1017,1051),N	SU23 120
1014	M=PICK2(Z(I),R(J),2)	SU23 121
	DO 1016 K=1,8	SU23 122
	ANS=TAB2(M,K,2)+(TAB2(M+1,K,2)-TAB2(M,K,2))*(R(J)-TAB2(M,2,2))/(TAB2(M+1,2,2)-TAB2(M,2,2))	SU23 123
	IF (K.NE.1) GO TO 1015	SU23 124
	ANS1=ANS	SU23 125
	GO TO 1016	SU23 126
1015	CONTINUE	SU23 127
	IF (K.EQ.2) GO TO 1016	SU23 128
	KX=K-2	SU23 129
	XMESH2(I,J,KX)=ANS+(XMESH2(L,J,KX)-ANS)*(Z(I)-ANS1)/(Z(L)-ANS1)	SU23 130
1016	CONTINUE	SU23 131
	GO TO 1000	SU23 132
1017	L=J-1	SU23 133
	N=TEST(Z(I),R(L))	SU23 134
	GO TO (1024,1030,1030,1030,1051),N	SU23 135
1024	M=PICK2(Z(I),R(J),2)	SU23 136
	DO 1026 K=2,8	SU23 137
	ANS=TAB2(M,K,2)+(TAB2(M+1,K,2)-TAB2(M,K,2))*(Z(I)-TAB2(M,1,2))/(TAB2(M+1,1,2)-TAB2(M,1,2))	SU23 138
	IF (K.NE.2) GO TO 1025	SU23 139
	ANS1=ANS	SU23 140
	GO TO 1026	SU23 141
		SU23 142
		SU23 143

1025	CONTINUE	SU23 144
	KX=K-2	SU23 145
	IF (ABS(Z(I)).GT.EPS) GO TO 9125	SU23 146
	IF (K.GT.5.OR.K.LT.4) GO TO 9125	SU23 147
	ANS=TAB2(M+1,K,2)	SU23 148
9125	CONTINUE	SU23 149
	XMESH2(I,J,KX)=ANS+(XMESH2(I,L,KX)-ANS)*(R(J)-ANS1)/(R(L)-ANS1)	SU23 150
	IF (ABS(Z(I)).GT.EPS) GO TO 1026	SU23 151
	XMESH2(I,J,1)=0.	SU23 152
	XMESH2(I,J,4)=RHOSTR	SU23 153
	XMESH2(I,J,5)=0.	SU23 154
	XMESH2(I,J,6)=SQRT(BIGAPR/RHOSTR)	SU23 155
1026	CONTINUE	SU23 156
	GO TO 1000	SU23 157
1100	M=PICK2(Z(I),R(J),3)	SU23 158
	ANS1=RARF2(M+1,2)+(RARF2(M,2)-RARF2(M+1,2))*(Z(I)-RARF2(M+1,1))/(R	SU23 159
	ARF2(M,1)-RARF2(M+1,1))	SU23 160
	L=J+1	SU23 161
	M=TEST(Z(I),R(L))	SU23 162
	GO TO (1101,1030,1051,1030),M	SU23 163
1101	CONTINUE	SU23 164
	DO 1106 K=1,6	SU23 165
	LL=K+2	SU23 166
	XMESH2(I,J,K)=RARF(1,LL)+(XMESH2(I,L,K)-RARF(1,LL))*(R(J)-ANS1)/(R	SU23 167
	1(L)-ANS1)	SU23 168
1106	CONTINUE	SU23 169
	GO TO 1000	SU23 170
1050	JJ1=J	SU23 171
	II1=1	SU23 172
	KOD1=1	SU23 173
	GO TO 1000	SU23 174
1051	JJ2=J	SU23 175
	II2=1	SU23 176
	KOD2=1	SU23 177
1000	CONTINUE	SU23 178
	IF (KOD1.EQ.0) GO TO 2000	SU23 179

	M=PICK2(Z(II1),R(JJ1),1)	SU23 180
	DO 2016 K=1,8	SU23 181
	ANS=TAB2(M,K,1)+(TAB2(M+1,K,1)-TAB2(M,K,1))*(R(JJ1)-TAB2(M,2,1))/(	SU23 182
	1TAB2(M+1,2,1)-TAB2(M,2,1))	SU23 183
	IF (K.NE.1) GO TO 2005	SU23 184
	ANS1=ANS	SU23 185
	GO TO 2016	SU23 186
2005	CONTINUE	SU23 187
	I=II1	SU23 188
	J=JJ1	SU23 189
	L=II1+1	SU23 190
	IF (K.EQ.2) GO TO 2016	SU23 191
	KX=K-2	SU23 192
	XMESH2(I,J,KX)=ANS+(XMESH2(L,J,KX)-ANS)*(Z(I)-ANS1)/(Z(L)-ANS1)	SU23 193
2016	CONTINUE	SU23 194
2000	IF (KOD2.EQ.0) GO TO 3000	SU23 195
	M=PICK2(Z(II2),R(JJ2),2)	SU23 196
	DO 3016 K=1,8	SU23 197
	ANS=TAB2(M,K,2)+(TAB2(M+1,K,2)-TAB2(M,K,2))*(R(JJ2)-TAB2(M,2,2))/(	SU23 198
	1TAB2(M+1,2,2)-TAB2(M,2,2))	SU23 199
	IF (K.NE.1) GO TO 3015	SU23 200
	ANS1=ANS	SU23 201
	GO TO 3016	SU23 202
3015	CONTINUE	SU23 203
	I=II2	SU23 204
	J=JJ2	SU23 205
	L=II2-1	SU23 206
	IF (K.EQ.2) GO TO 3016	SU23 207
	KX=K-2	SU23 208
	XMESH2(I,J,KX)=ANS+(XMESH2(L,J,KX)-ANS)*(Z(I)-ANS1)/(Z(L)-ANS1)	SU23 209
3016	CONTINUE	SU23 210
3000	CONTINUE	SU23 211
	GO TO 3017	SU23 212
1030	WRITE (3,1040) I,J	SU23 213
1040	FORMAT (27H0 TIME STEP TOO LARGE AT I=,I4,2HJ=,I4,///)	SU23 214
	CALL EXIT	SU23 215

3017	CONTINUE	SU23	216
C		SU23	217
C		SU23	218
	RETURN	SU23	219
	END	SU23	220
	SUBROUTINE EXIT	SU24	1
C		SU24	2
	COMMON CASEID(14),ITS1,ITS2,ITS3,ITS4,ITI1,ITI2,ITI3,ITI4,EPS1,EPSSU24		3
	12,EPS3,EPS4,EPS5,EPS6,EPI1,EPI2,EPI3,EPI4,EPI5,EPI6,EPI7,VP,AR,LENSU24		4
	1GTH,APR,BPR,BIGAPR,BIGBPR,ESTAR,ALPHA,BETA,RHOSTR,EPRS,RHOS	SU24	5
	COMMON XMESH(20,20,6),XMESH2(20,20,6),Z(20),R(20),SURF(15,8),SURF2SU24		6
	1(15,8),TAB(15,14,2),TAB2(15,14,2),SPART(15,2,2),RARF(15,11),RARF2(SU24		7
	115,4),RPART(15,2)	SU24	8
C		SU24	9
C		SU24	10
	COMMON ZO,RO,PO,UO,VO,LO,MO,RHOO,EO,AO,UBARO,VBARO	SU24	11
C		SU24	12
	COMMON NP,NT,NR,NI,NDEL,ISUB	SU24	13
C		SU24	14
	COMMON ZMIN,ZMAX,RMIN,RMAX,RADIUS,GZ,GR,DELTA,H	SU24	15
	COMMON DIRCOS	SU24	16
	COMMON TIME	SU24	17
	COMMON IRARF	SU24	18
	COMMON KSTOP	SU24	19
	COMMON TPSI	SU24	20
	COMMON KKK	SU24	21
	REAL LO,MO,LENGTH,MU,KO	SU24	22
	KSTOP=1	SU24	23
	STOP	SU24	24
	END	SU24	25
	SUBROUTINE FGOFI(ZX,RX,SS,QQ)	SU25	1
C		SU25	2
C	COMPUTES SI,QI FOR INTERIOR REGION	SU25	3
C	ITERATION FOR ZI,RI	SU25	4
C		SU25	5
	COMMON CASEID(14),ITS1,ITS2,ITS3,ITS4,ITI1,ITI2,ITI3,ITI4,EPS1,EPSSU25		6

	12,EPS3,EPS4,EPS5,EPS6,EPI1,EPI2,EPI3,EPI4,EPI5,EPI6,EPI7,VP,AR,LENS	SU25	7
	1GTH,APR,BPR,BIGAPR,BIGBPR,ESTAR,ALPHA,BETA,RHOSTR,EPRS,RHDS	SU25	8
	COMMON XMESH(20,20,6),XMESH2(20,20,6),Z(20),R(20),SURF(15,8),SURF2	SU25	9
	1(15,8),TAB(15,14,2),TAB2(15,14,2),SPART(15,2,2),RARF(15,11),RARF2	SU25	10
	115,4),RPART(15,2)	SU25	11
C		SU25	12
C		SU25	13
	COMMON ZO,RC,PO,UO,VO,LO,MO,RHOO,E0,AO,UBARO,VBARO	SU25	14
C		SU25	15
	COMMON NP,NT,NR,NI,NDEL,ISUB	SU25	16
C		SU25	17
	COMMON ZMIN,ZMAX,RMIN,RMAX,RADIUS,GZ,GR,DELTA,H	SU25	18
	COMMON DIRCOS	SU25	19
	COMMON TIME	SU25	20
	COMMON IRARF	SU25	21
	COMMON KSTOP	SU25	22
	COMMON TPSI	SU25	23
	COMMON KKK	SU25	24
	REAL LO,MO,LENGTH,MU,KO	SU25	25
C		SU25	26
	DIMENSION ANS(6),PSI(4),SPSI(11),CPSI(11)	SU25	27
C		SU25	28
C		SU25	29
C		SU25	30
C		SU25	31
C		SU25	32
	CALL DBLTRP(ZX,RX,ANS)	SU25	33
	UI=ANS(2)	SU25	34
	VI=ANS(3)	SU25	35
	AI=ANS(6)	SU25	36
	SS=ZX-ZO+H*(VI+AI*SIN(TPSI))	SU25	37
	QQ=RX-RO+H*(UI+AI*COS(TPSI))	SU25	38
	RETURN	SU25	39
	END	SU25	40



III.1. "Elementary Solutions of Coupled Model Equations in the Kinetic Theory of Gases"

III.2. "Tricritical Points in Multicomponent Fluid Mixtures"

III.3. "Generalized Scaling Hypothesis in Multicomponent Systems.  
I. Classification of Critical Points by Order and Scaling at Tricritical Points"

III.4. "Double-Power Scaling Functions Near Tricritical Points"

PAPERS INTENTIONALLY OMITTED

**AIAA Paper  
No. 69-355**

75-04939  
N75-15329



## **STRESS WAVES RESULTING FROM HYPERVELOCITY IMPACT**

by

**R. MADDEN**

Northeastern University

Boston, Massachusetts

and

**T. S. CHANG**

North Carolina State University

Raleigh, North Carolina

# **AIAA Hypervelocity Impact Conference**

**CINCINNATI, OHIO / APRIL 30 – MAY 2, 1969**

First publication rights reserved by American Institute of Aeronautics and Astronautics, 1290 Avenue of the Americas, New York, N. Y. 10019.  
Abstracts may be published without permission if credit is given to author and to AIAA. (Price: AIAA Member \$1.00. Nonmember \$1.50)

# STRESS WAVES RESULTING FROM HYPERVELOCITY IMPACT<sup>†</sup>

R. Madden

Assistant Professor of Mechanical Engineering  
Northeastern University  
Boston, Massachusetts

and

T. S. Chang

NSF Professor and Chairman of Mechanics Program  
North Carolina State University  
Raleigh, North Carolina

## Abstract

Results from a numerical scheme based on the method of characteristics are presented for the axially symmetric, hypervelocity impact of similar materials. The analysis is restricted to the early stages of the impact of a right circular cylinder on a halfspace. The resulting rarefaction and shock waves produced by the impact are considered as discrete wavefronts which divide the impacted zone into regions. Numerical diffusion is then controlled by requiring that the values of the dependent variables at a given point in the impacted zone to depend on only the calculated values at earlier times at points in the same region as the point in question. The numerical results give accurate representations of the stress wave profiles (i.e., rarefaction and shock waves) which should be useful as inputs for a later stage elastoplastic analysis and/or spallation analysis. The effects of "numerical diffusion" on the calculated pressure and flow fields when the rarefaction wave is not considered as discrete is investigated and the "diffused" results are compared with the more exact analysis.

## Nomenclature

$a$  = isentropic speed of sound  
 $e$  = specific internal energy  
 $e_s$  = sublimation energy  
 $h$  = time step  
 $P$  = pressure  
 $r$  = radial coordinate  
 $t$  = time  
 $U$  = radial velocity  
 $V$  = axial velocity  
 $z$  = axial coordinate  
 $\eta$  =  $\rho/\rho^*$   
 $\theta$  = parameter defining a bicharacteristic,  
( $0 \leq \theta \leq 2\pi$ )  
 $\mu$  =  $\eta - 1$   
 $\rho$  = mass density  
 $\rho^*$  = ambient density  
 $\phi$  = function of  $r$ ,  $z$ , and  $t$

## Introduction

Most of the existing numerical codes<sup>1-3</sup> for hypervelocity impact calculations are based on procedures which allow some smearing of the resulting rarefaction and shock waves. The present analysis of the initial hydrodynamic phase of an axially symmetric, hypervelocity impact is based on the method of characteristics while treating the rarefaction and shock waves as discrete discontinuities. The definitiveness of the resulting flow field obtained from such an analysis should be useful as inputs to a subsequent elastoplastic analysis for studying later stage cratering effects and/or spallation calculations which require rather accurate representations of both the peak pressure and the incident shock wave profile at reflection. The results based on a numerical code using the method of characteristics for the impact of a right circular aluminum cylinder on an aluminum halfspace are presented. The impact configuration is depicted schematically in Fig. 1.

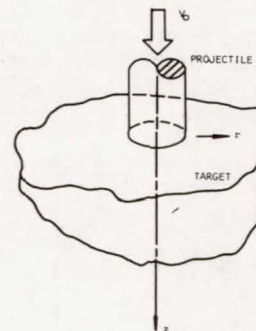


Figure 1 Impact configuration

In order to give some insight into the mechanism of "numerical diffusion", an analysis using the method of characteristics by not considering the rarefaction as discrete is also considered. In

<sup>†</sup>The authors are grateful to Mr. P. Townsend of Northeastern University for his assistance in adapting the computer program to the Northeastern University Computer, the running of the programs, and the preparation of the figures. The research of one of us (T.S.C.) was partially supported by the National Aeronautics and Space Administration under Contract No. NGR 34-002-084, and the Advanced Research Projects of the Department of Defense while monitored by the Office of Naval Research under Contract No. N00014-68-A-0187.



doing so, the speed of the release wave from the free surface of the projectile and the free surface of the target is not controlled. Results from such an approximate analysis are compared with the discrete rarefaction case and the limitations of the "diffused" solution are delineated.

### Characteristic Surfaces

As described in references 4 and 5, during the initial stages of a hypervelocity impact, the material in the impacted zone may be assumed to obey the inviscid fluid dynamic equations. For axially symmetric impact, these equations may be expressed as follows:

#### Conservation of Mass

$$\frac{D\rho}{Dt} + \rho \left( \frac{\partial U}{\partial r} + \frac{\partial V}{\partial z} + \frac{U}{r} \right) = 0, \quad (1)$$

#### Conservation of Momentum

$$\rho \frac{DU}{Dt} + \frac{\partial P}{\partial r} = 0, \quad (2)$$

$$\rho \frac{DV}{Dt} + \frac{\partial P}{\partial z} = 0, \quad (3)$$

#### Conservation of Entropy along a Particle Path

$$\frac{DP}{Dt} - a^2 \frac{D\rho}{Dt} = 0, \quad (4)$$

where,

$$\frac{D}{Dt} = \frac{\partial}{\partial t} + U \frac{\partial}{\partial r} + V \frac{\partial}{\partial z}, \quad (5)$$

and  $P$  is the pressure,  $\rho$  is the density,  $a$  is the isentropic speed of sound,  $t$  is the time, and  $(r, z)$  and  $(U, V)$  are the radial and axial coordinates and velocities, respectively.

Equations (1) to (4) form a system of non-linear, hyperbolic, partial differential equations. The corresponding characteristic equation for this system of equations is:

$$\begin{vmatrix} 0 & \frac{D\phi}{Dt} & \rho \frac{\partial \phi}{\partial r} & \rho \frac{\partial \phi}{\partial z} \\ \frac{\partial \phi}{\partial r} & 0 & \rho \frac{D\phi}{Dt} & 0 \\ \frac{\partial \phi}{\partial z} & 0 & 0 & \rho \frac{D\phi}{Dt} \\ \frac{D\phi}{Dt} & -a^2 \frac{D\phi}{Dt} & 0 & 0 \end{vmatrix} = 0 \quad (6)$$

where  $\phi = \phi(r, z, t)$ , and surfaces of  $\phi = \text{constants}$  are the characteristic surfaces.

The solutions of Eq. (6) are given by

$$\left( \frac{D\phi}{Dt} \right)^2 - a^2 \left[ \left( \frac{\partial \phi}{\partial r} \right)^2 + \left( \frac{\partial \phi}{\partial z} \right)^2 \right] = 0, \quad (7)$$

and

$$\frac{D\phi}{Dt} = 0. \quad (8)$$

The characteristic surfaces described by Eqs. (7) and (8) correspond to two distinct types of characteristic propagations. Corresponding to Eq. (7), the characteristic propagation is described by the differential equations of the bicharacteristics

$$\frac{dr}{dt} = U + a \cos \theta, \quad (9)$$

$$\frac{dz}{dt} = V + a \sin \theta, \quad (10)$$

where,  $0 \leq \theta \leq 2\pi$ . These bicharacteristics describe the propagation of pressure, density, or velocity disturbances. Corresponding to Eq. (8), the characteristic propagation is described by

$$\frac{dr}{dt} = U, \quad (11)$$

$$\frac{dz}{dt} = V, \quad (12)$$

which are the particle path equations and describe the propagation of entropy disturbances.

The set of bicharacteristics from a point, with  $0 \leq \theta \leq 2\pi$ , forms the conoid of dependence for the point which is at its vertex. The interior of the conoid contains all the points whose values of  $U, V, P, \rho$ , etc. may influence the corresponding values at the point at the vertex. The intersection of this conoid and a particular time plane forms the domain of dependence of the point at the vertex of the conoid and contains all the points whose values of  $U, V, P, \rho$ , etc. influence the corresponding values at the point at the vertex. A schematic representation of these ideas are given in Fig. 2.

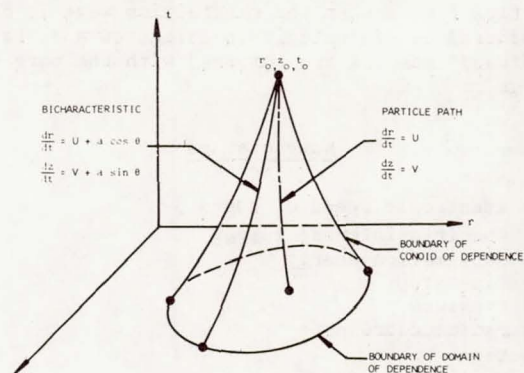


Figure 2 Conoid and domain of dependence

### Compatibility Conditions

It will not be difficult to demonstrate that along a bicharacteristic,  $U, V$ , and  $P$  must satisfy the following differential relation in a time interval  $dt$ :

$$\begin{aligned} dP + \rho a \cos \theta dU + \rho a \sin \theta dV \\ = - \rho a^2 dt \left[ \left( \frac{\partial U}{\partial r} \right) \sin^2 \theta - \left( \frac{\partial U}{\partial z} + \frac{\partial V}{\partial r} \right) \sin \theta \cos \theta \right. \\ \left. + \left( \frac{\partial V}{\partial z} \right) \cos^2 \theta + \frac{U}{r} \right]. \end{aligned} \quad (13)$$



Similarly, along the particle path, the following differential expression must be satisfied:

$$\rho^2 de = p d\rho, \quad (14)$$

where  $e$  is the specific internal energy. Equations (13) and (14) are called the bicharacteristic and particle path compatibility conditions, respectively.

Equation (14) is essentially the first law of thermodynamics expressed along the particle path for an isentropic process. This choice of a particle path compatibility equation was made in order to introduce the internal energy variable. The  $P, \rho, e$  variables are related by an equation of state of the form,

$$P = P(\rho, e). \quad (15)$$

The particular form of the equation of state used in this analysis is that of Tillotson.<sup>6</sup> For aluminum, it can be expressed as follows:

For  $\rho > \rho_*$ , with  $e > 0$  or  $e \leq e_s$ ,

$$P = [0.5 + \frac{1.63}{1+e/(e_s \eta^2)}] \rho e + 0.752\mu + 0.65\mu^2, \quad (16)$$

and for  $\rho < \rho_*$ , with  $e > e_s$ ,

$$P = 0.5 \rho e + [\frac{1.63 \rho e}{1+e/(e_s \eta^2)} + 0.752 \rho e^{5(1-1/\eta)}] e^{-5(1-1/\eta)^2}, \quad (17)$$

where,

$$\eta = \rho/\rho_*, \quad \mu = \eta - 1, \quad (18)$$

$\rho_* = 2.70 \text{ gm/cm}^3$  is the ambient density for aluminum, and  $e_s = 0.03 \text{ megabar cm}^3/\text{gm}$  is the sublimation energy for aluminum. In Eqs. (16) and (17),  $P$  is expressed in megabars,  $\rho$  in  $\text{gm/cm}^3$ , and  $e$  in  $\text{megabars cm}^3/\text{gm}$ .

#### Numerical Procedure

The differential expressions, Eqs. (9)-(14), are cast in finite difference forms accurate to the order of  $h^2$ , where  $h$  is the time step. For example, the bicharacteristic compatibility equation for a particular value of  $\theta$  is

$$\begin{aligned} P_o - P_i + \rho_i a_i [\cos \theta_i (U_o - U_i) + \sin \theta_i (V_o - V_i)] \\ = -\rho_i a_i^2 h \left[ \left( \frac{\partial U}{\partial r} \right)_i \sin^2 \theta_i \right. \\ \left. - \left( \frac{\partial U}{\partial z} + \frac{\partial V}{\partial r} \right)_i \sin \theta_i \cos \theta_i \right. \\ \left. + \left( \frac{\partial V}{\partial z} \right)_i \sin^2 \theta_i + \frac{U_i}{r_i} \right] + O(h^2), \quad (19) \end{aligned}$$

where the subscript "o" refers to  $t = t_o$  and the point where the values of  $U, V, P, \rho$ , etc. are being calculated and the subscript "i" refers to the corresponding values at the intersection of the bi-

characteristic  $\theta_i$  with an  $(t_o - h)$  - time plane at which all data has been previously calculated. In spite of the fact that the error over each time step is of order  $h^2$ , the accumulated errors reduce the aggregate solution to the order of  $h$ .

The unknowns in Eq. (19) are  $P_o, U_o, V_o$  and therefore unless one (or more) of these values is specified, three bicharacteristics are required for each calculation. After  $P_o, U_o, V_o$  are determined, the values  $\rho_o$  and  $e_o$  are obtained with the aid of the particle path compatibility condition and the equation of state. This procedure is applicable at points not on the boundary of the impacted zone, (i.e., on the shocks, rarefaction, free surfaces, or axis of symmetry). At points on the boundary, auxiliary relations are available and consequently, fewer independent bicharacteristic conditions are required for each calculation. A scheme is also used to insure that finite difference relations are not written across discontinuities and "numerical diffusion" across these discontinuities is minimized. The details of the various calculational procedures are given in references 4 and 5.

#### Numerical Stability

The problem of constructing a stable numerical procedure for the present analysis is resolved by following certain qualitative guidelines. The basic idea is suggested by the stability criterion of Courant, Friedrichs, and Lewy, (or the C.F.L. Condition). According to this condition, the domain of dependence of the difference equations must encompass the domain of dependence of the original hyperbolic differential equations for numerical stability. The following is a brief account of the approach used in this analysis to ascertain numerical stability.

Consider the domain of dependence of the partial differential equations in the  $(t_o - h)$  - time plane as illustrated in Fig. 3(a). If the conoid of dependence is approximated by the three bicharacteristics passing through the triangular points (1,2,3), the domain of dependence is described by the triangle of dashed lines connecting the three points. Since, for the purpose of attaining numerical convergence, the points (1,2,3) must be relatively close to the circular region which is the domain of dependence of the differential equations, instabilities cannot be avoided. To insure numerical stability, the values at points (1,2,3) are obtained by interpolation using the values at the twelve grid points (circular dots) which surround the three original points as shown in Fig. 3(b). In doing so, the domain of depend-

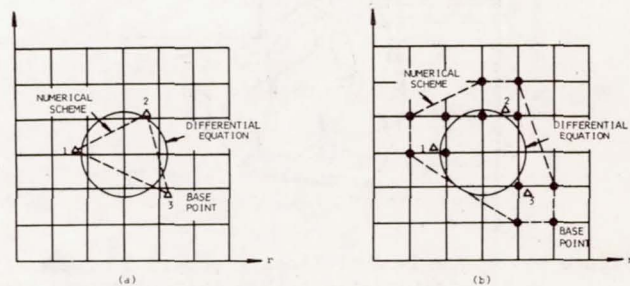


Figure 3 Domains of dependence: (a) without interpolation, (b) with interpolation



ence of the difference equations is increased to the convex hull of dashed lines indicated in Fig. 3(b). This convex hull should encompass the circular domain of the differential equations. Such an interpolation scheme seems to be sufficient to insure the required numerical stability for the present analysis.

### Results and Discussion

The example chosen in this paper to illustrate the results of the characteristic method is the axially symmetric impact of an infinitely long cylindrical aluminum projectile with a diameter  $d_0$  equal to 2.5 cm on an aluminum halfspace. The initial velocity  $V_0$  of the projectile is taken to be 7.6 km/sec and the halfspace is assumed to be at rest. The results of the characteristic method are compared with the results obtained from the well-known "OIL Code" of reference 1. Results from the discrete rarefaction case is then compared with those for a case where the "numerical diffusion" of the rarefaction wave is allowed.

Figure 4 shows the pressure distributions for both the "OIL" solution of reference 1 and the method of characteristics with discrete rarefaction at a time of  $t = 0.74$   $\mu\text{sec}$  after impact when the rarefaction has not yet propagated near the axis of symmetry. The pressure distributions are compared by mapping the isobars for  $P = 1.08, 0.8, 0.5$ , and  $0.2$  megabars (MB). The results of the method of characteristics are shown as solid lines and the "OIL" distributions as dashed lines. The locations of the two shocks and the rarefaction ( $P = 1.08$  MB) are quite clearly defined for the characteristic method. One difference immediately apparent between the two sets of results is that the isobars for the "OIL" approach begin and end on the axis of symmetry, whereas the isobars for the characteristic method begin and end on the projectile and target shocks. The difference, of course, comes from the smearing of the shock fronts in the "OIL" solution. The "OIL" approach predicts additionally two regions of pressure higher than the one-dimensional region which is bounded by the two shocks and the rarefaction. The reduction in pressure in the rarefied region compares quite favorably for both methods. Major differences among the isobars of  $P = 0.5$  and  $0.2$  MB obtained from the two methods are noted in the region near the original free surface where the pressure has been controlled by the characteristic method.

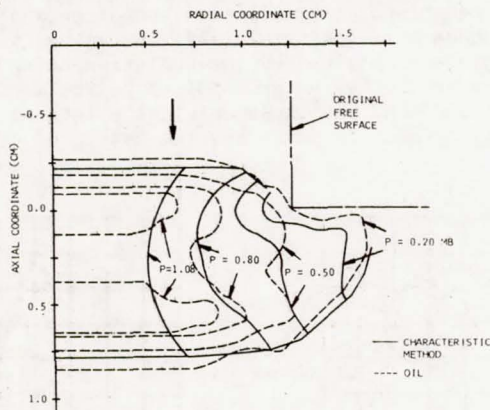


Figure 4 Comparison of isobars obtained by the characteristic method (with discrete rarefaction) and the "OIL" results.  $V_0 = 7.6$  km/sec,  $t = 0.74$   $\mu\text{sec}$ ,  $d_0 = 2.5$  cm

Figure 5 shows the pressure distribution along the axis of symmetry at a time of  $t = 1.28$   $\mu\text{sec}$  after impact just prior to the actual reflection of the rarefaction wave from the axis of symmetry. The dashed curve shows the correct uniform pressure distribution based on the discrete rarefaction solution. The solid line shows the pressure distribution predicted by the numerical method which allows "diffusion" across the rarefaction wave. In the latter case, the pressure along the axis is underestimated. The lowest value is approximately 60% of the actual value. This drop in pressure is due to the fact that the effective speed of the rarefaction for the "diffused" case is equal to the actual rarefaction speed plus the mesh speed (i.e., the rarefaction front travels one additional grid spacing in each time cycle). The fact that the pressures are in error by 40% could be serious if the target shock wave were to be reflected from a free surface at the back of a target with a finite thickness or if these results were to be used as inputs for an elastoplastic analysis for later stage cratering and subsequent spallation calculations.

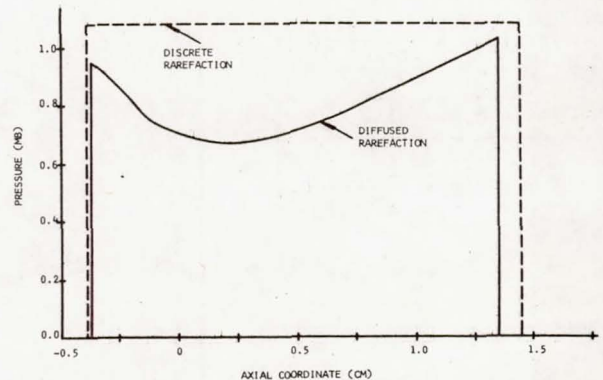


Figure 5 Pressure distribution along the axis of symmetry.  $V_0 = 7.6$  km/sec,  $t = 1.28$   $\mu\text{sec}$ ,  $d_0 = 2.5$  cm

Figure 6 shows the pressure distribution along the axis of symmetry at a later time ( $t = 1.55$   $\mu\text{sec}$ ) after the rarefaction has been re-

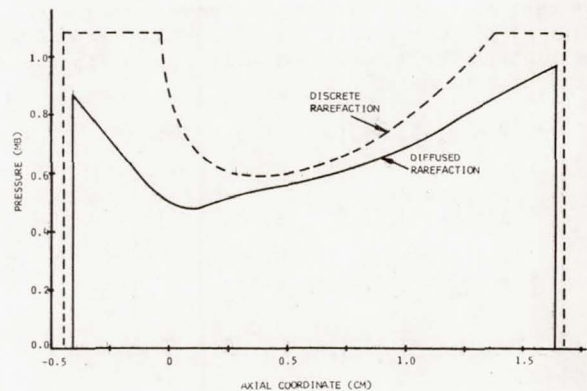


Figure 6 Pressure distribution along the axis of symmetry.  $V_0 = 7.6$  km/sec,  $t = 1.28$   $\mu\text{sec}$ ,  $d_0 = 2.5$  cm



flected. Again the dashed curve is that of the discrete rarefaction solution and the solid curve is the "diffused" solution. At or near this time and for subsequent times, the results of the two solutions are very close to each other and the discrepancies among the results diminish with the increase of time.

Figure 7 maps the isobars for the entire flow field for both the discrete rarefaction solution (dashed curves) and the "diffused" solution (solid curves) at  $t = 1.28 \mu\text{sec}$  after impact. It is noted that in regions close to the axis of symmetry and the rarefaction, there are large discrepancies among the numerically calculated pressures using the two different methods. In addition, due to the premature decay of the projectile shock near the projectile free surface, the calculated pressures near the target shock close to the free surface using the "diffused" scheme are much higher than those for the discrete rarefaction solution. This effect also causes a slightly higher target shock velocity near the free surface. In other regions far away from the free surface and the rarefaction front, the calculated pressures from the two methods are in good agreement.

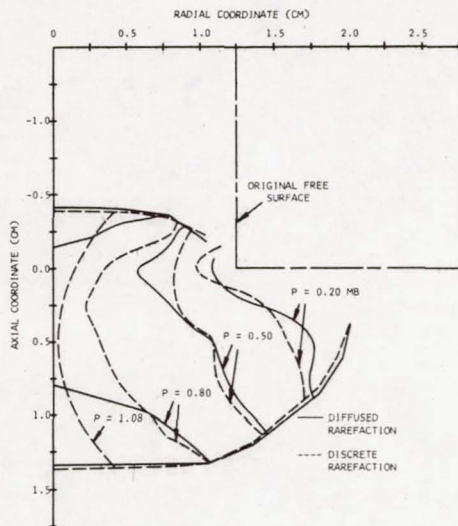


Figure 7 Pressure field.  $V_0 = 7.6 \text{ km/sec}$ ,  $t = 1.28 \mu\text{sec}$ ,  $d_0 = 2.5 \text{ cm}$

Figure 8 shows a comparison of the isobars in the impacted zone at  $t = 1.55 \mu\text{sec}$  after impact. At this time, the isobars are in close agreement throughout the flow field. Nevertheless, some of the effects of the "diffused" rarefaction can still be observed. For instance, there is a slightly higher pressure region predicted by the "diffused" results near the target shock close to the axis of symmetry.

Figure 9 compares the velocity vectors for the two methods of calculations at  $t = 1.50 \mu\text{sec}$  after impact. For all practical purposes, the results are nearly identical. It is apparent that the effect of "numerical diffusion" is more important in the pressure calculations.

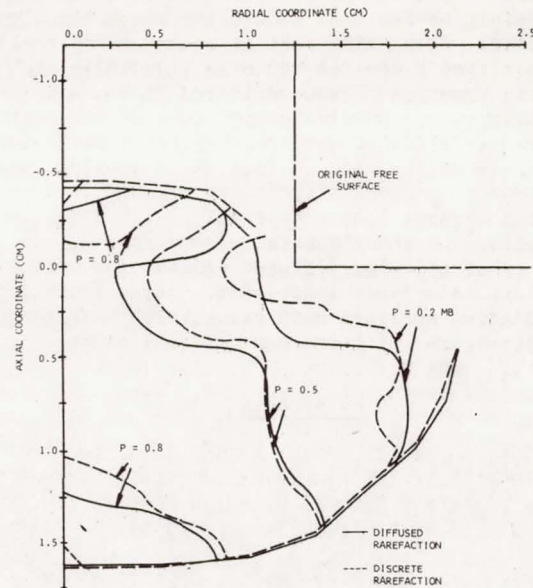


Figure 8 Pressure fields.  $V_0 = 7.6 \text{ km/sec}$ ,  $t = 1.55 \mu\text{sec}$ ,  $d_0 = 2.5 \text{ cm}$

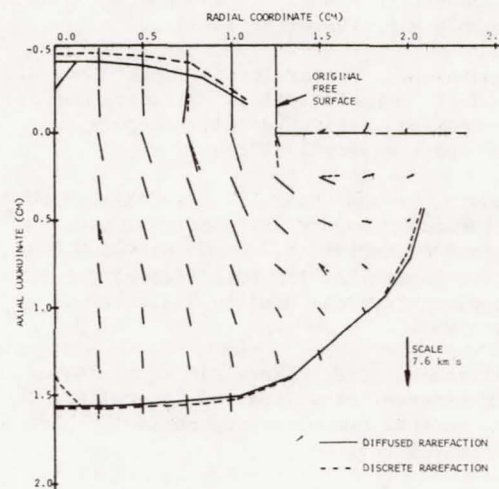


Figure 9 Velocity vectors.  $V_0 = 7.6 \text{ km/sec}$ ,  $t = 1.50 \mu\text{sec}$ ,  $d_0 = 2.5 \text{ cm}$

#### Concluding Remarks

It may be surmised from the calculated results using the method of characteristics that, if the rarefaction is not considered as a discrete discontinuity, the pressures for the initial stages of an axially symmetric hypervelocity impact may be quite different from their actual values before the rarefaction is reflected from the axis of symmetry. This is particularly true for the pressure distribution at the axis of symmetry. After the reflec-

tion of the rarefaction wave, however, the effect of numerical "diffusion" introduced by not treating the rarefaction front as a discrete discontinuity diminishes. This means that if the pressure fields and shock fronts are desired at a time after the rarefaction wave has been reflected from the axis of symmetry, an approximate procedure of the method of characteristics by not treating the rarefaction as discrete may be used. Since the computing time required for hypervelocity impact calculations using the method of characteristics with discrete rarefaction and shock fronts is very large, this procedure of allowing diffused rarefaction can be useful for relatively long impact time calculations or spallation analyses with relatively thick target plates (compared with the projectile diameter).

#### References

<sup>1</sup>Johnson, W. E., "OIL: A Continuous Two-Dimensional Eulerian Hydrodynamic Code," General Atomics Division, General Dynamics Corporation, Report No. 55-80-Revised (January 1965).

<sup>2</sup>Riney, T. D., "Theoretical Hypervelocity Impact Calculations Using the PICWICK Code," General Electric Space Sciences Laboratory Report, No. R64SD13 (February 1964).

<sup>3</sup>Bjork, R., Brooks, N. and Papette, R., "A Numerical Technique for Solution of Multidimensional Hydrodynamic Problems," Rand Corporation Report, No. R.M. 2628 P.R. (December 1963).

<sup>4</sup>Madden, R., "Hypervelocity Impact Analysis by the Method of Characteristics," National Aeronautics and Space Administration Technical Report, No. NASA TR-R-298 (January 1969).

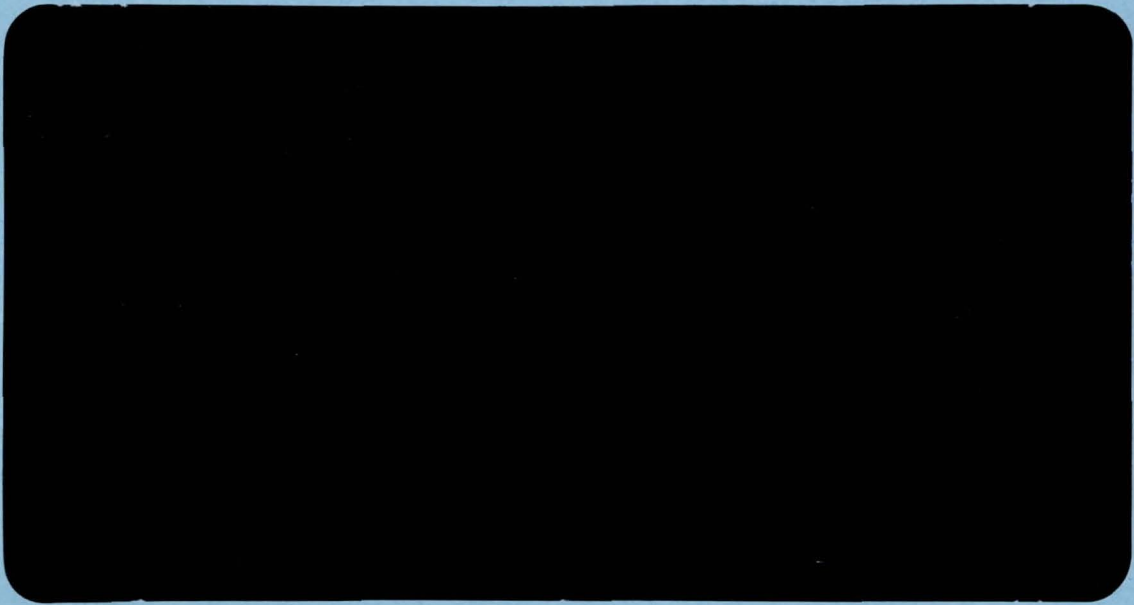
<sup>5</sup>Madden, R. and Chang, T. S., "Axially Symmetric Hypervelocity Impact Calculations Using the Method of Characteristics," North Carolina State University, Report No. TSC-68-1 (February 1968). Also, American Physical Society Bulletin, 111(5), 821 (May 1968).

<sup>6</sup>Tillotson, J. H., "Metallic Equations of State for Hypervelocity Impact," General Atomic Division, General Dynamics Corporation, Report No. GA-3216 (July 1962).



Reprinted from

75-04939



**PERGAMON PRESS**  
OXFORD NEW YORK LONDON PARIS

1075-1532-9

## NONLINEAR WAVES IN A RATE-SENSITIVE, ELASTOPLASTIC MATERIAL

E. E. BURNISTON

Department of Mathematics, North Carolina State University, Raleigh, North Carolina, U.S.A.

and

T. S. CHANG†

Center for Space Research, Massachusetts Institute of Technology, Cambridge, Massachusetts, U.S.A.

(Communicated by A. C. ERINGEN)

**Abstract**—Two classes of closed form solutions of one-dimensional, nonlinear waves in a rate-sensitive, elastoplastic material are reported. One class of these solutions is self-similar and the other class consists of constant speed propagations. Applications of these solutions to unsteady motions behind propagating discontinuities are also considered.

### 1. INTRODUCTION

THE PURPOSE of this paper is to discuss two interesting classes of closed form solutions of one-dimensional, unsteady motion of a rate-sensitive, elastoplastic material. One class of these solutions is self-similar and is deduced from the invariant theorems of continuous groups of transformations. This class of unsteady motion is governed by a single, first-order, nonlinear, ordinary differential equation of the Riccati type and closed form solutions in terms of elementary functions are obtained under special circumstances. If the material in consideration possesses the additional property of instantaneous linear elasticity [1] under 'high rate' of straining, it may be demonstrated that one of these self-similar solutions can be used to describe the dispersed nonlinear wave motion behind a propagating shockfront into an initially quiescent region.

The second class of solutions is obtained by searching for one-dimensional wave motions with constant speeds of propagation. These solutions are expressible as simple quadratures and closed form expressions can be obtained for specific constitutive relations. Such solutions represent non-characteristic propagations, i.e. they are not propagations of weak discontinuities of arbitrary wave forms. It may be demonstrated, using the Poincaré–Bendixon theorem, that these solutions, in general, are not periodic. Assuming a sub-elastic, constant-speed, propagating discontinuity preceded by an elastic precursor with an unloading, relaxation zone, or a constant stress region, the nonlinear wave solution with a constant propagation speed equal to that of the discontinuity can be used to describe the 'unsteady'‡ motion behind the discontinuity.

One-dimensional rectilinear motion, in the strict sense, involves not just one spatial coordinate but also only one component of stress, strain, and particle velocity. For such a type of motion, only a one-dimensional stress–strain or constitutive relation is required. Various rate-sensitive, constitutive equations have been proposed in the

†Permanent address: North Carolina State University.

‡Such an 'unsteady' motion, of course, becomes essentially steady for a moving observer following the propagating discontinuity.



literature and a comprehensive review of this subject can be found in Cristescu [2]. The solutions described in this paper are obtained based on a model first proposed by Sokolovskii [3, 4]. This model cannot, in general, be used to describe the structure or generation of shock waves [5, 6]. In applying the solutions given in this paper to the unsteady motions behind propagating shock layers or relaxation zones, additional material properties may have to be assumed within these shock or relaxation regions.

## 2. MATHEMATICAL FORMULATION

One-dimensional motion may be described by a scalar deformation field,

$$\bar{x} = \bar{x}(\bar{X}, \bar{t}), \quad (2.1)$$

where  $\bar{x}$  is the instantaneous position coordinate at time  $\bar{t}$  of a generic particle whose position coordinate at  $\bar{t} = 0$  was  $\bar{X}$ . The Lagrangian equation of motion and kinematic compatibility condition for rectilinear, one-dimensional motion are†

$$\rho \partial u / \partial \bar{t} = \partial \bar{\sigma} / \partial \bar{X}, \quad (2.2)$$

$$\partial \epsilon / \partial \bar{t} = \partial u / \partial \bar{X}, \quad (2.3)$$

where  $\bar{\sigma}$  is the longitudinal stress, and

$$u = \partial \bar{x} / \partial \bar{t}, \quad (2.4)$$

$$\epsilon = \partial \bar{x} / \partial \bar{X} - 1. \quad (2.5)$$

are the particle velocity and linear Lagrangian strain, respectively. The material is assumed to be initially unstressed and unstrained with a constant density  $\rho$ .

In this analysis, the material under consideration will be assumed to follow the special constitutive relation for a rate-sensitive, elastoplastic material generalized from a model suggested by Sokolovskii [3, 4],

$$\partial \epsilon / \partial \bar{t} = \partial u / \partial \bar{X} = E^{-1} \partial \bar{\sigma} / \partial \bar{t} + \gamma f(\bar{\sigma} / \sigma_0 - 1) 1_+(\bar{\sigma} / \sigma_0 - 1), \quad (2.6)$$

where  $f(\cdot)$  is a dimensionless  $C^1$  function with  $f(\eta) > 0$  for  $\eta > 0$ ,  $1_+(\cdot)$  is the Heaviside function,  $E$  is the modulus of elasticity which is assumed to be a constant,  $\sigma_0$  is the static yield stress, and  $\gamma$  is a material constant. Thus, the material is assumed to have an elastic range with a constant modulus. If the strain rate is held constant, Equation (2.6) may be integrated by simple quadrature‡. Typical stress-strain curves for  $\partial \epsilon / \partial \bar{t} = \text{constant}$  are displayed in Fig. 1. It is seen that the dynamic yield stress is rate-sensitive and there are no strain-hardening effects. Equation (2.6) includes the well-known models suggested by Cowper and Symonds [8], and Perzyna [9], as special cases. It is a special form of a more general constitutive equation suggested by Malvern [10].

Equations (2.2) and (2.6) are the basic equations describing the functions,  $u(\bar{X}, \bar{t})$ ,  $\bar{\sigma}(\bar{X}, \bar{t})$ , [and  $\epsilon(\bar{X}, \bar{t})$ ], characterizing the one-dimensional motions to be considered in this paper. These equations may be combined into one single, second-order, nonlinear,

†See e.g. Courant and Friedrichs [7].

‡The authors are grateful to Professor A. C. Eringen for suggesting this.

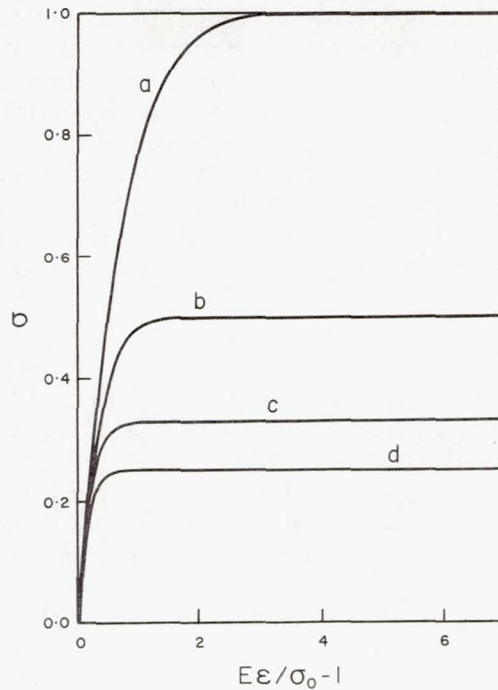


Fig. 1. Typical stress-strain curves for constant strain rates. (a)  $\sqrt{\gamma/k} = 1$ , (b)  $\sqrt{\gamma/k} = 2$ , (c)  $\sqrt{\gamma/k} = 3$ , (d)  $\sqrt{\gamma/k} = 4$ ,  $k = \partial\epsilon/\partial t$ .

hyperbolic, partial differential equation of the evolution type in dimensionless form as follows:

$$\beta(\partial^2\sigma/\partial x^2 - \partial^2\sigma/\partial t^2) = [1_+(\sigma)df(\sigma)/d\sigma + \delta(\sigma)f(0)]\partial\sigma/\partial t, \quad (2.7)$$

where

$$\sigma(x, t) \equiv \bar{\sigma}/\sigma_0 - 1, \quad (2.8)$$

is the dimensionless overstress,

$$x \equiv \alpha\bar{X}, \quad (2.9)$$

$$t \equiv \alpha c\bar{t}, \quad (2.10)$$

$$c \equiv \sqrt{E/\rho}, \quad (2.11)$$

$$\alpha \equiv \beta\gamma\sqrt{\rho E/\sigma_0}, \quad (2.12)$$

$\delta(\cdot)$  is the Dirac delta functional, and  $\beta > 0$  is a dimensionless constant included here in the definition of  $\alpha$  for convenience.

Materials described by the constitutive relation given in (2.6) probably cannot support shock layers or explain the generation of shockfronts. If a shock layer is dissipative, then generalized viscoelastic theories and constitutive relations such as those considered by Varley and Rogers[6], Coleman and Gurtin[11], Dunwoody and Dun-

woody [12] and Pipkin [5], or further generalizations of these models, should be used to describe it. For propagation in a rod, the shock layer may be dispersive due to lateral deformation<sup>†</sup> instead of due to any dissipative mechanism. Such a shock transition may be described in terms of a low frequency, large rate of straining expansion of a three-dimensional deformation field similar to that considered by Parker and Varley [13]. In applying one of the self-similar motions described in this paper to a nonlinear wave motion behind a propagating shockfront, it will be assumed that the rate of straining in the shock layer is high enough to allow the material to exhibit instantaneous linear elasticity<sup>‡</sup> [1]. Thus, across such a shock layer, it will be assumed that

$$[\bar{\sigma}] = E[\epsilon], \quad (2.13)$$

where  $[\chi]$  denotes the jump in value of  $\chi$  across the shock layer, and the value of  $E$  will be assumed to be a constant and have the same value as the modulus of the elastic range of the constitutive relation given by (2.6).

From the Lagrangian equation of motion (2.2) and the kinematic compatibility condition (2.3), two additional jump conditions relating  $[u]$ , and  $[\epsilon]$ , can be deduced formally following a technique suggested by Courant and Friedrichs [7]. The results are:

$$\rho U[u] + [\bar{\sigma}] = 0, \quad (2.14)$$

$$U[\epsilon] + [u] = 0, \quad (2.15)$$

where  $U$  is the propagation speed of the shockfront. Equations (2.14) and (2.15) can also be deduced from physical arguments directly. The jump conditions, (2.13)–(2.15), indicate that the speed of propagation of a shock layer of a material exhibiting instantaneous elasticity is

$$|U| = \sqrt{E/\rho}, \quad (2.16)$$

which is, in fact, the same as the elastic speed of propagation of small disturbances.

In applying the constant speed solutions to the 'unsteady' motion behind a propagating discontinuity which moves at a constant sub-elastic speed, it will be assumed that there is an elastic precursor and an unloading, relaxation zone, or a constant stress region, ahead of the discontinuity. The details of the unsteady motion of a relaxation zone ahead of such a discontinuity may be very complicated and will not be considered in this paper.

### 3. A CLASS OF SELF-SIMILAR SOLUTIONS

Cowper and Symonds [8] proposed, in 1957, a power law,

$$f(\sigma) = \sigma^{\delta}, \quad (3.1)$$

<sup>†</sup>The authors are indebted to Professor E. Varley for a discussion pertaining to this point.

<sup>‡</sup>The range of rate of straining within which materials exhibit instantaneous elasticity varies from one material to another. There is usually an upper (and lower) cutoff point in rate of straining above (and below) which a material may have to be considered viscoelastic. The authors are indebted to Professor R. S. Rivlin for pointing this out to them.



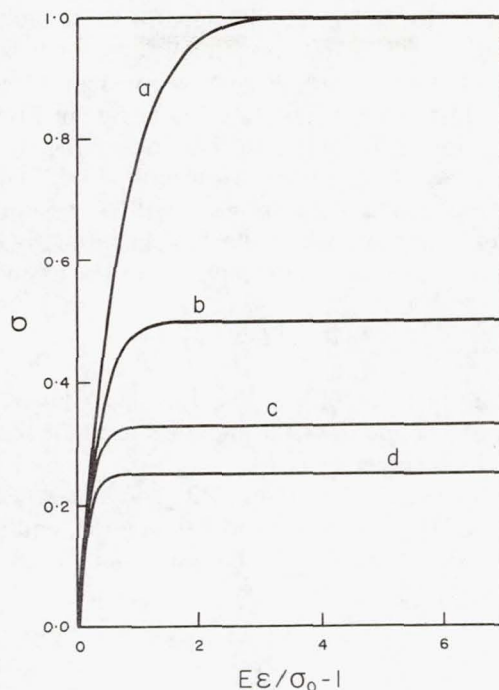


Fig. 1. Typical stress-strain curves for constant strain rates. (a)  $\sqrt{\gamma}/k = 1$ , (b)  $\sqrt{\gamma}/k = 2$ , (c)  $\sqrt{\gamma}/k = 3$ , (d)  $\sqrt{\gamma}/k = 4$ ,  $k = \partial\epsilon/\partial t$ .

hyperbolic, partial differential equation of the evolution type in dimensionless form as follows:

$$\beta(\partial^2\sigma/\partial x^2 - \partial^2\sigma/\partial t^2) = [1_+(\sigma)df(\sigma)/d\sigma + \delta(\sigma)f(0)]\partial\sigma/\partial t, \quad (2.7)$$

where

$$\sigma(x, t) \equiv \bar{\sigma}/\sigma_0 - 1, \quad (2.8)$$

is the dimensionless overstress,

$$x \equiv \alpha\bar{X}, \quad (2.9)$$

$$t \equiv \alpha c\bar{t}, \quad (2.10)$$

$$c \equiv \sqrt{E/\rho}, \quad (2.11)$$

$$\alpha \equiv \beta\gamma\sqrt{\rho E/\sigma_0}, \quad (2.12)$$

$\delta(\cdot)$  is the Dirac delta functional, and  $\beta > 0$  is a dimensionless constant included here in the definition of  $\alpha$  for convenience.

Materials described by the constitutive relation given in (2.6) probably cannot support shock layers or explain the generation of shockfronts. If a shock layer is dissipative, then generalized viscoelastic theories and constitutive relations such as those considered by Varley and Rogers[6], Coleman and Gurtin[11], Dunwoody and Dun-

woody[12] and Pipkin[5], or further generalizations of these models, should be used to describe it. For propagation in a rod, the shock layer may be dispersive due to lateral deformation† instead of due to any dissipative mechanism. Such a shock transition may be described in terms of a low frequency, large rate of straining expansion of a three-dimensional deformation field similar to that considered by Parker and Varley [13]. In applying one of the self-similar motions described in this paper to a nonlinear wave motion behind a propagating shockfront, it will be assumed that the rate of straining in the shock layer is high enough to allow the material to exhibit instantaneous linear elasticity‡[1]. Thus, across such a shock layer, it will be assumed that

$$[\bar{\sigma}] = E[\epsilon], \quad (2.13)$$

where  $[\chi]$  denotes the jump in value of  $\chi$  across the shock layer, and the value of  $E$  will be assumed to be a constant and have the same value as the modulus of the elastic range of the constitutive relation given by (2.6).

From the Lagrangian equation of motion (2.2) and the kinematic compatibility condition (2.3), two additional jump conditions relating  $[u]$ , and  $[\epsilon]$ , can be deduced formally following a technique suggested by Courant and Friedrichs[7]. The results are:

$$\rho U[u] + [\bar{\sigma}] = 0, \quad (2.14)$$

$$U[\epsilon] + [u] = 0, \quad (2.15)$$

where  $U$  is the propagation speed of the shockfront. Equations (2.14) and (2.15) can also be deduced from physical arguments directly. The jump conditions, (2.13)–(2.15), indicate that the speed of propagation of a shock layer of a material exhibiting instantaneous elasticity is

$$|U| = \sqrt{E/\rho}, \quad (2.16)$$

which is, in fact, the same as the elastic speed of propagation of small disturbances.

In applying the constant speed solutions to the 'unsteady' motion behind a propagating discontinuity which moves at a constant sub-elastic speed, it will be assumed that there is an elastic precursor and an unloading, relaxation zone, or a constant stress region, ahead of the discontinuity. The details of the unsteady motion of a relaxation zone ahead of such a discontinuity may be very complicated and will not be considered in this paper.

### 3. A CLASS OF SELF-SIMILAR SOLUTIONS

Cowper and Symonds[8] proposed, in 1957, a power law,

$$f(\sigma) = \sigma^\delta, \quad (3.1)$$

†The authors are indebted to Professor E. Varley for a discussion pertaining to this point.

‡The range of rate of straining within which materials exhibit instantaneous elasticity varies from one material to another. There is usually an upper (and lower) cutoff point in rate of straining above (and below) which a material may have to be considered viscoelastic. The authors are indebted to Professor R. S. Rivlin for pointing this out to them.

where  $\delta > 0$  is a dimensionless material constant, to describe the rate-sensitivity of perfectly plastic materials. This law seems to be quite adequate in approximating the dynamic responses of certain metallic alloys [14, 15] under moderately high rates of straining. The material constants,  $\gamma$  and  $\delta$ , for such a material may be determined by explosive ring-tests as suggested by Perrone [16]. Recent investigators [17–21] have applied this model to impulsively loaded beams, rods, and plates. The class of self-similar solutions described in this paper is based on the constitutive relation (2.6) and the special form of  $f(\sigma)$  given by (3.1). Under these constitutive assumptions, equation (2.7) may be expressed as follows:

$$\phi(\sigma_{xx}, \sigma_{tt}, \sigma_t, \sigma; x, t) = 0, \quad (3.2)$$

where

$$\phi \equiv \sigma_{xx} - \sigma_{tt} - \sigma^{\delta-1} \sigma_t I_+(\sigma), \quad (3.3)$$

and subscripts denote partial differentiation. The constant  $\beta$  which appeared in the definition of  $\alpha$  in (2.12) has been replaced by the material constant  $\delta$ .

Consider a one-parameter continuous group of transformations defined by

$$(X, T, \Sigma) = (bx, b^m t, b^n \sigma), \quad (3.4)$$

$$(\Sigma_{XX}, \Sigma_{TT}, \Sigma_T) = (b^{n-2} \sigma_{xx}, b^{n-2m} \sigma_{tt}, b^{n-m} \sigma_t), \quad (3.5)$$

where  $b$  is the parameter, and  $m, n$  are constants. It can be shown that for the special case of  $m = 1, n = 1/(1 - \delta)$ ,

$$\phi(\sigma_{xx}, \sigma_{tt}, \sigma_t, \sigma; x, t) = b^{(1-2\delta)/(1-\delta)} \phi(\Sigma_{XX}, \Sigma_{TT}, \Sigma_T, \Sigma; X, T), \quad (3.6)$$

where it is assumed that  $\delta \neq 1$ . For  $\delta = 1$ , equation (3.2) is linear and the analytical solution has been discussed in detail by Malvern [10]. Thus,  $\phi$  is a constant conformal invariant under the group defined by equations (3.4) and (3.5) with  $m = 1$ , and  $n = 1/(1 - \delta)$ . According to a theorem proven by Morgan [22], the solution to equation (3.2) may be expressed in terms of a function  $F(\xi)$  of an absolute invariant  $\xi$  of the transformation group defined by

$$(X, T) = (bx, bt). \quad (3.7)$$

The function  $F(\xi)$  is an absolute invariant of the transformation group defined by

$$(X, T, \Sigma) = (bx, bt, b^{1/(1-\delta)} \sigma). \quad (3.8)$$

It will be straightforward to verify that

$$\xi = t/x, \quad (3.9)$$

$$F(\xi) = x^{1/(\delta-1)} \sigma(x, t), \quad (3.10)$$

are absolute invariants of the groups defined by equations (3.7) and (3.8), respectively.



Thus, there exists a class of self-similar solutions to equation (3.2) of the form

$$\sigma = x^{1/(1-\delta)} F(\xi), \quad (3.11)$$

where  $\xi$  is given by (3.9).

Substituting equation (3.11) into equation (3.2) and using equation (3.3), a non-linear, second-order ordinary differential equation results. For  $\sigma > 0$ , this equation is expressible as follows:

$$(\xi^2 - 1)F'' - \{[2\delta/(1-\delta)]\xi + F^{\delta-1}\}F' + [\delta/(1-\delta)^2]F = 0, \quad (3.12)$$

where prime denotes differentiation.

For the special case of  $\delta = 2$ ,  $\xi > 0$ , equation (3.12) is immediately integrable to the following Riccati equation:

$$2(\xi^2 - 1)F' + 4\xi F - F^2 = 4K, \quad (3.13)$$

where  $K$  is an arbitrary constant. This equation may be converted into a linear, second-order, ordinary differential equation by the following transformation:

$$(\xi^2 - 1)^r V(z) = \text{Exp} \left[ -\frac{1}{2} \int_{\xi}^{\xi} \frac{F(\xi')}{\xi'^2 - 1} d\xi' \right], \quad (3.14)$$

$$2z = \xi + 1. \quad (3.15)$$

The result is:

$$z(1-z)V'' + 2(1+r)(1-2z)V' - (2r-K)V = 0, \quad (3.16)$$

where  $r$  satisfies the quadratic equation,

$$4r^2 + 4r + K = 0. \quad (3.17)$$

Equation (3.16) has three regular singular points at  $z = 0, 1$ , and  $\infty$ . The solutions to this equation are expressible in terms of hypergeometric functions. For  $\xi > 1$ , the appropriate general solution to (3.16) is, in the usual notation,

$$V(z) = Cz^{-2r-3} {}_2F_1[2r+3, 2, 4; 1/z], \quad (3.18)$$

where  $C$  is an arbitrary constant. Thus, from equation (3.14), the corresponding expression for  $F(\xi)$  is

$$F(\xi) = 6(\xi - 1) - 4r + 2(2r + 3) \frac{(\xi - 1) {}_2F_1[2r+4, 3, 5; 2/(\xi+1)]}{(\xi + 1) {}_2F_1[2r+3, 2, 4; 2/(\xi+1)]}. \quad (3.19)$$

The expression (3.19) for  $F(\xi)$  assumes some particularly simple forms in terms of elementary functions for special values of  $K$ . As examples, typical expressions for  $F(\xi)$  and  $\sigma(x, t)$  for two different values of  $K$  are listed below:

$K = 0$ , (i.e.  $r = 0$ , or  $-1$ )

$$F(\xi) = 8\{2\xi + (\xi^2 - 1) \ln [(\xi - 1)/(\xi + 1)] + A_1(\xi^2 - 1)\}^{-1}. \quad (3.20)$$

$$\sigma(x, t) = 8x\{2xt + (t^2 - x^2) \ln [(t - x)/(t + x)] + A_1(t^2 - x^2)\}^{-1}. \quad (3.21)$$

$K = -3$ , (i.e.  $r = 1/2$  or  $-3/2$ )

$$F(\xi) = 6(1 + A_2\xi + \xi^2)/(A_2 + 3\xi - \xi^2), \quad (3.22)$$

$$\sigma(x, t) = 6(x^2 + A_2xt + t^2)/(A_2x^3 + 3x^2t - t^3). \quad (3.23)$$

In these expressions,  $A_1$  and  $A_2$  are arbitrary constants.

It is interesting to note that the solution given by (3.21) is invariant under the translation defined by  $(x', t') = (x + a, t + a)$ , where  $a$  is an arbitrary constant. This property will be utilized in Section 5 to derive a closed form solution of a self-similar, unsteady, dispersed, nonlinear wave motion behind a constant 'elastic-speed' shockfront propagating into an initially quiescent region.

#### 4. NONLINEAR WAVES WITH CONSTANT SPEEDS

Equation (2.7) is a nonlinear, hyperbolic differential equation of the evolution type. The characteristic speeds related to this equation are given by,

$$D_{\pm} \bar{X}/Dt = \pm c, \quad (4.1)$$

or,

$$D_{\pm} x/Dt = \pm 1, \quad (4.2)$$

where  $D_{\pm}(\cdot)/D\bar{t}$  and  $D_{\pm}(\cdot)/Dt$  denote differentiation along the characteristics.

Due to the presence of the evolution or dissipative term,  $[1_+(\sigma)df(\sigma)/d\sigma + \delta(\sigma)f(0)] \cdot \partial\sigma/\partial t$ , in equation (2.7), it is expected that, in the plastic range, the material can also support dissipative, dispersive waves in addition to the characteristic propagations of discontinuities given by equation (4.1) or (4.2). To demonstrate the existence of non-characteristic propagations, a class of constant speed solutions to equation (2.7) is considered in this section. This class of solutions is obtained by searching for expressions of the form:

$$\sigma(x, t) = g(s), \quad (4.3)$$

where

$$s \equiv c\bar{t} - x, \quad (4.4)$$

and  $\bar{c}$  = constant determines the speed of propagation.

Substituting equation (4.3) into equation (2.7), a nonlinear, second-order, ordinary differential equation results:

$$\beta(1 - \bar{c}^2)g'' = \bar{c}[1_+(g)f'(g) + \delta(g)f(0)]g', \quad (4.5)$$

where primes denote differentiation. This equation can be integrated once immediately

to yield,

$$\beta(1 - \bar{c}^2)g' = \bar{c}1_+(g)f(g) + A, \quad (4.6)$$

where  $A$  is an arbitrary constant. Actually, the fact that equation (4.5) can be integrated once in closed form is not due to the special choice of the constitutive equation, (2.6), since, by assuming solutions of constant speeds of propagation, equation (2.2) can be integrated at once without making any additional assumptions. By comparing the expression (4.6) with the basic equations, (2.2) and (2.6), it is easily demonstrated that  $A = 0$ . Thus,

$$\beta(1 - \bar{c}^2)g' = \bar{c}1_+(g)f(g), \quad (4.7)$$

for constant speeds of propagation.

If  $g < 0$ , then equation (4.7) becomes

$$(1 - \bar{c}^2)g' = 0. \quad (4.8)$$

Except for the trivial case of  $g = \text{constant}$ , equation (4.8) requires that  $\bar{c} = \pm 1$ , which of course is the elastic speed of propagation. For  $g > 0$ , equation (4.7) requires that

$$(i) \quad \bar{c}^2 < 1, \text{ for } (g'/\bar{c}) > 0, \quad (4.9)$$

$$(ii) \quad \bar{c}^2 > 1, \text{ for } (g'/\bar{c}) < 0. \quad (4.10)$$

Thus, for the physically more meaningful case  $\bar{c}^2 < 1$ , the overstress may increase or decrease with  $s$  depending on whether  $\bar{c} > 0$  or  $< 0$ . Equations (4.9) and (4.10) also indicate that if solutions for  $g > 0$  exist, the waves represented by these solutions are not characteristic propagations.<sup>†</sup>

On setting  $h = g'$ , equation (4.5) for  $g > 0$  may be written as

$$\frac{h'}{g'} = \frac{\bar{c}}{\beta(1 - \bar{c}^2)} f'(g). \quad (4.11)$$

Since  $f(g)$  is a  $C^1$  function, equation (4.11) does not have any singular points. Thus, according to the Poincaré-Bendixon theorem, it may be concluded that equation (4.11), in general, does not possess periodic solutions.

For  $g > 0$ , equation (4.7) may be integrated, in general, by quadrature as follows:

$$s = [\beta(1 - \bar{c}^2)/\bar{c}] \int^g f^{-1}(\zeta) d\zeta + C', \quad (4.12)$$

where  $C'$  is an arbitrary constant.

Perzyna[9] in 1963, suggested two interesting expressions for  $f(\zeta)$ . In slightly generalized forms, these expressions are given as follows:

<sup>†</sup>In fact, these waves are similar to the so-called solitary waves which are constant-speed, nonlinear propagations of special wave forms. The authors are indebted to Professor G. S. S. Ludford for pointing this out to them.



$$(i) f(\zeta) = \sum_{l=0}^L a_l \zeta^l, \quad (4.13)$$

$$(ii) f(\zeta) = b_0 + \sum_{l=1}^L b_l (\text{Exp } \zeta^l - 1), \quad (4.14)$$

where  $a_l, b_l$  are constants. Expression (i) or equation (4.13) includes the model  $f(\zeta) = \zeta^\delta$  suggested by Cowper and Symonds[8] as a special case. For  $F(\zeta) = \zeta^\delta$ , and  $\delta \neq 1$ , equation (4.12) becomes,

$$s - s_1 = \frac{\delta(1 - \bar{c}^2)}{(1 - \delta)\bar{c}} (g^{1-\delta} - g_1^{1-\delta}), \quad (4.15)$$

where  $g_1 = g(s_1)$ ,  $s_1$  is a constant, and  $\beta$  has been chosen as  $\delta$ .

Another simple result is obtained for the constitutive relation (ii) or equation (4.14) with  $L = 1$ . The integrated expression is

$$s - s_1 = \frac{(1 - \bar{c}^2)}{\bar{c}} \left[ (g_1 - g) + \ln \left( \frac{e^g - 1}{e^{g_1} - 1} \right) \right], \quad (4.16)$$

where, again,  $g_1 = g(s_1)$ ,  $s_1$  is a constant, and  $\beta$  has been chosen as  $b_1$ .

It is of interest to note that for the constitutive relation (i), or equation (4.13),  $f^{-1}(\zeta)$  may be expressed in the form:

$$f^{-1}(\zeta) = \sum_{k=1}^m c_k (\alpha_1 \zeta + \alpha_2)^{-k} + \sum_{p=1}^n (d_p \zeta + e_p) (\beta_1 \zeta^2 + 2\beta_2 \zeta + \beta_3)^{-p}, \quad (4.17)$$

where  $\alpha_1, \alpha_2, \beta_1, \beta_2, \beta_3, c_k, d_p$ , and  $e_p$  are real constants, with  $\beta_2^2 < \beta_1 \beta_3$ . Thus, the integral in equation (4.12) can always be evaluated in closed form in terms of elementary functions.

## 5. NONLINEAR WAVE MOTION BEHIND PROPAGATING DISCONTINUITIES

### 5.1 Self-similar solution behind a constant-speed shockfront

Consider a one-dimensional shockfront propagating at some speed  $U(> 0)$  into an initially quiescent one-dimensional region ( $x \geq 0$ ). As it had been remarked earlier, if the range of the rate of straining within the shock layer renders the material to exhibit instantaneous linear elasticity, then the shockfront will propagate at a constant speed,

$$U = \sqrt{E/\rho}, \quad (5.1)$$

where  $E$  is the instantaneous modulus of elasticity. If the value of  $E$  is chosen to be the same as the modulus of the elastic range of the constitutive equation, (2.6), then the shock speed has the same value as the characteristic speed  $D_+ X/D\bar{t}$  given by equation (4.1). Under such an assumption, the values of  $u$  and  $\bar{\sigma}$  immediately behind the shock layer must satisfy the characteristic compatibility condition[10]:

$$d\bar{\sigma} - \rho c du = -E\gamma f(\bar{\sigma}/\sigma_0 - 1) 1_+(\bar{\sigma}/\sigma_0 - 1) d\bar{t}, \quad (5.2)$$

where  $c = U = \sqrt{E/\rho}$ .

The values of  $u$ ,  $\bar{\sigma}$ , and  $\epsilon$ , immediately behind the shock layer must also satisfy the jump conditions given by equations (2.13) to (2.15). Since  $u$ ,  $\bar{\sigma} = 0$  in the quiescent region in front of the shock layer, equation (2.14) requires that,

$$\bar{\sigma} = -\rho U u = -\rho c u, \quad (5.3)$$

immediately behind the shock layer. Combining equations (5.2) and (5.3), the following differential equation results:

$$2\beta d\sigma = -f(\sigma) 1_+(\sigma) dt, \quad (5.4)$$

where as before,  $\sigma \equiv (\bar{\sigma}/\sigma_0 - 1)$  and  $t \equiv \alpha c \bar{t}$  with  $\alpha \equiv \beta \gamma \sqrt{\rho E/\sigma_0}$ . Equation (5.4) indicates that, if  $\sigma > 0$ , then the overstress immediately behind the shockfront always attenuates with time along the shock.

Assuming that  $\sigma > 0$  behind the shockfront, equation (5.4) can be integrated by quadrature as follows:

$$t = 2\beta \int^\sigma f^{-1}(\zeta) d\zeta + C'', \quad (5.5)$$

where the integral is identical to that of equation (4.12). Thus, closed-form solutions of equation (5.5) are possible for special constitutive assumptions. For  $f(\zeta) = \zeta^\delta$  with  $\delta \neq 1$ , equation (5.5) becomes

$$t = [2\delta/(1-\delta)] (\sigma_1^{1-\delta} - \sigma^{1-\delta}), \quad (5.6)$$

where  $\sigma_1 \equiv \sigma(0)$ , and  $\beta$  has been chosen as  $\delta$ . Therefore, the overstress immediately behind the shock attenuates monotonically with time along the shockfront from  $\sigma = \sigma_1$  at  $t = 0$  to  $\sigma = 0$  at  $t = \infty$ .

It is interesting to note that for  $\delta = 2$ , equation (5.6) can be satisfied by one of the self-similar solutions given in Section 3:

$$8\sigma^{-1} = (x+a) [2\eta + (\eta^2 - 1) \{A_1 + \ln [(\eta - 1)/(\eta + 1)]\}], \quad (5.7)$$

where  $\eta = (t+a)/(x+a)$ , and  $a, A_1$  are constants. To satisfy the compatibility condition (5.6) for  $\delta = 2$ , the constant  $a$  in (5.7) must be chosen as follows:

$$a = 4/\sigma_1. \quad (5.8)$$

Therefore, the dimensionless overstress  $\sigma(x, t)$  behind the shockfront is given by,

$$\sigma = 8/\left[(t+4/\sigma_1) \left\{2 + (\eta - 1/\eta) \left[A_1 + \ln \left(\frac{\eta - 1}{\eta + 1}\right)\right]\right\}\right], \quad (5.9)$$

and the stress boundary condition at  $x = 0$  is,

$$\sigma(0, t) = 8/[2(t+4/\sigma_1) + (2t + \sigma_1 t^2/4) \{A_1 - \ln [1 + 8/(\sigma_1 t)]\}]. \quad (5.10)$$

The behavior of this function for various values of  $A_1$  is shown in Fig. 2.

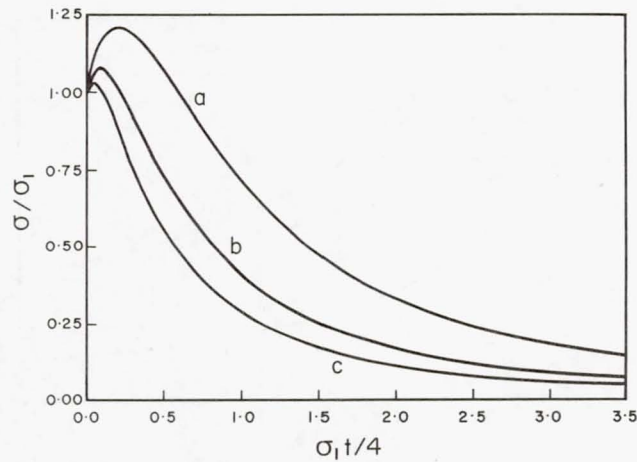


Fig. 2. Variation of  $\sigma/\sigma_1$  with  $\sigma_1 t/4$  at  $\bar{X} = 0$ . Self-similar solution ( $\delta = 2$ ). (a)  $A_1 = \ln 2$ , (b)  $A_1 = \ln 4$ , (c)  $A_1 = \ln 8$ .

In dimensional forms, the resulting expressions for  $\sigma(\bar{X}, \bar{t})$ ,  $u(\bar{X}, \bar{t})$ , and  $\epsilon(\bar{X}, \bar{t})$  for this case are given as follows:

$$\sigma = \bar{\sigma}/\sigma_0 - 1 = [4c\sigma_0/(E\gamma)](\bar{X} + ct_0)[2c(\bar{X} + ct_0)(\bar{t} + \bar{t}_0) - [c^2\bar{t}(\bar{t} + 2t_0) - \bar{X}(\bar{X} + 2ct_0)]\{\ln[(c\bar{t} + \bar{X} + 2ct_0)/(c\bar{t} - \bar{X})] + B\}]^{-1}, \quad (5.11)$$

$$u = -(\sigma_0/\rho)[\sigma(\bar{t} + t_0)/(\bar{X} + ct_0) + c^{-1}], \quad (5.12)$$

$$\epsilon = (\sigma_0/\rho)[\sigma(\bar{t} + t_0)^2/(\bar{X} + ct_0)^2 + c^{-2}], \quad (5.13)$$

where

$$t_0 = 2\sigma_0/(\gamma\sigma_1 E), \quad (5.14)$$

and  $B$  is a constant. The behavior of the functions  $u(0, \bar{t})$  and  $\epsilon(0, \bar{t})$  for various values of  $A_1$  are indicated in Figs. 3 and 4. It is of interest to note that (5.13) yields a permanent strain  $\epsilon_p$  given by

$$\epsilon_p = \lim_{\bar{t} \rightarrow \infty} \epsilon = (\sigma_0/E)[(4c\sigma_0/A_1\gamma E)(\bar{X} + ct_0)^{-1} + 1]. \quad (5.15)$$

Typical distributions of the permanent strain are shown in Fig. 5.

### 5.2. Constant speed solution behind an elastic precursor

Duvall [23] suggested that the one-dimensional, unsteady motion in a semi-infinite ( $x \geq 0$ ), rate-sensitive, elastoplastic region generated by a continuously applied load at its boundary ( $x = 0$ ) may eventually consist of an elastic precursor propagating into an initially quiescent region, an unloading, relaxation zone, and a sub-elastic, constant-speed, nonlinear wave motion as depicted in Fig. 6. After a reasonable length of time, the elastic precursor will be far ahead of the leading wave of the constant speed region

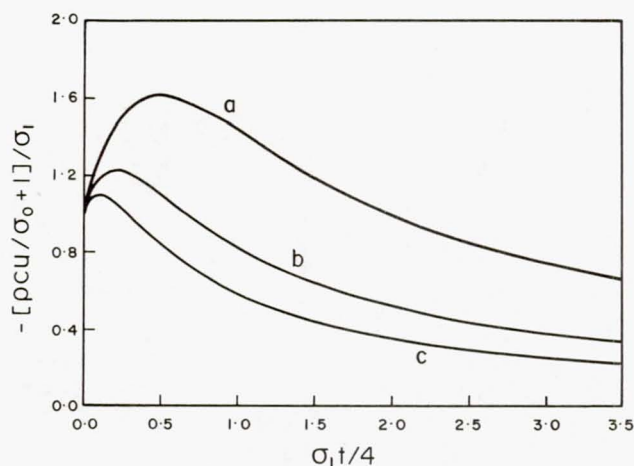


Fig. 3. Variation of  $-[pcu/\sigma_0 + 1]/\sigma_1$  with  $\sigma_1 t/4$  at  $\bar{X} = 0$ . Self-similar solution ( $\delta = 2$ ). (a)  $A_1 = \ln 2$ , (b)  $A_1 = \ln 4$ , (c)  $A_1 = \ln 8$ .

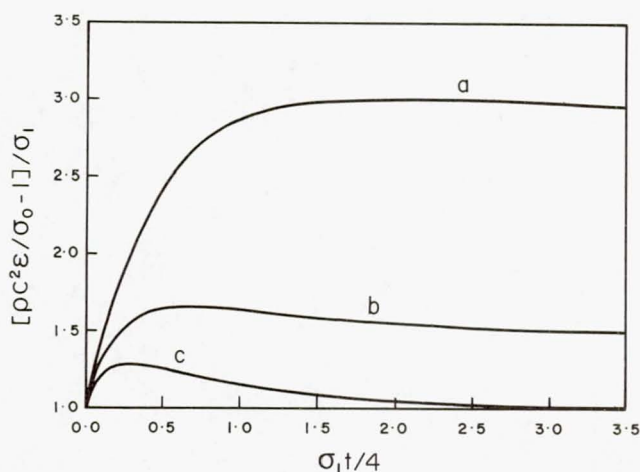


Fig. 4. Variation of  $[pc^2\epsilon/\sigma_0 - 1]/\sigma_1$  with  $\sigma_1 t/4$  at  $\bar{X} = 0$ . Self-similar solution ( $\delta = 2$ ). (a)  $A_1 = \ln 2$ , (b)  $A_1 = \ln 4$ , (c)  $A_1 = \ln 8$ .

and the boundary of  $x = 0$  will be far behind it. Relative to an observer moving with the leading wave of the constant speed region, the unsteady motion behind the leading wave becomes essentially steady.

Any of the constant-speed, nonlinear wave solutions described by equation (4.12) in section 4 with  $\bar{c} < 1$  may be considered as a constant-speed portion of such an 'unsteady' motion. If the overstress on the leading wave  $s = s_1$  is  $\sigma_1 > 0$ , then the quadrature expression, (4.12), becomes,

$$s - s_1 = [\beta(1 - \bar{c}^2)/\bar{c}] \int_{\sigma_1}^{\sigma} f^{-1}(\zeta) d\zeta, \quad (5.16)$$

where  $s \equiv \bar{c}t - x$ , and  $\bar{c} < 1$ . From equation (5.16), the stress boundary condition



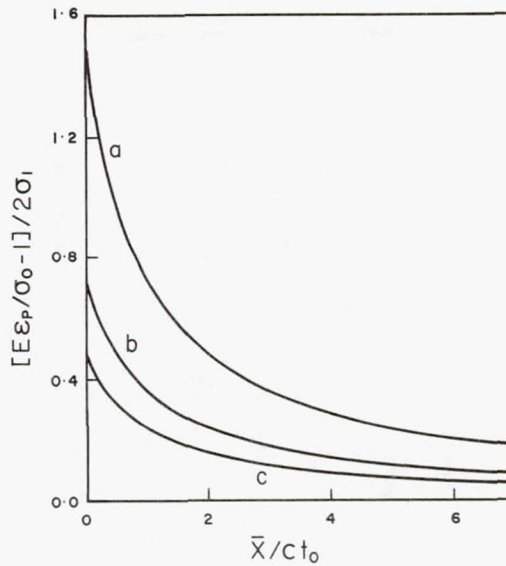


Fig. 5. Typical distributions of the permanent strain. Self-similar solution ( $\delta = 2$ ). (a)  $A_1 = \ln 2$ , (b)  $A_1 = \ln 4$ , (c)  $A_1 = \ln 8$ .

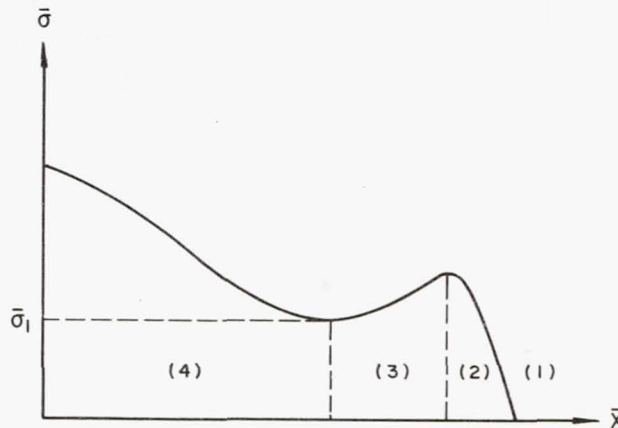


Fig. 6. Schematic representation of a nonlinear wave motion behind a relaxation zone. (1) quiescent region, (2) elastic precursor, (3) relaxation zone, (4) sub-elastic, constant speed region.

required to maintain the constant-speed motion can be evaluated in a straightforward manner.

It is of interest to note that, if the initial rate of loading of the applied stress at the boundary is not too high such that the time required to raise the stress  $\bar{\sigma}$  from zero to the value of the static yield stress  $\sigma_0$  is much longer than the pertinent characteristic relaxation time of the medium, then a complete description of a possible non-linear wave motion for a continuously loading boundary may be constructed exactly. Figure 7 is a schematic representation of such a motion. It consists of four solution regions



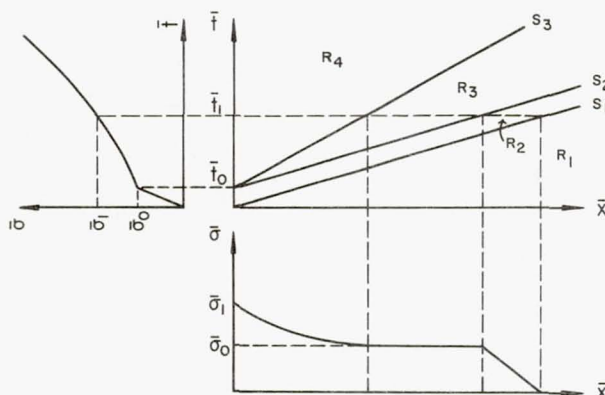


Fig. 7. Schematic representation of a possible nonlinear wave motion due to a continuously loading boundary at  $\bar{x} = 0$ .

separated by three discontinuities described as follows:

(1) *Solution regions*

$R_1$ : the undisturbed region,  $\bar{\sigma} = 0$

$R_2$ : the elastic region,  $\bar{\sigma} < \sigma_0$

$R_3$ : the constant stress region,  $\bar{\sigma} = \sigma_0$

$R_4$ : the constant speed solution region,  $\bar{\sigma} > \sigma_0$ .

(2) *Discontinuities*

$S_1$ : the leading elastic wave

$S_2$ : the trailing elastic wave

$S_3$ : the leading constant speed wave.

Such an unsteady motion may be generated by a monotonically increasing stress boundary condition. The manner in which the stress varies at the boundary in the elastic range can be quite arbitrary (so long as the rate of loading is small enough so that there will be no dynamic overstressing in the elastic precursor) and has been chosen as a linear function of  $\bar{t}$  in Fig. 7 for simplicity, while the rate of stressing beyond the static yield stress must follow the expression given in equation (4.12) or the differential equation, (4.7). It is clear from equation (4.7) that nontrivial solutions in  $R_4$  can be generated from a leading wave  $S_3$  on which the stress is  $\bar{\sigma} = 0$  only if  $f(0) > 0$ . The value of  $f(0)$  can be arbitrarily small. Alternatively, if  $f(0) = 0$  for a specific constitutive relation, a solution such as the one depicted by Fig. 7 can still be generated by viewing  $S_3$  as a small discontinuity in the value of  $\bar{\sigma}$  such that the overstress jumps across this 'plastic shock' from zero to some small constant positive value  $\sigma_1 \ll 1$ . The jump in  $\sigma$  from 0 to  $\sigma_1$  at the boundary of  $\bar{x} = 0$  may be viewed as the result of a very fast rate of loading  $r$  in a small interval of time  $\Delta\bar{t}$  near  $\bar{t} = \bar{t}_0$  such that  $\lim_{\Delta\bar{t} \rightarrow 0} (r\Delta\bar{t}) = \bar{\sigma}_1 = (1 + \sigma_1)\sigma_0$  and  $0 < \sigma_1 \leq 1$ . The fact that  $\bar{\sigma} = \sigma_0$  in  $R_3$  is an admissible solution can be deduced immediately from equation (2.7).

*Acknowledgment*—This investigation was partially supported by the Advanced Research Projects Agency of the Department of Defense and monitored by the Office of Naval Research under Contract Number N00014-68-A-0187, and partially supported by the National Aeronautics and Space Administration under Grant Number NASA-NGL34-002-084. A portion of this work was completed when one of us (T. S. C.) was visiting the Center for the Application of Mathematics, Lehigh University, and the Department of

Theoretical and Applied Mechanics, Cornell University. The authors are indebted to Professors A. C. Eringen, Y. Horie, G. S. S. Ludford, R. S. Rivlin, and E. Varley for their comments and suggestions.

## REFERENCES

- [1] R. S. RIVLIN, *Q. appl. Math.* **14**, 83 (1956).
- [2] N. CRISTESCU, *Dynamic Plasticity*. North-Holland (1967).
- [3] V. V. SOKOLOVSKII, *Dokl. Akad. Nauk SSSR* **60**, 775 (1948).
- [4] V. V. SOKOLOVSKII, *Prikl. Mat. Mekh.* **12**, 261 (1948).
- [5] A. C. PIPKIN, *Q. appl. Math.* **23**, 297 (1965).
- [6] E. VARLEY and T. G. ROGERS, *Proc. R. Soc. Series A* **296**, 498 (1967).
- [7] R. COURANT and K. O. FRIEDRICHS, *Supersonic Flow and Shock Waves*. Interscience (1948).
- [8] G. R. COWPER and P. S. SYMONDS, *Technical Report No. 28, Contract Nonr 562 (10)*. Brown University (1957).
- [9] P. PERZYNA, *Archw. Mech. stosow* **15**, 113 (1963).
- [10] L. E. MALVERN, *Q. appl. Math.* **8**, 405 (1951).
- [11] B. D. COLEMAN and M. E. GURTIN, *Proc. IUTAM Symp. Vienna 54*, Springer-Verlag (1968).
- [12] J. DUNWOODY and N. DUNWOODY, *Int. J. Engng Sci.* **3**, 417 (1965).
- [13] D. F. PARKER and E. VARLEY, *Q. Jl Mech. appl. Math.* **21(3)**, 329 (1968).
- [14] M. J. MANJOINE, *J. appl. Mech.* **11**, 211 (1944).
- [15] E. W. PARKES, *Proc. Instn civil Engrs* **10**, 277 (1958).
- [16] N. PERRONE, *Exp. Mech.* **8**, 232 (1968).
- [17] S. R. BODNER and P. S. SYMONDS, *Proc. 2nd Symp. nav. struct. Mech.* 488, Pergamon Press (1960).
- [18] T. C. T. TING and P. S. SYMONDS, *Proc. 4th U.S. natn. Congr. appl. Mech.* 1153 (1962).
- [19] S. R. BODNER and P. S. SYMONDS, *J. appl. Mech.* **29**, 719 (1962).
- [20] T. C. T. TING, *Q. appl. Math.* **21**, 133 (1963).
- [21] N. PERRONE, *J. appl. Mech.* **32**, 489 (1965).
- [22] A. J. A. MORGAN, *Q. J. Math.* **2**, 250 (1952).
- [23] G. E. DUVALL, *Proc. IUTAM Symp. Stress Waves in Anelastic Solids 20*, Springer-Verlag (1964).

(Received 20 July 1971)

**Résumé**—Deux classes de solutions du type fermé d'ondes non-linéaires à une dimension, dans un matériau élasto-plastique sensible à la vitesse sont présentées. Une classe de ces solutions est auto-semblable et l'autre classe consiste en des propagations à vitesse constante. Des applications de ces solutions à des mouvements instables en arrière de la propagation de discontinuités sont également considérées.

**Zusammenfassung**—Zwei Klassen von Lösungen geschlossener Form von eindimensionalen, nicht-linearen Wellen in einem ratenempfindlichen elastoplastischen Stoffe werden mitgeteilt. Eine Klasse dieser Lösungen ist selbst-ähnlich und die andere Klasse besteht aus konstanten Geschwindigkeitsfortpflanzungen. Anwendungen dieser Lösungen auf unstetige Bewegungen hinter sich fortpflanzenden Diskontinuitäten werden auch untersucht.

**Sommario**—Si tratta di una relazione su due classi di soluzioni di forma chiusa di onde monodimensionali e non lineari in un materiale elastoplastico e sensibile al ritmo. Una classe di queste soluzioni è autosimilare e l'altra consiste in propagazioni a velocità costante. Si prendono anche in considerazione le applicazioni di queste soluzioni ai movimenti instabili dietro le discontinuità di propagazione.

**Абстракт**—Установлены два класса решений замкнутого вида для одномерных нелинейных волн в эластопластическом материале чувствительном к скорости. Один класс этих решений — самоподобным, а другой состоит из распространений постоянной скорости. Рассмотрены и применения эти решений к нестационарным движениям за распространяющиеся разрывы.



## Research Notes

Research Notes published in this Section include important research results of a preliminary nature which are of special interest to the physics of fluids and new research contributions modifying results already published in the scientific literature. Research Notes

cannot exceed five printed columns in length including space allowed for title, abstract, figures, tables, and references. The abstract should have three printed lines. Authors must shorten galley proofs of Research Notes longer than five printed columns before publication.

### Curved Characteristics Behind Blast Waves

O. LAPORTE

Department of Physics, University of Michigan, Ann Arbor, Michigan 48104

AND

T. S. CHANG\*

Center for Space Research, Massachusetts Institute of Technology, Cambridge, Massachusetts 02139

(Received 22 December 1970; final manuscript received 6 August 1971)

Exact solutions, expressed in closed form in terms of elementary functions, are presented for the three sets of curved characteristics behind a self-similar, strong blast wave.

Blast waves are produced in gaseous media due to the sudden deposition of large amounts of energy in relatively small regions. The propagation of a point-source blast wave into an ideal gas, whose initial pressure is assumed to be negligibly low, is known to be self-similar. This property can be deduced using either dimensional arguments<sup>1</sup> or invariant theorems of continuous groups of transformations.<sup>2</sup> Closed form solutions describing the flow variables in the nonisentropic region behind such a blast wave in  $n=1, 2, 3$  dimensions were obtained independently by von Neumann<sup>3</sup> and Sedov.<sup>4</sup> The reflection of strong blast waves was discussed in an earlier paper<sup>5</sup> by the authors.

It is known that the basic equations governing the nonisentropic flow behind a propagating blast wave admit three distinct characteristic directions given by

$$\frac{dr}{dt} = u, \quad u \pm a, \quad (1)$$

where  $r$  is the radial distance from the point of explosion,  $t$  is the elapsed time,  $u$  is the velocity, and  $a$  is the isentropic speed of sound. The first characteristic direction coincides with the local particle velocity and the family of characteristics is, therefore, composed of particle lines. This direction corresponds to the speed of propagation of entropy disturbances. The other two characteristic directions correspond to the local speeds of propagation of pressure, density, or velocity disturbances. The purpose of this note is to report the interesting result that these three families of curved characteristics can also be represented in closed form, and remarkably, still in terms of elementary functions.

First, consider the  $(u)$  characteristics or particle lines. According to its definition and the self-similar solution of Ref. 5, it may be easily deduced that along

a  $(u)$  characteristic,

$$dr/dt = (2+n)U\hat{u}y(\hat{u})/2, \quad (2)$$

where

$$U = [2K_n/(2+n)](E_0/\rho_0)^{1/(2+n)}t^{-n/(2+n)} \quad (3)$$

is the shock speed,  $y(\hat{u})$  is given by Eq. (5) of Ref. 5,  $\hat{u} = ut/r$ ,  $E_0$  is the energy released per unit area for a planar wave, per unit length for a cylindrical wave, and the total energy released for a spherical wave,  $\rho_0$  is the initial density, and  $K_n$  is determined by the condition of conservation of total energy.

But, from the definition of the similarity parameter and the expression for the shock radius of Ref. 5, it can be shown that, in general,

$$dr/dt = K_n(E_0/\rho_0)^{1/(2+n)}t^{-n/(2+n)}[2y/(2+n) + t dy/dt]. \quad (4)$$

Therefore, from Eq. (5) of Ref. 5 and Eqs. (2)–(4), it is found that,

$$d \ln t = \frac{d \ln y}{d\hat{u}} \frac{d\hat{u}}{\hat{u} - [2/(2+n)]}, \quad (5)$$

along a particle line, where,

$$\frac{d \ln y}{d\hat{u}} = \frac{(\gamma-1)\hat{u}^2/2 + [\hat{u} - 2/(2+n)][\hat{u} - 2/\gamma(2+n)]}{\hat{u}[2/\gamma(2+n) - \hat{u}][(2-n+n\gamma)\hat{u}/2 - 1]}, \quad (6)$$

and  $\gamma$  is the adiabatic index. Thus, Eq. (5) can be integrated in terms of elementary functions. The result is

$$\hat{t} = \alpha \hat{u} (A_2 - \hat{u})^{\beta_1} (\hat{u} - A_2/\gamma)^{\beta_2} (\hat{u} - A_2^{-1})^{\beta_3}, \quad (7)$$

where



$$\begin{aligned}\alpha &= A_1(A_2 - A_1^{-1})^{-\beta_1}(A_1^{-1} - A_2/\gamma)^{-\beta_2}(A_1^{-1} - A_5^{-1})^{-\beta_3}, \\ \beta_1 &= (2\gamma + n - 2)[n(\gamma - 2)]^{-1}\beta_2, \\ \beta_2 &= n\gamma(2 + n)(2 - \gamma)(\gamma - 1)[2(2n\gamma + 2\gamma - n + 2) \\ &\quad \times (2 - n - 2\gamma) + 2n\gamma(2 - \gamma)(n\gamma + 4) + 2(\gamma + 1)(2 + n) \\ &\quad \times (n\gamma^2 - 2n\gamma + n + 2\gamma - 2)]^{-1}, \\ \beta_3 &= (2 + n)(n\gamma^2 - 2n\gamma + n + 2\gamma - 2)[n(2 - \gamma) \\ &\quad \times (n\gamma - n + 2)]^{-1}\beta_2 - 1, \quad (8)\end{aligned}$$

$\hat{t} = t/t_0$  is a dimensionless time normalized with respect to some convenient time scale  $t_0$ , and the  $A$ 's are given by Eqs. (6) of Ref. 5.

To complete the solution for the particle lines, an expression relating  $(r, t, \hat{u})$  is obtained from Eqs. (2) and (5) of Ref. 5. In dimensionless form, this expression becomes,

$$\begin{aligned}\hat{r} &= (A_1\hat{u})^{-A_2}[A_3(\gamma\hat{u}/A_2 - 1)]^{A_8} \\ &\quad \times [A_1(1 - A_5\hat{u})/(A_1 - A_5)]^{A_6 - A_9\hat{t}^{2/(2+n)}}, \quad (9)\end{aligned}$$

where  $\hat{r} = r/R(t_0)$ . Equations (8) and (9) form the closed form parametric solution for the family of  $(u)$  characteristics or particle lines behind a self-similar blast wave.

For the  $(u \pm a)$  characteristics, we have

$$\begin{aligned}\frac{d_{\pm}r}{dt} &= u'f \pm \left[ \frac{\gamma p'g}{\rho'h} \right]^{1/2} \\ &= [U/(\gamma + 1)] \{ 2A_1\hat{u}y(\hat{u}) \\ &\quad \pm [2\gamma(\gamma - 1)g(\hat{u})/h(\hat{u})]^{1/2} \}, \quad (10)\end{aligned}$$

where  $g(\hat{u})$ ,  $h(\hat{u})$ , and  $y(\hat{u})$  are given by Eqs. (4) and (5) of Ref. 5, and the shock speed  $U$  by Eq. (3). Combining with Eq. (4) and after considerable manipu-

lation, it is found that

$$d \ln t = G(\hat{u}) d\hat{u}, \quad (11)$$

where,

$$\begin{aligned}G(\hat{u}) &= (d \ln y/d\hat{u}) \{ [\hat{u} - 2/(2 + n)] \\ &\quad \pm [\gamma(\gamma - 1)(2 - 2\hat{u} - n\hat{u})/2(2\gamma\hat{u} + n\gamma\hat{u} - 2)]^{1/2}\hat{u} \}^{-1}. \quad (12)\end{aligned}$$

The expression  $d \ln y/d\hat{u}$  in  $G(\hat{u})$  is known and given by Eq. (6). Therefore,  $G(\hat{u})$  may be reduced to an algebraic function involving square roots of second degree polynomials of  $\hat{u}$  as radicals. This means that Eq. (11) can be integrated in terms of elementary, albeit transcendental, functions. The results are

$$\begin{aligned}\ln \hat{t} &= K_{\pm} + \ln |A_5\hat{u}/(1 - A_5\hat{u})| \pm (m/l^{1/2}) \\ &\quad \times \sin^{-1} \{ [l/(A_5^{-1} - \hat{u}) - k]/(k^2 - l)^{1/2} \}, \quad (13)\end{aligned}$$

where,

$$\begin{aligned}k &= A_5^{-1} - (\gamma + 1)[\gamma(2 + n)]^{-1}, \\ l &= A_5^{-2} - 2A_5^{-1}(\gamma + 1)[\gamma(2 + n)]^{-1} + 4[\gamma(2 + n)^2]^{-1}, \\ m &= -A_5^{-1}[(\gamma - 1)/2]^{1/2}. \quad (14)\end{aligned}$$

Equation (13) and the parametric expression for  $(\hat{r}, \hat{t}, \hat{u})$  given by Eq. (9) form the closed form parametric solutions for the two families of  $(u \pm a)$  characteristics in the dimensionless  $\hat{r}-\hat{t}$  plane. The constant  $K_{\pm}$  in Eq. (13) must be evaluated for each characteristic from a set of known values of  $(\hat{r}, \hat{t}, \hat{u})$ .

Figure 1 displays a typical set of solution curves expressing the dimensionless time  $\hat{t}$  as functions of the dimensionless distance  $\hat{r}$  for  $n=3$  and  $\gamma=5/3$ . The terminating curve A is the path of the front of the blast wave. Behind A, there are three families of characteristics: (1) The solid curves are the  $(u)$  characteristics or particle lines; (2) the dashed curves are the  $(u+a)$  characteristics; and (3) the dot-dashed curves are the  $(u-a)$  characteristics.

The authors are grateful to Mr. T. Tucker of Oak Ridge National Laboratory for computational assistance.

This research was supported in part by the Department of Defense Project Themis at Lehigh University under Contract Number DAAD05-69-C-0053 monitored by the Ballistic Research Laboratories, and by the National Aeronautics and Space Administration Grant number NASA-NGL34-002-084.

A portion of this manuscript was completed when one of us (T.S.C.) was visiting Cornell University under the auspices of the Army Research Office, Durham.

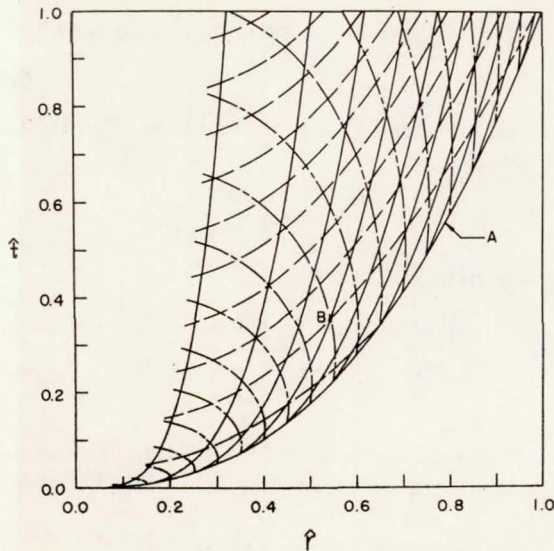


FIG. 1. Curved characteristics behind a strong blast wave for  $n=3$ ,  $\gamma=5/3$ .

\* Permanent address: North Carolina State University, Raleigh, North Carolina 27607.

<sup>1</sup> G. I. Taylor, Report of Civil Defense Research Committee of the Ministry of Home Security, RC-210, 12 (1941); also, Proc. Roy. Soc. (London) A201, 159 (1950).

<sup>2</sup> O. Laporte and T. S. Chang, Ballistic Research Laboratories Technical Report, CAM-110-14 (1971).

- <sup>3</sup> J. von Neumann, *Collected Works of von Neumann*, edited by A. H. Taub (Pergamon, New York, 1963), Vol. 6, p. 219. and *Dimensional Methods in Mechanics* (Academic, New York, 1959), Chap. IV.
- <sup>4</sup> L. I. Sedov, *Prikl. Mat. Mekh.* **10**, 241 (1946); also, *Similarity*
- <sup>5</sup> T. S. Chang and O. Laporte, *Phys. Fluids* **7**, 1225 (1964).



# Comments on "Application of singular eigenfunction expansions to the propagation of periodic disturbances in a radiating grey gas"

T. S. Chang\*

Physics Department, Massachusetts Institute of Technology, Cambridge, Massachusetts 02139

and

K. H. Kim and M. N. Özisik

Departments of Engineering Mechanics and Mechanical and Aerospace Engineering, North Carolina State University, Raleigh, North Carolina 27607

(Received 5 June 1972)

Recently, we have been extending our analysis<sup>1</sup> of sound propagation in dissociative, radiative media to include the effects of scattering. It is of interest to note that the set of pertinent integrodifferential equations can also be solved exactly using the singular eigenfunction expansion technique. For the special case of an ideal, grey, scattering gas, our resulting integral equation for the elementary solutions (in terms of the notations of Cheng and Leonard<sup>2</sup>) becomes

$$\left(1 - \frac{\mu}{\text{Bu}\nu}\right) \Psi_\nu(\mu) = \frac{1}{2} \{ [\bar{g}(\nu; c)]^{-1} + c \} \int_{-1}^1 \Psi_\nu(\mu') d\mu', \quad (1)$$

with

$$\bar{g}(\nu; c) = \frac{[(1-c) + i\beta](\nu^2 - \bar{\xi}^2)}{(\nu^2 + 1/\gamma)(1-c)^2},$$

and

$$\bar{\xi}^2 = -\frac{(1-c)/\gamma + i\beta}{(1-c) + i\beta},$$

where  $c$  denotes the single scattering albedo which is the ratio of the scattering coefficient to the extinction coefficient.

It can be shown that Eq. (1) admits both discrete eigenvalues and a continuous spectrum. The discrete eigenvalues are determined by the dispersion relation

$$\Lambda(\nu) = 1 - \frac{1}{2}(\text{Bu}\nu) \{ [\bar{g}(\nu; c)]^{-1} + c \} \int_{-1}^1 \frac{d\mu}{\text{Bu}\nu - \mu} = 0, \quad (2)$$

which for  $c=0$  corresponds to Eq. (11) of Ref. 2. Using the argument principle we are able to show that Eq. (2) admits either two or four discrete roots in plus-minus complex pairs. In Figs. 1 and 2 we present the discrete eigenvalues of  $\nu_0$  and  $\nu_1$  for  $\text{Bo}$  (Boltzmann number) = 3.23,  $\gamma = 1.4$ , and  $c = 0.2$ . We note that, similar to the results of Cheng and Leonard, there exists a frequency cutoff of the second pair of roots  $\pm\nu_1$  below a critical Bouguer number,  $\text{Bu} \cong 0.08161$ .

We find that it is possible to obtain explicit expressions for the eigenroots of the transcendental equation (2). For example, to determine the explicit expressions for the four roots for  $c=0$  with  $\text{Bu} \geq \text{Bu}_1 = 0.1107$ , we merely calculate  $\Lambda(z)$  and  $X(\pm z)$  at two arbitrary values of  $z = z_{1,2}$  (preferably along the imaginary axis) according to Eqs. (12) and (26) of Ref. 2. Equation (34) of Ref. 2 then provides a pair of coupled polynomial equations for  $\nu_0$  and  $\nu_1$ ,

$$(\nu_0^2 - z_i^2)(\nu_1^2 - z_i^2) = \frac{\Lambda(z_i)(\bar{\xi}^2 - z_i^2)[1 + (1/i\beta)]}{X(z_i)X(-z_i)} \quad \text{for } i=1 \text{ and } 2. \quad (3)$$

Equations (3) can be solved readily to yield the desired explicit expressions for  $\pm\nu_0$  and  $\pm\nu_1$ . Results of some

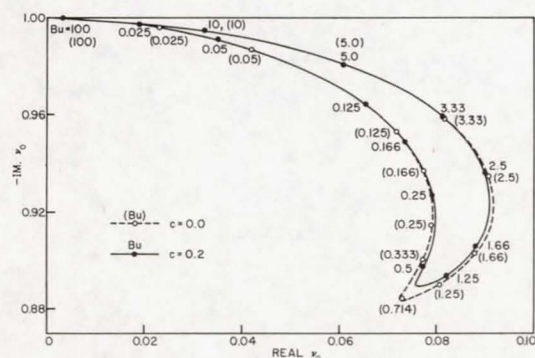


FIG. 1. The first discrete root ( $\nu_0$ ) of  $\Lambda(\nu) = 0$  for  $\text{Bo} = 3.23$ ,  $\gamma = 1.4$ , and  $c = 0.0, 0.2$ .

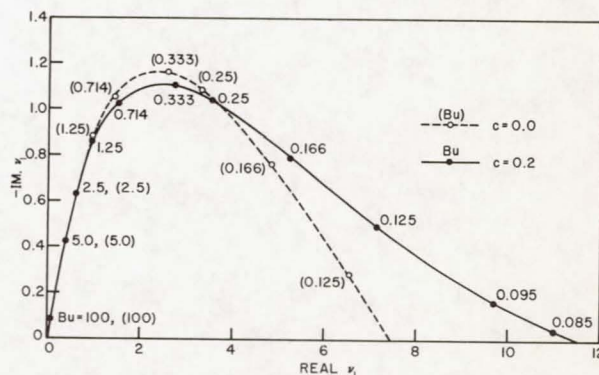


FIG. 2. Second discrete root ( $\nu_1$ ) of  $\Lambda(\nu) = 0$  for  $\text{Bo} = 3.23$ ,  $\gamma = 1.4$ , and  $c = 0.0, 0.2$ .

TABLE I. Discrete eigenvalues for  $Bu=1/6$ ,  $Bo=3.23$ ,  $\gamma=1.4$ , and  $c=0$ .

	a	b	c
$Re\nu_0$	0.07738627380	0.07738629373	0.07738
$Im\nu_0$	-0.9372360013	-0.9372359958	-0.9372
$Re\nu_1$	4.860766870	4.860766867	4.860
$Im\nu_1$	-0.7599477400	-0.7599477363	-0.7599

<sup>a</sup> Calculated using a bisection method where the roots are determined by simultaneous sign changes of the real and imaginary parts of  $\Lambda(z)$ .

<sup>b</sup> Calculated using the explicit expressions.

<sup>c</sup> Values provided by P. Cheng.

sample calculations of the discrete eigenvalues based on this method have been compared with those obtained using the more conventional numerical schemes in Table I. In general, we are able to obtain an accuracy

up to eight significant figures using the explicit expressions.

The authors are indebted to Professor P. Cheng for his assistance and for providing us with the numerical values quoted in Table I.

We are grateful to Dr. E. E. Burniston and Dr. C. E. Siewert for valuable discussion and to Dr. J. T. Kriese for his help in calculating the eigenroots using the explicit scheme.

This research was supported in part by National Aeronautics and Space Administration grant NGL34-002-084 and National Science Foundation grant GU-1590.

\* Permanent address: Riddick Laboratories, North Carolina State University, Raleigh, North Carolina 27607.

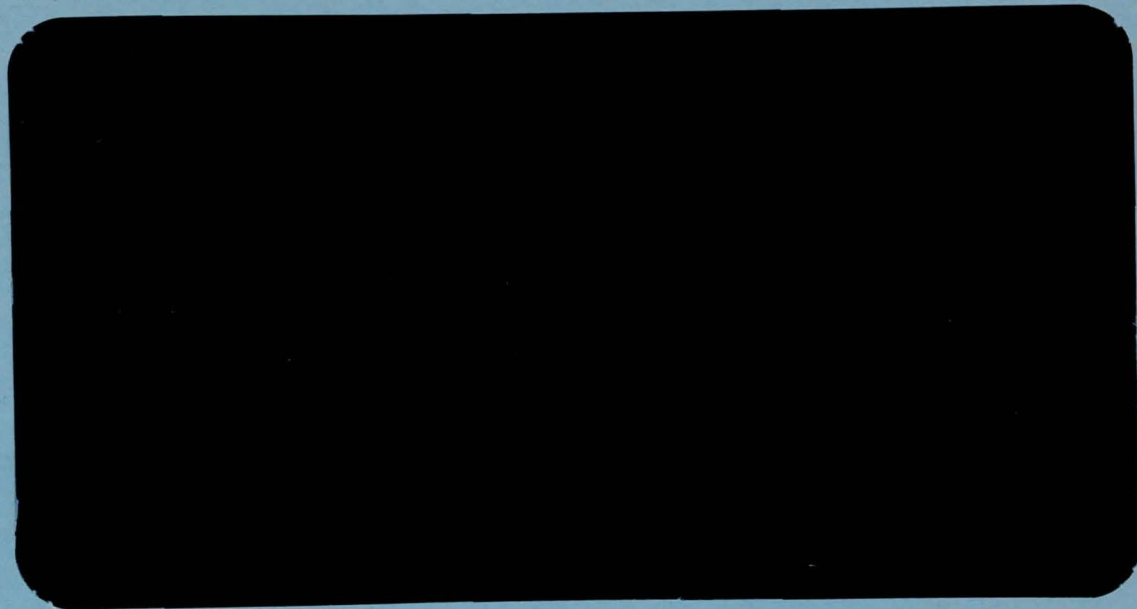
<sup>1</sup> G. K. Lea and T. S. Chang, Phys. Fluids **12**, 983 (1969).

<sup>2</sup> P. Cheng and A. Leonard, Phys. Fluids **14**, 906 (1971).



Reprinted from

75-04939



**PERGAMON PRESS**

OXFORD · NEW YORK



N75-15329

## ELEMENTARY SOLUTIONS OF COUPLED MODEL EQUATIONS IN THE KINETIC THEORY OF GASES

J. T. KRIESE†

Department of Nuclear Engineering, North Carolina State University, Raleigh, North Carolina 27607, U.S.A.

T. S. CHANG‡

Physics Department, Massachusetts Institute of Technology, Cambridge, Massachusetts 02139, U.S.A.

C. E. SIEWERT

Department of Nuclear Engineering, North Carolina State University, Raleigh, North Carolina 27607, U.S.A.

**Abstract**—The method of elementary solutions is employed to solve two coupled integrodifferential equations sufficient for determining temperature-density effects in a linearized BGK model in the kinetic theory of gases.

Full-range completeness and orthogonality theorems are proved for the developed normal modes and the infinite-medium Green's function is constructed as an illustration of the full-range formalism.

The appropriate homogeneous matrix Riemann problem is discussed, and half-range completeness and orthogonality theorems are proved for a certain subset of the normal modes. The required existence and uniqueness theorems relevant to the  $\mathbf{H}$  matrix, basic to the half-range analysis, are proved, and an accurate and efficient computational method is discussed. The half-space temperature-slip problem is solved analytically, and a highly accurate value of the temperature-slip coefficient is reported.

### 1. INTRODUCTION

THERE EXISTS in the kinetic theory of gases a class of one-dimensional problems for which the transverse momentum and heat-transfer effects can be separated by projecting the basic kinetic equation describing the particle distribution function onto certain properly chosen directions in a Hilbert space. The resulting expression describing the heat-transfer and compressibility effects is a vector integrodifferential equation with a matrix kernel similar in form to one studied previously by Bond and Siewert[4] and Burniston and Siewert[5] in connection with the scattering of polarized light. It can be shown that such a vector integrodifferential equation admits a general solution similar to that suggested by Case[7] for scalar transport problems and applied by Cercignani[12] to kinetic equations.

We develop in this paper the elementary solutions to the vector integrodifferential equation basic to a linearized, constant collision frequency (BGK) model suggested by Bhatnagar *et al.*[3] and Welander[29]. The elementary solutions, some of which are generalized functions[14], can be shown to possess rather general full-range and half-range completeness and orthogonality properties. The expansion (or completeness) theorems are proved by reducing a system of singular integral equations to an equivalent matrix Riemann problem and subsequently making use of the theory of Mandžavidze and Hvedelidze[20] and Muskhelishvili[21] to establish the solubility of the resulting equations.

†Present Address: Bettis Atomic Power Laboratory, Westinghouse Electric Corporation, Pittsburgh, Pennsylvania 15122, U.S.A.

‡Permanent Address: Riddick Laboratories, North Carolina State University, Raleigh, North Carolina 27607, U.S.A.

As an application of our established analysis, we construct in this paper the infinite-medium Green's function useful for developing particular solutions to the basic transport equation. We also make use of the half-range expansion theorem to solve the notoriously difficult temperature slip problem considered previously [2, 19, 23, 28, 29] by approximate methods. Our solution permits an accurate computation of the 'temperature slip coefficient' which may be used to evaluate the merits of approximate techniques.

## 2. THE KINETIC MODEL AND LINEARIZATION

Basically, the BGK model is constructed by replacing the collision integral in the Boltzmann equation by a more tractable relaxation term; we therefore write

$$\left[ \frac{\partial}{\partial \tau} + \mathbf{u} \cdot \nabla \right] f(\mathbf{y}, \mathbf{u}, \tau) = \nu [\hat{f}(\mathbf{y}, \mathbf{u}, \tau) - f(\mathbf{y}, \mathbf{u}, \tau)], \quad (2.1)$$

where  $f(\mathbf{y}, \mathbf{u}, \tau)$  is the particle distribution function,  $\mathbf{y}$  is the position vector,  $\mathbf{u}$  is the particle velocity,  $\tau$  is the time, and  $\nu$  is a characteristic collision frequency. To ensure that the model conserves particles, momentum and energy, we require that

$$\int [\hat{f}(\mathbf{y}, \mathbf{u}, \tau) - f(\mathbf{y}, \mathbf{u}, \tau)] \mathbf{U} d^3 u = 0, \quad (2.2)$$

where the integration is to be taken over all velocity space and  $\mathbf{U}$  is a five-element vector with components 1,  $u_1$ ,  $u_2$ ,  $u_3$ , and  $u^2$ , the collisional invariants. Here  $u_\alpha$ ,  $\alpha = 1, 2$ , and 3, and  $u$  are respectively the components and magnitude of  $\mathbf{u}$ . The invariance requirements given by equation (2.2) can be satisfied by choosing

$$\hat{f}(\mathbf{y}, \mathbf{u}, \tau) = n(\mathbf{y}, \tau) \left[ \frac{m}{2\pi k T(\mathbf{y}, \tau)} \right]^{3/2} \exp \left[ -\frac{m |\mathbf{u} - \mathbf{q}(\mathbf{y}, \tau)|^2}{2k T(\mathbf{y}, \tau)} \right], \quad (2.3)$$

the local Maxwellian distribution. Here  $m$  is the particle mass and  $k$  is the Boltzmann constant. In addition

$$\begin{bmatrix} n(\mathbf{y}, \tau) \\ n(\mathbf{y}, \tau) \mathbf{q}(\mathbf{y}, \tau) \\ 3n(\mathbf{y}, \tau) k T(\mathbf{y}, \tau) \end{bmatrix} = \int f(\mathbf{y}, \mathbf{u}, \tau) \begin{bmatrix} 1 \\ \mathbf{u} \\ m |\mathbf{u} - \mathbf{q}(\mathbf{y}, \tau)|^2 \end{bmatrix} d^3 u \quad (2.4)$$

defines the local number density  $n(\mathbf{y}, \tau)$ , the fluid velocity  $\mathbf{q}(\mathbf{y}, \tau)$ , and the absolute temperature  $T(\mathbf{y}, \tau)$ .

It is not difficult to demonstrate that the model given by equations (2.1), (2.3), and (2.4) admits an H theorem, such that

$$\frac{\partial}{\partial \tau} \int f(\mathbf{u}, \tau) \ln f(\mathbf{u}, \tau) d^3 u \leq 0, \quad (2.5)$$

for spatially uniform conditions. Thus the model possesses many of the important properties of the full Boltzmann equation.

Because of equation (2.4), the model is described by a nonlinear functional equation; however, we consider circumstances for which the particle distribution function



$f(\mathbf{y}, \mathbf{u}, \tau)$  differs only slightly from an initial Maxwellian distribution  $f_0(\mathbf{u})$  characterized by a set of constant initial values of the number density  $n_0$ , fluid velocity  $\mathbf{q}_0$ , and temperature  $T_0$ . If we now write

$$f(\mathbf{y}, \mathbf{u}, \tau) = f_0(\mathbf{u}) + f_1(\mathbf{y}, \mathbf{u}, \tau), \quad (2.6)$$

and truncate  $\hat{f}(\mathbf{y}, \mathbf{u}, \tau)$  at the linear terms in a Taylor series expansion about  $f_0$ , we find that equation (2.1) can be approximated by

$$\left[ \frac{\partial}{\partial t} + (\mathbf{c} + \mathbf{v}) \cdot \nabla + 1 \right] \hat{h}(\mathbf{x}, \mathbf{c}, t) = \int \hat{h}(\mathbf{x}, \mathbf{c}', t) K(\mathbf{c}' : \mathbf{c}) e^{-c'^2} d^3 c', \quad (2.7)$$

with

$$K(\mathbf{c}' : \mathbf{c}) = \frac{1}{\pi^{3/2}} \left[ 1 + 2\mathbf{c} \cdot \mathbf{c}' + \frac{2}{3} \left( c^2 - \frac{3}{2} \right) \left( c'^2 - \frac{3}{2} \right) \right], \quad (2.8)$$

and where

$$\mathbf{x} = \nu \left( \frac{m}{2kT_0} \right)^{1/2} \mathbf{y}, \quad t = \nu\tau, \quad (2.9a,b)$$

$$\mathbf{c} = \left( \frac{m}{2kT_0} \right)^{1/2} (\mathbf{u} - \mathbf{q}_0), \quad \mathbf{v} = \left( \frac{m}{2kT_0} \right)^{1/2} \mathbf{q}_0, \quad (2.10a,b)$$

and

$$f_0(\mathbf{c}) \hat{h}(\mathbf{x}, \mathbf{c}, t) = f_1(\mathbf{x}, \mathbf{c}, t). \quad (2.11)$$

A model equation more general than equation (2.7) may be constructed, as suggested by Gross and Jackson[13] and Sirovich[27], by expanding the kernel of a linearized Boltzmann equation in an appropriately chosen complete and orthonormal set of eigenfunctions. We shall, however, restrict our attention to the linearized model described by equation (2.7).

If we now let  $\phi_\alpha(\mathbf{c})$ ,  $\alpha = 1, 2, \dots, 5$ , denote the elements of the vector

$$\boldsymbol{\phi}(\mathbf{c}) = \frac{1}{\pi^{3/4}} \begin{bmatrix} 1 \\ \sqrt{\frac{2}{3}}(c^2 - \frac{3}{2}) \\ \sqrt{2} c_2 \\ \sqrt{2} c_3 \\ \sqrt{2} c_1 \end{bmatrix}, \quad (2.12)$$

where  $c_1$ ,  $c_2$ ,  $c_3$ , and  $c$  are respectively the components and magnitude of  $\mathbf{c}$ , then equation (2.8) can be written as

$$K(\mathbf{c}' : \mathbf{c}) = \tilde{\boldsymbol{\phi}}(\mathbf{c}) \boldsymbol{\phi}(\mathbf{c}'). \quad (2.13)$$

Here the superscript tilde is used to denote the transpose operation. We note that the

elements of  $\phi(\mathbf{c})$  obey the orthonormal conditions

$$(\phi_\alpha, \phi_\beta)_a = \delta_{\alpha,\beta}; \quad \alpha, \beta = 1, 2, \dots, 5, \quad (2.14)$$

in a Hilbert space  $(a)$  of the functions of  $\mathbf{c}$  defined by the inner product

$$(A_1, A_2)_a = \int A_1(\mathbf{c}) A_2(\mathbf{c}) e^{-c^2} d^3c. \quad (2.15)$$

The elements  $\phi_\alpha(\mathbf{c})$  are, of course, related to the collisional invariants which define the  $\mathbf{U}$  vector in equation (2.2), and the orthogonality conditions stated in equation (2.14) are therefore direct consequences of the invariance requirements of equation (2.2).

### 3. THE VECTOR KINETIC EQUATION

As stated in the Introduction, we are primarily interested in steady-state gas-kinetic problems with plane symmetry. Without loss of generality, we set  $\mathbf{q}_0 = \mathbf{0}$ , and thus the steady-state version of equation (2.7) for

$$h(x_1, \mathbf{c}) \stackrel{\Delta}{=} \hat{h}(x_1, \mathbf{c}) - 2\pi^{-3/2} c_1(c_1, \hat{h})_a \quad (3.1)$$

becomes

$$\left[ c_1 \frac{\partial}{\partial x_1} + 1 \right] h(x_1, \mathbf{c}) = \sum_{\alpha=1}^4 \phi_\alpha(\mathbf{c}) (\phi_\alpha, h)_a. \quad (3.2)$$

We now follow Cercignani[12] and consider the functions

$$\begin{aligned} g_1(c_2, c_3) &= \pi^{-1/2}, & g_2(c_2, c_3) &= \pi^{-1/2}(c_2^2 + c_3^2 - 1), \\ g_3(c_2, c_3) &= \left(\frac{\pi}{2}\right)^{-1/2} c_2, & \text{and } g_4(c_2, c_3) &= \left(\frac{\pi}{2}\right)^{-1/2} c_3. \end{aligned} \quad (3.3)$$

It is a straightforward matter to demonstrate that the  $g$  functions given by equations (3.3) satisfy the orthonormal conditions

$$(g_\alpha, g_\beta)_b = \delta_{\alpha,\beta}, \quad \alpha = 1, 2, 3, \text{ and } 4, \quad (3.4)$$

in a subspace  $(b)$  of the functions of  $c_2$  and  $c_3$  defined by the inner product

$$(B_1, B_2)_b = \int_{-\infty}^{\infty} \int_{-\infty}^{\infty} B_1(c_2, c_3) B_2(c_2, c_3) e^{-(c_2^2 + c_3^2)} dc_2 dc_3. \quad (3.5)$$

We now span the Hilbert space  $(b)$  by the subspace  $(c)$  characterized by the  $g_\alpha$ 's and a subspace  $(d)$ , the orthogonal complement to  $(c)$ ; subsequently we expand  $h(x_1, \mathbf{c})$  of equation (3.2) in the manner

$$h(x_1, \mathbf{c}) = \sum_{\alpha=1}^4 \Psi_\alpha(x_1, c_1) g_\alpha(c_2, c_3) + \Psi_5(x_1, \mathbf{c}), \quad (3.6)$$

where  $\Psi_5(x_1, \mathbf{c})$  is the component of  $h(x_1, \mathbf{c})$  belonging to the subspace  $(d)$ . Such an



expansion yields the interesting property that the inner products  $(\Psi_\alpha, \phi_\alpha)_\alpha$ ,  $\alpha = 1, 2, 3$ , and 4, are simply related to the perturbations of the number density, the temperature, and the transverse components of the fluid velocity, respectively.

Substituting equation (3.6) into equation (3.2) and projecting each term onto the appropriate directions of  $g_\alpha$  in the Hilbert space ( $b$ ), we obtain

$$\left[ \mu \frac{\partial}{\partial x} + 1 \right] \hat{\Psi}(x, \mu) = \frac{1}{\sqrt{\pi}} \mathbf{J}(\mu) \int_{-\infty}^{\infty} \tilde{\mathbf{J}}(\mu') \hat{\Psi}(x, \mu') e^{-\mu'^2} d\mu', \quad (3.7)$$

where  $\hat{\Psi}(x, \mu)$  is a four-element vector with components  $\Psi_\alpha(x, \mu)$ ,  $\alpha = 1, 2, \dots, 4$ , and

$$\mathbf{J}(\mu) = \begin{bmatrix} \sqrt{\frac{2}{3}}(\mu^2 - \frac{1}{2}) & 1 & 0 & 0 \\ \sqrt{\frac{2}{3}} & 0 & 0 & 0 \\ 0 & 0 & 1 & 0 \\ 0 & 0 & 0 & 1 \end{bmatrix}. \quad (3.8)$$

For convenience, we have changed the variables  $x_1$  and  $c_1$  to  $x$  and  $\mu$ . We note that the two functions  $\Psi_1(x, \mu)$  and  $\Psi_2(x, \mu)$ , characterizing the perturbations of the number density and temperature respectively, are described by a set of two coupled integrodifferential equations. These two equations are, of course, uncoupled from the functions  $\Psi_3(x, \mu)$  and  $\Psi_4(x, \mu)$  which describe the perturbations of the transverse momenta.

#### 4. ELEMENTARY SOLUTIONS OF THE TWO-VECTOR TRANSPORT EQUATION RELEVANT TO TEMPERATURE-DENSITY EFFECTS

We are interested in the steady-state, gas-kinetic effects of temperature-density variations in plane-parallel media. According to equation (3.7), the relevant coupled equations are

$$\mu \frac{\partial}{\partial x} \Psi(x, \mu) + \Psi(x, \mu) = \frac{1}{\sqrt{\pi}} \mathbf{Q}(\mu) \int_{-\infty}^{\infty} \tilde{\mathbf{Q}}(\mu') \Psi(x, \mu') e^{-\mu'^2} d\mu', \quad (4.1)$$

where  $\tilde{\mathbf{Q}}(\mu)$  is the transpose of

$$\mathbf{Q}(\mu) = \begin{bmatrix} \sqrt{\frac{2}{3}}(\mu^2 - \frac{1}{2}) & 1 \\ \sqrt{\frac{2}{3}} & 0 \end{bmatrix}, \quad (4.2)$$

and  $\Psi_1(x, \mu)$  and  $\Psi_2(x, \mu)$ , which are sufficient to determine the temperature-density effects, are respectively the upper and lower entries in the two-vector  $\Psi(x, \mu)$ . We should like to note that equation (4.1) is quite similar to the equation of transfer used in a related study [4, 5] of the scattering of polarized light.

Following Case [7] who introduced the method of normal modes in regard to one-speed neutron-transport theory, we search for elementary solutions to equation (4.1) of the form

$$\Psi_\epsilon(x, \mu) = \mathbf{F}(\xi, \mu) e^{-x/\xi}, \quad (4.3)$$

where  $\xi$  and  $\mathbf{F}(\xi, \mu)$  are the eigenvalues and eigenvectors to be determined. From equa-

tion (4.1), we obtain

$$(\xi - \mu)F(\xi, \mu) = \frac{1}{\sqrt{\pi}} \xi Q(\mu) M(\xi) \quad (4.4)$$

where the normalization vector  $M(\xi)$  is given by

$$M(\xi) = \int_{-\infty}^{\infty} \tilde{Q}(\mu) F(\xi, \mu) e^{-\mu^2} d\mu. \quad (4.5)$$

Equation (4.4) admits both discrete eigenvalues and a continuous spectrum. We consider first the discrete spectrum:  $\xi = \eta_i$ ,  $\text{Im } \eta_i \neq 0$ , and solve equation (4.4) to obtain

$$F(\eta_i, \mu) = \frac{1}{\sqrt{\pi}} \frac{\eta_i}{\eta_i - \mu} Q(\mu) M(\eta_i), \quad (4.6)$$

where  $\eta_i$  are the zeros (in the complex plane cut along the entire real axis) of the dispersion function

$$\Lambda(z) = \det \Lambda(z). \quad (4.7)$$

Here the dispersion matrix is

$$\Lambda(z) = I + z \int_{-\infty}^{\infty} \Psi(\mu) \frac{d\mu}{\mu - z}, \quad (4.8)$$

with  $I$  denoting the unit matrix and the characteristic matrix given by

$$\Psi(\mu) = \frac{1}{\sqrt{\pi}} \tilde{Q}(\mu) Q(\mu) e^{-\mu^2}. \quad (4.9)$$

Further,  $M(\eta_i)$  is a null vector of  $\Lambda(\eta_i)$  such that

$$\Lambda(\eta_i) M(\eta_i) = 0. \quad (4.10)$$

The argument principle [10] may be used to show that  $\Lambda(z)$  has no zeros in the finite cut plane; however, since  $\Lambda(z) \sim (a/z^4) + \dots$ , for  $|z|$  tending to infinity, we may deduce four 'discrete' solutions to equation (4.1). In the limit  $|z| \rightarrow \infty$ , we obtain from equations (4.6) and (4.10)

$$F_1(\mu) = Q(\mu) \begin{bmatrix} 1 \\ 0 \end{bmatrix} = \sqrt{\frac{2}{3}} \begin{bmatrix} \mu^2 - \frac{1}{2} \\ 1 \end{bmatrix}, \text{ and } F_2(\mu) = Q(\mu) \begin{bmatrix} 0 \\ 1 \end{bmatrix} = \begin{bmatrix} 1 \\ 0 \end{bmatrix}. \quad (4.11)$$

To construct the other two solutions requires a technique discussed by Case and Zweifel [8] to split the degeneracy at infinity. The resulting solutions are

$$\Psi_3(x, \mu) = (\mu - x) \sqrt{\frac{2}{3}} \begin{bmatrix} \mu^2 - \frac{1}{2} \\ 1 \end{bmatrix}, \text{ and } \Psi_4(x, \mu) = (\mu - x) \begin{bmatrix} 1 \\ 0 \end{bmatrix}. \quad (4.12)$$



It should be noted that equations (4.11) are solutions to equation (4.1) and to equation (4.4) in the limit  $|\xi| \rightarrow \infty$ ; whereas, equations (4.12) are solutions only to equation (4.1).

We now consider the continuous spectrum:  $\xi = \eta$ , with  $\text{Im } \eta = 0$ , and the solutions to equation (4.4) are

$$\mathbf{F}(\eta, \mu) = \frac{1}{\sqrt{\pi}} \left[ \eta P v \left( \frac{1}{\eta - \mu} \right) + \lambda^*(\eta) \delta(\eta - \mu) \right] \mathbf{Q}(\mu) \mathbf{M}(\eta), \quad (4.13)$$

where  $Pv(1/x)$  denotes the Cauchy principal-value distribution, and  $\delta(x)$  represents the Dirac delta distribution. Pre-multiplying equation (4.13) by  $\tilde{\mathbf{Q}}(\mu) e^{-\mu^2}$  and integrating over all  $\mu$ , we find

$$[\boldsymbol{\lambda}(\eta) - \lambda^*(\eta) \boldsymbol{\Psi}(\eta)] \mathbf{M}(\eta) = \mathbf{0}, \quad (4.14)$$

where

$$\boldsymbol{\lambda}(\eta) = \mathbf{I} + \eta P \int_{-\infty}^{\infty} \boldsymbol{\Psi}(\mu) \frac{d\mu}{\mu - \eta}; \quad (4.15)$$

and hence from

$$\det [\boldsymbol{\lambda}(\eta) - \lambda^*(\eta) \boldsymbol{\Psi}(\eta)] = 0, \quad (4.16)$$

we obtain a quadratic equation for the function  $\lambda^*(\eta)$ . In general there are two solutions which we label  $\lambda_1^*(\eta)$  and  $\lambda_2^*(\eta)$ , and thus we write the two-fold degenerate continuum solutions as

$$\mathbf{F}_\alpha(\eta, \mu) = \frac{1}{\sqrt{\pi}} \left[ \eta P v \left( \frac{1}{\eta - \mu} \right) + \lambda_\alpha^*(\eta) \delta(\eta - \mu) \right] \mathbf{Q}(\mu) \mathbf{M}_\alpha(\eta), \quad \alpha = 1 \text{ or } 2, \eta \in (-\infty, \infty), \quad (4.17)$$

where the vectors  $\mathbf{M}_\alpha(\eta)$  are to be determined by the corresponding  $\lambda_\alpha^*(\eta)$ , through equation (4.14).

Having established the elementary solutions, we write our general solution to equation (4.1) as

$$\boldsymbol{\Psi}(x, \mu) = \sum_{\alpha=1}^2 A_\alpha \mathbf{F}_\alpha(\mu) + \sum_{\alpha=3}^4 A_\alpha \boldsymbol{\Psi}_\alpha(x, \mu) + \sum_{\alpha=1}^2 \int_{-\infty}^{\infty} A_\alpha(\eta) \mathbf{F}_\alpha(\eta, \mu) e^{-x/\eta} d\eta, \quad (4.18)$$

where the expansion coefficients  $A_\alpha$  and  $A_\alpha(\eta)$  are to be determined once the boundary conditions of a particular problem are specified. Although in general the integral terms in equation (4.18) may diverge for  $x \neq 0$ , this will not be the case when the specific problems of sections 7 and 13 are considered.

## 5. A FULL-RANGE EXPANSION THEOREM

To ensure that the normal modes developed in the previous sections are sufficiently general for full-range,  $\mu \in (-\infty, \infty)$ , boundary-value problems, we should now like to prove a basic result.

**Theorem 1.** *The functions  $\mathbf{F}_1(\mu)$ ,  $\mathbf{F}_2(\mu)$ ,  $\mathbf{F}_3(\mu) = \boldsymbol{\Psi}_3(0, \mu)$ ,  $\mathbf{F}_4(\mu) = \boldsymbol{\Psi}_4(0, \mu)$ , and  $\mathbf{F}_\alpha(\eta, \mu)$ ,  $\alpha = 1$  and  $2$ ,  $\eta \in (-\infty, \infty)$ , form a complete basis set for the expansion of an*

arbitrary two-vector  $\mathbf{I}(\mu)$ , which is Hölder continuous on any open interval of the real axis and, for sufficiently large  $|\mu|$ , satisfies

$$|I_{\alpha}(\mu)| \exp(-|\mu|) < \infty, \alpha = 1 \text{ or } 2,$$

in the sense that

$$\mathbf{I}(\mu) = \sum_{\alpha=1}^4 A_{\alpha} \mathbf{F}_{\alpha}(\mu) + \sum_{\alpha=1}^2 \int_{-\infty}^{\infty} A_{\alpha}(\eta) \mathbf{F}_{\alpha}(\eta, \mu) d\eta, \mu \in (-\infty, \infty). \quad (5.1)$$

To prove the theorem, we shall construct an analytical solution to the above coupled singular integral equations. For the sake of brevity, we write

$$\hat{\mathbf{I}}(\mu) = \mathbf{I}(\mu) - \sum_{\alpha=1}^4 A_{\alpha} \mathbf{F}_{\alpha}(\mu), \quad (5.2)$$

introduce the  $(2 \times 2)$  matrix

$$\mathbf{G}(\eta, \mu) = [\mathbf{F}_1(\eta, \mu) \quad \mathbf{F}_2(\eta, \mu)], \quad (5.3)$$

let  $\mathbf{A}(\eta)$  denote a vector with elements  $A_{\alpha}(\eta)$ ,  $\alpha = 1$  and  $2$ , and thus write equation (5.1) as

$$\hat{\mathbf{I}}(\mu) = \int_{-\infty}^{\infty} \mathbf{G}(\eta, \mu) \mathbf{A}(\eta) d\eta, \mu \in (-\infty, \infty). \quad (5.4)$$

Pre-multiplying equation (4.13) by  $\tilde{\mathbf{Q}}(\mu) e^{-\mu^2}$  and invoking equation (4.14), we obtain

$$\tilde{\mathbf{Q}}(\mu) \mathbf{G}(\eta, \mu) e^{-\mu^2} = \left[ \eta P v \left( \frac{1}{\eta - \mu} \right) \Psi(\mu) + \delta(\eta - \mu) \lambda(\eta) \right] \mathbf{V}(\eta), \quad (5.5)$$

where

$$\mathbf{V}(\eta) = [\mathbf{M}_1(\eta) \quad \mathbf{M}_2(\eta)] \quad (5.6)$$

is the  $(2 \times 2)$  normalization matrix. We now pre-multiply equation (5.4) by  $\tilde{\mathbf{Q}}(\mu) e^{-\mu^2}$ , make use of equation (5.5), and integrate the  $\delta$  term to obtain

$$\tilde{\mathbf{Q}}(\mu) \hat{\mathbf{I}}(\mu) e^{-\mu^2} = \lambda(\mu) \mathbf{B}(\mu) + \Psi(\mu) P \int_{-\infty}^{\infty} \eta \mathbf{B}(\eta) \frac{d\eta}{\eta - \mu}, \quad (5.7)$$

where  $\mathbf{B}(\eta) = \mathbf{V}(\eta) \mathbf{A}(\eta)$ . Equation (5.7) may now be solved explicitly by using the theory of Muskhelishvili [21]. To convert equation (5.7) to a special form of a matrix Riemann problem, we introduce the sectionally holomorphic matrix

$$\mathbf{N}(z) = \frac{1}{2\pi i} \int_{-\infty}^{\infty} \eta \mathbf{B}(\eta) \frac{d\eta}{\eta - z}. \quad (5.8)$$

The boundary values of  $\mathbf{N}(z)$  as  $z$  approaches the real line from above (+) and below



(-) follow from the Plemelj formulae[21]:

$$\pi i [N^+(\mu) + N^-(\mu)] = P \int_{-\infty}^{\infty} \eta B(\eta) \frac{d\eta}{\eta - \mu} \quad (5.9a)$$

and

$$N^+(\mu) - N^-(\mu) = \mu B(\mu). \quad (5.9b)$$

In a similar manner, the boundary values of the dispersion matrix follow from equation (4.8):

$$\Lambda^+(\mu) + \Lambda^-(\mu) = 2\lambda(\mu), \quad (5.10a)$$

and

$$\Lambda^+(\mu) - \Lambda^-(\mu) = 2\pi i \mu \Psi(\mu). \quad (5.10b)$$

Equations (5.9) and (5.10) may now be used in equation (5.7) to yield

$$\mu \tilde{Q}(\mu) \hat{I}(\mu) e^{-\mu^2} = \Lambda^+(\mu) N^+(\mu) - \Lambda^-(\mu) N^-(\mu), \quad (5.11)$$

which can be solved to give

$$N(z) = \Lambda^{-1}(z) \frac{1}{2\pi i} \int_{-\infty}^{\infty} \mu \tilde{Q}(\mu) \hat{I}(\mu) e^{-\mu^2} \frac{d\mu}{\mu - z}. \quad (5.12)$$

We note that for large  $|z|$ ,

$$\Lambda(z) \sim -\frac{1}{z^2} \begin{bmatrix} \frac{7}{6} & \frac{1}{\sqrt[3]{6}} \\ \frac{1}{\sqrt[3]{6}} & \frac{1}{2} \end{bmatrix}, \text{ as } |z| \rightarrow \infty, \quad (5.13)$$

and

$$\Lambda^{-1}(z) \sim -\frac{12}{5} z^2 \begin{bmatrix} \frac{1}{2} & \frac{-1}{\sqrt[3]{6}} \\ \frac{-1}{\sqrt[3]{6}} & \frac{7}{6} \end{bmatrix}, \text{ as } |z| \rightarrow \infty, \quad (5.14)$$

and therefore if the  $N(z)$  as given by equation (5.12) is to vanish when  $|z|$  tends to infinity, as equation (5.8) prescribes, we must impose on the vector  $\hat{I}(\mu)$  the four constraints

$$\int_{-\infty}^{\infty} \mu^\alpha \tilde{Q}(\mu) \hat{I}(\mu) e^{-\mu^2} d\mu = 0, \quad \alpha = 1 \text{ and } 2. \quad (5.15)$$

Recalling equation (5.2) for  $\hat{I}(\mu)$ , we observe that equation (5.15) will be inherently

satisfied if we specify the expansion coefficients  $A_\alpha$ ,  $\alpha = 1, 2, 3$ , and 4, to be

$$\begin{bmatrix} A_1 \\ A_2 \\ A_3 \\ A_4 \end{bmatrix} = \frac{12}{5\sqrt{6}\pi} \begin{bmatrix} -\frac{3}{2}I_{12} + I_{14} + I_{22} \\ \frac{8}{\sqrt{6}}I_{12} - \sqrt{\frac{2}{3}}I_{14} - \sqrt{\frac{2}{3}}I_{22} \\ -\frac{3}{2}I_{11} + I_{13} + I_{21} \\ \frac{8}{\sqrt{6}}I_{11} - \sqrt{\frac{2}{3}}I_{13} - \sqrt{\frac{2}{3}}I_{21} \end{bmatrix}, \quad (5.16)$$

where

$$I_{\alpha\beta} \triangleq \int_{-\infty}^{\infty} \mu^\beta I_\alpha(\mu) e^{-\mu^2} d\mu, \quad \alpha = 1 \text{ or } 2; \beta = 1, 2, 3 \text{ or } 4, \quad (5.17)$$

and  $I_1(\mu)$  and  $I_2(\mu)$  are respectively the upper and lower entries of  $\mathbf{I}(\mu)$ . Theorem 1 is therefore established.

Although we could pursue equations (5.9b) and (5.12) to obtain explicit results for the continuum coefficients  $A_\alpha(\eta)$ ,  $\alpha = 1$  or 2, we prefer to summarize the final expressions in terms of the formalism of the full-range orthogonality relations given in the next section.

## 6. ORTHOGONALITY RELATIONS AND EXPLICIT SOLUTIONS

We should first like to state the general orthogonality relation relevant to all solutions including the special distributions,  $\mathbf{F}(\xi, \mu)$ , of the separated equation (4.4).

*Theorem 2.* All eigenvectors  $\mathbf{F}(\xi, \mu)$  which are solutions of equation (4.4) are orthogonal on the full range,  $\mu \in (-\infty, \infty)$ , in the sense that

$$\int_{-\infty}^{\infty} \tilde{\mathbf{F}}(\xi', \mu) \mathbf{F}(\xi, \mu) e^{-\mu^2} \mu d\mu = 0, \quad \xi' \neq \xi. \quad (6.1)$$

To prove the theorem, equation (4.4) is first pre-multiplied by  $\tilde{\mathbf{F}}(\xi', \mu) e^{-\mu^2}/\xi$ , the transpose of equation (4.4) with  $\xi$  changed to  $\xi'$  is post-multiplied by  $\mathbf{F}(\xi, \mu) e^{-\mu^2}/\xi'$ , and the two resulting equations are then integrated over all  $\mu$  and subtracted one from the other to yield

$$\left( \frac{1}{\xi} - \frac{1}{\xi'} \right) \int_{-\infty}^{\infty} \tilde{\mathbf{F}}(\xi', \mu) \mathbf{F}(\xi, \mu) e^{-\mu^2} \mu d\mu = 0, \quad (6.2)$$

which establishes equation (6.1). Though equation (6.2) is a general statement of full-range orthogonality, it is clear that several additional relations are required here. First of all, since  $\mathbf{F}_1(\mu)$  and  $\mathbf{F}_2(\mu)$  are both associated with  $\xi \rightarrow \infty$ , equation (6.2) does not ensure that they will be mutually orthogonal in the sense of equation (6.1). In addition, the vectors  $\mathbf{F}_3(\mu)$  and  $\mathbf{F}_4(\mu)$ , being derived from the solutions of equation (4.1), rather than equation (4.4), are not included in Theorem 2. However, it can be easily shown that  $\mathbf{F}_1(\mu)$  and  $\mathbf{F}_2(\mu)$  are mutually orthogonal, and, in fact, self-orthogonal; the same is true for  $\mathbf{F}_3(\mu)$  and  $\mathbf{F}_4(\mu)$ . In addition,  $\mathbf{F}_3(\mu)$  and  $\mathbf{F}_4(\mu)$  are orthogonal to the continuum



solutions  $F_1(\eta, \mu)$  and  $F_2(\eta, \mu)$ . We note that  $F_1(\mu)$  and  $F_2(\mu)$  are not orthogonal to  $F_3(\mu)$  and  $F_4(\mu)$ ; however, suitably defined adjoint vectors for these special cases can be developed by employing a Schmidt-type procedure.

Considering first the normalization integrals related to the solutions given by equation (4.13), we find

$$\int_{-\infty}^{\infty} \tilde{F}_{\alpha}(\eta', \mu) F_{\beta}(\eta, \mu) e^{-\mu^2} \mu d\mu = S(\eta) \delta(\eta - \eta') \delta_{\alpha\beta}; \alpha, \beta = 1, 2, \quad (6.3)$$

where

$$S(\eta) = \frac{\eta}{\sqrt{\pi}} [\pi^2 \eta^2 + \lambda_{\alpha}^*(\eta) \lambda_{\beta}^*(\eta)] \tilde{M}_{\alpha}(\eta) \Psi(\eta) M_{\beta}(\eta). \quad (6.4)$$

The Kronecker  $\delta_{\alpha\beta}$  appearing in equation (6.3) should be noted since it ensures that the degenerate continuum solutions given by equation (4.13) are orthogonal even for  $\eta' = \eta$ . To establish equation (6.3) requires the use of the Poincaré-Bertrand formula [21] and

$$[\lambda_{\alpha}^*(\eta) - \lambda_{\beta}^*(\eta)] \tilde{M}_{\alpha}(\eta) \Psi(\eta) M_{\beta}(\eta) = 0, \quad (6.5)$$

a relation which can be deduced from equation (4.14).

Though the representations of the two continuum solutions given by equation (4.13) were convenient for proving the full-range expansion theorem, we choose to make use of more explicit forms for actual applications. We note that equation (4.16) is quadratic in  $\lambda^*(\eta)$ , and thus the two solutions will in general involve radicals. To avoid the cumbersome nature of the ensuing solutions, we prefer the linear combinations

$$\Phi_{\alpha}(\eta, \mu) = T_{\alpha 1}(\eta) F_1(\eta, \mu) + T_{\alpha 2}(\eta) F_2(\eta, \mu), \quad \alpha = 1 \text{ and } 2, \quad (6.6)$$

which, for judicious choices of  $T_{\alpha\beta}(\eta)$ , enable us to deduce the more tractable solutions

$$\Phi_1(\eta, \mu) = \begin{bmatrix} \frac{1}{\sqrt{\pi}} \eta \left( \mu^2 - \frac{1}{2} \right) P v \left( \frac{1}{\eta - \mu} \right) e^{-\eta^2} + \lambda_1(\eta) \delta(\eta - \mu) \\ \frac{1}{\sqrt{\pi}} \eta P v \left( \frac{1}{\eta - \mu} \right) e^{-\eta^2} + \left[ \frac{1}{2} + \lambda_0(\eta) \right] \delta(\eta - \mu) \end{bmatrix} \quad (6.7a)$$

and

$$\Phi_2(\eta, \mu) = \begin{bmatrix} \frac{1}{\sqrt{\pi}} \eta P v \left( \frac{1}{\eta - \mu} \right) e^{-\eta^2} + \lambda_0(\eta) \delta(\eta - \mu) \\ \frac{1}{2} \delta(\eta - \mu) \end{bmatrix}, \quad (6.7b)$$

where

$$\lambda_0(\eta) = 1 + \frac{1}{\sqrt{\pi}} \eta P \int_{-\infty}^{\infty} e^{-\mu^2} \frac{d\mu}{\mu - \eta}, \quad (6.8a)$$

or

$$\lambda_0(\eta) = 1 - 2\eta e^{-\eta^2} \int_0^\eta e^{\mu^2} d\mu, \quad (6.8b)$$

and

$$\lambda_1(\eta) = \frac{1}{2} + (\eta^2 - \frac{1}{2})\lambda_0(\eta). \quad (6.9)$$

We note that equations (6.7) are not mutually orthogonal for  $\eta' = \eta$ ; however, a Schmidt-type procedure may be used here as well. Since our final adjoint vectors follow in a manner analogous to that reported by Siewert and Zweifel[26], we shall simply summarize our conclusions below. For the case of the degenerate continuum modes, we find that the procedure discussed in reference [26] can be used to establish the required adjoint vectors. To unify our notation, we also define

$$\Phi_\alpha(\mu) \triangleq F_\alpha(\mu), \quad \alpha = 1, 2, 3 \text{ and } 4. \quad (6.10)$$

The *orthonormal* full-range adjoint set is given by:

$$X_1(\mu) = \frac{1}{5\sqrt{\pi}}[6\Phi_3(\mu) - 2\sqrt{6}\Phi_4(\mu)], \quad (6.11a)$$

$$X_2(\mu) = \frac{1}{5\sqrt{\pi}}[-2\sqrt{6}\Phi_3(\mu) + 14\Phi_4(\mu)], \quad (6.11b)$$

$$X_3(\mu) = \frac{1}{5\sqrt{\pi}}[6\Phi_1(\mu) - 2\sqrt{6}\Phi_2(\mu)], \quad (6.11c)$$

$$X_4(\mu) = \frac{1}{5\sqrt{\pi}}[-2\sqrt{6}\Phi_1(\mu) + 14\Phi_2(\mu)], \quad (6.11d)$$

$$X_1(\eta, \mu) = \frac{1}{N(\eta)}[N_{22}(\eta)\Phi_1(\eta, \mu) - N_{12}(\eta)\Phi_2(\eta, \mu)], \quad (6.11e)$$

and

$$X_2(\eta, \mu) = \frac{1}{N(\eta)}[N_{11}(\eta)\Phi_2(\eta, \mu) - N_{12}(\eta)\Phi_1(\eta, \mu)], \quad (6.11f)$$

where

$$N_{11}(\eta) = [\lambda_0(\eta) + \frac{1}{2}]^2 + \lambda_1^2(\eta) + \pi\eta^2[(\eta^2 - \frac{1}{2})^2 + 1]e^{-2\eta^2},$$

$$N_{12}(\eta) = \lambda_0(\eta)\lambda_1(\eta) + \frac{1}{2}\lambda_0(\eta) + \frac{1}{4} + \pi\eta^2(\eta^2 - \frac{1}{2})e^{-2\eta^2},$$

$$N_{22}(\eta) = \lambda_0^2(\eta) + \frac{1}{4} + \pi\eta^2e^{-2\eta^2},$$

and

$$N(\eta) = \frac{9}{4}\eta e^{-\eta^2}\Lambda^+(\eta)\Lambda^-(\eta). \quad (6.12)$$



The required orthogonality relations among the full-range basis and adjoint sets are:

$$\int_{-\infty}^{\infty} \tilde{X}_{\alpha}(\mu) \Phi_{\beta}(\mu) e^{-\mu^2} \mu d\mu = \delta_{\alpha,\beta}; \alpha, \beta = 1, 2, 3, \text{ or } 4, \quad (6.13a)$$

$$\int_{-\infty}^{\infty} \tilde{X}_{\alpha}(\mu) \Phi_{\beta}(\eta, \mu) e^{-\mu^2} \mu d\mu = 0; \alpha = 1, 2, 3, \text{ or } 4, \beta = 1 \text{ or } 2, \quad (6.13b)$$

$$\int_{-\infty}^{\infty} \tilde{X}_{\alpha}(\eta', \mu) \Phi_{\beta}(\eta, \mu) e^{-\mu^2} \mu d\mu = \delta(\eta - \eta') \delta_{\alpha,\beta}; \alpha, \beta = 1 \text{ or } 2, \quad (6.13c)$$

$$\int_{-\infty}^{\infty} \tilde{X}_{\alpha}(\eta', \mu) \Phi_{\beta}(\mu) e^{-\mu^2} \mu d\mu = 0; \alpha = 1 \text{ or } 2, \beta = 1, 2, 3, \text{ or } 4. \quad (6.13d)$$

With the formalism thus established, we note that all expansion coefficients in equations of the form

$$I(\mu) = \sum_{\alpha=1}^4 A_{\alpha} \Phi_{\alpha}(\mu) + \sum_{\alpha=1}^2 \int_{-\infty}^{\infty} A_{\alpha}(\eta) \Phi_{\alpha}(\eta, \mu) d\eta, \mu \in (-\infty, \infty), \quad (6.14)$$

may be expressed immediately in terms of inner products:

$$A_{\alpha} = \int_{-\infty}^{\infty} \tilde{X}_{\alpha}(\mu) I(\mu) e^{-\mu^2} \mu d\mu, \alpha = 1, 2, 3 \text{ and } 4, \quad (6.15)$$

and

$$A_{\alpha}(\eta) = \int_{-\infty}^{\infty} \tilde{X}_{\alpha}(\eta, \mu) I(\mu) e^{-\mu^2} \mu d\mu, \alpha = 1 \text{ and } 2. \quad (6.16)$$

## 7. THE INFINITE-MEDIUM GREEN'S FUNCTION

In order to illustrate the use of the elementary solutions of equation (4.1) and the relevant orthogonality relations, we should now like to develop the infinite-medium Green's function. Here we seek a solution to

$$\mu \frac{\partial}{\partial x} \Psi(x, \mu) + \Psi(x, \mu) = \frac{1}{\sqrt{\pi}} Q(\mu) \int_{-\infty}^{\infty} \tilde{Q}(\mu') \Psi(x, \mu') e^{-\mu'^2} d\mu' + S(x_0, \mu_1, \mu_2; x, \mu), \quad (7.1)$$

where

$$S(x_0, \mu_1, \mu_2; x, \mu) = \delta(x - x_0) \begin{bmatrix} \rho_1 & \delta(\mu - \mu_1) \\ \rho_2 & \delta(\mu - \mu_2) \end{bmatrix}. \quad (7.2)$$

Clearly, since the kinetic equation conserves particles, kinetic energy, and momentum, there will exist no bounded (at infinity) solution to equation (7.1); however, the Green's function we develop may be used in the classical manner to construct particular solutions to equation (7.1) for arbitrary inhomogeneous source terms for semi-infinite or finite media. As discussed by Case and Zweifel [8], we neglect the inhomogeneous term

in equation (7.1) and require the solution to the resulting homogeneous equation to satisfy the 'jump' boundary condition

$$\mu [\Psi(x_0, \mu_1, \mu_2; x_0^+, \mu) - \Psi(x_0, \mu_1, \mu_2; x_0^-, \mu)] = \begin{bmatrix} \rho_1 \delta(\mu - \mu_1) \\ \rho_2 \delta(\mu - \mu_2) \end{bmatrix}, \quad \mu \in (-\infty, \infty), \quad (7.3)$$

where the argument list has been extended to include the parameters  $x_0$ ,  $\mu_1$ , and  $\mu_2$ . We therefore write the desired solution as

$$\Psi(x_0, \mu_1, \mu_2; x, \mu) = \sum_{\alpha=1}^2 A_\alpha \Phi_\alpha(\mu) + \sum_{\alpha=1}^2 \int_0^\infty A_\alpha(\eta) \Phi_\alpha(\eta, \mu) e^{-(x-x_0)/\eta} d\eta, \quad (7.4a)$$

and for  $x > x_0$ ,

$$\Psi(x_0, \mu_1, \mu_2; x, \mu) = - \sum_{\alpha=3}^4 A_\alpha \Psi_\alpha(x - x_0, \mu) - \sum_{\alpha=1}^2 \int_{-\infty}^0 A_\alpha(\eta) \Phi_\alpha(\eta, \mu) e^{-(x-x_0)/\eta} d\eta \quad (7.4b)$$

for  $x < x_0$ .

Substitution of equations (7.4) into equation (7.3) yields the full-range expansion

$$\begin{bmatrix} \rho_1 \delta(\mu - \mu_1) \\ \rho_2 \delta(\mu - \mu_2) \end{bmatrix} = \mu \left\{ \sum_{\alpha=1}^4 A_\alpha \Phi_\alpha(\mu) + \sum_{\alpha=1}^2 \int_{-\infty}^\infty A_\alpha(\eta) \Phi_\alpha(\eta, \mu) d\eta \right\}, \quad \mu \in (-\infty, \infty). \quad (7.5)$$

Though the left-hand side of equation (7.5) certainly is not a Hölder function, Case and Zweifel[8] have concluded that expansion theorems similar to our Theorem 1 remain valid formally even for this type of delta distribution. We therefore pre-multiply equation (7.5) by  $\tilde{X}_\alpha(\mu) e^{-\mu^2}$ ,  $\alpha = 1, 2, 3$ , or 4 and  $\tilde{X}_\alpha(\eta', \mu) e^{-\mu^2}$ ,  $\alpha = 1$  or 2, and integrate over all  $\mu$  to find, after invoking equation (6.13),

$$A_\alpha = \rho_1 X_{\alpha 1}(\mu_1) e^{-\mu_1^2} + \rho_2 X_{\alpha 2}(\mu_2) e^{-\mu_2^2}, \quad \alpha = 1, 2, 3, \text{ and } 4, \quad (7.6a)$$

and

$$A_\alpha(\eta) = \rho_1 X_{\alpha 1}(\eta, \mu_1) e^{-\mu_1^2} + \rho_2 X_{\alpha 2}(\eta, \mu_2) e^{-\mu_2^2}, \quad \alpha = 1 \text{ and } 2, \quad (7.6b)$$

where the subscripts 1 and 2 are used to denote the upper and lower elements of the  $\mathbf{X}$  vectors. Since all expansion coefficients required in equations (7.4) are given by equations (7.6), the infinite-medium Green's function is established.

## 8. A HALF-RANGE EXPANSION THEOREM

Having developed in sections 5 and 6 the necessary completeness and orthogonality properties of our normal modes, we should now like to discuss the analysis required for the considerably more interesting problems defined by half-range,  $\mu \in (0, \infty)$ , boundary conditions. The following theorem states the very important half-range expansion properties basic to a certain subset of our derived elementary solutions.

*Theorem 3. The functions  $F_1(\mu)$ ,  $F_2(\mu)$  and  $F_\alpha(\eta, \mu)$ ,  $\alpha = 1$  and 2,  $\eta \in (0, \infty)$ , form a complete basis set for the expansion of an arbitrary two-vector  $\mathbf{I}(\mu)$  which is Hölder*



continuous on any open interval of the positive real axis and, for sufficiently large  $|\mu|$ , satisfies

$$|I_\alpha(\mu)| \exp(-|\mu|) < \infty, \alpha = 1 \text{ or } 2,$$

in the sense that

$$I(\mu) = \sum_{\alpha=1}^2 A_\alpha F_\alpha(\mu) + \sum_{\alpha=1}^2 \int_0^\infty A_\alpha(\eta) F_\alpha(\eta, \mu) d\eta, \mu \in (0, \infty). \quad (8.1)$$

To prove this theorem, we premultiply equation (8.1) by  $e^{-\mu^2} \tilde{Q}(\mu)$ , integrate the  $\delta$  term and use equations (4.13) and (4.14) to obtain

$$\tilde{Q}(\mu) \hat{I}(\mu) e^{-\mu^2} = \Lambda(\mu) B(\mu) + \Psi(\mu) P \int_0^\infty \eta B(\eta) \frac{d\eta}{\eta - \mu}, \mu \in (0, \infty), \quad (8.2)$$

where

$$\hat{I}(\mu) = I(\mu) - \sum_{\alpha=1}^2 A_\alpha F_\alpha(\mu) \quad (8.3)$$

and

$$B(\eta) = V(\eta) A(\eta). \quad (8.4)$$

In addition,  $V(\eta)$  is given by equation (5.6) and the unknown  $A(\eta)$  has elements  $A_1(\eta)$  and  $A_2(\eta)$ . In a manner similar to that used to prove Theorem 1, we now introduce

$$N(z) = \frac{1}{2\pi i} \int_0^\infty \eta B(\eta) \frac{d\eta}{\eta - z}. \quad (8.5)$$

The  $N$  matrix is clearly analytic in the complex plane cut along the positive real axis. Further, the Plemelj formulae[21] can be used, with equation (8.5), to show that the boundary values of  $N(z)$  satisfy

$$\pi i [N^+(\mu) + N^-(\mu)] = P \int_0^\infty \eta B(\eta) \frac{d\eta}{\eta - \mu} \quad (8.6a)$$

and

$$N^+(\mu) - N^-(\mu) = \mu B(\mu). \quad (8.6b)$$

Equations (8.6) can now be used, along with equations (5.10), to express equation (8.2) in the form

$$\mu \tilde{Q}(\mu) \hat{I}(\mu) e^{-\mu^2} = \Lambda^+(\mu) N^+(\mu) - \Lambda^-(\mu) N^-(\mu), \mu \in (0, \infty). \quad (8.7)$$

If we now let  $\tilde{X}(z)$  denote a canonical (non-singular in the finite plane) solution to the homogeneous Riemann problem defined by

$$\tilde{X}^+(\mu) = G(\mu) \tilde{X}^-(\mu), \mu \in (0, \infty), \quad (8.8a)$$

where

$$\mathbf{G}(\mu) = \Lambda^+(\mu)[\Lambda^-(\mu)]^{-1}, \quad (8.8b)$$

then equation (8.7) can be solved immediately to yield

$$\mathbf{N}(z) = \mathbf{X}^{-1}(z) \left[ \frac{1}{2\pi i} \int_0^\infty \Gamma(\mu) \tilde{\mathbf{Q}}(\mu) \hat{\mathbf{I}}(\mu) e^{-\mu^2} \frac{d\mu}{\mu - z} + \mathbf{P}(z) \right]. \quad (8.9)$$

Here,  $\mathbf{P}(z)$  is a matrix of polynomials, and

$$\Gamma(\mu) = \mu \mathbf{X}^+(\mu) [\Lambda^+(\mu)]^{-1}. \quad (8.10)$$

Since the  $\mathbf{G}$  matrix given by equation (8.8b) is continuous for  $\mu \in [0, \infty)$ ,  $\mathbf{G}(0) = \mathbf{I}$  and  $\mathbf{G}(\mu) \rightarrow \mathbf{I}$  as  $\mu \rightarrow \infty$ , the analysis of Mandžavidze and Hvedelidze [20] can be used, after an elementary transformation of variables, to ensure the existence of a canonical solution to the Riemann problem defined by equation (8.8a). In section 9 we argue that the partial indices  $\kappa_1$  and  $\kappa_2$  associated with our canonical solution  $\tilde{\mathbf{X}}(z)$  are

$$\kappa_1 = \kappa_2 = 1, \quad (8.11)$$

and thus if we allow our canonical matrix  $\tilde{\mathbf{X}}(z)$  to be of normal form at infinity [21], we may write

$$\lim_{z \rightarrow \infty} z \mathbf{X}(z) = \mathbf{\Delta}, \quad (8.12)$$

where  $\mathbf{\Delta}$  is nonsingular and bounded.

From the defining equation (8.5), we observe that  $z \mathbf{N}(z)$  must be bounded as  $|z| \rightarrow \infty$ , and thus from equation (8.9) we conclude that

$$\lim_{|z| \rightarrow \infty} z \mathbf{\Delta}^{-1} \left[ \frac{1}{2\pi i} \int_0^\infty \Gamma(\mu) \tilde{\mathbf{Q}}(\mu) \hat{\mathbf{I}}(\mu) e^{-\mu^2} d\mu + z \mathbf{P}(z) \right] < \infty; \quad (8.13)$$

we must therefore set  $\mathbf{P}(z) = \mathbf{0}$  and, in addition, require that

$$\int_0^\infty \Gamma(\mu) \tilde{\mathbf{Q}}(\mu) \hat{\mathbf{I}}(\mu) e^{-\mu^2} d\mu = \mathbf{0}. \quad (8.14)$$

Equation (8.14) is, of course, not satisfied by all  $\hat{\mathbf{I}}(\mu)$ , but recalling equation (8.3), we conclude that choosing the discrete expansion coefficients to be solutions of

$$\int_0^\infty \Gamma(\mu) \Psi(\mu) d\mu \begin{bmatrix} A_1 \\ A_2 \end{bmatrix} = \frac{1}{\sqrt{\pi}} \int_0^\infty \Gamma(\mu) \tilde{\mathbf{Q}}(\mu) \mathbf{I}(\mu) e^{-\mu^2} d\mu \quad (8.15)$$

renders equation (8.1) valid for all appropriate  $\mathbf{I}(\mu)$ . The matrix in equation (8.15) whose inverse is required to obtain  $A_1$  and  $A_2$  can be shown to be non-singular by making use of a Cauchy integral representation of  $\mathbf{X}(z)$ . The theorem is therefore proved.



Though, as for the full-range case, we could pursue this completeness proof to construct the continuum expansion coefficients  $A(\eta)$ ,  $\eta \in (0, \infty)$ , we find it more convenient to express the final results in terms of half-range orthogonality relations.

#### 9. A PROOF REGARDING THE PARTIAL INDICES OF THE RIEMANN PROBLEM

The proof of the half-range expansion theorem given in section 8 is based on the proposition that the partial indices  $\kappa_1$  and  $\kappa_2$  are both non-negative. In fact, equation (8.13) is valid only if the partial indices are given by  $\kappa_1 = \kappa_2 = 1$ . In this section we develop the required proof that  $\kappa_1 = \kappa_2 = 1$ .

We consider then the homogeneous matrix Riemann problem defined by

$$\Phi^+(\mu) = G(\mu)\Phi^-(\mu), \mu \in [0, \infty), \quad (9.1)$$

where

$$G(\mu) = \Lambda^+(\mu)[\Lambda^-(\mu)]^{-1}, \mu \in [0, \infty). \quad (9.2)$$

Here we seek a matrix  $\Phi(z)$  analytic in the plane cut along the positive real axis, non-singular in the finite plane, and with boundary values  $\Phi^\pm(\mu)$  which satisfy equation (9.1).

Since  $G(0) = I$  and  $G(\mu) \rightarrow I$  in the limit as  $\mu \rightarrow \infty$ , we can define  $G(\mu) = I$  on the entire negative real axis and thus consider equation (9.1) for  $\mu \in (-\infty, \infty)$ . To make use of the results developed by Mandžavidze and Hvedelidze[20], valid for closed contours, we make the change of variables

$$\zeta = \frac{i-z}{i+z} \quad (9.3)$$

which maps the upper half of the  $z$  plane into the interior of the unit circle in the  $\zeta$ -plane. We note that the positive (negative) real axis maps into  $|\zeta| = 1$ ,  $\text{Im } \zeta > (<) 0$ . The existence of a solution to the Riemann problem in the  $\zeta$  plane follows from the theory of Mandžavidze and Hvedelidze[20], since the resulting  $G$  matrix is continuous on the unit circle, and  $\Phi(z)$ , the canonical solution in the  $z$ -plane, is the image of the solution in the  $\zeta$  plane postmultiplied by an appropriate matrix of rational functions.

It can be demonstrated[5] that the  $\Lambda$  matrix can be factored as

$$\Lambda(z) = \Phi(z)\mathcal{P}(z)\tilde{\Phi}(-z) \quad (9.4)$$

where  $\Phi(z)$  is any canonical solution (of ordered normal form at infinity) to equation (9.1) and  $\mathcal{P}(z)$  is a matrix of polynomials, which depends on the particular choice for  $\Phi(z)$ .

The fact that  $\overline{G(\mu)} = [G(\mu)]^{-1}$ , where the bar indicates the complex conjugate, enables us to extend the results of Siewert and Burniston's[25] Theorem II to the Riemann problem defined by equation (9.1):

*Theorem 4. There exists at least one canonical matrix  $\Phi_1(z)$  of ordered normal form at infinity for the Riemann problem defined by equation (9.1) such that  $\overline{\Phi_1(\bar{z})} = \Phi_1(z)$ .*

Since the proof of Theorem 4 follows very closely one previously reported [25], it will not be given here.

If we use  $\Phi_1(z)$  in the factorization of  $\Lambda(z)$ , the resulting polynomial matrix  $\mathcal{P}(z)$  is such that  $\mathcal{P}(z) = \tilde{\mathcal{P}}(-z)$  and  $\mathcal{P}(z) = \overline{\mathcal{P}(\bar{z})}$ , since  $\Lambda(z) = \tilde{\Lambda}(z) = \Lambda(-z)$  and  $\Lambda(z) = \overline{\Lambda(\bar{z})}$ .

By definition [21], a canonical solution of ordered normal form at infinity is such that

$$\lim_{|z| \rightarrow \infty} \Phi_1(z) \begin{bmatrix} z^{\kappa_1} & 0 \\ 0 & z^{\kappa_2} \end{bmatrix} = \mathbf{K}, \det \mathbf{K} \neq 0, \quad (9.5)$$

where  $\kappa_1$  and  $\kappa_2 \geq \kappa_1$  are the partial indices. Furthermore the sum of  $\kappa_1$  and  $\kappa_2$  must yield the total index  $\kappa$ , which in the manner of Muskelishvili [21] can be computed directly once the  $\mathbf{G}$  matrix and the appropriate contour are specified. For this problem, we find

$$\kappa_1 + \kappa_2 = \kappa = 2. \quad (9.6)$$

If we now evaluate equation (9.4), for  $\Phi(z) = \Phi_1(z)$  at  $z = 0$ , we obtain

$$\mathcal{P}(0) = \Phi_1^{-1}(0) \tilde{\Phi}_1^{-1}(0), \quad (9.7)$$

and since  $\Phi_1(0)$  is real (recall that  $\Phi_1(z) = \overline{\Phi_1(\bar{z})}$ ), we conclude from equation (9.7) that  $\mathcal{P}_{11}(0) \neq 0$  and  $\mathcal{P}_{22}(0) \neq 0$ . Again from equation (9.4), for  $\Phi(z) = \Phi_1(z)$ , we can write, after using equation (5.13),

$$\mathcal{P}(z) \rightarrow -\frac{1}{z^2} \begin{bmatrix} z^{\kappa_1} & 0 \\ 0 & z^{\kappa_2} \end{bmatrix} \mathbf{K}^{-1} \begin{bmatrix} \frac{7}{6} & \frac{\sqrt{6}}{6} \\ \frac{\sqrt{6}}{6} & \frac{1}{2} \end{bmatrix} \tilde{\mathbf{K}}^{-1} \begin{bmatrix} (-z)^{\kappa_1} & 0 \\ 0 & (-z)^{\kappa_2} \end{bmatrix}, \quad (9.8)$$

$$\text{as } |z| \rightarrow \infty,$$

from which it follows, since  $\mathbf{K}$  is real, that

$$\kappa_1 = \kappa_2 = 1. \quad (9.9)$$

It is clear, since  $\Phi_1(z)$  is a canonical solution of ordered normal form at infinity, and since  $\kappa_1 = \kappa_2 = 1$ , that

$$\Phi_0(z) \triangleq \Phi_1(z) \mathbf{K}^{-1} \sqrt{2} \begin{bmatrix} \sqrt{\frac{3}{12}} & \frac{\sqrt{6}}{6} \\ 0 & \frac{1}{2} \end{bmatrix} \quad (9.10)$$

is also a canonical solution of ordered normal form at infinity and is such that  $\Phi_0(z) = \overline{\Phi_0(\bar{z})}$ . In view of equations (9.8) and (9.10), we can therefore write equation (9.4) as

$$\Lambda(z) = \Phi_0(z) \tilde{\Phi}_0(-z), \quad (9.11)$$

where

$$\Phi_0(0) \tilde{\Phi}_0(0) = \mathbf{I} \quad (9.12a)$$



and

$$\lim_{|z| \rightarrow \infty} z \Phi_0(z) = \sqrt{2} \begin{bmatrix} \sqrt{\frac{5}{12}} & \frac{\sqrt{6}}{6} \\ 0 & \frac{1}{2} \end{bmatrix}. \quad (9.12b)$$

We note that Cercignani [11] has reported a factorization in the spirit of our equation (9.11). We have been unable, however, to justify some of Cercignani's results [11; pp. 84–85] since, for example, upon 'taking' determinants of his equation (311) we find an inconsistency in the number of poles on the two sides of the equality sign. We have found that the extension of scalar results to the case of matrix Riemann problems, in general, does not follow immediately [6].

#### 10. HALF-RANGE ORTHOGONALITY AND NORMALIZATION INTEGRALS

The half-range orthogonality relations developed by Kuščer, McCormick, and Summerfield [18] for the elementary solutions of the one-speed neutron-transport equation have proved to be useful for establishing concisely the solutions to a scalar singular integral equation somewhat analogous to equation (8.1). We should thus like to prove, in a manner similar to that reported by Siewert [24] for an equation of transfer basic to the scattering of polarized light, the following theorem concerning the half-range orthogonality properties of a subset of our developed normal modes.

*Theorem 5. The eigenvectors  $F_1(\mu)$ ,  $F_2(\mu)$ ,  $F_1(\eta, \mu)$ , and  $F_2(\eta, \mu)$ ,  $\eta \in (0, \infty)$ , are orthogonal to the related set  $G_1(\mu)$ ,  $G_2(\mu)$ ,  $G_1(\eta, \mu)$  and  $G_2(\eta, \mu)$ ,  $\eta \in (0, \infty)$ , on the half-range,  $\mu \in (0, \infty)$ , in the sense that*

$$\int_0^\infty \tilde{G}(\xi', \mu) F(\xi, \mu) e^{-\mu^2} \mu d\mu = 0, \quad \xi \neq \xi'; \quad \xi, \xi' = \infty \text{ or } \in (0, \infty). \quad (10.1)$$

Here  $F(\xi, \mu)$ ,  $\xi = \infty$  or  $\in (0, \infty)$ , denotes any of the eigenvectors  $F_1(\mu)$ ,  $F_2(\mu)$ , for  $\xi = \infty$ , or  $F_1(\eta, \mu)$ ,  $F_2(\eta, \mu)$ , for  $\eta \in (0, \infty)$ . In a similar manner,  $G(\xi, \mu)$ , represents either

$$G_\alpha(\mu) = Q(\mu)H(\mu)H^{-1}Q^{-1}(\mu)F_\alpha(\mu), \quad \alpha = 1 \text{ or } 2, \quad (10.2a)$$

or

$$G_\alpha(\eta, \mu) = Q(\mu)H(\mu)H^{-1}(\eta)Q^{-1}(\mu)F_\alpha(\eta, \mu), \quad \eta \in (0, \infty), \quad \alpha = 1 \text{ or } 2. \quad (10.2b)$$

In addition

$$\tilde{H}_1 = \int_0^\infty \tilde{H}(\mu)\Psi(\mu) \mu d\mu \quad (10.3)$$

and  $H(\mu)$  is the  $H$  matrix basic to our half-range analysis. In section 11 we prove the existence of a unique solution to the system of singular integral equations

$$\tilde{H}(\mu)\lambda(\mu) = I + \mu P \int_0^\infty \tilde{H}(\eta)\Psi(\eta) \frac{d\eta}{\eta - \mu}, \quad \mu \in (0, \infty), \quad (10.4a)$$

plus the constraint

$$\int_0^\infty \tilde{\mathbf{H}}(\mu) \boldsymbol{\Psi}(\mu) d\mu = \mathbf{I}, \quad (10.4b)$$

which we take to specify  $\mathbf{H}(\mu)$ . As shall be shown,  $\mathbf{H}(\mu)$  can be expressed in terms of  $\boldsymbol{\Phi}_0(z)$ , our canonical solution, of ordered normal form at infinity, of the matrix Riemann problem defined by equation (9.1); that is

$$\mathbf{H}(\mu) = \tilde{\boldsymbol{\Phi}}_0^{-1}(-\mu) \tilde{\boldsymbol{\Phi}}_0(0), \quad (10.5)$$

which can be extended to the complex plane cut along the negative real axis to yield a factorization of  $\Lambda(z)$ :

$$\Lambda(z) = \tilde{\mathbf{H}}^{-1}(z) \mathbf{H}^{-1}(-z). \quad (10.6)$$

To establish our Theorem 5, we first pre-multiply equation (4.4) by  $\tilde{\mathbf{G}}(\xi', \mu) e^{-\mu^2}/\xi$ , we then post-multiply the transpose of equation (4.4), having changed  $\xi$  to  $\xi'$ , by  $\tilde{\mathbf{Q}}^{-1}(\mu) \tilde{\mathbf{H}}^{-1}(\xi') \tilde{\mathbf{H}}(\mu) \tilde{\mathbf{Q}}(\mu) \mathbf{F}(\xi, \mu) \exp(-\mu^2)/\xi'$ , integrate the two resulting equations over  $\mu$  from 0 to  $\infty$  and subtract the two equations, one from the other, to obtain

$$\left(\frac{1}{\xi} - \frac{1}{\xi'}\right) \int_0^\infty \tilde{\mathbf{G}}(\xi', \mu) \mathbf{F}(\xi, \mu) e^{-\mu^2} \mu d\mu = \frac{1}{\sqrt{\pi}} [K_1(\xi', \xi) - K_2(\xi', \xi)], \quad \xi \text{ and } \xi' > 0. \quad (10.7)$$

Here

$$K_1(\xi', \xi) = \tilde{\mathbf{M}}(\xi') \tilde{\mathbf{H}}^{-1}(\xi') \int_0^\infty \tilde{\mathbf{H}}(\mu) \tilde{\mathbf{Q}}(\mu) \mathbf{F}(\xi, \mu) e^{-\mu^2} d\mu \quad (10.8)$$

and

$$K_2(\xi', \xi) = \int_0^\infty \tilde{\mathbf{F}}(\xi', \mu) \tilde{\mathbf{Q}}^{-1}(\mu) \tilde{\mathbf{H}}^{-1}(\xi') \tilde{\mathbf{H}}(\mu) \tilde{\mathbf{Q}}(\mu) \mathbf{Q}(\mu) e^{-\mu^2} d\mu \mathbf{M}(\xi). \quad (10.9)$$

If now, in the manner similar to that previously reported [24], we make use of equations (4.5), (4.11), (4.13), (4.14) and (10.4) to evaluate equations (10.8) and (10.9) for all appropriate  $\xi$  and  $\xi'$ , we find

$$K_1(\xi', \xi) = K_2(\xi', \xi); \quad \xi' \in (0, \infty), \quad \xi = \infty \text{ or } \in (0, \infty), \quad (10.10)$$

and from equation (10.7) we obtain

$$\left(\frac{1}{\xi} - \frac{1}{\xi'}\right) \int_0^\infty \tilde{\mathbf{G}}(\xi', \mu) \mathbf{F}(\xi, \mu) e^{-\mu^2} \mu d\mu = 0; \quad \xi, \xi' > 0, \quad (10.11)$$

which proves the theorem. We have only established equation (10.11) formally for  $\xi' \neq \infty$ . However, considering that case separately, we do find that  $\mathbf{G}_\alpha(\mu)$ ,  $\alpha = 1$  or  $2$ , is orthogonal to  $\mathbf{F}(\xi, \mu)$  in the sense of Theorem 5. Of course, since  $\mathbf{F}_1(\mu)$  and  $\mathbf{F}_2(\mu)$  both correspond to the eigenvalue  $\xi = \infty$ , equation (10.1) does not ensure that the inner product, in the sense of Theorem 5, of  $\mathbf{G}_1(\mu)$  with  $\mathbf{F}_2(\mu)$  and  $\mathbf{G}_2(\mu)$  with  $\mathbf{F}_1(\mu)$  is zero.



However, for this special case we have carried out the algebra prescribed by equation (10.1) to show explicitly that

$$\int_0^\infty \tilde{G}_\alpha(\mu) F_\beta(\mu) e^{-\mu^2} \mu d\mu = 0, \alpha \neq \beta, \quad (10.12)$$

so that all of the half-range eigenvectors are orthogonal in the manner of Theorem 5.

Having established the required half-range orthogonality results, we should now like to consider again the normalized solutions given by equation (6.7) in order to present our half-range normalization integrals in a form analogous to that used for the full-range theory. We consider then the half-range adjoint set

$$\Theta_\alpha(\mu) = \frac{1}{\sqrt{\pi}} Q(\mu) H(\mu) H^{-1} Q^{-1}(\mu) \Phi_\alpha(\mu), \alpha = 1 \text{ and } 2, \quad (10.13a)$$

and

$$\Theta_\alpha(\eta, \mu) = Q(\mu) H(\mu) H^{-1}(\eta) Q^{-1}(\mu) X_\alpha(\eta, \mu), \eta \in (0, \infty), \alpha = 1 \text{ and } 2, \quad (10.13b)$$

where the vectors  $X_\alpha(\eta, \mu)$ ,  $\alpha = 1$  and  $2$ , are given by equations (6.11e) and (6.11f); we can therefore summarize our results in the manner

$$\int_0^\infty \tilde{\Theta}_\alpha(\mu) \Phi_\beta(\mu) e^{-\mu^2} \mu d\mu = \delta_{\alpha\beta}; \alpha, \beta = 1 \text{ or } 2, \quad (10.14a)$$

$$\int_0^\infty \tilde{\Theta}_\alpha(\mu) \Phi_\beta(\eta, \mu) e^{-\mu^2} \mu d\mu = 0, \eta \in (0, \infty); \alpha, \beta = 1 \text{ or } 2, \quad (10.14b)$$

$$\int_0^\infty \tilde{\Theta}_\alpha(\eta', \mu) \Phi_\beta(\eta, \mu) e^{-\mu^2} \mu d\mu = \delta_{\alpha\beta} \delta(\eta - \eta'); \eta, \eta' \in (0, \infty), \alpha, \beta = 1 \text{ or } 2, \quad (10.14c)$$

and

$$\int_0^\infty \tilde{\Theta}_\alpha(\eta, \mu) \Phi_\beta(\mu) e^{-\mu^2} \mu d\mu = 0; \eta \in (0, \infty), \alpha, \beta = 1 \text{ or } 2. \quad (10.14d)$$

With the half-range formalism thus established, we note that the solutions for all expansion coefficients in equations of the form

$$I(\mu) = \sum_{\alpha=1}^2 A_\alpha F_\alpha(\mu) + \sum_{\alpha=1}^2 \int_0^\infty A_\alpha(\eta) F_\alpha(\eta, \mu) d\eta, \mu \in (0, \infty), \quad (10.15)$$

can be expressed concisely as

$$A_\alpha = \int_0^\infty \tilde{\Theta}_\alpha(\mu) I(\mu) e^{-\mu^2} \mu d\mu, \alpha = 1 \text{ and } 2, \quad (10.16a)$$

and

$$A_\alpha(\eta) = \int_0^\infty \tilde{\Theta}_\alpha(\eta, \mu) I(\mu) e^{-\mu^2} \mu d\mu, \alpha = 1 \text{ and } 2. \quad (10.16b)$$

We note that a set of integrals of the form

$$T(\xi', \xi) = \int_0^\infty \tilde{\Theta}(\xi', \mu) \Phi(-\xi, \mu) e^{-\mu^2} \mu d\mu, \quad \xi \text{ and } \xi' > 0, \quad (10.17)$$

has been evaluated and is listed elsewhere [16].

## 11. EXISTENCE AND UNIQUENESS OF THE $\mathbf{H}$ MATRIX

We first wish to prove

*Theorem 6. The equations*

$$\tilde{\mathbf{H}}(\mu) \boldsymbol{\lambda}(\mu) = \mathbf{I} + \mu P \int_0^\infty \tilde{\mathbf{H}}(\eta) \boldsymbol{\Psi}(\eta) \frac{d\eta}{\eta - \mu}, \quad \mu \in (0, \infty), \quad (11.1a)$$

and

$$\int_0^\infty \tilde{\mathbf{H}}(\mu) \boldsymbol{\Psi}(\mu) d\mu = \mathbf{I} \quad (11.1b)$$

possess a unique solution in the class of functions continuous on every open interval of the positive real axis.

Though for the sake of brevity we do not give an explicit derivation of equations (11.1), we note that the  $\mathbf{H}$  matrix specified by equations (11.1) is sufficient for establishing the half-range orthogonality theorem.

To prove Theorem VI we make use of the equivalence of the given singular-integral equations to a certain matrix version of the Riemann problem. In the manner of Muskhelishvili [21], we introduce the matrix

$$\mathbf{N}(z) = \frac{1}{2\pi i} \int_0^\infty \tilde{\mathbf{H}}(\eta) \boldsymbol{\Psi}(\eta) \frac{d\eta}{\eta - z} \quad (11.2)$$

which is analytic in the plane cut along the real axis and vanishes at least as fast as  $1/z$  as  $|z|$  tends to infinity. The Plemelj formulae [21] can be used with equation (11.2) to yield

$$\pi i [\mathbf{N}^+(\mu) + \mathbf{N}^-(\mu)] = P \int_0^\infty \tilde{\mathbf{H}}(\eta) \boldsymbol{\Psi}(\eta) \frac{d\eta}{\eta - \mu}, \quad \mu \in (0, \infty), \quad (11.3)$$

and

$$\mathbf{N}^+(\mu) - \mathbf{N}^-(\mu) = \tilde{\mathbf{H}}(\mu) \boldsymbol{\Psi}(\mu), \quad \mu \in (0, \infty). \quad (11.4)$$

If we make use of equations (5.10), (11.3) and (11.4) then equation (11.1a) can be cast in the equivalent form of an inhomogeneous Riemann problem:

$$\tilde{\mathbf{N}}^+(\mu) = \mathbf{G}(\mu) \tilde{\mathbf{N}}^-(\mu) + \boldsymbol{\Psi}(\mu) [\boldsymbol{\Lambda}^-(\mu)]^{-1}, \quad \mu \in (0, \infty), \quad (11.5)$$

where

$$\mathbf{G}(\mu) = \boldsymbol{\Lambda}^+(\mu) [\boldsymbol{\Lambda}^-(\mu)]^{-1}. \quad (11.6)$$



The solution to equation (11.5) can be written as

$$\tilde{\mathbf{N}}(z) = \frac{1}{2\pi i} \boldsymbol{\Phi}(z) \left[ \int_0^\infty \mathbf{K}(\eta) \frac{d\eta}{\eta - z} + \hat{\mathbf{P}}(z) \right] \quad (11.7)$$

where  $\hat{\mathbf{P}}(z)$  is a matrix of polynomials,

$$\mathbf{K}(\mu) = [\boldsymbol{\Phi}^+(\mu)]^{-1} \boldsymbol{\Psi}(\mu) [\boldsymbol{\Lambda}^-(\mu)]^{-1}, \quad (11.8)$$

and  $\boldsymbol{\Phi}(z)$  is any canonical solution (of ordered normal form at infinity) to the homogeneous Riemann problem defined by equation (9.1). In order that equation (11.7) have behavior as  $|z|$  approaches infinity consistent with equation (11.2), we must take  $\hat{\mathbf{P}}(z)$  to be a constant matrix.

Following closely Siewert and Burniston's [25] work on the scattering of polarized light, we can now use the constraint to specify uniquely the constant  $\hat{\mathbf{P}}(z)$  in equation (11.7). It thus follows that equation (11.7) along with equations (9.11) and (11.4) yields the result

$$\mathbf{H}(\mu) = \tilde{\boldsymbol{\Phi}}_0^{-1}(-\mu) \tilde{\boldsymbol{\Phi}}_0(0), \quad \mu \in (0, \infty), \quad (11.9)$$

where  $\boldsymbol{\Phi}_0(z)$  is the canonical solution (of ordered normal form at infinity) used in equation (9.11). We note from equation (11.9), since  $\boldsymbol{\Phi}_0(z) = \overline{\boldsymbol{\Phi}_0(\bar{z})}$ , that  $\mathbf{H}(\mu)$  is real for  $\mu \in (0, \infty)$ . Further, equation (11.9) can be used to extend the definition of  $\mathbf{H}(\mu)$  to the complex plane:

$$\mathbf{H}(z) = \tilde{\boldsymbol{\Phi}}_0^{-1}(-z) \tilde{\boldsymbol{\Phi}}_0(0), \quad (11.10)$$

so that the  $\boldsymbol{\Lambda}$  matrix can now be factored as

$$\boldsymbol{\Lambda}(z) = \tilde{\mathbf{H}}^{-1}(-z) \mathbf{H}^{-1}(z).$$

We note that equations (5.10), (9.11) and (11.10) can be used in the Cauchy integral representation

$$\boldsymbol{\Phi}_0(z) = \frac{1}{2\pi i} \int_0^\infty [\boldsymbol{\Phi}_0^+(\mu) - \boldsymbol{\Phi}_0^-(\mu)] \frac{d\mu}{\mu - z} \quad (11.11)$$

to obtain

$$\mathbf{H}(z) = \mathbf{I} + z \mathbf{H}(z) \int_0^\infty \tilde{\mathbf{H}}(\eta) \boldsymbol{\Psi}(\eta) \frac{d\eta}{\eta + z} \quad (11.12)$$

or

$$\mathbf{H}(\mu) = \mathbf{I} + \mu \mathbf{H}(\mu) \int_0^\infty \tilde{\mathbf{H}}(\eta) \boldsymbol{\Psi}(\eta) \frac{d\eta}{\eta + \mu}, \quad \mu \in [0, \infty). \quad (11.13)$$

Since we have established the existence of a unique solution to equations (11.1) and developed equation (11.13) specifically to be used, along with equation (11.1b), as the

basis for our procedure for computing the  $\mathbf{H}$  matrix, it follows that we require proof of *Theorem 7. The equations*

$$\mathbf{H}(\mu) = \mathbf{I} + \mu \mathbf{H}(\mu) \int_0^\infty \tilde{\mathbf{H}}(\eta) \Psi(\eta) \frac{d\eta}{\eta + \mu}, \quad \mu \in [0, \infty), \quad (11.14a)$$

and

$$\int_0^\infty \tilde{\mathbf{H}}(\mu) \Psi(\mu) d\mu = \mathbf{I} \quad (11.14b)$$

possess a unique solution in the class of functions continuous on every open interval of the positive real axis.

We have shown that equations (11.1) possess a unique solution; thus we need only show that any solution of equation (11.14a) is also a solution of equation (11.1a). We first write equation (11.14a) as

$$\mathbf{H}(\mu) \left[ \mathbf{I} - \mu \int_0^\infty \tilde{\mathbf{H}}(\eta) \Psi(\eta) \frac{d\eta}{\eta + \mu} \right] = \mathbf{I} \quad (11.15a)$$

or, alternatively,

$$\left[ \mathbf{I} - \mu \int_0^\infty \tilde{\mathbf{H}}(\eta) \Psi(\eta) \frac{d\eta}{\eta + \mu} \right] \mathbf{H}(\mu) = \mathbf{I}. \quad (11.15b)$$

If the transpose of equation (11.15b) is post-multiplied by

$$\mathbf{I} + \mu P \int_0^\infty \tilde{\mathbf{H}}(\eta) \Psi(\eta) \frac{d\eta}{\eta - \mu}$$

then, after making use of some partial-fraction analysis and equations (4.15) and (11.15), we obtain

$$\tilde{\mathbf{H}}(\mu) \boldsymbol{\lambda}(\mu) = \mathbf{I} + \mu P \int_0^\infty \tilde{\mathbf{H}}(\eta) \Psi(\eta) \frac{d\eta}{\eta - \mu}, \quad \mu \in (0, \infty), \quad (11.16)$$

which proves Theorem 7.

## 12. AN EXPEDIENT METHOD FOR COMPUTING THE $\mathbf{H}$ MATRIX

It is clear from the previous sections of this paper that the  $\mathbf{H}$  matrix is the basic quantity required in the solutions of problems defined in terms of equation (4.18) and specified by half-range,  $\mu \in (0, \infty)$ , boundary conditions. It is also apparent from the analysis of section 11 that the basic proofs regarding the existence and uniqueness of the  $\mathbf{H}$  matrix have been established; however, to demonstrate the utility of our analysis, we must now establish a procedure by which we can compute the  $\mathbf{H}$  matrix accurately and efficiently.

As we have discussed, the  $\mathbf{H}$  matrix is uniquely specified by the nonlinear equation



$$\mathbf{H}(\mu) = \mathbf{I} + \mu \mathbf{H}(\mu) \int_0^\infty \tilde{\mathbf{H}}(\eta) \Psi(\eta) \frac{d\eta}{\eta + \mu}, \mu \in [0, \infty), \quad (12.1a)$$

and the constraint

$$\int_0^\infty \tilde{\mathbf{H}}(\mu) \Psi(\mu) d\mu = \mathbf{I}. \quad (12.1b)$$

Rather than seek a numerical solution to equation (12.1a) which must also satisfy equation (12.1b), we prefer [15, 22] first to write

$$\mathbf{H}(\mu) = (1 + \mu) \mathbf{L}(\mu), \mu \in [0, \infty). \quad (12.2)$$

If we now substitute equation (12.2) into equation (12.1a), perform some elementary partial-fraction analysis, and make use of the constraint, equation (12.1b), then we find that  $\mathbf{L}(\mu)$  must satisfy

$$\mathbf{L}(\mu) = \mathbf{I} + \mu \mathbf{L}(\mu) \int_0^\infty (1 - \eta^2) \tilde{\mathbf{L}}(\eta) \Psi(\eta) \frac{d\eta}{\eta + \mu}, \mu \in [0, \infty), \quad (12.3a)$$

and

$$\int_0^\infty \tilde{\mathbf{L}}(\mu) \Psi(\mu) (1 + \mu) d\mu = \mathbf{I}. \quad (12.3b)$$

It follows from Theorem 7 that equations (12.3) have a unique solution. We regard equations (12.3) as the basic equations to be solved numerically because an iterative procedure based on these equations has proven to converge faster than a similar iterative solution of equations (12.1).

For calculational convenience, we now prefer to make in equations (12.3) the change of variable

$$t = \frac{\mu}{1 + \mu} \quad (12.4)$$

and thus to write

$$\mathbf{L}_*(t) = \mathbf{I} + t \mathbf{L}_*(t) \int_0^1 \frac{1 - 2s}{(1 - s)^3} \tilde{\mathbf{L}}_*(s) \Psi_*(s) \frac{ds}{t(1 - s) + s(1 - t)}, t \in [0, 1), \quad (12.5)$$

where we have introduced the notation  $g_*(t) = g[t/(1 - t)]$ . We have found that equation (12.5) can be solved quite effectively by iteration.

The computations were performed in double-precision arithmetic on an IBM 370/165 computer, and we used an improved Gaussian-quadrature [17] representation of the integration process. The iterative procedure was terminated when successive calculations of  $\mathbf{L}_*(t)$  differed by no more than  $10^{-15}$ .

To substantiate confidence in our computations, several "checks" were incorporated in the calculation. As expected  $\mathbf{L}_*(t)$  satisfied

$$\mathbf{I} - \int_0^1 \tilde{\mathbf{L}}_*(t) \Psi_*(t) \frac{dt}{(1 - t)^3} = \mathbf{0}, \quad (12.6)$$

an identity corresponding to the constraint, equation (12.1b), to thirteen significant figures. The equation in terms of  $L_*(t)$  corresponding to the identity [16]

$$2 \int_0^\infty \Psi(\mu) \mu^2 d\mu - \int_0^\infty \Psi(\mu) H(\mu) \mu d\mu \int_0^\infty \tilde{H}(\mu) \Psi(\mu) \mu d\mu = 0 \quad (12.7)$$

was also verified to thirteen significant figures.

The analytical solution [16]

$$H(z) = \det \mathbf{H}(z) = \sqrt{\frac{12}{5}} z^2 \exp \left\{ -\frac{1}{\pi} \int_0^\infty \arg \Lambda^+(\mu) \frac{d\mu}{\mu + z} \right\}, \quad (12.8)$$

where  $\arg \Lambda^+(0) = -2\pi$ , can be shown to satisfy

$$H(\mu) = 1 + \mu H(\mu) \int_0^\infty f(\eta) H(\eta) \frac{d\eta}{\eta + \mu}, \quad \mu \in [0, \infty), \quad (12.9)$$

where

$$f(\eta) = \frac{1}{3} \frac{1}{\sqrt{\pi}} e^{-\eta^2} \left[ \frac{11}{2} - \eta^2 - 8\eta e^{-\eta^2} \int_0^\eta e^{t^2} dt \right]. \quad (12.10)$$

Rather than solve equation (12.9) and the appropriate constraint for  $H(\mu)$  we prefer to write

$$H(\mu) = (1 + \mu)^2 L(\mu), \quad \mu \in [0, \infty). \quad (12.11)$$

If we substitute equation (12.11) into equation (12.9), perform some partial-fraction analysis and make use of two identities [16] for  $H(\mu)$  then we find that (after an appropriate change of variables)  $L_*(t) = \det \mathbf{L}_*(t)$  must satisfy

$$\frac{1}{L_*(t)} = 1 - t \int_0^1 \frac{(1-2s)^2}{(1-s)^5} f_*(s) L_*(s) \frac{ds}{s(1-t) + t(1-s)}, \quad t \in [0, 1). \quad (12.12)$$

We have compared  $L_*(t)$  as computed from equation (12.5) to a direct solution of equation (12.12) and the appropriate constraint to find agreement to nine significant figures.

Finally the number of quadrature points used to represent the integration process was increased to suggest that the numerical values of the  $L_*$  matrix given in the accompanying Table (1) were insensitive to further refinements in the quadrature scheme.

### 13. AN APPLICATION OF THE THEORY: THE TEMPERATURE SLIP PROBLEM

We consider the effect of a body surface on the behavior of the particle distribution function of a rarefied gaseous medium. It is known that, in the absence of boundaries, the particle distribution function in a gas with slowly varying physical parameters obeys the Chapman-Enskog equations (and therefore the macroscopic variables obey the



Table 1. The  $L_{\alpha}$  matrix

$t$	$L_{\alpha 11}(t)$	$L_{\alpha 12}(t)$	$L_{\alpha 21}(t)$	$L_{\alpha 22}(t)$
0.0	1.0	0.0	0.0	1.0
0.05	1.05781	-0.0409718	-0.0406202	1.08988
0.10	1.08842	-0.0702992	-0.0691920	1.14897
0.15	1.10976	-0.0960791	-0.0939297	1.19824
0.20	1.12527	-0.119749	-0.116314	1.24158
0.25	1.13648	-0.141931	-0.136989	1.28073
0.30	1.14424	-0.162963	-0.156307	1.31664
0.35	1.14909	-0.183053	-0.174483	1.34992
0.40	1.15139	-0.202341	-0.191658	1.38097
0.45	1.15138	-0.220921	-0.207929	1.41009
0.50	1.14926	-0.238862	-0.223361	1.43748
0.55	1.14514	-0.256214	-0.238000	1.46333
0.60	1.13912	-0.273011	-0.251873	1.48774
0.65	1.13125	-0.298278	-0.264997	1.51082
0.70	1.12157	-0.305030	-0.277373	1.53265
0.75	1.11008	-0.320274	-0.288995	1.55328
0.80	1.09678	-0.335010	-0.299844	1.57276
0.85	1.08162	-0.349228	-0.309887	1.59111
0.90	1.06454	-0.362913	-0.319081	1.60835
0.95	1.04545	-0.376036	-0.327361	1.62449
0.99	1.02864	-0.386105	-0.333271	1.63660

Navier-Stokes equations). Near the body surface, the behavior of the gas is described by a rarefied Knudsen layer in which the collisional effects are only of secondary importance. It is natural to ask how the outer Chapman-Enskog (or Navier-Stokes) region can be matched consistently with the inner Knudsen layer. Saying it differently, we ask what are the velocity and temperature slip boundary conditions at a body surface for the Navier-Stokes equations due to the presence of the Knudsen layer adjacent to the body surface.

To understand the asymptotic behavior of the Knudsen layer, we may stretch locally the coordinate normal to the body surface such that the gas-kinetic motion in the Knudsen layer reduces to a locally defined half-space problem and the kinetic equation takes on a one-dimensional character in the form studied in this paper.

Since the asymptotic boundary condition of the Knudsen layer is given by the Chapman-Enskog equations, the asymptotic form of the particle distribution function is nearly Maxwellian. If we also assume that the effect of the body surface is to re-emit molecules described by a suitably chosen Maxwellian distribution and that the macroscopic variables do not vary appreciably throughout the Knudsen layer, a linearization scheme for the one-dimensional kinetic equation in the sense described in sections 2 and 3 is justified. Based on the constant collision frequency BGK model, the pertinent linearized kinetic equation for the Knudsen layer is that given by equation (3.7). The velocity-slip (or Kramers problem) for this equation for a diffusely reflecting wall has been solved exactly by Cercignani[9] and an accurate velocity-slip coefficient has been calculated,[1]. Although approximate analyses of the associated temperature slip problem have been reported by a number of authors[2, 19, 23, 28, 29], an accurate calculation of the temperature-slip coefficient has not been previously reported. Since the temperature-density effects for the problem for a diffusely reflecting wall are uncoupled from the transverse momentum effects, we will show that an accurate determi-

nation of the temperature slip coefficient for steady gas-kinetic motion may be effected by using the method of elementary solutions and the half-range expansion theorem developed in this paper for the vector integrodifferential equation (4.1).

It is straightforward to demonstrate that the heat flux in the normal direction in the Knudsen layer is a constant and since the Chapman–Enskog solution relates the heat flux linearly to the temperature gradient, to match the Chapman–Enskog region and the Knudsen layer it is only necessary to consider an asymptotic boundary condition with a constant temperature gradient. It is interesting to note that such an asymptotic boundary condition, as far as the temperature-density effects are concerned, can be satisfied by taking the asymptotic perturbation distribution function to be

$$h_{asy}(x, \mathbf{c}) = \left[ c_2^2 + c_3^2 - 1 \right]^T \left[ \sum_{\alpha=1}^2 A_{\alpha} \Phi_{\alpha}(\mu) + \sum_{\beta=3}^4 A_{\beta} \Psi_{\beta}(x, \mu) \right], \quad (13.1)$$

where the  $\Phi'_{\alpha}$ s and  $\Psi'_{\beta}$ s are the discrete solutions to equation (4.1), and  $c_2, c_3$  are the components of the dimensionless particle velocity in the transverse directions. Since the Chapman–Enskog theory requires the medium to obey the perfect gas law and the pressure in the Knudsen layer far from the wall is a specified constant, we deduce from the definitions

$$n_{asy}(x) \triangleq \pi^{-3/2} \int h_{asy}(x, \mathbf{c}) e^{-c^2} d^3c, \quad (13.2)$$

and

$$T_{asy}(x) \triangleq \frac{2}{3} \pi^{-3/2} \int h_{asy}(x, \mathbf{c}) (c^2 - \frac{3}{2}) e^{-c^2} d^3c, \quad (13.3)$$

the requirements

$$A_2 = -\sqrt{\frac{2}{3}} A_1 \text{ and } A_4 = -\sqrt{\frac{2}{3}} A_3. \quad (13.4)$$

For an asymptotic temperature gradient of unity, it is clear that the temperature slip coefficient  $\xi$  defined by  $T_{asy}(0) = \xi(d/dx)T_{asy}(x)|_{x=0}$  will be given by  $\xi = \epsilon' l_i$ , [19], where

$$\epsilon' = \sqrt{\frac{2}{3}} A_1, \quad (13.5)$$

$l_i = (4/5)(\mathcal{K}/nk)(m/2kT)^{1/2}$  is a mean free path, and  $\mathcal{K}$  is the thermal conductivity.

For a diffusely reflecting wall, the boundary condition at  $x = 0$  requires

$$\begin{bmatrix} B \\ 0 \end{bmatrix} = \sum_{\alpha=1}^4 A_{\alpha} \Phi_{\alpha}(\mu) + \sum_{\alpha=1}^2 \int_0^{\infty} A_{\alpha}(\eta) \Phi_{\alpha}(\eta, \mu) d\eta, \quad \mu \in (0, \infty). \quad (13.6)$$

The unknown constant  $B$  is related to the density of the gas near the wall and need not be specified for temperature-slip coefficient calculations. We make use of equation (13.4) and the specified asymptotic temperature gradient to write equation (13.6) as

$$\sqrt{\frac{2}{3}} \Phi_3(\mu) - \Phi_4(\mu) = A_1 \Phi_1(\mu) + (A_2 - B) \Phi_2(\mu) + \sum_{\alpha=1}^2 \int_0^{\infty} A_{\alpha}(\eta) \Phi_{\alpha}(\eta, \mu) d\eta. \quad (13.7)$$



Theorem 3 and equation (10.16a) enable us to solve equation (13.7) for  $A_1$ :

$$A_1 = \int_0^\infty \tilde{\Theta}_1(\mu) [\sqrt{\frac{3}{2}} \Phi_3(\mu) - \Phi_4(\mu)] e^{-\mu^2} \mu d\mu. \quad (13.8)$$

It is clear from the definition of  $\Theta_1(\mu)$  that  $A_1$  may be expressed in terms of appropriate moments of the  $\mathbf{H}$  matrix discussed in section 11. The numerical procedure used to evaluate integrals involving the  $\mathbf{H}$  matrix was given in section 12. We find

$$\epsilon' = \frac{5}{8}\pi^{1/2} (1.17597). \quad (13.9)$$

This compares with the variational result of  $\epsilon' = \frac{5}{8}\pi^{1/2} (1.1621)$ , [2, 19, 23], Wang Chang and Uhlenbeck's result of  $\epsilon' = \frac{5}{8}\pi^{1/2} (1.150)$ , [28], and Welander's value of  $\epsilon' = \frac{5}{8}\pi^{1/2} (1.173)$ , [29]. We believe our result to be accurate to the number of significant figures quoted.

*Acknowledgement*—The authors are grateful to Professor E. E. BURNISTON for many valuable discussions during the course of this investigation. This research was supported in part by NSF grants GK-11935 and GU-1590, and NASA grant NGL34-002-084, and the Triangle Universities Consortium on Air Pollution (comprising Duke University, North Carolina State University and the University of North Carolina at Chapel Hill), which is funded by the Office of Manpower Development of the U.S. Environmental Protection Agency.

#### REFERENCES

- [1] S. ALBERTONI, C. CERCIGNANI and L. GOTUSSO, *Phys. Fluids* **6**, 993 (1963).
- [2] P. BASSANINI, C. CERCIGNANI and C. D. PAGANI, *Int. J. Heat Mass Transfer* **10**, 447 (1967).
- [3] P. L. BHATNAGAR, E. P. GROSS and M. KROOK, *Phys. Rev.* **94**, 511 (1954).
- [4] G. R. BOND and C. E. SIEWERT, *Astrophys. J.* **164**, 97 (1971).
- [5] E. E. BURNISTON and C. E. SIEWERT, *J. Math. Phys.* **11**, 3416 (1970).
- [6] E. E. BURNISTON, C. E. SIEWERT, P. SILVENNOINEN and P. F. ZWEIFEL, *Nucl. Sci. Engng* **45**, 331 (1971).
- [7] K. M. CASE, *Ann. Phys.* **9**, 1 (1960).
- [8] K. M. CASE and P. F. ZWEIFEL, *Linear Transport Theory*. Addison-Wesley (1967).
- [9] C. CERCIGNANI, *J. Math. Analysis Applic.* **10**, 568 (1965).
- [10] R. V. CHURCHILL, *Complex Variables and Applications* McGraw-Hill (1960).
- [11] C. CERCIGNANI, *Elementary solutions of linearized kinetic models and boundary value problems in the kinetic theory of gases*. Brown Univ. Report (1965).
- [12] C. CERCIGNANI, *Mathematical Methods in Kinetic Theory*. Plenum (1969).
- [13] E. P. GROSS and E. A. JACKSON, *Physics Fluids* **2**, 432 (1959).
- [14] I. M. GELFAND and G. E. SHILOV, *Generalized Functions*. Academic (1964).
- [15] J. T. KRIESE and C. E. SIEWERT, *Astrophys. J.* **164**, 389 (1971).
- [16] J. T. KRIESE, Ph.D. Thesis, North Carolina State University (1972).
- [17] A. S. KRONROD, *Nodes and Weights of Quadrature Formulas*. Consultants Bureau (1965).
- [18] I. KUSCER, N. J. McCORMICK and G. C. SUMMERFIELD, *Ann. Phys.* **30**, 411 (1964).
- [19] S. K. LOYALKA and J. H. FERZIGER, *Physics Fluids* **11**, 1668 (1968).
- [20] G. F. MANDŽAVIDZE and B. V. HVEDELIDZE, *Dokl. Akad. Nauk SSSR* **123**, 791 (1958).
- [21] N. I. MUSKHELISHVILI, *Singular Integral Equations*. Noordhoff (1953).
- [22] S. PAHOR, *Nucl. Sci. Engng* **31**, 110 (1968).
- [23] S. F. SHEN, *Rarefied Gas Dynamics*, (Edited by C. L. BAUNDIN). Academic Press (1967).
- [24] C. E. SIEWERT, *J. Quant. Spectrosc. Radiat. Transfer* **12**, 683 (1972).
- [25] C. E. SIEWERT and E. E. BURNISTON, *Astrophys. J.* **174**, 629 (1972).
- [26] C. E. SIEWERT and P. F. ZWEIFEL, *Ann. Phys.* **36**, 61 (1966).
- [27] L. SIROVICH, *Phys. Fluids* **5**, 908 (1962).
- [28] C. S. WANG CHANG and G. E. UHLENBECK, University of Michigan Engineering Research Institute Project Report M999 (1954).
- [29] P. WELANDER, *Ark. Fy.* **7**, 507 (1954).

(Received 8 June 1972)

**Résumé**—La méthode des solutions élémentaires est employée pour résoudre deux équations integro-différentielles couplées pour la détermination des effets du rapport température-densité, dans un modèle BGK linéarisé dans la théorie cinétique des gaz. L'état complet de tout le domaine et les théorèmes d'orthogonalité sont démontrés pour les modes normaux développés et la fonction de Green pour un milieu infini est établie comme illustration du formalisme sur tout le domaine.

Le problème de Riemann approprié à une matrice homogène est étudiée et l'état complet de tout le domaine et les théorèmes d'orthogonalité sont démontrés pour un certain sous-système des modes normaux. Les théorèmes nécessaires d'existence et d'unicité concernant la matrice  $H$ , fondamentale pour l'analyse du domaine complet, sont démontrés et une méthode de calcul précise et efficace est présentée. Le problème du glissement de température d'un demiespace est résolu analytiquement et une valeur très précise du coefficient de glissement de température est donnée.

**Zusammenfassung**—Das Verfahren elementarer Lösungen wird verwendet, um zwei gekoppelte Integro-differentialgleichungen zu lösen, die genügen, um die Temperatur-Dichtewirkungen in einem linearisierten BGK-Modell in der kinetischen Theorie von Gasen zu bestimmen.

Vollbereichs-Vollständigkeits- und Orthogonalitätstheoreme werden für die entwickelten Normalformen bewiesen und Green's Funktion des unendlichen Stoffes wird als eine Illustration des Vollbereichsformalismus konstruiert.

Das entsprechende Riemann'sche Problem einer homogenen Matrix wird besprochen und Halbbereichs-Vollständigkeits- und Orthogonalitätstheoreme werden für eine bestimmte Untergruppe der Normalformen bewiesen. Die für die  $H$ -Matrix belangreichen erforderlichen Existenz- und Eindeutigkeits-theoreme, grundlegend für die Halbbereichs-Analyse, werden bewiesen, und eine genaue und wirksame Berechnungsmethode wird besprochen. Das Temperaturgleitproblem des Halbraumes wird analytisch gelöst und ein sehr genauer Wert des Temperaturgleitkoeffizienten wird berichtet.

**Sommario**—Il metodo delle soluzioni elementari viene usato per risolvere due equazioni integrodifferenziali accoppiate, sufficienti a determinare gli effetti della densità di temperatura in un modello BGK linearizzato nella teoria cinetica dei gas.

Vengono dimostrati i teoremi della completezza e dell'ortogonalità su tutta la gamma per i modi normali sviluppati e, per illustrare il formalismo sull'intera gamma, viene costruita la funzione di Green per un mezzo infinito.

Viene discusso il problema di Riemann per una matrice omogenea appropriata e, per un certo sottoinsieme dei modi normali, vengono dimostrati i problemi di completezza e ortogonalità per la semigamma. Vengono dimostrati i necessari teoremi di esistenza e unicità relativi alla matrice  $H$ , fondamentali per l'analisi della semigamma, e viene discusso un metodo di calcolo accurato ed efficiente. Il problema temperatura/scorrimento del semispazio viene risolto analiticamente e viene dato un valore molto accurato del coefficiente temperatura/scorrimento.

**Абстракт** — Применен метод элементарных решений для решения двух интегро-дифференциальных уравнений достаточных для определения эффектов температуры и плотности в линеаризованной модели (BGK) в кинетической теории газов. Даны доказательства теорем об общей полноте и ортогональности для развиваемых нормальных режимов, построена функция Грина для бесконечной среды в качестве иллюстрации общего формализма. Обсуждена соответствующая римановская проблема однородной матрицы, даны доказательства теорем о половинной полноте и ортогональности для определенной подсистемы нормальных режимов. Доказаны искомые теоремы о существовании и единственности относительно матрицы  $H$ , лежащие в основе анализа половинной полноты, а также обсужден точный рациональный метод вычисления. Аналитически решена проблема полупространственного скольжения и температуры, сообщено высокоточное значение коэффициента скольжения и температуры.



75-04939

N75-15329

## Tricritical points in multicomponent fluid mixtures\*

Alex Hankey<sup>†</sup>

Stanford Linear Accelerator Center, Stanford University, Stanford, California 94305

T. S. Chang<sup>†</sup> and H. E. Stanley<sup>§</sup>

Department of Physics, Massachusetts Institute of Technology, Cambridge, Massachusetts 02139

(Received 2 July 1973)

In view of experimental considerations, we give a model-independent argument that the novel tricritical points in multicomponent fluid mixtures, where three phases simultaneously become critical, are points on the boundary of a *single two-dimensional surface of critical points*. This result is corroborated by the Landau model suggested by Griffiths. The relationship between these tricritical points and the complex "higher-order" critical points proposed to exist in certain magnetic systems is elucidated.

## I. INTRODUCTION

In 1970 Griffiths<sup>1</sup> proposed the concept of a tricritical point as being the point of intersection of three lines of critical points in a phase diagram using intensive thermodynamic variables. He further suggested, as examples, metamagnets,<sup>2</sup> He<sup>3</sup>-He<sup>4</sup> mixtures,<sup>3</sup> and ammonium chloride.<sup>4</sup> There has also been considerable speculation<sup>1,5</sup> that similar points might exist and might be found in the phase diagrams of complex fluid mixtures. That such points have already been proposed and, indeed, that they had been investigated prior to 1970 has recently been pointed out by Widom and Griffiths.<sup>6-8</sup> A full and very complete discussion of experimental evidence for these points has been given in Refs. 6-8, and we refer the reader to these papers for details.

A different way in which critical points more complex than tricritical points can occur has been shown to involve intersecting lines of tricritical points, and a classification of critical points has been introduced to differentiate these points from tricritical points or ordinary critical points.<sup>5</sup> The question has been raised<sup>6,8</sup> as to how the new points discovered in fluids are related to such a classification.

Properties of the phase diagram<sup>9</sup> were the basis of the approach we suggested previously.<sup>5,10</sup> In particular, we emphasized the importance of the connectivity properties of different spaces of critical points and tricritical points. Accordingly it is the connectivity of the different critical points of multicomponent fluid mixtures in the space of truly intensive or "field" variables that we emphasize here.

## II. DEMONSTRATION THAT ALL CRITICAL POINTS FORM A SINGLE CONNECTED SURFACE

The basic idea is to consider a system where three distinct phases can be in equilibrium. These might be three liquids or two liquids and a vapor phase. On changing the thermodynamic variables (temperature, pressure, chemical potentials of different components) one pair of phases will become critical, in the presence of the third. In a binary system the point where this occurs is the end point of a line of critical points which bounds the surface of points where the two phases coexist. There are no degrees of freedom and such a point is unique in the phase diagram.<sup>7</sup>

In a ternary, quaternary, or more complicated system this point has one or more degrees of freedom. Thus a line of "critical end points" is possible. Such a line is the boundary of a surface of critical points where two phases are critical.

In the particular systems of interest it is possible, by varying physical conditions, to make a different pair of the three phases become critical in the presence of the third, thus producing a second line of critical end points.

Finally, by achieving exactly the correct physical conditions it is possible for all three phases to become critical simultaneously. In a ternary system such a point is unique; there are zero degrees of freedom. Here, only this and similarly simple cases are considered.

Experimentally there is the following arrangement. A tube containing a three-component mixture with a three-phase system is cooled to observe the appearance of successive phases. We



will call these phases  $\alpha$ ,  $\beta$ , and  $\gamma$ , where for purposes of argument  $\rho_\alpha < \rho_\beta < \rho_\gamma$ . The ratio of the various components is varied until the second meniscus appears via a critical mode. This could be the lower meniscus in which case phases  $\gamma$  and  $\beta$  become critical at a lower temperature. If pressure, temperature, and one other intensive parameter are allowed to vary, a phase diagram of the type shown in Fig. 1(a) will be observed. At the point  $P$ , the phases  $\gamma$  and  $\beta$  become critical in the presence of a third phase  $\alpha$ . If pressure is increased, the lightest phase  $\alpha$  will disappear and a line of critical points between phases  $\gamma$  and  $\beta$  will develop. For increasing temperatures above  $P$ , there will be a line of critical points bounding the surface of coexistence points which separates the region of light phase  $\alpha$  from the region of the heavier phase  $\gamma\beta$ .

By varying the ratios of components appropriately, it is possible, in the physical systems of interest, to make the upper meniscus, separating phase  $\beta$  from phase  $\alpha$ , appear second on cooling. The corresponding phase diagram is shown in Fig. 1(c). Again there is a special point  $P'$  which is the end point of a line of critical points for phases  $\beta$  and  $\alpha$ , and which is also the end point of the line of points where three phases coexist. If the temperature is increased above  $P'$  then the coexistence surface separating phase  $\gamma$  from the

combined phases  $\beta\alpha$  will terminate in a line of critical points.

If the transition to the phase diagram of Fig. 1(c) happens by a continuous variation from Fig. 1(a) then there must be a situation where both menisci become critical simultaneously.

The corresponding phase diagram is shown in Fig. 1(b). It may be seen that the point  $P$  of Fig. 1(a) has migrated along the coexistence surface to the point  $P_t$  on the boundary. At the point  $P_t$  all three lines of critical points,  $a$  ( $\gamma\beta$  critical),  $b$  ( $\gamma\alpha$  critical), and  $c$  ( $\beta\alpha$  critical) meet.

The purpose of constructing Figs. 1(a)–1(c) is to consider the behavior of the critical surface in the immediate neighborhood of the tricritical point  $P_t$ , and the figures should therefore be understood to represent the phase diagram close to  $P_t$  and not far away from the tricritical point. Also, since our primary interest is the connectivity of the surface of critical points, and not its specific shape, we do not have to choose the variables precisely, since the connectedness would remain unchanged even if different variables were chosen. [Similar remarks apply to Figs. 2(a) and 2(b) in what follows.]

We can now demonstrate that the lines of critical points  $a, b, c$  in Figs. 1(a)–1(c) form a single continuous surface of critical points bounded by the line of critical end points  $P$ – $P_t$ – $P'$ . Consider a

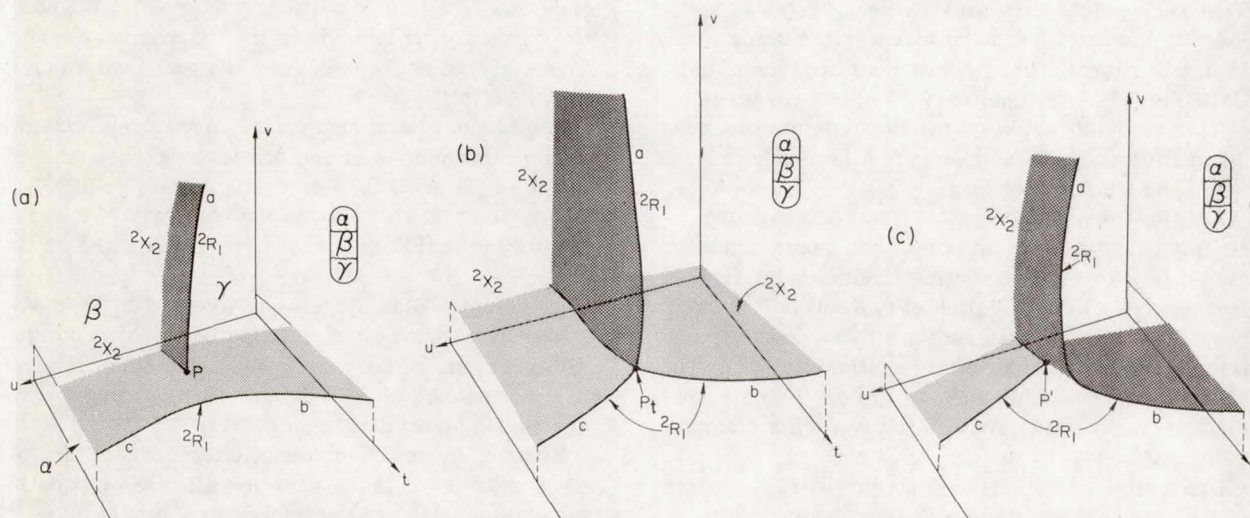


FIG. 1. Three-dimensional subspaces of the full four-dimensional space of field variables of a three-component system (or of five dimensions for four components). The variable  $t$  may be thought of as the temperature, the variable  $v$  as the pressure, and the third variable  $u$  as a suitable combination of chemical potentials. We use the notation of Ref. 5 to indicate lines and surfaces of critical points in the diagram. Lines of critical points are indicated  ${}^2R_1$  (order 2, dimension 1). Coexistence surfaces are indicated by  ${}^2X_2$  (two phases and dimension 2). (a) Section containing a point  $P$  where the two heavier phases  $\gamma, \beta$  are critical in the presence of the lightest  $\alpha$ , as represented by the schematic tube showing the  $\gamma\beta$  meniscus critical and the  $\beta\alpha$  meniscus stable. (b) Section through the point  $P_t$  where all three phases become critical simultaneously, the  $\gamma\beta$  and  $\beta\alpha$  menisci are simultaneously critical in the schematic tube. (c) Section containing a point  $P'$  where the lighter phases  $\beta, \alpha$  are critical in the presence of the heaviest  $\gamma$ , as shown in the schematic representation.



point on line  $a$  in Fig. 1(a); move continuously through Figs. 1(b) to 1(c). Now move along the line  $a-b$  to a point at the "b" end, and now move along continuously through Figs. 1(b) to 1(a). Still being on line  $b$ , we can move along the line  $b-c$  to the "c" end. Now move continuously through Figs. 1(b) to 1(c) and our assertion is demonstrated. We have not passed through the point  $P_t$  and so the lines  $a, b, c$  form sections of a single continuous surface of critical points bounded by lines of critical end points  $P-P_t-P'$ .

The fact that there is only a single surface of critical points is also corroborated by the model of Griffiths<sup>8</sup> (see his Fig. 3). This fact is in strong contrast to the metamagnet where it is not possible to go from a point on the wing boundaries to a point on the physical critical line without passing through a tricritical point<sup>1,10</sup> and the spaces of critical points are distinct and separate.

It will be plausible to conjecture that since all the critical points form a single surface, the critical-point exponents are the same at all critical points except the tricritical point itself. In contrast, for a metamagnet no reasons have been presented for why the critical-point exponents should be the same along all three of the critical lines meeting at the tricritical point. However, it has been suggested<sup>11</sup> that for most tricritical points the existence of a hidden variable linking the wing boundaries to the physical critical line (the variable called  $a_3$  by Griffiths<sup>8</sup>) might force the equality of exponents.

### III. MODEL SURFACE OF CRITICAL POINTS

The phase diagrams of Figs. 1(a)–1(c) were three dimensional and so parametrizing them with an extra field variable introduces a fourth dimension to the phase diagram. The connectivity, and other properties, of the surface of critical points formed by the critical lines  $a, b, c$  of Fig. 1, are most easily studied in a three-dimensional subspace of the full phase diagram which contains the whole critical surface. The shape of the critical surface in such a subspace may be determined as follows.

Consider the critical lines as they appear on the paper in Figs. 1(a)–1(c) and consider how these lines would form a smooth surface in three dimensions if the extra parameter were used to plot the height of the paper, with Fig. 1(c) above 1(b) above 1(a). By this combined projection and motion we generate a single connected surface of critical points with a boundary formed by the line of points  $P-P_t-P'$ .

A surface, which is topologically equivalent to the surface of critical points thus obtained, is

shown in Figs. 2(a) and 2(b). Fig. 2(a) is a contour map of the surface, and the heights  $h$  of the contours are given by the hyperbolae  $xy = h$ . The boundary of the surface  $P-P_t-P'$  is represented by the parabola  $y = -cx^2$  in the lower half of Fig. 2(a). The topological equivalence of the surface of Fig. 2(a) to the surface of critical points may be seen as follows.

Consider a section of Fig. 2(a) at constant height  $h$ . If  $h > 0$  there are two hyperbolae, one in the upper right quadrant and one which terminates on the portion of the parabola labeled  $P$  in the lower left. This is a representation of Fig. 1(a) for which there are two critical lines, one labeled (a) terminating at  $P$  and another labeled (b-c).

If  $h < 0$  there are again two hyperbolae, one in the upper left quadrant which corresponds to the line of critical points (a, b) of Fig. 1(c), and one

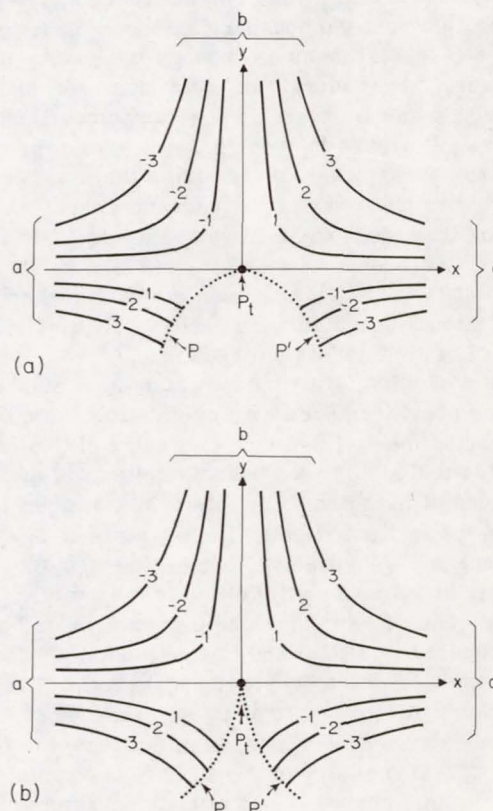


FIG. 2. Section of the four-dimensional space of field variables containing the full surface of critical points. The surface is represented by a contour map of hyperbolae and is fully explained in the text. The variables  $x$  and  $y$  are suitable field variables. (a) Boundary of the surface is smooth at  $P_t$ . The lines of critical end points  $P, P'$  form a smooth line in the four-dimensional space. (b) Boundary of the surface is cusplike at  $P_t$ . The lines of critical end points  $P, P'$  form a cusp in the four-dimensional space.



in the lower right quadrant of Fig. 2 which corresponds to the critical line  $c$  terminating at  $P$  in Fig. 1(c).

When  $h=0$  the hyperbolae degenerate into the three axes, for  $x<0$ ,  $y>0$ , and  $x>0$  corresponding to the lines  $a, b, c$  of Fig. 1(b) which terminate at  $P_t$ .

Accordingly, in Fig. 2, the ends of the hyperbolae are labeled  $a, b, c$  according to the parts of the critical lines in Fig. 1 to which they correspond.

The complete topological correspondence between the sections of the surface in Fig. 2 and the critical lines of Fig. 1 is therefore clear. The points  $P, P_t, P'$  are a line forming a boundary of the surface of critical points, and the point  $P_t$ , which is the tricritical point, corresponds to a saddle point of the surface in the projective space of Fig. 2.

It may seem that a very special space has been chosen, and that the boundary has been made to go in a very special fashion—through the saddle point. However, this is merely in accordance with the following general physical requirements: (i) Only one point  $P$  occurs in each phase diagram; therefore the boundary *has* to pass from the lower left quadrant to the lower right quadrant without passing through the upper two quadrants; (ii) Critical lines only split or end at a point like  $P$ . Thus the point  $P$  *has* to pass through the origin where the section would otherwise necessarily give four lines of critical points intersecting.

This analysis of the critical points as a single surface provides another viewpoint from which to understand the fact that only two pairs of the three possible pairs of phases became critical in the presence of the third. The simplest viewpoint is that of the test tube itself. If the phases  $\alpha, \beta, \gamma$  are ordered in increasing density, then  $(\alpha, \beta)$  can be critical (same density) in the presence of  $\gamma$ , and  $(\beta, \gamma)$  can be critical in the presence of  $\alpha$ , but  $(\alpha, \gamma)$  cannot be critical and of equal density without the phase  $\beta$  having a density equal to both. Thus the possibility  $(\alpha, \gamma)$  critical in the presence of  $\beta$  is eliminated. Widom<sup>7</sup> has related this fact to the geometric asymmetry of the solid figure containing three distinct phases  $\alpha, \beta, \gamma$  at constant temperature less than the tricritical temperature.

In terms of the phase diagrams in spaces of truly intensive variables (Widom used densities, or extensive variables), the existence of two lines of critical end points instead of three has a very simple topological interpretation: the boundary of a single surface is locally divided into *two* separate parts by the removal of a single point. Thus the tricritical point  $P_t$  divides the boundary of the surface of critical points into two lines of critical

end points but *cannot* divide it into three different lines of critical end points.

#### IV. SPECIAL DIRECTIONS

It was shown by Griffiths<sup>8</sup> that in his model there are four variables of scaling, each with different exponents at the special point. From a purely phenomenological point of view one can define four different directions at the special point  $P_t$  in the same spirit as Griffiths and Wheeler.<sup>9</sup> From Fig. 2 it may be seen that these directions are (i) the limiting "strong" direction for the surface of critical points, (ii) the limiting "weak" direction for the surface of critical points, (iii) the tangent to the line of critical end points at the tricritical point, and (iv) the limiting second direction parametrizing the surface of critical points. These correspond to the variables called  $a_1, a_2, a_4$ , and  $a_3$ , respectively, by Griffiths.<sup>8</sup>

#### V. TRANSLATION TO COMPOSITION VARIABLES

The variables over which the experimentalist has easy control are unfortunately not the intensive field variables like the chemical potentials, but only the densities. In these variables the phase diagrams have been discussed by Widom.<sup>7</sup> It has been pointed out by Griffiths<sup>8</sup> that the precise composition of the tricritical point  $P_t$  probably does not coincide with the composition of the regions of coexistence of three phases at temperatures smaller than the temperature at  $P_t$ .

Such behavior has probably been observed in the system carbon-dioxide-methanol-water because when a constant volume specimen (i.e., a sealed tube) of precisely the correct composition is increased in temperature, one does not observe the simultaneous disappearance of two menisci. Instead<sup>12</sup> one meniscus disappears critically and simultaneously a second appears critically. This remarkable behavior does not change any of our geometric conclusions, because it can be interpreted as follows: the constant volume, constant composition path does not follow the line of points where three phases coexist in Fig. 1(b), but rather it passes from one coexistence surface  $(\gamma, \beta)$  to another  $(\alpha, \beta)$  directly through the point  $P_t$ .

#### VI. RELATIONSHIP TO OTHER COMPLEX SYSTEMS

In previous work<sup>5,10</sup> we have given several examples of complex magnetic systems and we have attempted to systematically classify all the coexistence and critical points in such systems. For



points where several phases coexist without being critical this is relatively simple, since the appropriate quantities are the number of coexisting phases and the dimensionality of the space. These are related to the total number of thermodynamic intensive variables by the phase rule.<sup>5</sup>

For critical points, it can be argued that every phase that becomes critical after the first two implies the loss of an extra degree of freedom in addition to the one lost because of coexistence.<sup>7</sup> Hence if there is a system with  $n$  thermodynamic variables possessing a point where  $p$  phases are in coexistence, of which  $q$  are critical (altogether rather than in two separate groups  $q_1$  and  $q_2$ , although the generalization to such cases is simple). The dimensionality of the space on which this occurs will be given by

$$d = n - (p - 1) - m, \quad (1)$$

where  $m = \max(q - 1, 0)$  since the case  $q = 1$  is not meaningful and  $m = 0$  if  $q = 0$ . As a special case if all  $p$  of the phases are critical we obtain  $d = n + 2 - 2p$ .

While this equation holds for fluids, it is violated by the original tricritical points, for which  $n = p = 3$ ,  $d = 0$  and also by certain magnetic models<sup>10</sup> which contain highly symmetric points where lines of tricritical points intersect, and  $n = p = 4$  and  $d = 0$ . Before giving the equation which correctly describes both fluids and the complex magnetic systems let us contrast the two ways of classifying more complicated critical points that have been proposed.

For fluids Widom<sup>7</sup> has proposed that the important quantity is the number of phases becoming critical, and that this number should be used as the order of the critical points.

For complex magnetic systems we have proposed an apparently different scheme which is based on the original proposal for tricritical points<sup>1</sup> where three different lines of critical points intersected. Accordingly we gave examples of systems where different lines of tricritical points intersected, and gave the points of intersection an order different from (one larger than) that of tricritical points. Because of the symmetry of the various systems we investigated, there were no lines of critical end points, i.e., points where one or more phases coexist with others that are critical. Consequently the number of variables  $n$  needed to obtain a point where four phases are simultaneously critical was reduced from six to four.

For tricritical points in fluids, it is possible to artificially reduce the number of variables and eliminate the lines of critical end points from the phase diagram. For example, Fig. 1(b) is an illustration of this since it is a three-dimensional

section of the four-dimensional field space with all lines of critical points ending at the tricritical point. Similarly the  $h = 0$  section of Fig. 2 produces the same result. Griffiths<sup>8</sup> has shown how a similar phase diagram can be obtained by taking the section  $a_3 = 0$  of his four-dimensional phase diagram with variables  $a_1, a_2, a_3, a_4$ .

Let us now return to the case of the intersecting lines of tricritical points in the variable interaction metamagnet. It has been shown<sup>10</sup> that the point of intersection (the point of order 4) is a point where four phases become simultaneously critical. Thus in this case the definition of order suggested by us coincides with the definition suggested by Widom.<sup>7</sup> This fact may be generalized, because the only reason there should be more than one line of tricritical points is because there are more than three phases available. The different lines of tricritical points will intersect at points where more than three phases become simultaneously critical.

To obtain a version of Eq. (1) which is satisfied by all the cases considered so far, it is necessary to consider the number of variables which possess nonzero scaling power at the point under consideration. It is important to note that this number may be less than the number of significant directions picked out by the phase diagram. For example, on an ordinary line of critical points three directions are determined, but only two (the strong and weak) are associated with variables which scale. Alternatively, on the line of critical end points  $P, P_t, P'$ , all four of the directions (i)–(iv) are defined but only (i) and (ii) are associated with variables which scale (except at  $P_t$  where all four enter the scaling equation). The implications of the simple Landau model<sup>8</sup> are that for fluids the number of scaling directions  $s = 2(q - 1)$ . Another quantity that is important is the number of phases which are in equilibrium but which are not critical,  $x = p - q$ . In terms of the variables  $s$  and  $x$ , Eq. (1) may be rewritten as<sup>13</sup>

$$s + x + d = n. \quad (2)$$

It will be seen that this equation also holds for the old tricritical points, and the intersection of lines of tricritical points. It is satisfied by construction from (1) by all the points in generalizations of Widom's scheme for which the order is given by  $\Theta = q = \frac{1}{2}s + 1$  and by all the points in our scheme<sup>5</sup> for which the order is given by  $\Theta = s$ . These two possibilities express, respectively, the maximum and minimum number of scaling variables at a point where  $\Theta$  phases became critical,  $\Theta \leq s \leq 2(\Theta - 1)$ . For  $\Theta = 2$  there is only one possibility,  $s = 2$ ; for  $\Theta = 3$  there are two cases,  $s = 3, 4$ ; and for  $\Theta > 3$  there are many possibilities.



Thus we have proposed<sup>5</sup> a minimal scheme for complex critical points whereas Widom and Griffiths have proposed a maximal scheme.

In conclusion it should be reiterated that while the definition of order for critical points suggested in Ref. 5 does not appear to be applicable to fluids, it is consistent with the definition in terms of the number of phases becoming critical.<sup>7</sup>

#### ACKNOWLEDGMENT

We would like to thank Professor B. Widom and Professor R. B. Griffiths for drawing our attention to the references cited in the Soviet literature in this manuscript and for stimulating conversations. Also thanks are due to R. B. G. for comments on a previous version of this paper.

\*Supported in part by the U. S. Atomic Energy Commission, the National Science Foundation, the National Aeronautics and Space Administration, the Office of Naval Research, and the Air Force Office of Scientific Research.

†Lindemann Fellow.

‡Permanent address: Riddick Laboratories, North Carolina State University, Raleigh, N. C. 27607.

§Address to whom requests for reprints should be sent.

<sup>1</sup>R. B. Griffiths, Phys. Rev. Lett. 24, 715 (1970).

<sup>2</sup>V. A. Schmidt and S. A. Friedberg, Phys. Rev. B 1, 2250 (1970); F. Harbus and H. E. Stanley, Phys. Rev. Lett. 29, 58 (1972); Phys. Rev. B 8, 1141 (1973) and B 8, 1156 (1973).

<sup>3</sup>G. Goellner and H. Meyer, Phys. Rev. Lett. 26, 1543 (1971).

<sup>4</sup>C. W. Garland and B. B. Weiner, Phys. Rev. B 3, 1634 (1971).

<sup>5</sup>(a) T. S. Chang, A. Hankey, and H. E. Stanley, Phys. Rev. B 8, 346 (1973); (b) A. Hankey, T. S. Chang, and

H. E. Stanley, Phys. Rev. B 8, 1178 (1973). Preliminary accounts of this work are given by A. Hankey, T. S. Chang, and H. E. Stanley, AIP Conf. Proc. 10, 889 (1972).

<sup>6</sup>B. Widom and R. B. Griffiths, Phys. Rev. A 8, 2173 (1973).

<sup>7</sup>B. Widom, J. Phys. Chem. 77, 2196 (1973).

<sup>8</sup>R. B. Griffiths, Cornell University Material Science Center Report No. 1995 (unpublished).

<sup>9</sup>R. B. Griffiths and J. C. Wheeler, Phys. Rev. A 2, 1047 (1970).

<sup>10</sup>F. Harbus, A. Hankey, H. E. Stanley, and T. S. Chang, Phys. Rev. B 8, 2273 (1973).

<sup>11</sup>R. B. Griffiths (private communication).

<sup>12</sup>G. D. Efremova and A. V. Shvarts, Russ. J. of Phys. Chem. 43, 968 (1969).

<sup>13</sup>We are much indebted to J. Nicoll for discussions leading to this equation. A more complete account will be given in a separate paper.



# Generalized Scaling Hypothesis in Multicomponent Systems. I. Classification of Critical Points by Order and Scaling at Tricritical Points\*

T. S. Chang,<sup>†</sup> Alex Hankey,<sup>‡</sup> and H. Eugene Stanley<sup>§</sup>

Department of Physics, Massachusetts Institute of Technology, Cambridge, Massachusetts 02139

(Received 10 October 1972; revised manuscript received 29 January 1973)

The goal of this work is to provide an analysis of spaces of critical points for multicomponent systems. First, we propose the geometric concept of order  $\Theta$  for critical points; we distinguish it from a previous definition of a "multicritical" point. Specifically, we may define the intersection of spaces of critical points of order  $\Theta$  to be a space of critical points of order  $(\Theta+1)$ . Ordinary critical points are defined to be of order  $\Theta=2$ , so that the tricritical points introduced by Griffiths are of order  $\Theta=3$ . We discuss more general examples of critical spaces of order  $\Theta=3$  which are known for a wide variety of systems; we also propose several examples of models of magnetic systems showing critical points of order  $\Theta=4$ —i.e., systems having *intersecting lines of tricritical points*. The analysis of critical and coexistence spaces also provides a new form of the Gibbs phase rule suitable for complex magnetic models. Next we define—for the critical points of order  $\Theta$  of which examples have been given—special directions in terms of which to make a scaling hypothesis. We give the hypothesis for simple systems and then for tricritical points, and then, in a subsequent paper, part II, the special directions are used to make a scaling hypothesis at spaces of critical points of any order. Certain predictions (e.g., scaling laws and "single-power" scaling functions) follow in a simple and straightforward fashion. We consider the scaling hypothesis at a critical space of order  $\Theta$  in terms of a group of transformations. We can define a set of invariants of the group. It is possible, for  $\Theta \geq 3$ , to make a *second* scaling hypothesis for the space of order  $\Theta-1$  using certain of these invariants as *independent* variables. This is advantageous because certain "double-power" scaling functions then follow directly; these predict that for  $\Theta=3$ , experimental data collapse from a *volume* onto a *line*. This prediction is to be contrasted with ordinary scaling functions, which predict that data collapse by only a single dimension (e.g., from a volume onto a surface or from a surface onto a line).

## I. INTRODUCTION: THE ORDER OF A CRITICAL POINT

The purpose of this work is (i) to propose the concept of the "order" of a critical point, (ii) to give examples of critical points of orders three and four, and (iii) to present a form of the scaling hypothesis for spaces of *arbitrary* order. The work is divided into two parts. In this paper (I), we focus upon concrete examples illustrating critical points and scaling at critical points of order three, while in a subsequent paper<sup>1</sup> (II), we consider scaling for spaces of arbitrary order. First, we must develop the concept of the order of a critical point, and that is the task of this section.

The scaling hypothesis was originally formulated for the critical point of a simple magnet and a simple fluid.<sup>2-4</sup> These systems each have two purely intensive variables  $[(H, T)$  and  $(P, T)$ , respectively]. Such variables we call *fields*, adopting the terminology of Griffiths and Wheeler.<sup>5</sup>

A very wide variety of physical systems whose critical phenomena are under active study have more than two field variables; two common examples are antiferromagnets and binary mixtures. In such systems, one can have lines (or, in general, spaces of dimension larger than one) of critical points. Recently, special attention has come to focus on those systems for which *three* lines of

critical points intersect, and the point of intersection has been called a *tricritical point* by Griffiths.<sup>6</sup>

The scaling hypothesis has recently been extended<sup>7</sup> to treat some (but not all) aspects of this novel type of "critical point". In this work we present a comprehensive scaling treatment of general multicomponent systems. First we give a detailed treatment of tricritical points. Our approach is then generalized to more complex situations.

One example of a more complex situation is a system for which *four* lines of critical points intersect; in a natural extension of Griffiths's terminology, Nagle and Bonner<sup>8</sup> have called such points tetracritical points. We show here that, in the particular case studied by those authors, *the tetracritical point is qualitatively the same as a tricritical point* in the sense that the formulation of the scaling hypothesis there is the same as at tricritical points.

Qualitatively different points ("spaces")<sup>9</sup> can be achieved in systems with more than three field variables; a more general scaling hypothesis is needed and correspondingly more predictions are obtained. These are discussed in detail in Paper II.

Two simple examples of systems with more than three field variables are provided by  $\text{He}^3\text{-He}^4$  and ammonium chloride, and both these systems



show lines of tricritical points.

Liquid  $\text{He}^3\text{-He}^4$  mixtures have thermodynamic variables  $[P, T, \mu_4 - \mu_3, \eta]$ , where  $P$  denotes pressure,  $T$  denotes temperature,  $\mu_4$  and  $\mu_3$  are the chemical potentials of  $\text{He}^4$  and  $\text{He}^3$ , respectively, and  $\eta$  is a variable conjugate to the superfluid density. The " $\lambda$  line" in the  $P$ - $T$  plane becomes a two-dimensional surface of singularities with increasing mole fraction of  $\text{He}^3$ . This surface terminates at a line of special points,<sup>10(a)</sup> which is in fact a line of tricritical points.

Ammonium chloride possesses an order-disorder transition for which the transition temperature increases with increasing pressure, and changes from first order to second order at a tricritical point. If one replaces some of the hydrogen by deuterium in the ammonium group,<sup>10(b)</sup> then the position of the tricritical point (and the whole line of order-disorder transitions) changes. The variables are thus  $(P, T, \mu_H - \mu_D, \eta)$ , where  $\eta$  is a variable conjugate to the order parameter.

In a system of sufficient complexity, several lines of tricritical points can occur. A point of intersection of lines of tricritical points is qualitatively different from a point where lines of ordinary critical points intersect. This should be clear from the topology of the situation: At a line of tricritical points, surfaces of critical points meet, while at a point where lines of tricritical points intersect, several surfaces of critical points (bounded on each side by the tricritical lines) converge on the point.

To distinguish such points—and in general spaces of such points—we will refer to them as critical points of higher order, and we will associate a number with each order as follows. We define ordinary critical points to be of order  $\phi = 2$ ; then a critical point (or space of points) of order  $\phi + 1$  ( $\phi \geq 2$ ) is defined to be a special point where lines (or spaces) of points of order  $\phi$  intersect. Thus a tricritical point is of order  $\phi = 3$  and a point of intersection of lines of tricritical points is of order  $\phi = 4$ .

Griffiths and Wheeler<sup>5</sup> reasoned that the dimensionality of a space of ordinary critical points (of order  $\phi = 2$ ) is  $(n - 2)$ . In the systems we consider below the dimensionality,  $d$ , of a space of critical points of order  $\phi$  is always one less than the dimensionality of the spaces of critical points of order  $(\phi - 1)$  which intersect at it. Therefore, we find the value of  $d$  for arbitrary  $\phi$  by induction from  $\phi = 2$  to be, in these cases,

$$d = n - \phi, \quad (1.1)$$

where  $n$  is the total number of field (and fieldlike)<sup>11</sup> variables available.

Critical points of complex thermodynamic systems can also be analyzed by making the scaling

hypothesis from the outset. The significant quantity is then the number of relevant scaling variables. Using the renormalization group, it has been suggested<sup>12</sup> how more than two relevant scaling variables can occur, but the geometry of the phase diagram was not considered at all. In most of the examples known to the authors, the number of significant scaling directions is equal to the order. This may not always be true for more complex systems [e.g., fluid mixtures, for which Eq. (1.1) may need modification, becoming  $d \leq n - \phi$ ].

A specific example which demonstrates the importance of distinguishing the order of a critical point from the number of critical lines meeting there is the tetracritical point. This is a point of order  $\phi = 3$  with true field variables  $(H, H_2, T)$ , where  $H$  and  $H_2$  are direct and staggered (i.e., wavelength 2 lattice sites) magnetic fields. When a fieldlike variable  $\tilde{\alpha}$  (the ratio of short- to long-range-interaction strengths) is also included, (i.e.,  $n = 4$ ), Eq. (1.1) indicates that the system has a line of critical points of order  $\phi = 3$ . This is verified in the analysis of Sec. III, where it is shown that in this model there are three surfaces of critical points of order  $\phi = 2$ , meeting at the line of points of order  $\phi = 3$ . The tetracritical point is simply a point on a smooth line of tricritical points; the "tetracritical point" arises because we have chosen a section of the four-dimensional  $(H, H_2, T, \tilde{\alpha})$  space that is tangent to the line of tricritical points, rather than a section which intersects it.

First we give, in Sec. II, examples of systems exhibiting spaces of critical points of order  $\phi \geq 3$ , and explain a convenient notation for the phase diagrams of such systems. This leads to an equation equivalent to the Gibbs phase rule.

In Sec. III we explicitly demonstrate the importance of distinguishing between the order of a critical point and the number of lines meeting at a critical point—the former leads to an essential increase in complexity, while the latter does not. To do this, we compare several one-dimensional Ising models with long-range interactions, all of which are exactly soluble.

Special directions at spaces of order  $\phi$  are defined in Sec. IV; these are analogous to the strong and weak directions defined by Griffiths and Wheeler.<sup>5</sup> A way of deriving these directions for tricritical points using the renormalization group approach has been pointed out by Riedel and Wegner.<sup>12(c)</sup>

To make the formulation of a scaling hypothesis easier to follow, we give an account in Sec. V of the scaling hypothesis using generalized homogeneous functions and equations invariant under a one-parameter continuous group of transformations at points of order 2.

In Sec. VI we give a full account of the scaling



hypothesis at tricritical points and we include an account of a space of invariant variables as a very useful way to derive "double-power" scaling functions and to plot "crossover surfaces". These predictions have not yet been tested experimentally.

We present the scaling hypothesis at a critical point of arbitrary order in Paper II. The hypothesis is framed as a sequence of operations to be repeated as the hypothesis is formed successively at critical points of decreasing order. The proposed sequence is illustrated by detailed consideration of a system of Ising planes with a variable interplanar interaction.

## II. SYSTEMS EXHIBITING CRITICAL POINTS OF ORDER HIGHER THAN TWO: NOTATION FOR SUCH POINTS

Critical points more complex than ordinary  $\phi=2$  critical points have been found in many experimental and theoretical systems. Without doubt, the systems exhibiting the richest possibilities are multicomponent fluid mixtures; however, specific examples of critical points of order three or more in these systems have yet to be found.

Systems on which experiments have been analyzed are liquid helium,<sup>10(a)</sup> ammonium chloride,<sup>10(b)</sup> metamagnets,<sup>13</sup> and anisotropic antiferromagnets.<sup>14</sup> In addition, one-dimensional magnetic models provide a rich opportunity for theoretical and numerical investigations. Liquid helium<sup>10(a)</sup> and  $\text{NH}_4\text{Cl}$ <sup>10(b)</sup> provide excellent examples where there exist lines of tricritical points—as discussed in Sec. I. In metamagnets,<sup>13</sup> lines of tricritical points can be generated by introducing transverse fields, and also by introducing a parameter into the Hamiltonian which changes the strength of the interaction. Decreasing the latter causes the tricritical points to converge to a point on the temperature axis; this point is a critical point of order 4 and is treated in more detail below.

An anisotropic antiferromagnet,<sup>14</sup> which exhibits a spin-flop transition, contains a point in its phase diagram where two lines of ordinary critical points intersect a line of first-order transitions. This special point has an order of at least 3, but whether it is 3 or more has yet to be determined.

To be able to discuss phenomena in phase diagrams of any complexity easily, we introduce a notation for spaces of points where several phases coexist and for critical points of arbitrary order  $\phi$ . Critical spaces are denoted by an abbreviation of the notation CRS of Griffiths and Wheeler<sup>5</sup>; the order of the space will be given a preceding superscript and the dimensionality a subscript, and hence a critical space of order  $\phi$  and dimensionality  $d$  is written as  ${}^\phi R_d$ . The relation between  $\phi$ ,  $d$ , and the total number  $n$  of field (or fieldlike) variables, in general, is given by Eq. (1.1),  $\phi = n - d$ .

Coexistence spaces are designated by an abbrevi-

ation of the Griffiths-Wheeler notation CXS but now the number of coexisting phases is given by the preceding superscript; hence the general space of dimension  $d$  where  $p$  phases coexist is written as  ${}^p X_d$ . The equation analogous to Eq. (1.1) is

$$p = n - d + 1. \quad (2.1)$$

The dimension  $d$  of the CXS may be interpreted as the number of "degrees of freedom",  $f$ , and for a chemical system  $n$  is one greater than the number of components  $c$ . Thus (2.1) is similar to the usual statement of the Gibbs phase rule,  $p \geq c - f + 2$ , but it is in a form valid for all the systems considered in this work. The Gibbs phase rule contains an inequality because it refers to any phase diagram, even those in a restricted space of fields. For example, the  ${}^2 X_2$  in the  $H$ - $T$  plane of a simple nearest-neighbor antiferromagnet (with field variables  $H$ ,  $H_2$ , and  $T$ ) satisfies Eq. (2.1) as an equality providing all three fields are considered, but as an inequality if only  $T$  and  $H$  are considered. Consideration of other models<sup>6,15</sup> leads us to conclude that Eq. (2.1) is satisfied as an equality (for  $T > 0$ ) if and only if a sufficient set of conjugate fields (i.e., conjugate to every possible phase of the system) has been introduced. Thus Eq. (2.1) can be used as a criterion for whether enough conjugate fields have been considered or not. It is noteworthy that Eqs. (1.1) and (2.1) depend only on topologically significant quantities like the dimension of a subspace in the phase diagram, and should therefore be understood as topological statements.

To illustrate the notation and to provide a good example of a system with a phase diagram exhibiting critical spaces of orders 2, 3, and 4, we consider the  $d=3$  Ising model with variable interaction strength  $\mathcal{R}J$  between planes of constant  $z$ :

$$\mathcal{H} = - \sum_{x,y,z} S_{x,y,z} [J(S_{x+1,y,z} + S_{x,y+1,z}) + \mathcal{R}J S_{x,y,z+1} + H + (-1)^z H_2]. \quad (2.2)$$

Here the symbol  $S_{x,y,z}$  is the value of the spin on lattice site with coordinates  $(x, y, z)$ . The variable  $\mathcal{R}$  allows for a variation in the strength of interaction in the  $z$  direction. The phase diagram of this model is four dimensional, with fields  $H$ ,  $H_2$ ,  $T$ , and the fieldlike variable  $\mathcal{R}$ . For  $\mathcal{R} > 0$ , we have a three-dimensional Ising model with "lattice anisotropy," which tends as  $\mathcal{R} \rightarrow 0$  to the two-dimensional Ising model. The invariance of the Hamiltonian under the transformation  $S_{x,y,z} \rightarrow (-1)^z S_{x,y,z}$ ,  $\mathcal{R} \rightarrow -\mathcal{R}$ ,  $H \rightarrow H_2$ , and  $H_2 \rightarrow H$  relates the phase diagram for  $\mathcal{R} < 0$  to that for  $\mathcal{R} > 0$ .

For  $\mathcal{R} < 0$ , Eq. (2.2) describes a metamagnet. The phase diagram of this system is well known and shown in Fig. 1. As  $|\mathcal{R}|$  is decreased, the values of  $T_t$  and  $T_N$  decrease (unpublished results



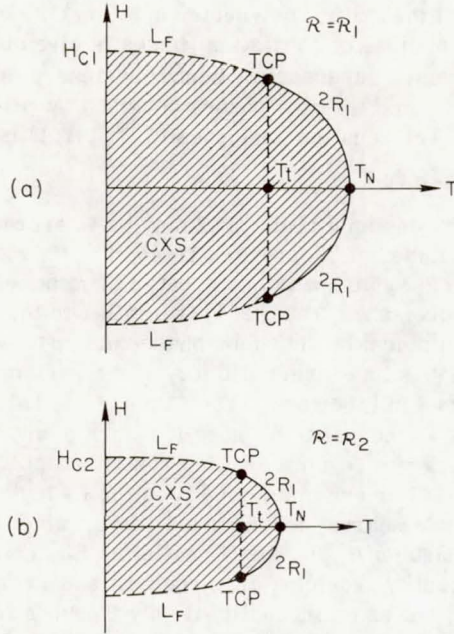


FIG. 1. (a) Phase diagram for  $R = R_1 < 0$ , in the  $(H, T)$  plane ( $H' = 0$ ). The  ${}^2R_1$  terminates at a pair of tricritical points ( ${}^3R_0$ ) shown as TCP. The  ${}^2X_2$  separating the anti-ferromagnetic phases  $A^+A^-$  is bounded below the tricritical temperature  $T_t$  by the lines of first-order transitions  $L_F$ , which terminate at a magnetic field value  $H_{C1}$ . (b) The same for  $R_2 < 0$ , where  $|R_2| < |R_1|$ . Note that  $H_{C2} < H_{C1}$  and that both  $T_t$  and  $T_N$  have decreased. See also, F. Harbus *et al.*, Ref. 1.

of F. Harbus). This is shown in the Fig. 1(b) as compared to Fig. 1(a).

As  $|R| \rightarrow 0$ , the behavior of  $T_N(R)$  is described by the well-known crossover exponent and symmetry between  $R < 0$  and  $R > 0$  mentioned above shows that in the plane  $H = H_2 = 0$  there is a reflection symmetry about  $R = 0$ .

From these considerations we obtain Fig. 2, which is a three-dimensional phase diagram in the  $H_2 = 0$  plane. For  $R < 0$  and constant, there is a phase diagram like Fig. 1, and for  $R > 0$  the ordinary crossover behavior holds.

The two tricritical points in Fig. 1 become lines of critical points of order 3,  ${}^3R_1$ , in Fig. 2. The symmetry of the Hamiltonian shows that there are two additional  ${}^3R_1$  for  $R > 0$  at nonzero  $H_2$ . The symmetry of the Hamiltonian forces these four lines (tricritical lines) to converge upon a point lying on the temperature axis—a critical point of order 4. On the temperature axis below the  ${}^4R_0$  four phases are in coexistence: it is a  ${}^4X_1$ .

The validity of Eqs. (1.1) and (2.1) may be verified and it can also be seen that in this system a  ${}^pX_{d+1}$  is bounded for increasing  $T$  by a  ${}^pR_d$ , where  $\phi = p$ . A CXS which in the full phase diagram is a  ${}^pX_{d+1}$  is, when considered in the zero-temperature

plane, only a  ${}^pX_d$ . In the model considered in this section, therefore, a coexistence hypersurface which in the  $T = 0$  phase diagram is a  ${}^pX_d$  evolves as the temperature increases into an  ${}^pR_d$ , with  $\phi = p$ . In other words, the space of critical points of order  $\phi$  is the upper bound (as temperature increases) of a space of points where  $\phi$  phases coexist.

This is a very significant point and can be understood by examples, and from the following consideration. In a phase diagram, a space where three phases coexist is necessarily a place of intersection of spaces where two phases coexist. The spaces where two phases coexist are bounded from above by spaces of critical points of order two. Therefore, the upper bound of the space where three phases coexist is either the boundary of one critical space of order 2 or the intersection of all three critical spaces of order 2. Because of the symmetry properties holding in the present model, and

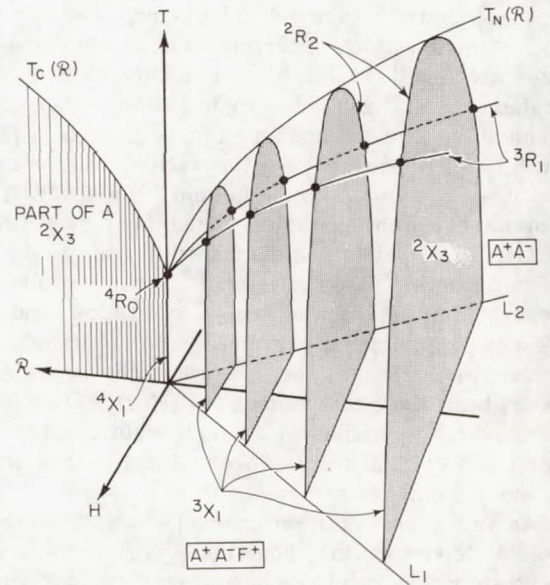


FIG. 2. Phase diagram in the  $H_2 = 0$  hyperplane for Ising model with variable interplanar interaction. For  $R < 0$  the  $R = \text{const}$  sections are similar to Fig. 1. These sections are schematically shaded. As  $R$  varies continuously the  ${}^pX_d$  and  ${}^pR_d$  of Fig. 1 become  ${}^pX_{d+1}$  and  ${}^pR_{d+1}$ . Thus the  ${}^2X_2$  of Fig. 1 becomes the interior of the "mountain"; this is a  ${}^2X_3$  separating phases  $A^+$ ,  $A^-$ . The lines  $L_F$  where three phases coexist become surfaces of the mountain ( ${}^3X_2$ ) below the line of tricritical points  ${}^3R_1$  corresponding to TCP of Fig. 1. The  ${}^2R_1$  of Fig. 1 becomes a  ${}^2R_2$ , the top of the "mountain" in Fig. 2. The  $T$  axis becomes a line of special points where all four phases  $A^+$ ,  $A^-$  and the ferromagnetic  $F^+$  and  $F^-$  all coexist; it is a  ${}^4X_0$ . The  ${}^3R_1$  meet at the  $T$  axis at the end of this line; at a  ${}^4R_0$ . The region  $R > 0$  appears simpler because it corresponds to the  $(H = 0)$  section of  $R < 0$ , and the rest of the mountain occurs at  $H_2 \neq 0$ . See also, F. Harbus *et al.*, Ref. 1.



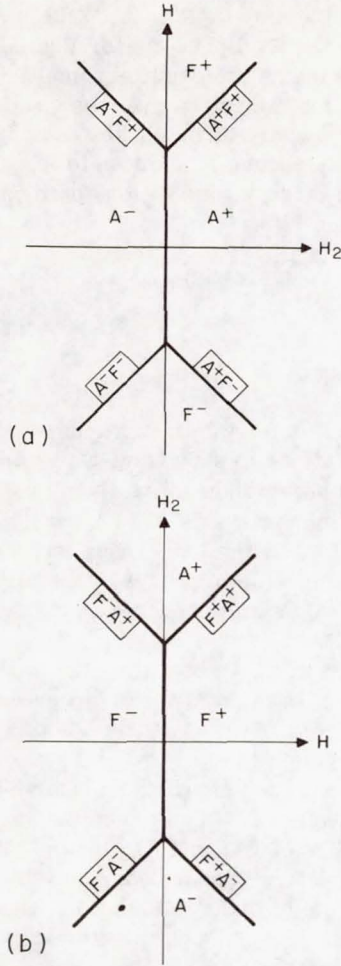


FIG. 3. The phase diagram at  $T=0$  of an Ising (a) anti-ferromagnet and (b) ferromagnet. The phases with spins parallel are indicated by  $F^\pm$  and with spins antiparallel by  $A^\pm$ . The lines indicate where the various phases are in equilibrium.

also because it is an Ising model, the latter condition holds. An entirely analogous argument can be constructed for critical points of order 4 or more.

It is therefore possible, for Ising models, to make predictions about the relationships between  $^0R_d$  in the full phase diagram, by considering the relationships between the  $^bX_d$  in the  $T=0$  phase diagram. We will make extensive use of this method in Sec. III.

### III. SPACES OF TRICRITICAL POINTS IN ONE-DIMENSIONAL MODELS

There has been much work recently on one-dimensional Ising models possessing a long-range interaction.<sup>8,15</sup> The effect of this interaction is to shift the critical temperature from the value  $T=0$  to a nonzero temperature, thereby enabling the critical points to obey scaling laws.

The purpose of this section is to display two

models for which critical points of order  $\phi=4$  occur; these are both Ising models with long-range interactions.<sup>16</sup>

Models exhibiting a critical point of order 4 also possess a line of points where four phases coexist, as explained at the end of Sec. II. Therefore, a simple method of deciding whether a particular model can possess a critical point of order 4 is to analyze the  $T=0$  hyperplane of the phase diagram and see if points where four phases coexist continue to have four distinct phases in equilibrium as  $T$  is increased. Cases where this does and does not happen are discussed below.

Before analyzing a case where there is a long-range interaction, let us consider the  $T=0$  phase diagram of a one-dimensional Ising antiferromagnet with only nearest-neighbor interactions.

#### Hamiltonians

The Hamiltonian is given by

$$\mathcal{H}_{\text{SR}} = -J_{\text{SR}} \sum_{i=1}^{N-1} s_i s_{i+1} - H \sum_{i=1}^N s_i - H_2 \sum_{i=1}^N (-)^{i+1} s_i, \quad (3.1)$$

where  $J_{\text{SR}}$  is the nearest-neighbor (nn) interaction strength and  $s_i = \pm 1$  are the Ising spins situated at site  $i$  of the chain. When  $J_{\text{SR}} > 0$  the interaction is ferromagnetic and when  $J_{\text{SR}} < 0$  the interaction is antiferromagnetic.  $H$  is the magnetic field and  $H_2$  is the staggered magnetic field of wavelength 2 lattice sites. The phase diagram will appear as in Fig. 3(a). Here the four phases  $F^\pm$ ,  $A^\pm$  are defined in Table I:  $F$  means ferromagnetic and  $A$  means antiferromagnetic. The  $T=0$  "critical point" of the

TABLE I. Definitions, energies, and equations of Figs. 3 and 5. Here  $\tilde{R} \equiv J_{\text{SR}}/J_{\text{LR}}$ ;  $h \equiv H/J_{\text{LR}}$ ;  $h_2 \equiv H_2/J_{\text{LR}}$ . Star means not shown in Fig. 5.

Configuration	Name	Field	Energy
$\uparrow \uparrow$	$F^+$	$H$	$E_F = -J_{\text{LR}} - J_{\text{SR}} - H$
$\downarrow \downarrow$	$F^-$		
$\uparrow \downarrow$	$A^+$	$H_2$	$E_2 = +J_{\text{SR}} - H_2$
$\downarrow \uparrow$	$A^-$		
Surface	Equation	Line	Equation
$[F^+, F^-]$	$H=0$	$L_1$	$h_2 = 1 + 2\tilde{R}; h=0$
			$\tilde{R} > -\frac{1}{2}$
$[A^+, A^-]$	$H_2=0$	$L_2$	$h_2 = 1 - 2\tilde{R}; h=0$
$[F^+, A^+]^*$	$h - h_2 + 1 + 2\tilde{R} = 0$	$L_3$	$h = -1 - 2\tilde{R}; h_2 = 0$
			$\tilde{R} < -\frac{1}{2}$
$[F^-, A^-]^*$	$h - h_2 - 1 + 2\tilde{R} = 0$	$L_4$	$h = -1 + 2\tilde{R}; h_2 = 0$
$[F^+, A^-]^*$	$h + h_2 + 1 + 2\tilde{R} = 0$		
$[F^-, A^+]^*$	$h + h_2 - 1 - 2\tilde{R} = 0$		



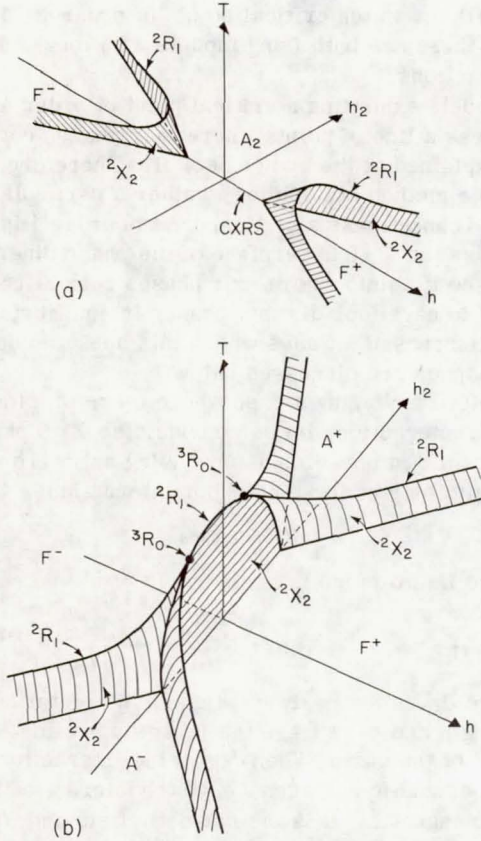


FIG. 4. (a) The extension of Fig. 3(a) into the space with  $T > 0$  when a weak long-range interaction is included. Note that the  $T = 0$  plane corresponds to Fig. 3(a), and that the  $[A^+, A^-]$  phase boundary only separates phases at  $T = 0$ . The other lines in Fig. 3(a) develop normally, giving coexistence surfaces ( ${}^2X_2$ ) ending in critical lines  ${}^2R_1$ . (b) The phase diagram of the same model but without the antiferromagnetic interaction ( $J_{SR} = 0$  or  $J_{SR} > 0$ ). Now all lines in the  $T = 0$  plane become coexistence surfaces  ${}^2X_2$ . The points of interaction become  ${}^3X_1$  (lines where three phases coexist) and there terminate at two  ${}^3R_0$  (triple critical points).

Ising antiferromagnet becomes a *line* of critical points for nonzero values of magnetic field. This line bifurcates at points where it is energetically more favorable<sup>17</sup> for the system to order ferromagnetically (i.e., with all spins parallel).

Normal scaling laws do not apply to one-dimensional Ising models with short-range interactions, as these display essential singularities at the  $T = 0$  critical point. Thus the lines in Fig. 3(a) are lines of both critical points and coexistence points. These lines do not have very much in common with either the conventional critical points  ${}^2R_d$  or the conventional coexistence surfaces  ${}^2X_d$  that divide up the field space at finite values of temperature. A suitable nomenclature for the lines of Fig. 3(a) might be "coexistence-critical surfaces" and we

will denote them by CXRS. A CXRS is necessarily confined to the  $T = 0$  plane as for Fig. 3(a). Thus we see that the nn Ising antiferromagnet contains five CXRS lines where two phases coexist and two CXRS points where three phases coexist.

Then we introduce in addition to  $\mathcal{H}_{SR}$  of Eq. (3.1), a long-range interaction, defined by the Hamiltonian

$$\mathcal{H}_{LR} = - \sum_{i=1}^N \sum_r J(r) s_i s_{i+r}, \quad (3.2a)$$

where

$$J(r) = \lim_{\gamma \rightarrow 0} a\gamma e^{-\gamma|r|}, \quad (3.2b)$$

the phases  $F^*$  are stabilized at nonzero temperature and continue to show long-range order for  $T > 0$ . The phase diagram is given in Fig. 4(a). The CXRS [on the  $H$  axis of Fig. 3(a)] is not stabilized at  $T > 0$  by the long-range interaction; the two antiferromagnetic phases  $A^*$  coexisting at the CXRS at  $T = 0$ , simply become a single disordered phase for  $T > 0$ .

There are two  ${}^2X_2$  separating the ordered (ferromagnetic) phase from the disordered phase at higher temperatures. These  ${}^2X_2$  end in  ${}^2R_1$  (lines of critical points).

If the dominating nearest-neighbor interactions are ferromagnetic,  $J_{SR} > 0$ , then the situation depicted in Figs. 3(b) and 4(b) results. The two points where three phases coexist at  $T = 0$  become the end points of two  ${}^3X_1$  lines where three phases coexist. Each  ${}^3X_1$  line terminates at a  ${}^3R_0$  (a triple critical point).

If sufficient care is taken to decide whether a space in the  $T = 0$  hyperplane is a CXRS or a CXS, then the nature of the extension of the space and its subspaces into  $T > 0$  can be easily ascertained. The rules exemplified from Figs. 3 and 4 are the following: (i) Two phases which can only be distinguished by a staggered magnetic field coexist on a CXRS. (ii) Such staggered phases give only one phase for  $T > 0$ . (iii) A line where one phase which maintains order for  $T > 0$  coexists with any other phase is *always* a CXS. (iv) A point where a CXRS meets a CXS has no special properties. It is simply a point on a CXS.

Using these rules we can analyze the model of Nagle and Bonner<sup>8</sup> which includes a long-range interaction, a variable short-range interaction, and the two fields of Fig. 3.<sup>18</sup> A point where four critical lines meet, a tetracritical point, is known for this model. We will show here that this point is a critical point of order 3. Since a variant of this model, which we discuss below, shows a critical point of order 4, it is worth treating the Nagle-Bonner model in some detail first.

Figure 5 depicts the surfaces of coexistence of the four phases in the  $T = 0$  plane. Definitions and



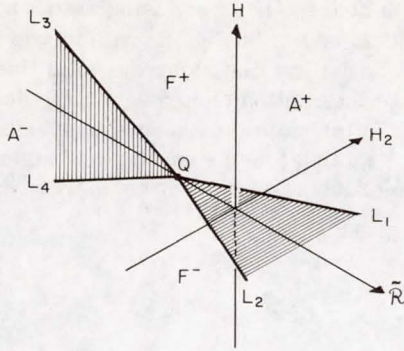


FIG. 5.  $T=0$  hyperplane for an Ising model with competing long- and short-range interactions. Here  $\tilde{R} \equiv J_{SR}/J_{LR}$  and  $H_2$  is a staggered magnetic field of wavelength 2 lattice sites. The lines  $L_1, L_2$  are in the  $(H_2, \tilde{R})$  plane, and the lines  $L_3, L_4$  are in the  $(H, \tilde{R})$  plane. The surfaces  $[A^+F^+]$ ,  $[A^+F^-]$ ,  $[F^+, A^+]$ ,  $[F^-, A^+]$  have been omitted. The surface  $[A^+, A^-]$  is a CXRS, Fig. 3(a) is an  $(H_2, H)$  plane for  $\tilde{R} < \tilde{R}_Q$ , while Fig. 3(b) is for  $\tilde{R} > \tilde{R}_Q$ .

equations are given in Table I. For clarity four surfaces are omitted; e.g., those that separate the phases  $[F^+A^+]$ ,  $[F^+A^-]$ ,  $[F^-A^-]$ , and  $[F^-A^+]$ . As may be seen there are four lines where three phases coexist and a point  $Q$  where all four phases coexist. The surface  $[A^+A^-]$  bounded by the lines  $L_3, L_4$ , is a CXRS since for constant values of  $\tilde{R}$  less than  $\tilde{R}_Q$ , the phase diagrams are the same as Figs. 3(a) and 4(a). Here

$$\tilde{R} \equiv J_{SR}/J_{LR}, \quad (3.3)$$

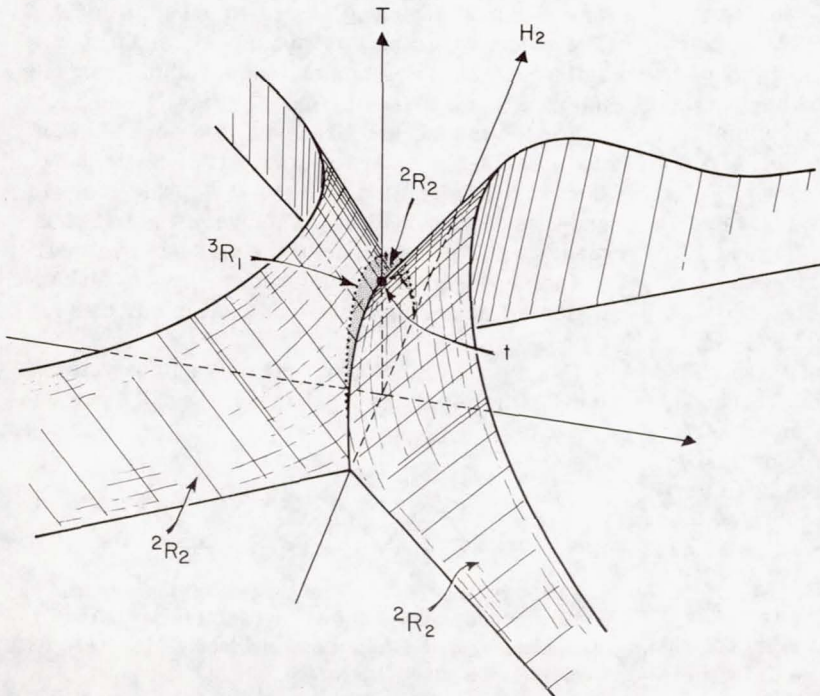


FIG. 7. Ray projection of the four-dimensional space, from  $Q$  onto  $\tilde{R}=0$  showing the topology of the surfaces of critical points. The  $\tilde{R}$  axis in Figs. 5 and 6 has become a combination of  $\tilde{R}$  and  $h$ . The curved  $^2R_2$  surfaces are the ends of those surfaces which end on  $L_3$  and  $L_4$  of Fig. 5. The  $^2R_1$  of Figs. 4(a) and 4(b) are lines in this surface. The flat  $^2R_2$  shown in the  $(T, H_2)$  plane is the surface  $^2R_2$  of Fig. 6.

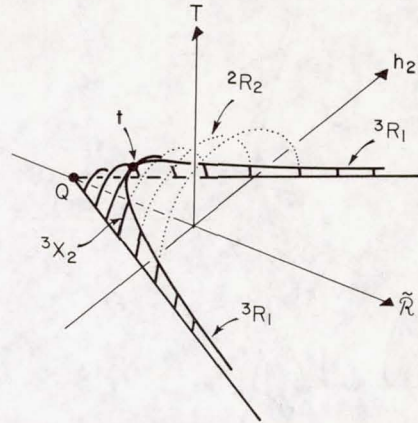


FIG. 6.  $H=0$  hyperplane of the model of Fig. 5. The lines  $L_1, L_2$  extend into  $T > 0$ . The lines where three phases coexist in Fig. 4(b) have become a single surface, denoted here by  $^3X_2$ . This terminates at a line of tri-critical points  $^3R_1$ ; the  $^3R_1$  also bounds a surface of ordinary critical points  $^2R_2$ . The point  $t$  where the  $^3R_1$  intersects the plane  $h_2=0$  is the location of the tetracritical point (Ref. 8). The  $\tilde{R}=0$  section of this figure corresponds to the  $H=0$  section of Fig. 4(b). Note that at  $t$  a surface  $\tilde{R}=\text{const}$  is parallel to the  $^3R_1$ .

where  $J_{LR}$  is the "equivalent neighbor" long-range parameter.<sup>8</sup>

For  $T \neq 0$ , the two  $^2X_2$  surfaces  $[A^+F^+]$  and  $[A^+F^-]$  of Fig. 5 end in a single surface of critical points, and the same is true for the  $[A^-F^-]$ ,  $[A^-F^+]$  surfaces; this is shown in Fig. 4(a).

The point  $Q$  of Fig. 5, where four phases coexist,



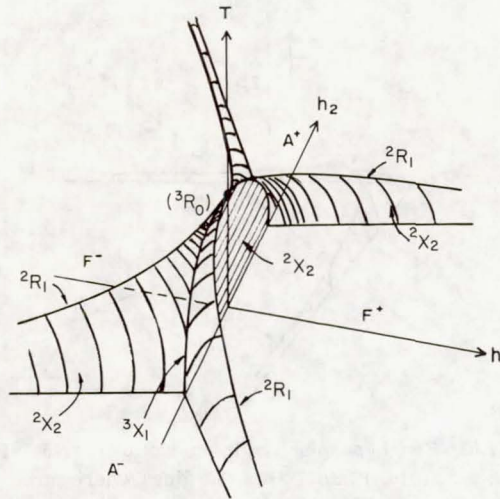


FIG. 8. Plot of the  ${}^2X_2$  and the four lines of critical points meeting at the tetracritical point  $t$ . The value of the interaction strength ratio  $\tilde{R} \equiv J_{SR}/J_{LR}$  is equal to its appropriate value  $\tilde{R}_c = 0$ .

is seen (Fig. 6) to be only a special point on a  ${}^3X_2$  and  $Q$  does not give rise to a  ${}^4X_1$  on increasing the temperature. To see this (in the full phase diagram) it is necessary to consider Figs. 4(b) and 5-7. First, in Fig. 4(b), the phase diagram of the system is shown at constant  $\tilde{R} > 0$ . The relationship of this figure to Fig. 5 can be understood by looking at the  $T=0$  plane of Fig. 4(b). The lines where two phases coexist are lines on the appropriate surfaces of Fig. 5, and points where lines in the  $T=0$  plane of Fig. 4(b) meet are points on the lines  $L_1, L_2$ . Therefore Fig. 4(b) shows that the lines  $L_1, L_2$  do give rise to coexistence surfaces and are lines on  ${}^3X_2$ , as shown in Fig. 6. The line of points where three phases coexist ( ${}^3X_1$ ) in Fig. 5 has become a surface ( ${}^3X_2$ ) in Fig. 6, and this surface is terminated by a single line of tricritical points,  ${}^3R_1$ . Figure 6 shows that the point  $Q$  is just a point on a  ${}^3X_2$ , and does not generate a  ${}^4X_1$ .

The three surfaces of critical points generated by the lines of critical points in Figs. 4(a) and 4(b) are shown schematically in Fig. 7. It can be seen that the two  ${}^3R_0$  (tricritical points) of Fig. 4(b) form a continuous line (a  ${}^3R_1$ ) bounding three  ${}^2R_2$  (surfaces of critical points). The point  $t$  was called a tetracritical point by Nagle and Bonner<sup>8</sup> because, for  $\tilde{R} = \tilde{R}_c$ , four lines of critical points meet there (see Fig. 8). However, Figs. 6 and 7 show that  $t$  is an indistinguishable point on a smooth line of tricritical points of order 3; this is corroborated by the fact<sup>8</sup> that the exponents at  $t$  are the same as at the other tricritical points.

To produce a model where the point  $Q$  is stable at higher temperatures demands only a slight change in the structure of the interactions. We draw the

linear-chain nearest-neighbor Ising antiferromagnet in the form shown in Fig. 9, with the nn antiferromagnetic interaction along the solid lines, and a long-range interaction along each of the dotted lines. The latter stabilizes each sublattice independently, enabling the system to adopt an antiferromagnetic ordering at nonzero temperature:

$$\mathcal{H}_I = \mathcal{H}_{SR} + \mathcal{H}_{LR}^0 + \mathcal{H}_{LR}^E, \quad (3.4a)$$

where

$$\mathcal{H}_{LR}^{0,E} = - \sum_i \sum_r J(2r) s_i s_{i+2r}. \quad (3.4b)$$

Here odd-numbered spins are on the top lattice of Fig. 9 and  $\mathcal{H}^0$  has all  $i$  odd. Even numbered spins are on the lower lattice and  $\mathcal{H}^E$  has all  $i$  even;  $J(2r)$  is defined by Eq. (3.2b). The point  $Q$  is now at the origin and stable for  $T > 0$ , and we are able to have four  ${}^3X_2$ ; these are generated by the lines  $L_1, L_2, L_3, L_4$  (of Fig. 5) meeting at the  ${}^4X_1$ , generated by  $Q$ . The  ${}^3X_2$  should end in a  ${}^3R_1$  (as in Fig. 6) but unlike the system of Fig. 6, the  ${}^3R_1$  all terminate at a  ${}^4R_0$ .

This Hamiltonian has an important discrete symmetry which will necessarily be reflected by the phase diagram of the solution of the model. It is given by the operation  $s_i \rightarrow (-)^i s_i, H \rightarrow H_2, H_2 \rightarrow H, J_{SR} \rightarrow -J_{SR}$ . Therefore,

$$G(H, H_2, T; +J_{SR}) = G(H_2, H, T; -J_{SR}).$$

Further, the point  $Q$  in Fig. 5 (which is now stable at  $T > 0$ ) is now located at the origin. There are now four  ${}^3R_1$ ; two of which lie in the  $H_2 = 0$  hyperplane for  $\tilde{R} < 0$  and these are symmetrically complemented by two more  ${}^3R_1$  in the  $H = 0$  for  $\tilde{R} > 0$ . These four  ${}^3R_1$  meet at the  $T$ -axis at some finite value of  $T$ . This point at which all four  ${}^3R_1$  meet is a  ${}^4R_0$ . The phase diagram for this model is the same as that for the Ising model with variable interplanar interaction discussed in Sec. II (Figs. 1 and 2).

For the model just discussed, we were able to make use of the extensive analysis of Nagle and Bonner in conjunction with the  $T=0$  phase diagram, and thus we deduced the structure of the full phase diagram. The existence of the discrete symmetry and the consequent analogy with the model discussed in Sec. II makes us more confident in our conclusions.

For the next model, we use only an analysis of the  $T=0$  phase diagram and we make the extrapolation

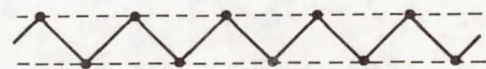


FIG. 9. Modified one-dimensional lattice exhibiting a critical point of order  $\Theta=4$ . The solid lines represent antiferromagnetic interactions and the dashed lines, long-range (ferromagnetic) interactions.



TABLE II. Definitions of spin orderings of phases and fields for an Ising model with two staggered fields.

Spin configuration	Name	Conjugate field
$\uparrow \uparrow \uparrow \uparrow$	$F^+$	$H$
$\downarrow \downarrow \downarrow \downarrow$	$F^-$	
$\uparrow \downarrow \uparrow \downarrow$	$A_2^+$	$H_2$
$\downarrow \uparrow \downarrow \uparrow$	$A_2^-$	
$\uparrow \uparrow \downarrow \downarrow$	$A_4^+$	$H_4$
$\downarrow \downarrow \uparrow \uparrow$	$A_4^-$	
$\uparrow \uparrow \uparrow \downarrow$	$M_a^+$	$\frac{1}{2}[H_2 + H_4 \pm H]$
$\uparrow \downarrow \downarrow \downarrow$	$M_a^-$	
$\uparrow \uparrow \downarrow \uparrow$	$M_b^+$	$\frac{1}{2}[-H_2 + H_4 \pm H]$
$\downarrow \uparrow \uparrow \downarrow$	$M_b^-$	
$\uparrow \downarrow \uparrow \uparrow$	$M_c^+$	$\frac{1}{2}[H_2 - H_4 \pm H]$
$\downarrow \downarrow \uparrow \uparrow$	$M_c^-$	
$\downarrow \uparrow \uparrow \uparrow$	$M_d^+$	$\frac{1}{2}[-H_2 - H_4 \pm H]$
$\downarrow \downarrow \downarrow \uparrow$	$M_d^-$	

tions explained at the end of Sec. II. Our knowledge of the extensive occurrence of tricritical points in certain Ising models gives us a reasonable basis from which to predict the existence of a critical point of order 4.

This second model for which an exact solution is fairly readily obtainable<sup>16</sup> is a model with a second staggered magnetic field. It turns out that the analysis for an exact solution is simplest if the staggered field, " $H_4$ ," is of wavelength four lattice sites.<sup>19</sup> The Hamiltonian will therefore be given by

$$\mathcal{H} = \mathcal{H}_{\text{SR}} + \mathcal{H}_{\text{LR}} - H_4 \sum_{i=1}^N u_i s_i, \quad (3.5)$$

where the number  $u_i = +1$  for  $i = 4n+1, 4n+2$  and

TABLE III. Energies of various phases at  $T=0$  for an Ising model with two staggered fields. Here the long-range energy is given by  $J_{\text{LR}}$  and the nearest neighbor by  $J_{\text{SR}}$ . Only the phase + is shown; to get the value of  $E_X^-$ , reverse the sign of the conjugate field.

Phase	Energy per spin
$F^+$	$E_F = -J_{\text{LR}} - J_{\text{SR}} - H$
$A_2^+$	$E_2 = +J_{\text{SR}} - H_2$
$A_4^+$	$E_4 = -H_4$
$M_a^+$	$E_a = -\frac{1}{2}J_{\text{LR}} - \frac{1}{2}[+H_2 + H_4 + H]$
$M_b^+$	$E_b = -\frac{1}{2}J_{\text{LR}} - \frac{1}{2}[-H_2 + H_4 + H]$
$M_c^+$	$E_c = -\frac{1}{2}J_{\text{LR}} - \frac{1}{2}[+H_2 - H_4 + H]$
$M_d^+$	$E_d = -\frac{1}{2}J_{\text{LR}} - \frac{1}{2}[-H_2 - H_4 + H]$

$u_i = -1$  for  $i = 4n-1, 4n$ . We define the names of the various phases in Table II and also the phase of  $H_4$  relative to  $H_2$ . We give the energies of the phases at  $T=0$  in Table III. The phase adopted at  $T=0$  is that of lowest energy, and so the problem of finding the phase diagram at  $T=0$  is simple. The phases coexist at points where the energies of two different phases are equal, and the most important equalities are given in Table IV(a).

An extended analysis<sup>16</sup> shows that the significant values of  $\tilde{R}$  are  $-1, -\frac{1}{2}$ , and  $0$ , and a sequence of phase diagrams can be drawn in the space of variables  $H, H_2, H_4$  for values of  $\tilde{R}$  greater than, equal to, and less than these numbers. A representative

TABLE IV. (a) Equations of planes and lines in Fig. 10 for an Ising model with two staggered fields. Here we have divided all energies through by  $J_{\text{LR}}$  and defined  $h_i = H_i/J_{\text{LR}}$ ,  $\tilde{R} \equiv J_{\text{SR}}/J_{\text{LR}}$ . In Fig. 10,  $\tilde{R}$  is positive, e.g.,  $\frac{1}{2}$  or  $\infty$ . Star means that the plane was omitted from Fig. 10. Double star indicates that this is only a line: (b) Equations of lines in Fig. 10.

Phase boundary	(a) Equation	Region
$[F^+, F^-]$	$h = 0$	
$[M_a^+, M_a^-]$	$h = 0$	
$[F^+, M_a^+]$ *	$h_2 + h_4 - 1 - 2\tilde{R} = h$	$h, h_2, h_4 > 0$
$[F^+, M_b^+]$ *	$h_2 - h_4 + 1 + 2\tilde{R} = -h$	$h, h_4 > 0, h_2 < 0$
$[F^+, A_4^+]$	$h_4 - 1 - \tilde{R} = h$	$h_4 > 0, h > 0$
$[A_4^+, M_a^+]$	$h_4 - h_2 - 1 = h$	$h, h_4 > 0, h_2 > 0$
$[A_4^+, M_b^+]$	$h_4 + h_2 - 1 = h$	$h, h_4 > 0, h_2 < 0$
$[F^+, A_2^+]$ **	$h_2 - 1 - 2\tilde{R} = h$	$h, h_2 > 0; h_4 = 0$
$[A_2^+, M_a^+]$	$h_2 - h_4 - 1 - 2\tilde{R} = h$	$h, h_2, h_4 > 0$
Line	(b) Intersection	Equation
$[4 : F^+ F^- M_a^+ M_a^-]$	$[F^+, F^-][M_a^+, M_a^-]$	$h_2 + h_4 = 1 + 2\tilde{R}$
	$[F^+, M_a^+], [F^-, M_a^-]$	$h = 0$
$[3 : F^+ F^- A_4^+]$	$[F^+, F^-][F^+, A_4^+]$	$h_4 = 1 + \tilde{R}$
	$[F^-, A_4^+]$ *	$h = 0$
$[3 : F^+ M_a^+ A_4^+]$	$[F^+, A_4^+][A_4^+, M_a^+]$	$h_4 - h = 1 + \tilde{R}$
	$[F^+, M_a^+]$ *	$h_2 = \tilde{R}$
$[3 : F^+ M_b^+ A_4^+]$	$[F^+ A_4^+][A_4^+, M_b^+]$	$h_4 - h = 1 + \tilde{R}$
	$[F^+, M_b^+]$ *	$h_2 = -\tilde{R}$
$[4 : F^+ M_a^+ M_c^+ A_2^+]$	$[F^+, M_a^+][F^+ M_c^+]$ *	$h_2 - h = 1 + 2\tilde{R}$
	$[M_a^+, A_2^+][M_c^+, A_2^+]$	$h_4 = 0$
$[3 : M_a^+, M_a^-, A_4^+]$	$[M_a^+, M_a^-][M_a^+, A_4^+]$	$h_4 - h_2 = 1$
	$[M_a^+, A_4^+]$ *	$h = 0$
$[3 : M_a^+, M_a^-, A_2^+]$	$[M_a^+, M_a^-], [M_a^+, A_2^+]$	$h_2 - h_4 = 1 + 2\tilde{R}$
	$[M_a^+, A_2^+]$	$h = 0$



diagram is shown in Fig. 10 for which the equations of the lines are given in Table IV(b). Some of the surfaces and lines of Fig. 10 are labeled and the reader can discover the labels for the rest by reference to Tables IV(a) and IV(b).

There are several important points about this model: firstly, the "mixed" phases  $M_a^\pm$  are distinguished at  $T=0$  as  $M_a^+ \cdots M_a^-$  but above absolute zero there are only phases  $M^+$  and  $M^-$ . The phases  $M^+$  are stable for  $T>0$  because they contain a long-range contribution to their energy; thus all the lines and surfaces on Fig. 10 will survive at  $T>0$  because they separate phases stabilized by the long-range interaction from phases ( $A_2^\pm, A_4^\pm$ ) stable only at  $T=0$ .

There are several points where many phases coexist. In particular, at the point  $P_2$  the phases  $F^+$ ,  $M_a^+$ , and  $A_4^+$  coexist. The lines where three or more phases coexist which meet at  $P_2$  are all stable at  $T>0$  and so should end in tricritical points. Thus  $P_2$  will give rise to a line of points where five phases coexist; this line ends at a critical point of order 4. Other points in Fig. 10 (viz.,  $P_1$ ) are much more complex in structure and will not be discussed here. The object of introducing the model given by Eq. (3.5) was to show a critical point of order four and this, at least, we have done.

In this section we have shown that it is reasonably easy to find model systems which are soluble and which show critical points of order 4 or more. The analysis of the two models suggested was omitted for the sake of brevity, and will be given in future work.<sup>16</sup>

#### IV. SPECIAL DIRECTIONS AT CRITICAL SPACES OF ORDER 0: A SET OF "CANONICAL DIRECTIONS"

In order to properly formulate the scaling hypothesis for multicomponent systems, it is important to choose the proper independent variables. It is this problem that is treated in the present section. We shall argue that the considerations that Griffiths and Wheeler<sup>5</sup> applied to their discussion of second-order critical spaces ( ${}^2R_d$ ) can be extended to spaces of higher order in a natural and straightforward fashion.

A  ${}^2X_d$  is, by definition, a hypersurface where two phases coexist; it necessarily divides the total space of  $n$  field variables locally into two regions and is therefore of dimension  $d=n-1$ , where  $n$  is the total number of truly intensive or "field" variables.<sup>5</sup> A  ${}^2R_d$  (a simple second-order critical space) is the boundary of a  ${}^2X_{n-1}$  and is therefore of dimension  $d=n-2$ .

At a  ${}^2R_{n-2}$  there are  $n-2$  directions parametrizing the critical space. The two remaining directions are of significance for the generalized scaling hypothesis. Directions not locally parallel to the  ${}^2X_{n-1}$  (coexistence surface) we call strong directions, and directions locally parallel to the  ${}^2X_{n-1}$  but not in the  ${}^2R_{n-2}$  we call weak directions. The strong and weak directions will be called directions of type 1 and 2, respectively; this terminology is useful in Sec. VI and in Paper II, where the appropriate generalization to critical spaces of order larger than 2 is made. Examples are given in Figs. 11 and 12.

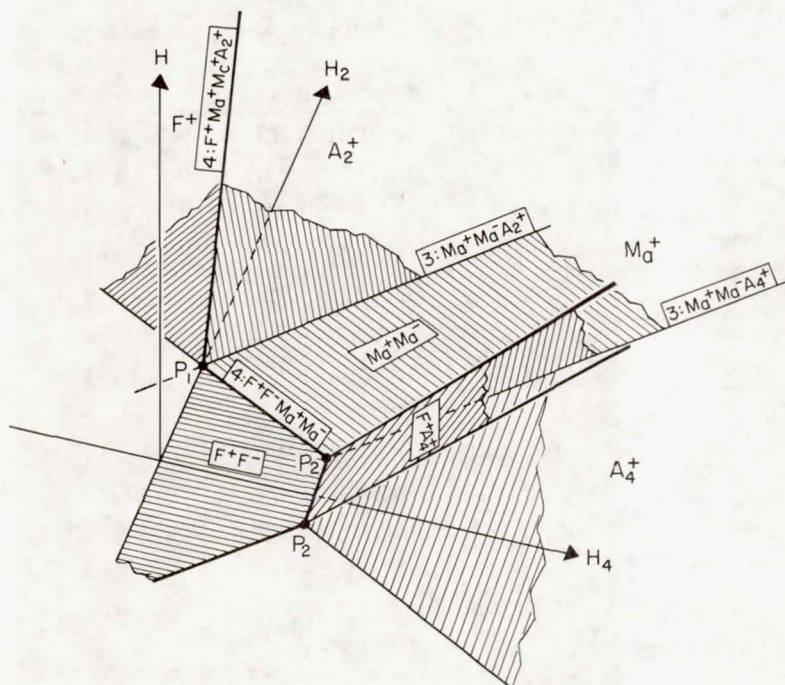


FIG. 10. Coexistence surfaces in the  $T=0$  phase for a system with a long-range interaction, an  $n$  interaction, magnetic field  $h$ , and staggered magnetic fields  $h_2, h_4$  of wavelengths 2 and 4. Here the short-range interaction is also ferromagnetic. The surfaces are labeled by the phases in coexistence. The surface  $[F^+, M_a^+]$  is omitted. The lines are labeled by the three or four phases in coexistence there. At the point  $P_2$ , five phases coexist; at  $P_1$ , seven phases coexist. The phases  $F$  and  $M$  are stable above  $T=0$ .



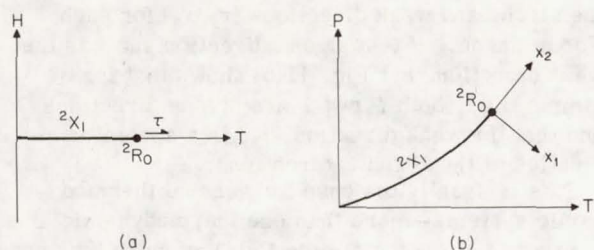


FIG. 11. (a) Phase transition for a ferromagnetic system. The coexistence surface  ${}^2X_1$  ends at a critical point  ${}^2R_0$ . The strong direction  $H$  and weak direction  $T$  are defined at the  ${}^2R_0$ . (b) Phase transition for a simple fluid. The coexistence surface  ${}^2X_1$  ends at a critical point  ${}^2R_0$ . The strong direction  $x_1$  and weak direction  $x_2$  are indicated; both  $P$  and  $T$  directions are strong.

Next, we introduce the concept of a direction of type 3. In the examples discussed, the critical spaces of order 3 have a dimension of  $d = n - 3$ . If one approaches a particular tricritical point along a line of critical points of order 2, then in addition to the two directions singled out by the  ${}^2R_1$  (and its associated  ${}^2X_2$ ), there is a third direction of significance for scaling. This direction, which we call a direction of type 3, is a direction tangent to the line of critical points (Figs. 12 and 14). This concept is easily generalized to  $n > 3$  for the case mentioned above, for which the dimension  $d$  of the space of critical points of order three is indeed given by  $d = n - 3$ . In this case directions of type 3 are those directions which are neither strong nor weak for a particular  ${}^2R_{n-2}$  bounded by the  ${}^3R_{n-3}$ , nor are they locally tangent to the space of critical points of

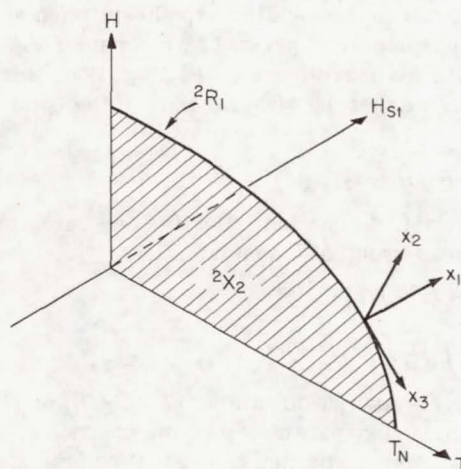


FIG. 12. Phase transition for an antiferromagnet. The coexistence surface  ${}^2X_2$  lies in the  $H, T$  plane and the line of critical points  ${}^2R_1$  bounds it. The strong direction is everywhere  $H_{st}$ , the staggered magnetic field. The weak direction may be either  $H$  or  $T$ , except at the Néel point where it can only be  $T$ . The independent direction  $x_0$  lies in the  ${}^2R_1$ .

third order.

In the similar cases where Eq. (1.1) holds as an equality, one can generalize the above concepts to define directions of types 1, 2, ...,  $\emptyset$ , and these are important in applying the scaling hypothesis to critical spaces of order  $\emptyset$ . Specifically, since a critical point of order  $\emptyset$  is, by definition, a particular point on a "line" of critical points of order  $\emptyset - 1$ , the generalization follows by analogy with the case treated above. The directions of types 1 through  $\emptyset$  are of great importance because they are used as the independent variables of the Gibbs function when the scaling hypothesis is made. Accordingly, they will be referred to in later sections as the "principal directions of scaling."

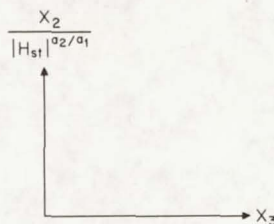
Thus, to set up a coordinate system at a  ${}^{\emptyset}R_{n-\emptyset}$  (a general critical space of order  $\emptyset$ ), a set of critical spaces  ${}^jR_{n-j}$  of orders  $j = 2, 3, \dots, \emptyset$  must be selected. This set of spaces must satisfy an inclusion principle:  ${}^{\emptyset}R_{n-\emptyset} \subset {}^jR_{n-j} \subset {}^iR_{n-i}$  for  $j < i < \emptyset$ . The directions of types 1, 2, ...,  $\emptyset$  are then sequentially defined. Here the inclusion symbol  $\subset$  means not only that the  ${}^iR_{n-i}$  is also part of a  ${}^jR_{n-j}$  (for  $i > j$ ) but also that the  ${}^iR_{n-i}$  can be reached as a limiting point or boundary of the  ${}^jR_{n-j}$ .

The hierarchy of spaces  ${}^jR_{n-j}$  is not unique, and the large number of choices available presents an apparent problem because many more than  $\emptyset$  linearly independent vector directions are definable. For the  $\emptyset = 3$  example of Fig. 14 the  ${}^3R_0$  can be approached along any of the three  ${}^2R_1$ , and each of these three "critical lines" (with its associated  ${}^2X_2$ ) defines a set of directions of types 1, 2, and 3. This apparent problem is resolved by the generalized scaling hypothesis, because the shape of each critical space of order  $j$  ( $j < \emptyset$ ) near the  ${}^{\emptyset}R_d$  is constrained by the scaling hypothesis so that all the different directions end up mutually consistent. Accordingly, we now turn our attention to the scaling hypothesis, making it firstly in Sec. V for simple systems ( $n = 2$ ), for  $n = 3$  systems with a  ${}^3R_0$  (tricritical point) in Sec. VI, and in Paper II for a  ${}^{\emptyset}R_{n-\emptyset}$  (a general critical space of order  $\emptyset$ ).<sup>20</sup>

#### V. INVARIANT THEOREMS OF ONE-PARAMETER CONTINUOUS GROUPS; APPLICATION TO THE SCALING HYPOTHESIS FOR CRITICAL SPACES OF ORDER 2

The scaling hypothesis for a simple system with two independent field variables can be made in

FIG. 13. Invariant space for an antiferromagnet. ( $x_3$  is merely a parameter.)





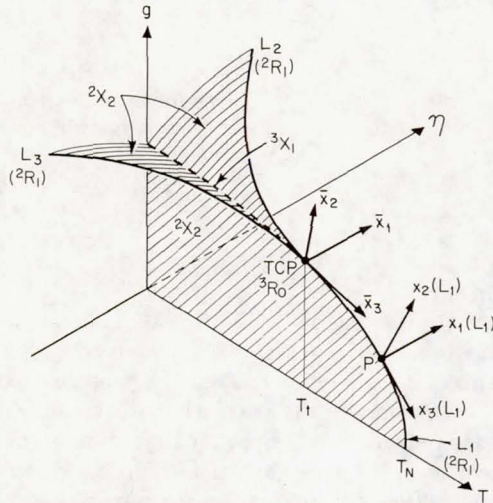


FIG. 14. Phase diagram for a metamagnet. The three  ${}^2X_2$  end in lines of critical points  ${}^2R_1$ . These lines intersect at the tricritical point  ${}^3R_0$ . At a point  $P$  on the line  $L_1$ , a triad of strong, weak, and parallel (to  $L_1$ ) directions is shown. This triad attains the limiting orientation  $(\bar{x}_1, \bar{x}_2, \bar{x}_3)$  at the tricritical point  ${}^3R_0$ .

several essentially equivalent fashions. One statement is that the singular part of the Gibbs potential is asymptotically a generalized homogeneous function (GHF) of the appropriate variables.<sup>21</sup> For the simple magnet, this statement takes the form that there exist two numbers  $a_H, a_\tau$  (called "scaling powers") such that for all positive  $\lambda$ ,

$$G(\lambda^{a_H} H, \lambda^{a_\tau} \tau) = \lambda G(H, \tau), \quad (5.1)$$

where  $H$  is the magnetic field and  $\tau \equiv T - T_c$ . Using Eq. (5.1), one can express all possible thermodynamic exponents in terms of  $(a_H, a_\tau)$ .<sup>21</sup>

This form of the scaling hypothesis implies that the singular part of the Gibbs potential

$$G = F(H, \tau) \quad (5.2)$$

is an invariant equation under the "scaling" transformation defined by

$$G' \equiv \lambda G, \quad (5.3a)$$

$$H' \equiv \lambda^{a_H} H; \tau' \equiv \lambda^{a_\tau} \tau, \quad (5.3b)$$

such that  $G' = F(H', \tau')$ . The transformations defined by Eq. (5.3) form a one-parameter group<sup>22</sup>  $\mathcal{G}_F$  and the scaling hypothesis may be restated in the following fashion: (5.2) is an invariant equation under the group of transformations  $\mathcal{G}_F$  of (5.3).

For a simple magnet the thermodynamic axes are parallel to the directions used in the scaling hypothesis (5.1) (the "principal axes of scaling"). In other systems, this is not always so. In Fig. 11 we contrast the phase diagrams of a simple fluid and a simple magnet, and show the orientations of

the strong and weak directions  $(x_1, x_2)$  for each. For a magnet,  $H$  is a strong direction and  $\tau$  is the weak direction, but Fig. 11(b) shows that for a simple fluid, both  $P$  and  $T$  are strong directions and that the weak direction,  $x_2$ , is a special combination of the  $P$  and  $T$  directions.

This is usually the case for general thermodynamic systems—more than one thermodynamic axis is strong (as for the simple fluid) or more than one axis is weak (as for an antiferromagnet, see Fig. 12).

The scaling hypothesis at a  ${}^2R_{n-2}$  for a general system can be made by choosing the strong and weak directions as the principal axes of scaling. Then the statement is that the singular part of the Gibbs function

$$G = \mathcal{F}(x_1, x_2; \dots, x_n) \quad (5.4)$$

is an invariant equation under the one-parameter<sup>23</sup> continuous group of transformations  $\mathcal{G}$ :

$$\mathcal{G} \begin{cases} G' = \lambda G, \\ x'_i = \lambda^{a_i} x_i, \quad i = 1, 2, \dots, n, \quad [a_i = 0, i > 2]. \end{cases} \quad (5.5a)$$

$$\mathcal{G} \begin{cases} G' = \lambda G, \\ x'_i = \lambda^{a_i} x_i, \quad i = 1, 2, \dots, n, \quad [a_i = 0, i > 2]. \end{cases} \quad (5.5b)$$

Equation (5.5) is defined for all positive  $\lambda$ ; the  $a_i$  are called scaling powers. This statement is equivalent to the scaling hypothesis

$$G(\lambda^{a_1} x_1, \lambda^{a_2} x_2; x_3, \dots, x_n) = \lambda G(x_1, x_2; \dots, x_n). \quad (5.6)$$

For future reference, we will use a superscript  $s$  to denote the subgroup generated by the transformations of the independent variables  $x_i$  ( $i = 1, 2, \dots, n$ ). Thus we may generally define the full group by two equations, where the second denotes the subgroup  $\mathcal{G}^s$ .

To illustrate the scaling hypothesis when an inactive parameter is present, we consider the example of the antiferromagnet (see Fig. 12). Here we hypothesize that the singular part of the Gibbs potential

$$G = \mathcal{F}_A(H_{st}, x_2, x_3) \quad (5.7)$$

is an invariant equation under the one parameter continuous group of transformations  $\mathcal{G}_A$ :

$$\mathcal{G}_A \begin{cases} G' = \lambda G, \\ H'_{st} = \lambda^{a_1} H_{st}, \quad x'_2 = \lambda^{a_2} x_2, \quad x'_3 = x_3, \end{cases} \quad (5.8)$$

where  $x_2$  is a weak direction,  $[T - T_c(H)]$  or  $[H - H_c(T)]$ , and  $x_3$  parametrizes the position of the critical point on the line of critical points. Equivalently  $G$  satisfies a GHF equation<sup>24</sup>

$$G(\lambda^{a_1} H_{st}, \lambda^{a_2} x_2; x_3) = \lambda G(H_{st}, x_2; x_3). \quad (5.9)$$

Here  $H_{st}$  denotes the staggered magnetic field.

Scaling functions for ferromagnets and antiferromagnets can be obtained the usual way<sup>21</sup> from



Eqs. (5.1) and (5.9), respectively. For example, by setting  $\lambda \equiv 1/|H|^{1/a_H}$  in Eq. (5.1), we obtain<sup>25</sup>

$$G(1, \tau/|H|^{a_\tau/a_H}) = |H|^{-1/a_H} G(H, \tau). \quad (5.10)$$

The function  $G(H, \tau)$  can be plotted as a curve in a two-dimensional plane with coordinates specified by  $G/|H|^{1/a_H}$  and  $\tau/|H|^{a_\tau/a_H}$ . We note that both  $G/|H|^{1/a_H}$  and  $\tau/|H|^{a_\tau/a_H}$  are absolute invariants of the group  $\mathcal{G}_F$  defined by Eq. (5.3), i. e.,

$$G_H \equiv \frac{G'}{|H'|^{1/a_H}} = \frac{G}{|H|^{1/a_H}}, \quad (5.11a)$$

$$\tau_H \equiv \frac{\tau'}{|H'|^{a_\tau/a_H}} = \frac{\tau}{|H|^{a_\tau/a_H}}, \quad (5.11b)$$

where the second equalities in (5.11) follow from (5.3).

Similarly, by setting  $\lambda \equiv 1/|H_{st}|^{1/a_1}$ , Eq. (5.9) may be written

$$G(1, x_2/|H_{st}|^{a_2/a_1}, x_3) = |H_{st}|^{-1/a_1} G(H_{st}, x_2; x_3), \quad (5.12)$$

and  $G/|H_{st}|^{1/a_1}$ ,  $x_2/|H_{st}|^{a_2/a_1}$ ,  $x_3$  are absolute invariants of the group  $\mathcal{G}_A$ . In addition, the last two quantities are absolute invariants of the subgroup  $\mathcal{G}_A^s$ .

To derive exponents and scaling laws for the antiferromagnet, the procedures developed in Ref. 21 can be simply applied to Eq. (5.9). At points where the critical line is not parallel to the  $T$  axis, it is easily shown that

$$\beta = (1 - a_1)/a_2, \quad (5.13a)$$

$$1/\delta = (1 - a_1)/a_1, \quad (5.13b)$$

$$-\gamma = (1 - 2a_1)/a_2, \quad (5.13c)$$

$$-\alpha = (1 - 2a_2)/a_2, \quad (5.13d)$$

where the order parameter  $M_{st}$  tends to zero when the critical line is approached in a weak direction with exponent  $\beta$ ,

$$M_{st} \propto |T - T_c(H)|^\beta, \quad (5.14a)$$

and with exponent  $1/\delta$  when it is approached in a strong direction

$$M_{st} \propto H_{st}^{1/\delta}. \quad (5.14b)$$

The staggered susceptibility  $\chi_{st} = \partial M_{st} / \partial H_{st}$  diverges with exponent  $\gamma$ ,

$$\chi_{st} \propto |T - T_c(H)|^{-\gamma}, \quad (5.14c)$$

and the specific heat at constant order parameter diverges with exponent  $\alpha$ :

$$C_{M_{st}} \propto |T - T_c(H)|^{-\alpha}. \quad (5.14d)$$

The last two exponents  $\gamma$  and  $\alpha$  refer to weak directions of approach (in the plane  $H_{st} = 0$ ) to the critical line.<sup>26</sup>

In the same way, exponents for the ordinary

magnetization  $M$ , and ordinary susceptibility  $\chi = \partial M / \partial H$  can be derived. It turns out on using Eq. (5.13d) that

$$M - M_c(H) \propto |T - T_c(H)|^{(1-\alpha)}, \quad (5.15a)$$

$$\chi \propto |T - T_c(H)|^{-\alpha}. \quad (5.15b)$$

From Eqs. (5.13a)–(5.13d) the usual scaling law equalities can be derived by eliminating the scaling powers  $a_1$  and  $a_2$ :

$$\alpha + 2\beta + \gamma = 2, \quad \beta(\delta - 1) = \gamma, \quad \beta(\delta + 1) = 2 - \alpha.$$

These results are also obtainable from two simple group invariant theorems which we shall find particularly useful in making the scaling hypothesis for critical subspaces of higher order.

**Theorem 1.** Consider a one-parameter continuous group of transformations:

$$\mathcal{G} \begin{cases} x'_0 = f(\lambda | x_0), \end{cases} \quad (5.16a)$$

$$\mathcal{G} \begin{cases} x'_i = f_i(\lambda | x_1, x_2, \dots, x_n), \quad i = 1, 2, \dots, n. \end{cases} \quad (5.16b)$$

There exist  $n$  functionally independent absolute invariants of the  $x_i$  ( $i = 0, 1, \dots, n$ ). This theorem is proved in Appendix A.

For our applications, we shall choose the invariants, denoted by  $y_i$  ( $i = 0, 1, \dots, n-1$ ), such that, for  $i = 0$ ,

$$\frac{\partial y_0}{\partial x_0} \neq 0, \quad (5.17a)$$

and for  $i > 0$ ,

$$(y_1, y_2, \dots, y_{n-1}) \quad (5.17b)$$

are the  $n-1$  functionally independent absolute invariants of the subgroup  $\mathcal{G}^s$ .

For the simple ferromagnet,  $G/|H|^{1/a_H}$  is an absolute invariant under  $\mathcal{G}_F$  [see Eq. (5.3)] and  $\tau/|H|^{a_\tau/a_H}$  is the functionally independent absolute invariant of  $(H, \tau)$  under the transformation  $\mathcal{G}_F^s$ . For the antiferromagnet,  $G/|H_{st}|^{1/a_1}$  is an absolute invariant under  $\mathcal{G}_A$ , and  $(x_2/|H_{st}|^{a_2/a_1}, x_3)$  are the two functionally independent absolute invariants under  $\mathcal{G}_A^s$ .

**Theorem 2.** If

$$x_0 = X_0(x_1, x_2, \dots, x_n) \quad (5.18)$$

is an invariant equation under  $\mathcal{G}$  defined by (5.16) (i. e., if  $X_0$  is a GHF), then it can be expressed as

$$y_0 = Y_0(y_1, y_2, \dots, y_{n-1}), \quad (5.19)$$

where the  $y_i$  ( $i = 0, 1, \dots, n-1$ ) form a set of functionally independent absolute invariants of  $\mathcal{G}$  given by (5.16), and satisfying (5.17).

The proof of this theorem is given in Appendix B. Equations (5.10) and (5.12) are simple applications of these theorems. The usefulness of theorems 1 and 2 will be apparent in Sec. VI.



## VI. SCALING HYPOTHESIS FOR TRICRITICAL POINTS

Before making the scaling hypothesis and examining its consequences for a critical space of arbitrary order  $\theta$ , we will make it for the special case of a  ${}^3R_0$  (tricritical point) for which there are three fields available ( $n=3$ ). This will clarify both notation and concepts, and make passage to the general case more painless.

As was shown in Sec. IV, it is possible at a critical point to select strong and weak directions (directions of types 1 and 2). These we call  $x_1$  and  $x_2$  as before. In a space of total dimension three, the critical subspaces terminating at a  ${}^3R_0$  are all  ${}^2R_1$ . At a point on a  ${}^2R_1$  we may select a direction tangent to the line. Thus as one approaches the  ${}^3R_0$  along a given  ${}^2R_1$ , the directions of types 1, 2, and 3 are uniquely defined (see Fig. 14).

Since three critical lines meet at a  ${}^3R_0$ , three "rival" coordinate systems exist at the point  ${}^3R_0$ . A scaling hypothesis cannot be made at the tricritical point unless a unique coordinate system can be defined, and this represents an apparent obstacle.

The solution of this problem is somewhat subtle, and the full details have been given in a previous paper.<sup>7(b)</sup> The basic idea is that a scaling hypothesis at the  ${}^3R_0$  determines the general shape of a line of critical points near the  ${}^3R_0$ ; thus a scaling hypothesis made in a coordinate system defined by one line will restrict the shapes of the other two lines meeting it (at the tricritical point).

The coordinate systems defined with reference to the other two lines are consistent in the sense that we could have selected any line first to make the scaling hypothesis and we would have obtained the same final result.

To set up a coordinate system in which to make a scaling hypothesis at the  ${}^3R_0$ , we choose a point  $P$  on one of the critical lines (say  $L_1$ ) and we set up a triad of directions  $x_i(L_1)$ . Two of these directions are of types 1 and 2, while the third is tangent to the  ${}^2R_1$ . The coordinate system at the tricritical point is now defined to be

$$\bar{x}_i \equiv \lim_{P \rightarrow {}^3R_0} x_i(P) \quad (6.1)$$

(see Fig. 14). The direction  $\bar{x}_3$  is of type 3. The bars are used in order that the present notation be consistent with that of Ref. 7(b).

We now introduce a scaling parameter  $\lambda$  ( $\lambda > 0$ ) and make the scaling hypothesis that the singular part of the Gibbs potential is a GHF, i.e.,

$$G(\lambda^{\bar{a}_1} \bar{x}_1, \lambda^{\bar{a}_2} \bar{x}_2, \lambda^{\bar{a}_3} \bar{x}_3) = \lambda G(\bar{x}_1, \bar{x}_2, \bar{x}_3), \quad (6.2)$$

where  $(\bar{a}_1, \bar{a}_2, \bar{a}_3)$  are the "tricritical scaling powers". Equation (6.2) is equivalent to the statement that  $G = \mathcal{F}(\bar{x}_1, \bar{x}_2, \bar{x}_3)$  is an invariant equation under the one-parameter continuous group of transformations

$$\mathcal{G}_3 \left\{ \begin{array}{l} G' = \lambda G, \\ \bar{x}_i' = \lambda^{\bar{a}_i} \bar{x}_i, \quad i=1, 2, 3. \end{array} \right. \quad (6.3a)$$

$$(6.3b)$$

According to theorem 1 of Sec. V, the hypothesized invariance property of (6.1) under  $\mathcal{G}_3$  implies that there exists a basis set of functionally independent absolute invariants of  $\mathcal{G}_3$ . We adopt a canonical form for the invariants  $y_i$  by scaling  $\bar{x}_i$  with respect to the tangent variable—here  $\bar{x}_3$ —as follows:

$$y_0 \equiv \frac{\bar{x}_0}{\bar{x}_3^{1/\bar{a}_3}}, \quad y_1 \equiv \frac{\bar{x}_1}{\bar{x}_3^{\bar{a}_1/\bar{a}_3}}, \quad y_2 \equiv \frac{\bar{x}_2}{\bar{x}_3^{\bar{a}_2/\bar{a}_3}}, \quad (6.4)$$

with  $\bar{x}_0 \equiv G$ . Thus, theorem 2 of Sec. V states that  $G(\bar{x}_1, \bar{x}_2, \bar{x}_3)$  may be expressed as<sup>27</sup>

$$y_0 = F_2(y_1, y_2). \quad (6.5)$$

Since the variables  $y_1$  and  $y_2$  forms a basis set of functionally independent absolute invariants of the scaling field variables  $\bar{x}_1, \bar{x}_2$ , and  $\bar{x}_3$  of the group of transformations  $\mathcal{G}_3$ , any point  $(k_1, k_2)$  in the two-dimensional space  $(y_1, y_2)$  gives rise to an invariant curve of points in the three-dimensional space  $(\bar{x}_1, \bar{x}_2, \bar{x}_3)$ . That is, the point given by

$$y_i = k_i, \quad i=1, 2 \quad (6.6)$$

corresponds to a line in the  $x_i$  space that may be conveniently parametrized by

$$(\bar{x}_1, \bar{x}_2, \bar{x}_3) = (k_1 \lambda^{\bar{a}_1}, k_2 \lambda^{\bar{a}_2}, \lambda^{\bar{a}_3}), \quad (6.7)$$

where  $\lambda$  is an arbitrary parameter (see Fig. 15). In particular the lines of critical points  $L_j$  converging on the tricritical point can be expressed in the form of Eq. (6.7), since according to the scaling hypothesis (6.2) they must be invariant under the group of symmetries  $\mathcal{G}_3$  of (6.3).

Previously<sup>7(b)</sup> we have derived Eq. (6.7) directly from Eq. (6.2) and demonstrated that if the scaling powers  $\bar{a}_i$  are all different, the curves parametrized by Eq. (6.7) end up parallel to the axis  $\bar{x}_i$  corresponding to the minimum  $\bar{a}_i$  (unless  $k_i=0$ ). Although the direction of type 3 defined for one line is not necessarily parallel to the direction of type 3 defined for another line, it will at least be parallel to *some* member of the triad defined for that other line. Thus all choices of scaling directions will be mutually consistent!<sup>7(b),28</sup>

Along a critical line  ${}^2R_1$ , the conventional scaling hypothesis is normally stated in terms of a GHF equation of the form

$$G(\mu^{\bar{a}_1} x_1, \mu^{\bar{a}_2} x_2; x_3) = \mu G(x_1, x_2; x_3), \quad (6.8)$$

where  $x_3$  is a parameter and does not scale. Near the  ${}^3R_0$ , however, the shape of the critical line is determined by Eq. (6.7). A  ${}^2R_1$  near the  ${}^3R_0$  maps into a point  $(k_1, k_2)$  in the  $y_1$ - $y_2$  plane given by Eq. (6.6). Furthermore, the value of  $y_0 \equiv \bar{x}_0 / \bar{x}_3^{1/\bar{a}_3}$



$= G/\bar{x}_3^{1/\bar{a}_3}$  changes only if  $y_1$  and/or  $y_2$  changes. It is therefore more proper to make a precise scaling hypothesis about the critical line  ${}^2R_1$  near the  ${}^3R_0$  making use of the variables  $(y_1, y_2)$ .

If we adopt the strong requirement that a point in one phase remains in that phase under the scale transformation  $\mathcal{G}_3$ , the CXS surfaces become lines in the  $y_1$ - $y_2$  plane. Hence, it is possible to choose the principal directions of scaling for the  ${}^2R_{n-2}$  as linear combinations of the variables  $y_1, y_2$ .

Because the scaled variables must be zero at the critical line we consider the variables

$$\hat{y}_1 \equiv y_1 - k_1, \quad (6.9a)$$

$$\hat{y}_2 \equiv y_2 - k_2. \quad (6.9b)$$

For the line  $L_1$  of Fig. 15,  $k_1=0$ , the coordinate  $y_1$ , is everywhere strong and  $(y_2+k)$  is weak. For  $L_2$  and  $L_3$ , the weak direction is parallel to the CXS mapped in the  $y_1$ - $y_2$  plane, and both  $\hat{y}_1, \hat{y}_2$  are strong directions unless the wings end up parallel to one axis.

We therefore define linear combinations of the variables  $(y_i - k_i)$ , which give the weak and strong directions (they are of necessity also absolute invariants of the group  $\mathcal{G}_3$ ):

$$\tilde{y}_i \equiv \sum_{j=1}^2 \tilde{R}_{ij}(y_j - k_j), \quad (6.10a)$$

where  $\tilde{R}_{ij}$  is a "rotation matrix". Defining

$$\tilde{y}_0 \equiv y_0, \quad (6.10b)$$

we hypothesize that along a  ${}^2R_1$  near the  ${}^3R_0$ ,  $\tilde{y}_0$  is a GHF of  $(\tilde{y}_1, \tilde{y}_2)$ ,

$$\tilde{y}_0(\mu^{a_1}\tilde{y}_1, \mu^{a_2}\tilde{y}_2) = \mu\tilde{y}_0(\tilde{y}_1, \tilde{y}_2), \quad (6.11)$$

i.e.,  $\tilde{y}_0 = \mathcal{F}_2(\tilde{y}_1, \tilde{y}_2)$  is an invariant equation under a group  $\mathcal{G}_2$  defined by

$$\mathcal{G}_2 \left\{ \begin{array}{l} \tilde{y}_0' = \mu\tilde{y}_0, \\ \tilde{y}_i' = \mu^{a_i}\tilde{y}_i, \quad i=1, 2. \end{array} \right. \quad (6.12a)$$

$$(6.12b)$$

In general, the group  $\mathcal{G}_2$  will be different (having different  $a_i$ ) for each critical line at the tricritical point, and will only be valid within a certain region close to the critical line. The different groups  $\mathcal{G}_2$  for the different lines  $L_i$  do not have regions of overlap and there is therefore no conflict.

We can now form absolute invariants of  $\mathcal{G}_2$ . Scaling with respect to the weak direction we obtain

$$z_0 \equiv \frac{\tilde{y}_0}{\tilde{y}_2^{1/a_2}}, \quad z_1 \equiv \frac{\tilde{y}_1}{\tilde{y}_2^{a_1/a_2}}. \quad (6.13)$$

Theorem 2 of Sec. V states that under the hypothesis (6.11),  $\tilde{y}_0(\tilde{y}_1, \tilde{y}_2)$  may be expressed as<sup>27</sup>

$$z_0 = \mathcal{F}_1(z_1). \quad (6.14)$$

The simplest example of this is for the line  $L_1$  of Fig. 15. Here the variables of scaling are

$$\hat{y}_1 = \bar{x}_1 / \bar{x}_3^{1/\bar{a}_3}, \quad (6.15a)$$

$$\hat{y}_2 = (\bar{x}_2 / \bar{x}_3^{1/\bar{a}_3} + k), \quad (6.15b)$$

where  $k$  is defined in Fig. 15. Rotation is not necessary and  $\tilde{R}_{ij} \equiv \delta_{ij}$ . Hence on using (6.13) and (6.15), Eq. (6.14) can be written in the "double-power law" form<sup>27</sup>

$$\frac{G}{\bar{x}_3^{1/\bar{a}_3}(\bar{x}_2 / \bar{x}_3^{1/\bar{a}_3} + k)^{1/a_2}} = \mathcal{F}_1 \left[ \frac{\bar{x}_1}{\bar{x}_3^{1/\bar{a}_3}(\bar{x}_2 / \bar{x}_3^{1/\bar{a}_3} + k)^{a_1/a_2}} \right]. \quad (6.16)$$

For a simple system with  $n=2$ , scaling functions predict data collapsing for functions of two variables from a surface onto a line. For  $n=3$  and functions of three variables, data collapse from a volume onto a surface. However, the double-power scaling function of Eq. (6.16) predicts that data will collapse from a volume onto a line. Clearly this happens only within the region of validity of both groups of transformations  $\mathcal{G}_2$  and  $\mathcal{G}_3$ .

The region of influence of  $\mathcal{G}_2$  in the neighborhood of the tricritical point  ${}^3R_0$  should also be controlled by the group  $\mathcal{G}_3$ . This means that the region of influence of  $\mathcal{G}_2$  should be bounded by a surface which scales toward the  ${}^3R_0$ . In Fig. 15, where a line which scales is represented by a point, a surface which scales will be represented by a line. We therefore plot the surfaces bounding the region of influence of the group  $\mathcal{G}_2$  (of transformations about a  ${}^2R_1, L_i$ ) as a line surrounding the point in the  $y_1$ - $y_2$  plane, representing the particular line  $L_i$ .

In terms of the variables  $y_1, y_2$  such a line will be represented by the equation

$$f(y_1, y_2) = 0 \quad (6.17a)$$

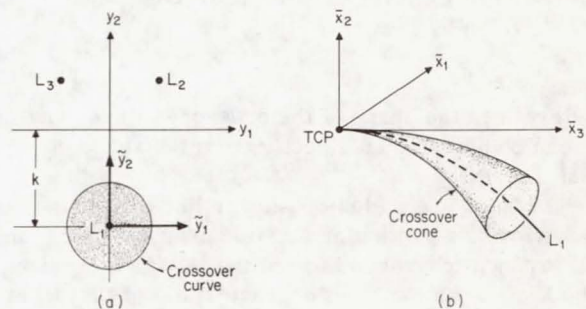


FIG. 15. (a) Plot of the invariants  $(y_1, y_2)$  for the group  $\mathcal{G}_3$  of transformations about the tricritical point. The strong and weak directions for the line  $L_1$  are  $y_1$  and  $y_2$ . The circle around  $L_1$  is a possible shape for the crossover region. (b) The principal points of interest of Fig. 15(a) in the full space  $(\bar{x}_1, \bar{x}_2, \bar{x}_3)$ . The point labeled  $L_1$  has become a line and the circle surrounding it has become a cone.



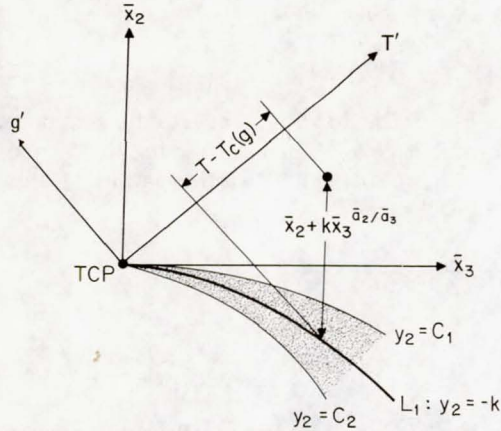


FIG. 16. Figure 15(b) sliced in the  $\bar{x}_2, \bar{x}_3$  plane. The cone has become the two lines labeled  $y_2 = C_1, C_2$  [see Fig. 15(a)]. These are generally referred to as crossover lines:  $(T', g') = (T - T_c, g - g_c)$ .

or

$$f(\bar{x}_1 / |\bar{x}_3|^{\bar{a}_1/\bar{a}_3}, \bar{x}_2 / |\bar{x}_3|^{\bar{a}_2/\bar{a}_3}) = 0. \quad (6.17b)$$

The area bounded by this curve (6.17) maps into a conical volume surrounding the critical line  $L_1$  (Fig. 15). Scaling will not tell us the actual shape of the curve in the  $y_1 - y_2$  plane but it does limit the shape in the  $(\bar{x}_1, \bar{x}_2, \bar{x}_3)$  space, since all points in the  $y_1 - y_2$  plane give rise to curves approaching the tricritical point along a particular direction—the axis corresponding to the minimum  $\bar{a}_i$ .

In the plane  $\bar{x}_1 = 0$ , Eq. (6.16) requires<sup>29</sup> that

$$G \propto \bar{x}_3^{1/\bar{a}_3} (\bar{x}_2 / \bar{x}_3^{\bar{a}_2/\bar{a}_3} + k)^{1/\bar{a}_2}, \quad (6.18)$$

and the conical surface of Eq. (6.17) becomes the two “crossover lines”

$$\bar{x}_2 = C_{1,2} \bar{x}_3^{\bar{a}_2/\bar{a}_3}, \quad (6.19)$$

as shown in Fig. 16. The crossover exponent  $\varphi$ ,<sup>7(a)</sup> given by

$$\varphi \equiv \bar{a}_3 / \bar{a}_2, \quad (6.20)$$

determines the shape of the crossover lines, and it can be determined directly from the shape of the line  $L_1$  ( ${}^2R_1$ ).

The lines are called crossover lines, because the behavior of a particular function crosses over from an exponent characteristic of the  ${}^3R_0$  far away from the line, to an exponent characteristic of the  ${}^2R_1$  at points close to the  ${}^2R_1$ . It is important to realize that the group  $\mathcal{G}_3$  does not cease to be valid, and the crossover does not refer to changing from one group to another. The group  $\mathcal{G}_3$  is everywhere valid, and the crossover merely marks the limits of validity of  $\mathcal{G}_2$ . This principle will be extended in Paper II and the groups  $\mathcal{G}_j$  will control cross-overs (or boundaries for the regions of validity) of

$\mathcal{G}_i$  where  $j > i$ .

Finally, a few remarks should be made about the exponents and the directions of approach to the tricritical point. Equation (6.18) shows that if  $\bar{x}_2 / |\bar{x}_3|^{\bar{a}_2/\bar{a}_3}$  is a constant the exponent for  $G$  is  $1/\bar{a}_3$ . For a function  $f$  with a tricritical-point (TCP) scaling power  $\bar{a}_f$ , and a critical-line scaling power  $a_f$ , the equation analogous to Eq. (6.18) predicts exponents  $\bar{a}_f/\bar{a}_3$  and  $a_f/a_2$ . For example, for the staggered susceptibility  $\chi_{st} \equiv \partial^2 G / \partial H_{st}^2$ , from (6.16),

$$\chi_{st} \propto \bar{x}_3^{(1-2\bar{a}_1)/\bar{a}_3} (\bar{x}_2 / \bar{x}_3^{\bar{a}_2/\bar{a}_3} + k)^{(1-2a_1)/a_2}, \quad (6.21)$$

and  $\bar{a}_f = 1 - 2\bar{a}_1$  and  $a_f = 1 - 2a_1$  for this case. Thus for all the exponents considered below the numerators can be appropriately replaced by  $\bar{a}_f$  or  $a_f$ .

If the  ${}^3R_0$  is approached along a direction not asymptotically parallel to the  $\bar{x}_3$  axis (i.e., outside the crossover lines),  $G$  scales with a power  $1/\bar{a}_2$ .

If the  ${}^2R_1$  is approached along a line of constant  $\bar{x}_3$ , in the plane  $\bar{x}_1 = 0$  Eq. (6.18) shows that  $G$  has an exponent  $1/\bar{a}_2$ . This is expected, of course, since  $G$  has an exponent  $1/a_2$  for any point (i.e., fixed  $x_3$ ) on the line  ${}^2R_1$  even when the point is far away from the  ${}^3R_0$  [see Eq. (6.8)].

In Sec. V, exponents were demonstrated in terms of the scaling powers  $a_i$  [Eqs. (5.13)] and the same can be done here for the  ${}^2R_1$  (exponents in terms of  $a_i$ ) and the  ${}^3R_0$  (exponents in terms of the  $\bar{a}_i$ ) separately. The only new exponents, which will be derived, are exponents for the directions of approach to the  ${}^3R_0$  along  $y_2 = \text{constant}$  and these give exponents of the form

$$f \sim |\bar{x}_3|^{\bar{a}_f/\bar{a}_3}. \quad (6.22)$$

These can be related to exponents of approach along directions of type 2 by relations of the form

$$\bar{a}_f/\bar{a}_3 = (\bar{a}_f/\bar{a}_2)/\varphi. \quad (6.23)$$

These are new predictions of scaling specific to tricritical points [the others are analogous to Eq. (5.13)].<sup>7(c)</sup>

Finally, we emphasize the importance of expressing the scaling relations in terms of invariants. For example, Eq. (6.21) may be written in the alternative “mixed-exponent form”

$$\chi_{st} \propto C(\bar{x}_2 + k\bar{x}_3^{1/\varphi})^{-\gamma}, \quad (6.24)$$

where

$$C \propto \bar{x}_3^{(\gamma-\bar{\gamma})/\varphi}, \quad (6.25)$$

with

$$-\gamma = \frac{1-2a_1}{a_2}, \quad -\bar{\gamma} = \frac{1-2\bar{a}_1}{\bar{a}_2}. \quad (6.26)$$

Expressions (6.24) and (6.25) appear more complicated than they actually are. The exponents are actually not mixed when expressed in the invariant form as shown in Eq. (6.21).



## ACKNOWLEDGMENTS

We wish to thank F. Harbus, R. B. Griffiths, J. C. Wheeler, and E. K. Riedel for stimulating discussions.

## APPENDIX A: PROOF OF THEOREM 1

*Theorem 1.* Consider a one-parameter continuous group of transformations

$$\mathcal{G}: x'_i = f_i(\lambda | x_0, x_1, \dots, x_n), \quad (\text{A1})$$

where  $i=0, 1, \dots, n$ . There exist  $n$  functionally independent absolute invariants of the  $x_i$  ( $i=0, 1, \dots, n$ ).

*Proof of theorem 1.* Consider a function  $F(x'_0, x'_1, \dots, x'_n)$ . Assume the derivatives of  $f_i$  with respect to  $\lambda$  exist. We expand  $F(x'_0, x'_1, \dots, x'_n)$  in a Maclaurin series

$$F(x'_0, x'_1, \dots, x'_n) = f + f'(\delta\lambda) + \frac{f''}{2!} (\delta\lambda)^2 + \dots, \quad (\text{A2})$$

where

$$\begin{aligned} f &= F(x_0, x_1, \dots, x_n), \\ f' &= \left( \frac{dF}{d\lambda} \right)_{\lambda=\lambda_0} = VF(x_0, x_1, \dots, x_n), \\ f'' &= \left( \frac{d^2F}{d\lambda^2} \right)_{\lambda=\lambda_0} = V^2F(x_0, x_1, \dots, x_n), \\ &\vdots \end{aligned} \quad (\text{A3})$$

with  $\lambda_0$  the value of  $\lambda$  corresponding to the identical transformation and

$$V \equiv \sum_{i=0}^n \xi_i \left( \frac{\partial}{\partial x_i} \right), \quad (\text{A4})$$

$$\xi_i \equiv \left( \frac{\partial f_i}{\partial \lambda} \right). \quad (\text{A5})$$

If, therefore,  $F(x_0, x_1, \dots, x_n)$  is an absolute invariant of the group  $\mathcal{G}$ , then

$$F(x'_0, x'_1, \dots, x'_n) = F(x_0, x_1, \dots, x_n). \quad (\text{A6})$$

The necessary and sufficient condition for  $F = \text{const}$  is that

$$VF = \sum_{i=0}^n \xi_i \left( \frac{\partial F}{\partial x_i} \right) = 0. \quad (\text{A7})$$

Thus,  $F$  is a solution of the partial differential equation (A7) and consequently,  $F(x_0, x_1, \dots, x_n) = \text{const}$  is a solution of the system of the equivalent ordinary differential equations

$$\frac{dx_0}{\xi_0} = \frac{dx_1}{\xi_1} = \dots = \frac{dx_n}{\xi_n}. \quad (\text{A8})$$

These equations admit  $n$  independent solutions (first integrals)<sup>30,31</sup> and theorem 1 is proved.

## APPENDIX B: PROOF OF THEOREM 2

*Theorem 2.* If the equation

$$x_0 = X_0(x_1, x_2, \dots, x_n) \quad (\text{B1})$$

is invariant under

$$\mathcal{G} \begin{cases} x_0 = f(\lambda | x_0), \\ x'_i = f_i(\lambda | x_1, x_2, \dots, x_n), \end{cases} \quad (\text{B2})$$

then it can be expressed as

$$y_0 = Y_0(y_1, y_2, \dots, y_{n-1}), \quad (\text{B3})$$

where  $(y_0, y_1, \dots, y_{n-1})$  form a set of functionally independent absolute invariants under  $\mathcal{G}$ , with

$$\frac{\partial y_0}{\partial x_0} \neq 0,$$

and  $(y_1, y_2, \dots, y_{n-1})$  the  $n-1$  functionally independent absolute invariants of  $\mathcal{G}^s$ .

By hypothesis,  $y_0$  is an absolute invariant of  $(x_0, x_1, \dots, x_n)$  of  $\mathcal{G}$ . Thus, (B3) implies that the invariant equation (B1) may be written

$$y_0(x_0; x_1, x_2, \dots, x_n) = Y_0(y_1, y_2, \dots, y_{n-1}). \quad (\text{B4})$$

Since  $(y_1, y_2, \dots, y_{n-1})$  form a basis set of functionally independent absolute invariants of  $(x_1, x_2, \dots, x_n)$  of  $\mathcal{G}^s$ , (B4) is equivalent to the statement that  $x_0$  is expressible as an implicit function of  $(x_1, x_2, \dots, x_n)$ :

$$y_0(x_0; x_1, x_2, \dots, x_n) = g(x_1, x_2, \dots, x_n), \quad (\text{B5})$$

where  $g$  is an absolute invariant of  $(x_1, x_2, \dots, x_n)$  under  $\mathcal{G}^s$ .

Before we launch into the proof of the theorem, we give a proof of the following lemma.<sup>32</sup>

*Lemma.* A necessary and sufficient condition for  $x_0$ , implicitly defined by (B5), as a function of  $(x_1, x_2, \dots, x_n)$ , to be the same function as  $x'_0$  of  $(x'_1, x'_2, \dots, x'_n)$  implicitly defined by

$$y_0(x'_0, x'_1, x'_2, \dots, x'_n) = g'(x'_1, x'_2, \dots, x'_n) \quad (\text{B6})$$

is that  $g$  is an absolute invariant of  $(x_1, x_2, \dots, x_n)$  under  $\mathcal{G}^s$ .

*Proof of lemma.* Since  $y_0$  is an absolute invariant of  $\mathcal{G}$ , we have

$$y_0(x_0; x_1, x_2, \dots, x_n) = y_0(x'_0; x'_1, x'_2, \dots, x'_n). \quad (\text{B7})$$

Since we require  $x_0(x_1, x_2, \dots, x_n)$  to be exactly the same function as  $x'_0(x'_1, x'_2, \dots, x'_n)$ , (B5)–(B7) require that

$$\begin{aligned} g(x_1, x_2, \dots, x_n) &= g'(x'_1, x'_2, \dots, x'_n) \\ &= g'(x'_1, x'_2, \dots, x'_n). \end{aligned} \quad (\text{B8})$$

This is the necessity proof.

We now demonstrate (B8) is sufficient to ensure (B5) and (B6) admit an invariant solution such that



$x_0(x_1, x_2, \dots, x_n)$  is exactly the same function as  $x'_0(x'_1, x'_2, \dots, x'_n)$ . Inverting (B5) and (B6), we obtain

$$\begin{aligned} x_0(x_1, x_2, \dots, x_n) &= h(g; x_1, x_2, \dots, x_n), \\ x'_0(x'_1, x'_2, \dots, x'_n) &= h'(g'; x_1, x_2, \dots, x_n), \end{aligned} \quad (\text{B9})$$

in some neighborhood of the  $(x_1, x_2, \dots, x_n)$  and  $(x'_1, x'_2, \dots, x'_n)$  spaces, respectively. It is obvious that  $h(g; x_1, x_2, \dots, x_n)$  is exactly the same function as  $h'(g'; x'_1, x'_2, \dots, x'_n)$ . But, by hypothesis,  $g(x_1, x_2, \dots, x_n)$  is exactly the same function as  $g'(x'_1, x'_2, \dots, x'_n)$ . Therefore,  $x_0(x_1, x_2, \dots, x_n)$  is exactly the same function as  $x'_0(x'_1, x'_2, \dots, x'_n)$ .

*Proof of theorem 2.* Using the lemma and the fact that  $g(x_1, x_2, \dots, x_n)$  in (B5) is an absolute invariant of  $(x_1, x_2, \dots, x_n)$  under  $\mathcal{G}^s$ , we immediately verify the statement of theorem 2.

#### APPENDIX C: PROOF OF THEOREM 3

*Theorem 3.* Consider a one-parameter continuous group of transformations  $\mathcal{G}$ :

$$\mathcal{G} \begin{cases} x'_0 = \lambda x_0, \\ x'_i = f_i(\lambda) x_i, \quad i = 1, 2, \dots, n. \end{cases} \quad (\text{C1})$$

If

$$x_0 = F(x_1, x_2, \dots, x_n) \quad (\text{C2})$$

is an invariant equation under  $\mathcal{G}$ , the most general form for  $f_i(\lambda)$  is  $\lambda^{a_i}$ , where  $a_i$  are constants.

*Proof of theorem 3.* We transform (C2) by means of (C1) for two successive values of  $\lambda = \lambda_1, \lambda_2$ ,

$$\lambda_1 \lambda_2 x_0 = F[f_1(\lambda_1) f_1(\lambda_2) x_1, f_2(\lambda_1) f_2(\lambda_2) x_2, \dots, f_n(\lambda_1) f_n(\lambda_2) x_n], \quad (\text{C3})$$

and again for the value of  $\lambda = \lambda_1 \lambda_2$ ,

$$\lambda_1 \lambda_2 x_0 = F[f_1(\lambda_1 \lambda_2) x_1, f_2(\lambda_1 \lambda_2) x_2, \dots, f_n(\lambda_1 \lambda_2) x_n]. \quad (\text{C4})$$

These results are to hold for all values of  $x_i$ . Setting  $x_2 = x_3 = \dots = x_n = 0$ , we have from (C3) and (C4)

$$F[f_1(\lambda_1) f_1(\lambda_2) x_1, 0, \dots, 0] = F[f_1(\lambda_1 \lambda_2) x_1, 0, \dots, 0]. \quad (\text{C5})$$

Therefore,

$$f_1(\lambda_1) f_1(\lambda_2) = f_1(\lambda_1 \lambda_2). \quad (\text{C6})$$

The solution<sup>33</sup> of the functional equation for  $f_1(\lambda)$  for  $\lambda > 0$  is

$$f_1(\lambda) = \lambda^{a_1}, \quad (\text{C7})$$

where  $a_1$  is a constant. This process may be repeated for each  $f_i(\lambda)$ ,  $i = 1, 2, \dots, n$ . Thus, theorem 3 is proved.

\*Work forms a part of a Ph.D. thesis to be submitted to the Physics Department of MIT by A. Hankey. Preliminary reports of aspects of this work appear in T. S. Chang, A. Hankey, and H. E. Stanley, AIP Conf. Proc. 10, 880 (1973).

<sup>†</sup>Supported by NSF Grant No. GU-1590 and NASA Grant No. NGL 34-002-084. Permanent address: Riddick Laboratories, North Carolina State University, Raleigh, N.C. 27607.

<sup>‡</sup>Supported by a Research Assistantship from the Laboratory for Nuclear Science, MIT Lindemann Fellow. Present address: SLAC, Stanford, Calif.

<sup>§</sup>Supported by NSF, ONR, and AFOSR

<sup>1</sup>A. Hankey, T. S. Chang, and H. E. Stanley, Phys. Rev. B (to be published), hereafter referred to as II. See also, F. Harbus, A. Hankey, H. E. Stanley, and T. S. Chang, Phys. Rev. B (to be published).

<sup>2</sup>(a) B. Widom, J. Chem. Phys. **43**, 3892 (1965); (b) C. Domb and D. L. Hunter, Proc. Phys. Soc. Lond. **86**, 1147 (1965); (c) L. P. Kadanoff, Physics (N.Y.) **2**, 263 (1966); (d) R. B. Griffiths, Phys. Rev. **158**, 176 (1967).

<sup>3</sup>E. K. Riedel and F. Wegner, Z. Phys. **225**, 195 (1969).

<sup>4</sup>E. K. Riedel and F. Wegner, Phys. Rev. Lett. **24**, 730 (1970).

<sup>5</sup>R. B. Griffiths and J. C. Wheeler, Phys. Rev. A **2**, 1047 (1970).

<sup>6</sup>R. B. Griffiths, Phys. Rev. Lett. **24**, 715 (1970).

<sup>7</sup>(a) E. K. Riedel, Phys. Rev. Lett. **28**, 675 (1972); (b) A. Hankey, H. E. Stanley, and T. S. Chang, Phys. Rev. Lett. **29**, 278 (1972). (c) See also, R. B. Griffiths, Phys. Rev. B **7**, 545 (1973).

<sup>8</sup>J. F. Nagle, Phys. Rev. A **2**, 2124 (1970); J. F. Nagle and J. C. Bonner, J. Chem. Phys. **54**, 729 (1971); J. C. Bonner and J. F. Nagle, J. Appl. Phys. **42**, 1280 (1971).

<sup>9</sup>We will use the word "spaces" to mean subspaces of the total space of field or fieldlike variables. Fieldlike refers to variables

which occur as parameters in the Hamiltonian and which are not discontinuous across coexistence surfaces.

<sup>10</sup>(a) E. H. Graf, D. M. Lee, and J. D. Reppy, Phys. Rev. Lett. **19**, 417 (1967). These authors only treat the tricritical point at the lowest pressure. See also, G. Goellner and H. Meyer, Phys. Rev. Lett. **26**, 1543 (1971); and G. Goellner, Ph.D. thesis (Duke University, 1972) (unpublished). (b) W. B. Yelon (private communication); see also, C. W. Garland and B. B. Weiner, Phys. Rev. B **3**, 1634 (1971).

<sup>11</sup>Parameters in a Hamiltonian which can be varied have similar properties to field variables with respect to the geometry of the surfaces. These are used in Sec. III.

<sup>12</sup>(a) F. J. Wegner, Phys. Rev. B **5**, 4529 (1972); (b) Phys. Rev. B **6**, 1891 (1972); (c) E. K. Riedel and F. J. Wegner, Phys. Rev. Lett. **29**, 349 (1972).

<sup>13</sup>I. S. Jacobs and P. E. Lawrence, Phys. Rev. **164**, 866 (1967); V. A. Schmidt and S. A. Friedberg, Phys. Rev. B **1**, 2250 (1970); B. E. Keen, D. P. Landau, B. Schneider, and W. P. Wolf, J. Appl. Phys. **37**, 1120 (1966); W. B. Yelon and R. J. Birgeneau, Phys. Rev. B **5**, 2615 (1972); F. Harbus and H. E. Stanley, Phys. Rev. Lett. **29**, 58 (1972); Phys. Rev. B (to be published).

<sup>14</sup>For an elementary account of anisotropic antiferromagnets, including a brief discussion of the spin-flop transition, see, e.g., D. H. Martin, *Magnetism in Solids* (MIT Press, Cambridge, Mass., 1967), pp. 261-263. The implications of scaling here are touched on in A. Hankey, Ph.D. thesis (MIT, 1973) (unpublished).

<sup>15</sup>W. K. Theuman and J. S. Hoye, J. Chem. Phys. **55**, 4159 (1971); see also P. C. Hemmer and G. Stell, Phys. Rev. Lett. **24**, 1284 (1970); and G. Stell and P. C. Hemmer, J. Chem. Phys. **56**, 2474 (1972); A. Hankey, Ref. 14.

<sup>16</sup>A more complete account of these models will be given else-



where; a preliminary account appears in A. Hankey, T. S. Chang, and H. E. Stanley, AIP Conf. Proc. 10, 899 (1973).

<sup>17</sup>This point occurs when  $2mH = 2J_{SR}$ , where  $2m = 1$ , in the remainder of this work and  $J_{SR}$  is the nearest-neighbor exchange energy [cf. Eq. (3.1)].

<sup>18</sup>The inclusion of a competing long-range interaction makes it possible to define a fourth variable, which is fieldlike, although it is strictly not a field. This variable is the ratio of interaction strengths in the Hamiltonians. In the figures, it is denoted by  $\bar{R} \equiv J_{SR}/J_{LR}$ . This variable is "fieldlike" because the CXS and CRS in the space including  $\bar{R}$  have the same properties as in spaces of fields.

<sup>19</sup>An exact analysis of an Ising model with several staggered fields requires consideration of a regularly repeating block of spins. The length of the block will be equal to the lowest common multiple of the wavelengths of the various staggered fields. If staggered fields of wavelengths 2 and 3 had been chosen, there would be six spins in a block, but with wavelengths 2 and 4, there are only four spins per block. The analysis for a block of  $n$  spins proceeds by multiplying together  $n$  transfer matrices and so  $H_2$  and  $H_4$  give the smallest number of matrices to multiply.

<sup>20</sup>Our ideas of using the invariant theorems of continuous groups of transformations for multicomponent scaling were first presented at the MIT Summer School on Critical Phenomena in 1971 (unpublished). Recently, important advances have been made by Wilson, Fisher, Wegner, Riedel and others in generating the scaling exponents using the linearized renormalization group equations. It was shown that the scaling fields may be deduced from the relevant operator densities. The number of references to work utilizing the renormalization group now exceeds 100, and the reader is urged to consult K. G. Wilson, Phys. Reports (to be published) or *Cooperative Phenomena Near Phase Transitions: A Bibliography with Selected Readings*, edited by H. E. Stanley (MIT Press, Cambridge, Mass., 1973).

<sup>21</sup>This form of the scaling hypothesis has been treated in detail by A. Hankey and H. E. Stanley [Phys. Rev. B 6, 3515 (1972)]. It is a more complete discussion of the statements of the hypothesis previously used by Riedel and Wegner (Refs. 3 and 4) and also by Kadanoff (Ref. 2c). For a complete set of references, see *Cooperative Phenomena near Phase Transitions: A Bibliography with Selected Readings*, edited by H. E. Stanley (MIT Press, Cambridge, Mass., 1973).

<sup>22</sup>The elements of the group are parametrized by the single

parameter  $\lambda$ . Thus the group is a one-parameter group.

<sup>23</sup>A more-general linear transformation will be  $x_i = f_i(\lambda)x_i$ . Because of the associativity property of groups, it can be shown that  $f_i(\lambda) = \lambda^{a_i}$  [Appendix C]. If some of the  $x_i$  do not scale and serve only as "inactive parameters" in Eq. (5.6), the corresponding scaling powers are equal to zero.

<sup>24</sup>We could, of course, replace  $H_{st}$  by  $x_1$  in Eq. (5.9), but we emphasize that (cf. Fig. 12) the only thermodynamic field axis which is a strong direction is  $H_{st}$ . Thus while the direction  $H_{st} + \epsilon(H - H_c)$  or  $H_{st} + \epsilon(T - T_c)$  are both strong and  $\partial/\partial H_{st}$  is the same as  $\partial/\partial x_1$ ,  $\partial/\partial T$ , and  $\partial/\partial H$  are only equivalent to differentiating with respect to  $x_2$ .

<sup>25</sup>Here we will formulate the scaling hypothesis only for the Gibbs function, because the scaling equation analogous to (5.1) for other functions can be obtained by appropriate differentiation with respect to its independent variables. Scaling functions for physically more interesting functions like  $M$  and  $\chi$  can then be obtained by the same method used here for  $G$ .

<sup>26</sup>Equations (5.14) can all be written in terms of  $|H - H_c(T)|$  except at the Néel point, where the line of critical points is parallel to the  $H$  axis.

<sup>27</sup>Occasionally, it turns out to be appropriate to scale with respect to a variable which is not tangent—see, e.g., Paper II. This is also true when all the  $^2R_i$  do not end up parallel and the tangent variable for one line is not the tangent variable for another line. We emphasize that scaled equations may change their values or functional forms when the scaling variables change signs.

<sup>28</sup>"Mutually consistent" means that if one chooses two different sets of axes for scaling, one set  $(\bar{x}_1, \bar{x}_2, \bar{x}_3)$  with reference to a line  $L$  and the second  $(\bar{x}'_1, \bar{x}'_2, \bar{x}'_3)$  with respect to  $L'$ , then the second set is none other than a permutation of the first set.

<sup>29</sup>Our expression differs from that given in Ref. 7 [Eq. (8)], where the constant  $k$  is not present. The constant  $k$  is needed to ensure the divergence property of  $\chi_{st}$  (and other second derivatives of  $G$ ) along the critical line.

<sup>30</sup>L. P. Eisenhart, *Continuous Groups of Transformations* (Princeton U. P., Princeton, N.J., 1933).

<sup>31</sup>L. S. Pontryagin, *Ordinary Differential Equations* (Addison-Wesley, Reading, Mass., 1962).

<sup>32</sup>A. J. A. Morgan, Q. J. Math. 2, 250 (1952).

<sup>33</sup>J. Aczél, *Lectures on Functional Equations and their Applications* (Academic, New York, 1966).



## Double-Power Scaling Functions near Tricritical Points\*

T. S. Chang,<sup>†</sup> Alex Hankey,<sup>‡</sup> and H. Eugene Stanley

Physics Department, Massachusetts Institute of Technology, Cambridge, Massachusetts 02139

(Received 11 September 1972)

We introduce invariants of the scaling equation about the tricritical point. Using these invariants, a modified version of the scaling hypothesis about the three critical lines meeting at the tricritical point is presented. From it we demonstrate that the thermodynamic equation of state near a tricritical point and near a critical line may be expressed as double-power scaling functions. These imply that experimental data should collapse from a *volume* onto a *line* (i.e., by two dimensions). This behavior is in contrast to ordinary "single-power" scaling functions, which predict data collapsing from a volume onto a surface or from a surface onto a line (i.e., by one dimension).

### I. INTRODUCTION

There have been recent experimental measurements<sup>1</sup> near tricritical points<sup>2</sup> (TCPs) in metamagnets,  $\text{NH}_4\text{Cl}$ , and  $^3\text{He}$ - $^4\text{He}$  mixtures.<sup>1</sup> These data have been partially interpreted recently in terms of scaling arguments in which one makes not one but two scaling hypotheses.<sup>3-5</sup> Riedel and Wegner<sup>6</sup> were perhaps the first authors to note that in regions for which two scaling hypotheses are simultaneously valid, double-power-law behavior of certain functions results. In this work we present a *variation* of scaling for tricritical points, utilizing generalized homogeneous functions<sup>7</sup> (GHF's) of invariants of the scaling equation about the tricritical point. We obtain, in regions near a critical line and a tricritical point, double-power scaling functions which permit data to collapse from a volume onto a line, in contrast to the behavior of single-power scaling functions, which permit data to collapse by only one dimension (e.g., from a surface onto a line, or a volume onto a surface).

Before we can proceed to make the scaling hypothesis for a TCP, it will be necessary to determine the relevant directions for scaling.<sup>3</sup> The three thermodynamic fields ( $T$ , temperature;  $\eta$ , ordering field; and  $g$ , nonordering field) near a TCP are believed to constitute an affine space in which directions may be defined by parallelism only. A TCP is a point of intersection of three critical lines in this three-dimensional affine space (cf. Fig. 1). At each point  $P$  on a critical line, three different types of directions can be established. The first direction,  $x_1(P)$ , is a direction not locally parallel to the coexistence surface. The second,  $x_2(P)$ , is locally parallel to the coexistence surface but not

parallel to the critical line. These are the "strong" and "weak" directions of Griffiths and Wheeler.<sup>8</sup> The third direction,  $x_3(P)$ , is locally parallel to the critical line.

As the point  $P$  moves toward the TCP, these directions attain limiting orientations. Since there are three critical lines terminating at a TCP, three "rival" sets of directions of this type exist at the TCP. It has been shown<sup>4</sup> that if scaling holds at a TCP, these three sets of directions are equivalent. Thus, we choose the relevant directions for scaling at a TCP as  $\bar{x}_i \equiv \lim_{P \rightarrow \text{TCP}} x_i(P)$ , where  $P$  is a point on the critical line  $L_i$  (see Fig. 1).<sup>9</sup>

### II. SCALING HYPOTHESIS FOR TCP

Having ascertained the relevant scaling directions  $\bar{x}_i$  for TCP, we now introduce a scaling parameter  $\lambda$  ( $> 0$ ) and make the homogeneity hypothesis<sup>3-7</sup> that the singular part of the Gibbs potential is asymptotically a GHF,

$$G(\lambda^{\bar{a}_1} \bar{x}_1, \lambda^{\bar{a}_2} \bar{x}_2, \lambda^{\bar{a}_3} \bar{x}_3) = \lambda G(\bar{x}_1, \bar{x}_2, \bar{x}_3), \quad (1)$$

where  $\bar{a}_i$  are the scaling powers. Equation (1) is *equivalent* to the statement that

$$G = F_3(\bar{x}_1, \bar{x}_2, \bar{x}_3) \quad (2)$$

is an invariant equation under the one-parameter ( $\lambda$ ) group ( $\mathcal{G}_3$ ) of transformations

$$G' = \lambda G, \quad \bar{x}_i' = \lambda^{\bar{a}_i} \bar{x}_i, \quad (i=1, 2, 3). \quad (3)$$

In other words, under the transformations, Eq. (2) becomes  $G' = F_3(\bar{x}_1', \bar{x}_2', \bar{x}_3')$ .

The group  $\mathcal{G}_3$  admits a basis set of three ( $i=0, 1, 2$ ) functionally independent absolute invariants,  $y_i(G', \bar{x}_1', \bar{x}_2', \bar{x}_3') = y_i(G, \bar{x}_1, \bar{x}_2, \bar{x}_3)$ , such that all



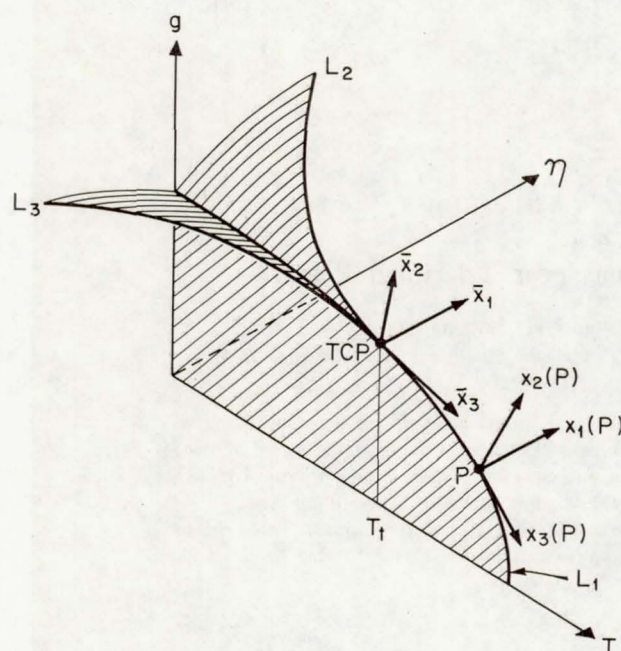


FIG. 1. Schematic phase diagram showing a TCP (at  $T = T_f$ ). Shaded areas are coexistence surfaces. At a point  $P$  on  $L_1$ , a triad of directions  $x_i(P)$  are shown. This triad becomes  $\bar{x}_i$  at TCP.

other absolute invariants are expressible in terms of these. One such basis set is

$$y_0 \equiv G/\bar{x}_3^{1/\bar{a}_3}, \quad y_1 \equiv \bar{x}_1/\bar{x}_3^{\bar{a}_1/\bar{a}_3}, \quad y_2 \equiv \bar{x}_2/\bar{x}_3^{\bar{a}_2/\bar{a}_3} \quad (4)$$

The scaling hypothesis, Eq. (1), requires Eq. (2) to be expressible in terms of the basis set as a "single-power" scaling function,

$$y_0 = \bar{F}_2(y_1, y_2), \quad (5)$$

which states that  $G$  (and other thermodynamic functions), when appropriately scaled, are functions of the invariants  $(y_1, y_2)$  alone. This result allows data near a TCP to collapse from a *volume* onto a *surface*.

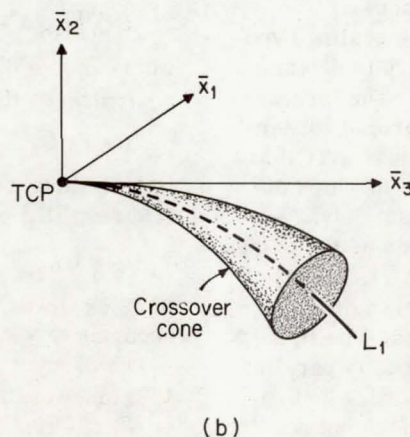
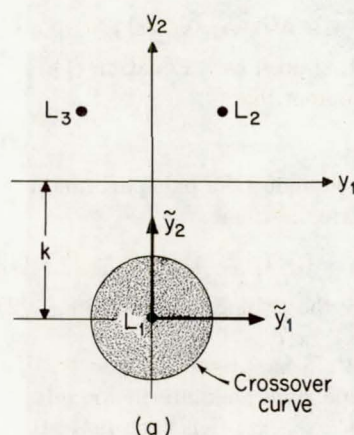


FIG. 2. (a) Invariant  $(y_1, y_2)$  plane. The strong and weak directions for  $L_1$  are  $y_1$  and  $y_2$ , and the crossover curve is shown (Ref. 8). (b) Principal points of interest of (a) in the  $(\bar{x}_1, \bar{x}_2, \bar{x}_3)$  space.

We remark that, using Eq. (1), it is possible to determine all exponent relations and "single-power" scaling laws for a TCP.<sup>3-5</sup>

### III. GEOMETRY OF SURFACES AND CURVES NEAR TCP

Since the quantities  $y_1$  and  $y_2$  defined in Eqs. (4) form a basis set of functionally independent absolute invariants of  $\bar{x}_i$  under the group of transformations  $\bar{x}_i' = \lambda^{\bar{a}_i} \bar{x}_i$ , points in the invariant  $(y_1, y_2)$  plane give rise to invariant curves in the  $(\bar{x}_1, \bar{x}_2, \bar{x}_3)$  space. We have seen that the scaling hypothesis requires scaled thermodynamic functions near a TCP to depend on  $y_1$  and  $y_2$  only. This implies that each of the three critical lines near the TCP can be expressed as a point  $y_i = k_i$  in the  $(y_1, y_2)$  plane, where  $k_i$  are constants.

Usually, for systems exhibiting a TCP, one of the critical lines is a planar curve lying entirely in the  $(g, T)$  plane (e.g.,  $L_1$  of Fig. 1). Since  $\bar{x}_1 = 0$ , Eq. (4) implies that  $L_1$  is given by  $(y_1, y_2) = (0, -k)$  in the invariant plane.

Near  $L_1$ , it is expected that the symmetry property of the critical line will also influence the asymptotic form of the thermodynamic functions. The region of influence is bounded by some "crossover" curve,  $f_x(y_1, y_2) = 0$  [Fig. 2(a)], or

$$f_x(x_1/x_3^{\bar{a}_1/\bar{a}_3}, \bar{x}_2/\bar{x}_3^{\bar{a}_2/\bar{a}_3}) = 0, \quad (6)$$

which is a conical surface surrounding  $L_1$  in the  $(\bar{x}_1, \bar{x}_2, \bar{x}_3)$  space [Fig. 2(b)]. Scaling cannot tell us the *actual* shape of the curve in the  $(y_1, y_2)$  plane,<sup>10</sup> but it does limit the shape of the conical "crossover" surface in the  $(\bar{x}_1, \bar{x}_2, \bar{x}_3)$  space, since all points in the  $(y_1, y_2)$  plane give rise to curves approaching the TCP along the  $\bar{x}_3$  axis (corresponding to the minimum  $\bar{a}_i$ ).<sup>11</sup>

### IV. DOUBLE-POWER SCALING FUNCTIONS FOR $L_1$

We now proceed to deduce the restriction on the asymptotic form of the thermodynamic functions near a TCP adjacent to the critical line  $L_1$ .<sup>12</sup> Along  $L_1$ , the conventional scaling hypothesis is



normally stated in terms of a GHF equation

$$G(\mu^{a_1} x_1, \mu^{a_2} x_2; x_3) = \mu G(x_1, x_2; x_3), \quad (7)$$

where  $\mu(>0)$  is an arbitrary parameter,  $a_1$  and  $a_2$  are the scaling powers for  $L_1$ , and  $x_3$  is an "inactive" variable which does not scale. Near the TCP, by Eq. (5) the value of  $y_0 \equiv G/\bar{x}_3^{1/\bar{a}_3}$  changes only if the values  $y_1$  and/or  $y_2$  change. It is much better therefore to make a scaling hypothesis about  $L_1$  near the TCP using  $y_1$  and  $y_2$ .<sup>13</sup>

Since the coexistence surface bounded by  $L_1$  maps into the vertical axis of the  $(y_1, y_2)$  plane, the direction  $y_1$  is strong and  $y_2$  is weak. Thus, we deduce that the proper scaling variables for  $L_1$  (near the TCP) are

$$\tilde{y}_1 \equiv y_1, \quad \tilde{y}_2 \equiv y_2 + k; \quad (8)$$

these vanish at the line  $(y_1, y_2) = (0, -k)$ .

We now hypothesize that along  $L_1$  near the TCP,  $\tilde{y}_0 \equiv y_0$  is a GHF of  $(\tilde{y}_1, \tilde{y}_2)$ :

$$\tilde{y}_0(\mu^{a_1} \tilde{y}_1, \mu^{a_2} \tilde{y}_2) = \mu \tilde{y}_0(\tilde{y}_1, \tilde{y}_2). \quad (9)$$

In other words, instead of (7) we postulate that

$$\tilde{y}_0 = F_2(\tilde{y}_1, \tilde{y}_2) \quad (10)$$

is an invariant equation under the group  $(\mathcal{G}_2)$  of transformations  $(\tilde{y}_0' = \mu \tilde{y}_0, \tilde{y}_1' = \mu^{a_1} \tilde{y}_1, \text{ and } \tilde{y}_2' = \mu^{a_2} \tilde{y}_2)$ .

By the same reasoning used for the derivation of Eq. (5), we see that (9) requires that (10) may be written in the form

$$z_0 = F_1(z_1), \quad (11)$$

where  $z_0 \equiv \tilde{y}_0/\tilde{y}_2^{1/a_2}$  and  $z_1 \equiv \tilde{y}_1/\tilde{y}_2^{a_1/a_2}$  form a set of functionally independent absolute invariants of  $\mathcal{G}_2$  and therefore of the variables  $G, \bar{x}_1, \bar{x}_2, \bar{x}_3$  under the direct-product group  $\mathcal{G}_2 \otimes \mathcal{G}_3$ .

Reexpressing Eq. (11) in terms of the original variables  $G, x_1, x_2$ , and  $x_3$  we obtain the "double-power" form<sup>14</sup>

$$\frac{G}{\bar{x}_3^{1/\bar{a}_3} (\bar{x}_2/\bar{x}_3^{\bar{a}_2/\bar{a}_3} + k)^{1/a_2}} = F_1\left(\frac{\bar{x}_1}{\bar{x}_3^{a_1/\bar{a}_3} (\bar{x}_2/\bar{x}_3^{\bar{a}_2/\bar{a}_3} + k)^{a_1/a_2}}\right). \quad (12)$$

Equation (12) predicts that near the TCP and  $L_1$ , data will collapse from a volume onto a line.

Clearly, this happens only within the crossover cone of Eq. (6) [cf. Fig. 2(b)].

In the plane  $\bar{x}_1 = 0$  [i. e., the  $(g, T)$  plane], Eq. (12) requires<sup>15</sup>

$$G \sim \bar{x}_3^{1/\bar{a}_3} (\bar{x}_2/\bar{x}_3^{\bar{a}_2/\bar{a}_3} + k)^{1/a_2}, \quad (13)$$

and the conical surface of Eq. (6) becomes two crossover lines (cf. Fig. 3)  $\bar{x}_2 = C_i \bar{x}_3^{\bar{a}_2/\bar{a}_3}$  or  $y_2 = C_i$ , where  $i = 1, 2$ . The crossover exponent  $\varphi \equiv \bar{a}_3/\bar{a}_2$ , which determines the shape of the crossover lines, can be obtained directly from the shape of  $L_1$ .<sup>3</sup>

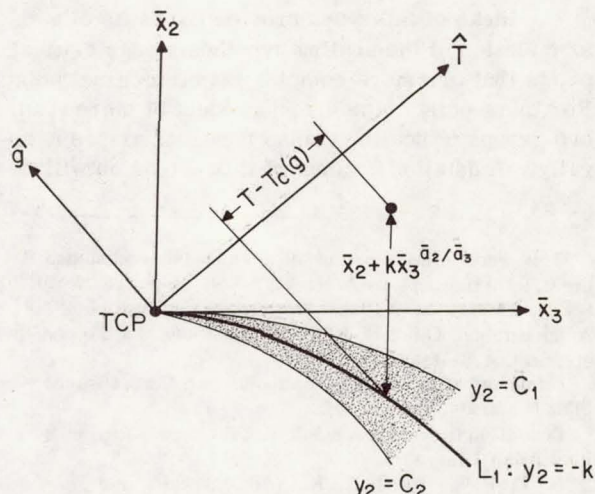


FIG. 3. Figure 2(b) sliced in the  $\bar{x}_1 = 0$  plane. The crossover lines are labeled  $y_2 = C_1, C_2$ . The projection of  $\bar{x}_2 + k\bar{x}_3^{\bar{a}_2/\bar{a}_3}$  along the  $T$  axis is  $T - T_c(g)$ , and  $(\hat{T}, \hat{g}) \equiv (T - T_t, g - g_t)$ .

## V. EXTENSIONS AND CONCLUDING REMARKS

The entire discussion in this paper may be extended to the scaling of any thermodynamic function  $f$ . For example, for the staggered susceptibility  $\chi_{st} \equiv \partial^2 G / \partial \eta^2 \propto \partial^2 G / \partial x_1^2$  (or  $\partial^2 G / \partial x_1^2$ ) and the direct susceptibility  $\chi \equiv \partial^2 G / \partial g^2 \propto \partial^2 G / \partial x_2^2$  (or  $\partial^2 G / \partial x_2^2$ ) of a metamagnet, the expression analogous to Eq. (13) is

$$f_i = \bar{x}_3^{(1-2\bar{a}_i)/\bar{a}_3} (\bar{x}_2/\bar{x}_3^{\bar{a}_2/\bar{a}_3} + k)^{(1-2a_i)/a_2}, \quad (14)$$

where  $f_1 \equiv \chi_{st}$  and  $f_2 \equiv \chi$ . We note that Eq. (13) has the appropriate divergence properties at the critical line and at the TCP.

Finally, we make a few remarks about the exponents and directions of approach toward the TCP and  $L_1$ . Using the experimentally accessible function  $\chi_{st}$  as an example, we note that if we approach the TCP along a curve  $\bar{x}_2/\bar{x}_3^{\bar{a}_2/\bar{a}_3} = \text{const}$ , the scaling exponent is  $-\bar{\gamma}_{st}\varphi^{-1} = (1 - 2\bar{a}_1)/\bar{a}_3$ . If we approach the critical line  $L_1$  along a line  $\bar{x}_3 = \text{const}$ , the scaling exponent is  $-\gamma_{st} = (1 - 2a_1)/a_2$  as expected. On the other hand, if the TCP is approached along a path outside the crossover lines,  $\chi_{st}$  scales with an exponent  $-\bar{\gamma}_{st} = (1 - 2\bar{a}_1)/\bar{a}_2$ . Similar remarks may be made with respect to the three-dimensional "double-power" scaling functions of Eq. (12).

Equation (14) may be cast in "mixed-exponent" forms; e. g.,  $\chi_{st} \sim C[T - T_c(g)]^{-\gamma_{st}}$ , in which  $\bar{x}_2 + k\bar{x}_3^{\bar{a}_2/\bar{a}_3}$  has been replaced by its projection along the  $T$  axis (Fig. 3), and  $C \sim \bar{x}_3^{(\gamma_{st} - \bar{\gamma}_{st})/\varphi}$  is the asymptotic amplitude. Depending on the relative magnitudes of  $\gamma_{st}$  and  $\bar{\gamma}_{st}$ , the asymptotic amplitude may diverge, vanish, or stay constant as the TCP is approached within the crossover cone.



The ideas of this work provide the basis of a formulation of the scaling hypothesis near critical points that are more complex than tricritical points. For these points, the direct product of more than two groups of scaling transformations arises naturally. A detailed account of this extension will be

published elsewhere.

#### ACKNOWLEDGMENTS

The authors wish to thank F. Harbus, R. B. Griffiths, E. K. Riedel, and J. C. Wheeler for stimulating discussions.

\*This work forms a portion of a Ph.D. thesis submitted to the MIT Physics Dept. by A. Hankey. Work supported by National Science Foundation, National Aeronautics and Space Administration, Office of Naval Research, and Air Force Office of Scientific Research.

<sup>†</sup>Permanent address: Riddick Laboratories, North Carolina State University, Raleigh, N. C.

<sup>‡</sup>Present address: SLAC, Stanford, Calif. Supported by a Lindemann Fellowship.

<sup>1</sup>(a) D. P. Landau, B. E. Keen, B. Schneider, and W. P. Wolf, Phys. Rev. B **3**, 2310 (1971); (b) C. W. Garland and B. B. Weiner, Phys. Rev. B **3**, 1634 (1971); (c) E. H. Graf, D. M. Lee, and J. D. Reppy, Phys. Rev. Lett. **19**, 417 (1967); (d) R. J. Birgeneau (private communication). For additional references to the vast experimental literature, see *Cooperative Phenomena near Phase Transitions*, edited by H. E. Stanley (MIT Press, Cambridge, Mass., 1973).

<sup>2</sup>R. B. Griffiths, Phys. Rev. Lett. **24**, 715 (1970).

<sup>3</sup>E. K. Riedel, Phys. Rev. Lett. **28**, 675 (1972).

<sup>4</sup>A. Hankey, H. E. Stanley, and T. S. Chang, Phys. Rev. Lett. **29**, 278 (1972).

<sup>5</sup>R. B. Griffiths, Phys. Rev. B **7**, 545 (1973).

<sup>6</sup>E. K. Riedel and F. Wegner, (a) Z. Phys. **225**, 195 (1969); (b) Phys. Rev. Lett. **24**, 730 (1970).

<sup>7</sup>A. Hankey and H. E. Stanley, Phys. Rev. B **6**, 3515 (1972). See also H. E. Stanley, *Introduction to Phase Transitions and*

*Critical Phenomena* (Oxford U.P., London and New York, 1971), Chap. 11. (1972). See also, H. E. Stanley, *Introduction to Phase Transitions and Critical Phenomena* (Oxford U. P., London, 1971), Chap. 11.

<sup>8</sup>R. B. Griffiths and J. C. Wheeler, Phys. Rev. A **2**, 1047 (1970).

<sup>9</sup>In general, the  $\bar{x}_j$  may be nonorthogonal, but in this work we need consider only rectilinear orthogonal coordinates.

<sup>10</sup>Although the crossover curve may be of any form, it is shown for convenience as a circle in Fig. 2(a).

<sup>11</sup>In this paper, we assume  $a_1 \neq a_2 \neq a_3$ . (See Ref. 4 for discussion of other cases.)

<sup>12</sup>The scaling ideas for  $L_{2,3}$  are similar. However, it will be necessary to rotate the invariant axis to determine the strong and weak directions.

<sup>13</sup>This assumption is equivalent to the scaling assertion of Ref. 6, that the extended homogeneity relation (1) must encompass the relation (7) asymptotically close to the critical line.

<sup>14</sup>Equation (12) is similar to that found in Ref. 6(b) for dynamic scaling in anisotropic magnetic systems. We emphasize that scaled equations may change their values or functional forms when the scaling variables change signs.

<sup>15</sup>Equation (13) is essentially equivalent to Eq. (8) of Ref. 3, provided the variable  $\mu_1$  is interpreted as the critical line scaling field.